RAYTHEON

COMMUNICATIONS AND DATA PROCESSING

STUDIES IN DEEP STRATA RADIO COMMUNICATIONS

STUDIES IN DEEP STRATA RADIO COMMUNICATIONS

by

Dr. Joseph T. deBettencourt

Raymond A. Sutcliffe

RAYTHEON COMPANY

Norwood, Massachusetts

Contract No. AF 19(604)-8359

Project No. 4610

FINAL REPORT

October, 1962

Prepared for

ELECTRONICS RESEARCH DIRECTORATE
AIR FORCE CAMBRIDGE RESEARCH LABORATORIES
OFFICE OF AEROSPACE RESEARCH
UNITED STATES AIR FORCE
BEDFORD, MASSACHUSETTS

Requests for additional copies by Agencies of the Department

of Defense, their contractors, and other government agencies

should be directed to the:

ARMED SERVICES TECHNICAL INFORMATION AGENCY
ARLINGTON HALL STATION
ARLINGTON 12, VIRGINIA

All other persons and organizations should apply to the:

U. S. DEPARTMENT OF COMMERCE
OFFICE OF TECHNICAL SERVICES
WASHINGTON 25, D. C.

CONTENTS

CONTENTS (cont)

CONTENTS (cont)

CONTENTS (cont)

LIST OF ILLUSTRATIONS

x

Section I. INTRODUCTION

A. Geological Aspects of Radio Propagation

1. Propagation Modes in the Atmosphere

To put into proper perspective Raytheon's work on Deep Strata Radio Propagation research, the large scale aspects of the pertinent propagation media for radio waves are reviewed first.

Figure I. 1 is an oversimplified sketch of the earth with the immediately surrounding tropospheric and ionospheric media. Radio propagation between points on the surface of the earth as affected by these media has been and is a large field of research covering the radio frequency spectrum. The troposphere extending upwards to about 10 km or more and the major ionospheric regions at 100 km (E region) and 150 to 250 km (F regions) play various roles in short line-of-sight, longer beyond-horizon, and much longer distance paths. At UHF and for distances beyond horizon, the principal effects of the troposphere are those of scattering, and tropospheric scattering modes have been studied from higher HF through microwave frequencies and at ranges up to hundreds of miles. At VHF and distances beyond horizon, turbulent and meteoric scattering in the ionosphere give rise to ionospheric and meteoric scatter modes at distances of 600 to 1200 miles. At frequencies up through HF (and neglecting sporadic E-layer propagation), reflection and refraction in the ionospheric regions give rise to well-known regular ionospheric layer modes for propagation to

REGULAR LAYER IONOSPHERIC REFLECTIONS,
IONOSPHERIC AND METEORIC SCATTER

TROPOSPHERE

IONOSPHERE

LINE OF SIGHT, TROPOSPHERIC
SCATTER, GROUND WAVES

CRUST

MANTLE

OUTER CORE

INNER CORE
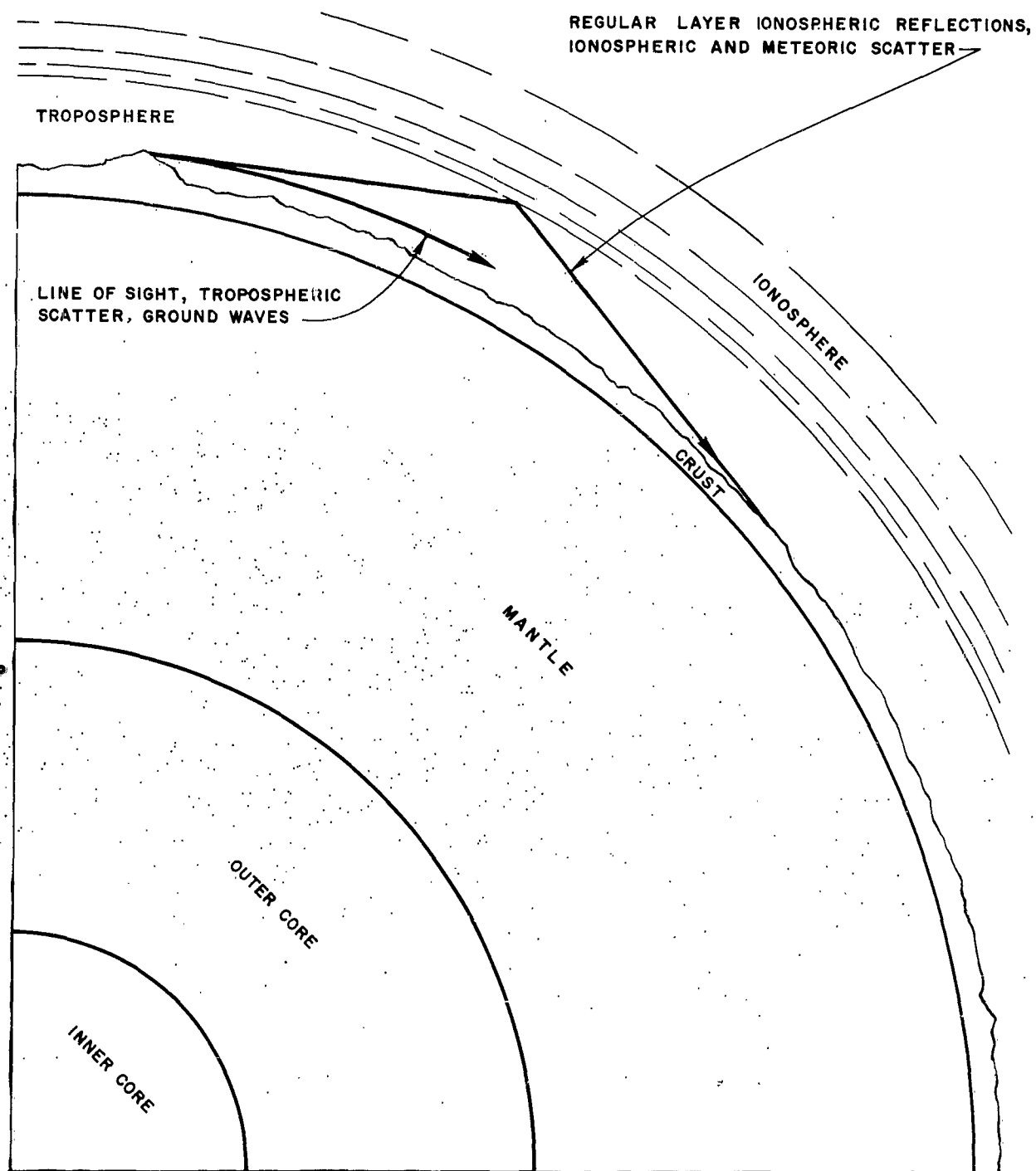
Figure I. 1. Oversimplified sketch of earth structure and radio propagation modes above the surface (not to scale)

great distances. The principal effect of the troposphere here is that of radio refraction. There is an additional mode, that of the surface wave along the air-ground interface, which contributes to vertically polarized wave propagation of particular importance at LF and MF.

An explanation of the mechanism of propagation in the spherical cavity between the earth's surface and the ionosphere can be found in the mode theory[25,76,81] at the low frequencies used in deep strata propagation. Our interest in the mode theory is twofold: first, external noise, which may limit the range for subsurface propagation, is due mainly to atmospheric radio noise propagated between the earth's surface and the ionosphere and then attenuated through the earth to the buried receiver; second, the mode theory for propagation in air between ground and ionosphere has a counterpart in certain possible propagation modes in the earth's crust in a "waveguide" of very low conductivity rock between highly conducting boundaries, e.g., overburden soil on top and the highly conducting "Moho" (Mohorovicic) discontinuity on the bottom. This is discussed further in Section IB and Appendix B.

2. Geological Structure of the Earth

We have discussed one of perhaps four major spherical regions of the earth: the atmosphere. Depending upon the definition used for these regions: the second is the hydrosphere, which includes the great oceans, seas, lakes, and rivers; the third region is the lithosphere; the fourth is the barysphere.

The lithosphere, according to one set of definitions,[20] refers to the solid, rocky outer portion of the earth——as distinguished from the barysphere, which designates the unknown interior supposed to consist of matter heavier than surface materials. More positively, the lithosphere is formed only of the types of rocks observable to geologists and is assumed to be about 60 miles thick. It is commonly termed the earth's crust.

The earth may be divided into shells according to reflections of seismic waves from discontinuities forming the boundaries of such spherical shells. The major discontinuities are:*

—— the earth's surface.

—— the Mohorovicic (Moho) discontinuity, which occurs at a depth $10 \pm$ km in deeper parts of the oceans, $30 \pm$ km under lower parts of continents, and perhaps up to 60 km under high mountain ranges.

—— outer core, boundary at a depth 2900 ± 20 km (radius 3470 km).

—— inner core, there is doubt as to whether the boundary (radius = $1300 \pm$ km) is sharp or whether the transition takes place over a range of 100 to 200 km in depth.

* See Reference 13, section 2-k.

I-4

Therefore, the earth has four shells: the <u>crust</u> extends above the Moho, with a thickness varying from 10 to 30 miles (its upper surface may vary by 12 miles when considering the variation from the top of Mt. Everest to the Mindinao Deep); the <u>mantle</u> extends to a depth of about 1900 miles; the <u>outer core</u> is about 1300 miles thick; the <u>inner core</u> is about 800 miles in radius. This division is depicted in an oversimplified fashion in Figure I.1.

We will not discuss further the characteristics of the core. The mantle is believed to be a plastic fluid area mostly of peridotite rock (with conductivity and dielectric constant comparable to those of surface soils). Conductivity was deduced from diurnal variations in the earth's magnetic field by Lahiri and Price[61] of about 4×10^{-3} mhos/meter at the Moho. The crust consists of rocks in various forms most often with lower conductivity.

Closer examination of the crust reveals more complexity in structure and distributions of rock types with depth, causing consequent difficulty in attaining suitably simplified, useful propagation models. The crust may be divided into two thin portions: the outer or <u>continental layer</u>, which is the foundation of all continents and consists largely of granite; the inner or <u>subcontinental layer</u>, which lies beneath continents and makes up ocean bottoms and consists mainly of basalt. An oversimplified sketch for the model postulated is depicted in Figure I.2.
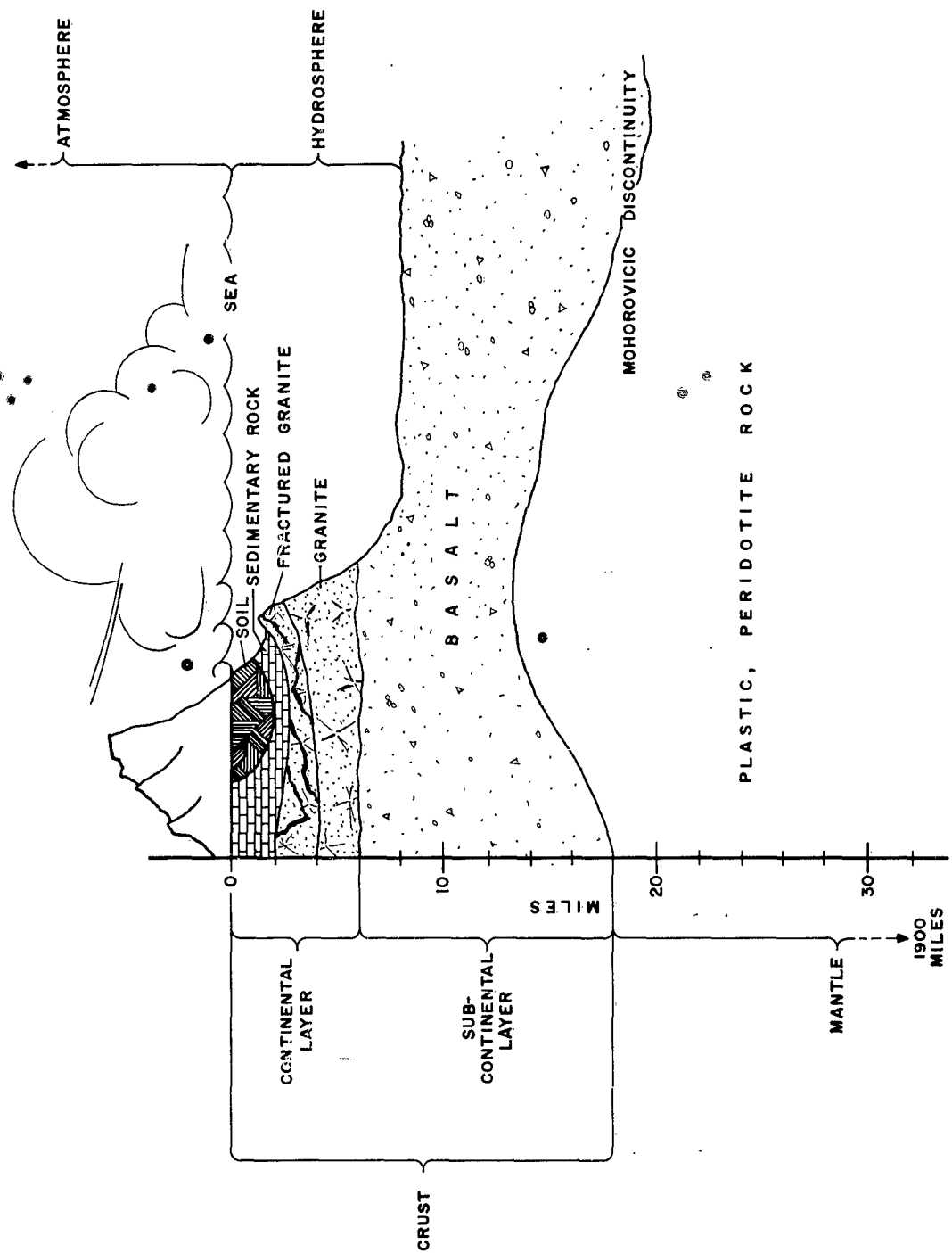
Figure I.2. Sketch of crust and mantle regions near
earth's surface (lithosphere)

3. Rocks and Structure of the Crust

A rock consists of one or more minerals.[20] A simple rock consists of one mineral; marble, for example, is formed from the single mineral calcite. A compound rock is made of more than one mineral; granite, for example, is formed from feldspar and quartz in various ratios, plus minor amounts of mica and other accessory minerals.

Rocks may be divided into three classes according to the code of origin:

a. Igneous - rocks formed from molten masses of material from within the earth, which have cooled and solidified. In part they are the lavas and other products of volcanoes; other masses cool slowly below the surface to form granite and other crystalline forms. The bulk of igneous types are intrusive——as distinct from the lavas, which are extrusive. Examples are:

(1) granite - a common and widely occurring deep seated igneous rock. As the amount of feldspar increases, granite becomes known as granodiorite.

(2) basalt - fine grained to dense, intrusive or extrusive; black or green-black, principally feldspar and pyroxene.

(3) gabbro - often coarse-grained, deep seated.

b. Sedimentary - material that "formed a part of pre-existent rocks, and that was moved from its former position, deposited by the action of water, atmosphere, or glacier ice, and subsequently converted into rock."

Examples are: conglomerate, sandstone, and limestone.

c. Metamorphic -- rocks which were originally igneous or sedimentary but changed for some (e.g., temperature and pressure) reason in texture, composition, or both, so that the original characteristics are altered markedly.

Examples are: Slate, formed from shale; marble, derived from pre-existent limestone.

Referring again to Figure I.2, the gross picture is that of surface soils of varying thicknesses overlying in general sedimentary rocks on top of "fractured" granites. One theory is that granites meld in depth with more solid granite and then blend into basaltic rock, which extends down to the Moho.

4. Gross Electrical Characteristics of Crust and Mantle

From a radio propagation point of view, we consider the region above the Moho; our immediate and perhaps more limited and practical concern is with that portion nearer the earth's surface. We wish to know the electrical characteristics of such media pertinent to the complex propagation constant k discussed in Section II. The electrical constants which affect k are the conductivity σ and relative dielectric constant ϵ_r (it is assumed

I-8

for simplicity that <u>relative permeability</u> μ_r = 1). The way in which σ and ϵ_r affect <u>attenuation constant</u> α and <u>phase constant</u> β (where k = β - j α) depends upon a ratio called the <u>loss tangent</u> p = $\sigma / \omega\epsilon$ = 60 $\sigma \lambda_o / \epsilon_r$; λ_o is the free space wavelength and mks units are employed. This ratio is that of conduction current to displacement current in the lossy dielectric media. If p is large (say p $\geq$ 10), propagation is similar to that in metals; if p is small (say p $\leq$ 0.5), propagation is similar to that in dielectrics with small heating loss (glass, polyethylene, etc.). For reasonable values of ϵ_r, the loss tangent p will be large unless σ is extremely small at the necessarily low frequencies where λ_o is large.

The accuracy of values of σ and ϵ_r is complicated by several factors, becoming worse as depth increases because of the indirect methods of measurement. It is also found that σ and ϵ_r are not independent of frequency, temperature, pressure, and water content; so that at best, a relatively simple but accurate picture is difficult. Nevertheless, typical ranges of values of these constants and the loss tangent may serve as a guide.

The ranges of conductivity for earth materials are shown sketched in Figure I.3, based principally on data from the American Institute of Physics Handbook.[*] These cover various forms of water, unconsolidated sediments (soils), and sedimentary, igneous, and metamorphic rocks. One notes the wide ranges of σ, particularly for igneous and metamorphic rock.

---

[*] See Reference 13, Table 5K-2.
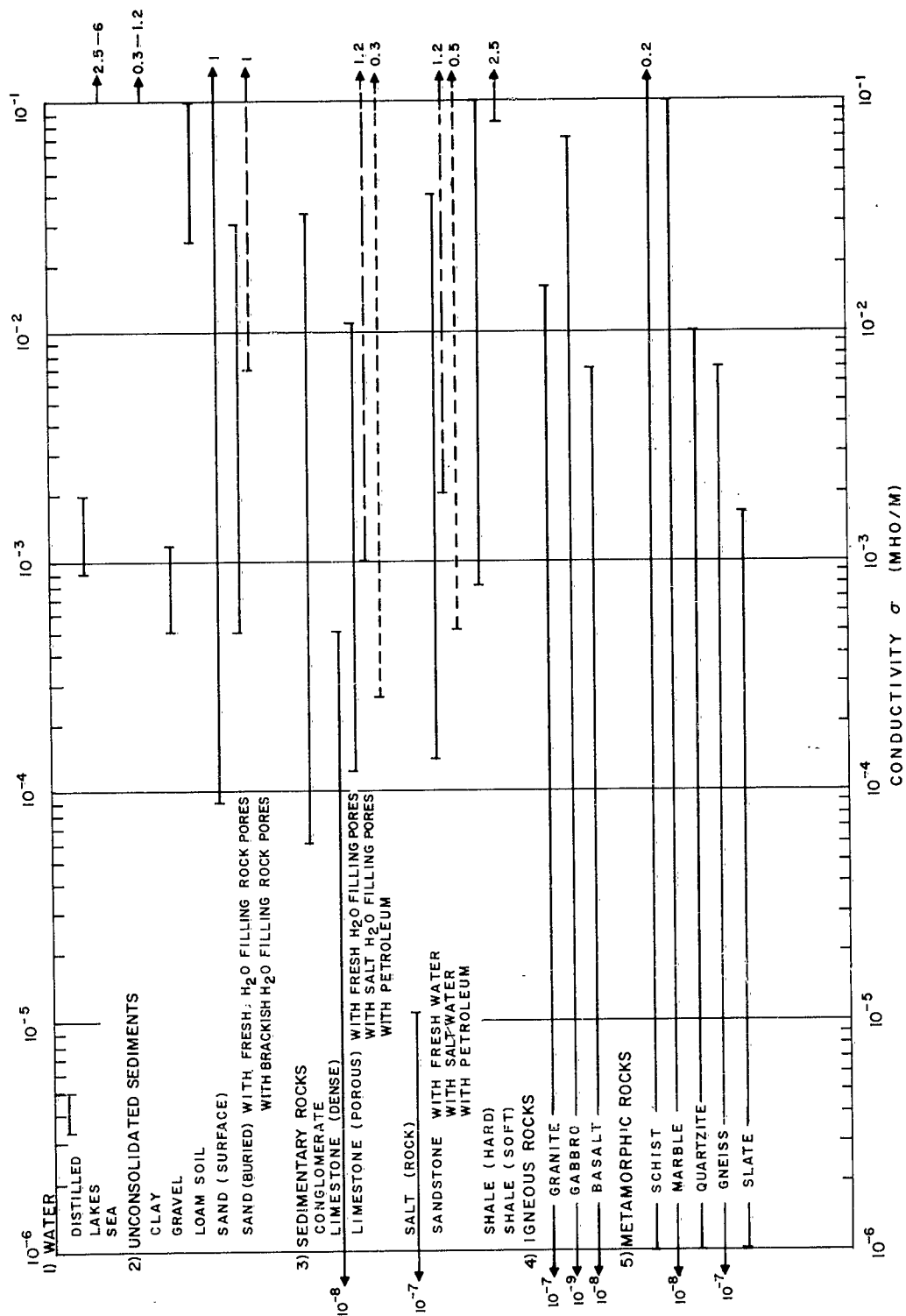
Figure I.3. Conductivity of earth materials (after Amer. Inst. Phys. Handbook)

At VLF where the loss tangent is large, the principal mechanism of conduction is electrolytic; hence, σ depends on the state and amount of water in the rock and the σ of that water. The amount of water depends upon whether the rocks are porous and upon the availability of water to fill the cracks. Dense rocks such as dense limestone have lower values of σ than their porous forms. Buried sand with water has higher σ than surface sand. The conductivity of the included water itself depends on amounts of dissolved salts. The salt content may be enhanced because the original rock minerals have been changed into more soluble mineral forms or because the water has been in contact for a very long time with rock normally thought insoluble.

In drill holes, from which much of the data was taken, temperature increases with depth (perhaps parabolically down to the Moho) and so does pressure (perhaps linearly with depth). The conductivity increases with increased temperature and decreases with decreased water content. From the tabulated data of von Hippel[14] for sandy soil and marble for example, the effect of water content at constant temperature may be seen. Since the percentage of water in rocks decreases as the temperature and pressure increase, the conductivity at first decreases with depth well into the crust. As the depth increases further and where the temperature is several hundred degrees centigrade, temperature increases result in a rising trend in σ. At the Moho, the conductivity is about 4 millimhos/m, which is comparable to that for surface soils.

The electrical properties of rocks are frequency dispersive, particularly when dry. The variation in σ with frequency is particularly marked, the variation in ϵ_r being much less frequency dependent. Thus, dry marble at $25°C$, measured over the range 100 cps to 100 mc, shows that ϵ_r decreases slightly from 9.5 to 8.5, but σ increases from about 10^{-9} to 6×10^{-4} mhos/m. Throughout this frequency range the loss tangent p is small, decreasing from 0.2 to about 0.03, respectively. A similar frequency behavior of σ, ϵ_r, and p is found for dry sandy soil. However, when wet with about 3.9% moisture, this soil shows ϵ_r decreasing slightly from 5 at 100 cps to 4.5 at 300 kc, while the values of σ vary from 5.3×10^{-4} at 100 cps, then decrease slightly and increase slowly to 2.25×10^{-3} at 300 kc. The loss tangent is 19 at 100 cps and decreases to .03 at 300 kc. Crudely, it appears that for $\sigma > 10^{-3}$ and at frequencies where the loss tangent is large, then σ and ϵ_r do not vary markedly with frequency. This seems to hold true for surface soils and some sediments. For smaller conductivities and loss tangents, σ increases markedly, and ϵ_r decreases somewhat with increasing frequency; consequently, p decreases markedly with frequency.

It is also found that earth materials are anisotropic in that σ in a direction perpendicular to bedding planes is notably less than σ in a direction parallel to such planes.

Most of the measurements on σ and ϵ_r to be reported have been done in drill holes of relatively small depth compared with the potentially larger depths into the crust previously discussed. The drill holes used

I-12

to date in New Hampshire and on Cape Cod are 1000 feet deep or less. From the discussion above, it is not expected that very small conductivities in situ will be encountered at the locations studied and values of 10^{-4} mhos/m and greater were typical, certainly not as low as 10^{-6} mhos/m. However, most of the work was that of developing adequate theory and techniques of measurement rather than attempting radio transmission over very great distances (the results of propagation tests over various paths are discussed in Section VI).

B. Subsurface Modes of Propagation

One may conveniently divide possible modes of radio propagation between buried antennas below the surface into three types by reference to the simplified sketches in Figure I.4. These are the up-over-and-down (UOD) mode, the short distance deep strata mode, and the potentially much longer distance very deep waveguide mode. The models shown for an example assume four media: (a) air, with $\sigma_0 = 0$ and $\epsilon_{r_0} = 1$; (b) an overburden, perhaps 500 feet thick with $\sigma_1 \cong 10^{-2}$ mhos/m, $\epsilon_{r_1} \cong 4$; (c) a rock transmission medium with σ_2 having two lower ranges of σ_2 values and $\epsilon_{r_2} \cong 4$ to 9; (d) the Moho discontinuity where σ_3 is of the order of 10^{-2} mhos/m with $\epsilon_{r_2} \cong 4$.

1. Up-Over-and-Down Mode

This mode for propagation up through, over, and down through sea water was suggested and analyzed by R. K. Moore[60] and more recently by Moore and colleagues at the University of New Mexico.[61] Experiments
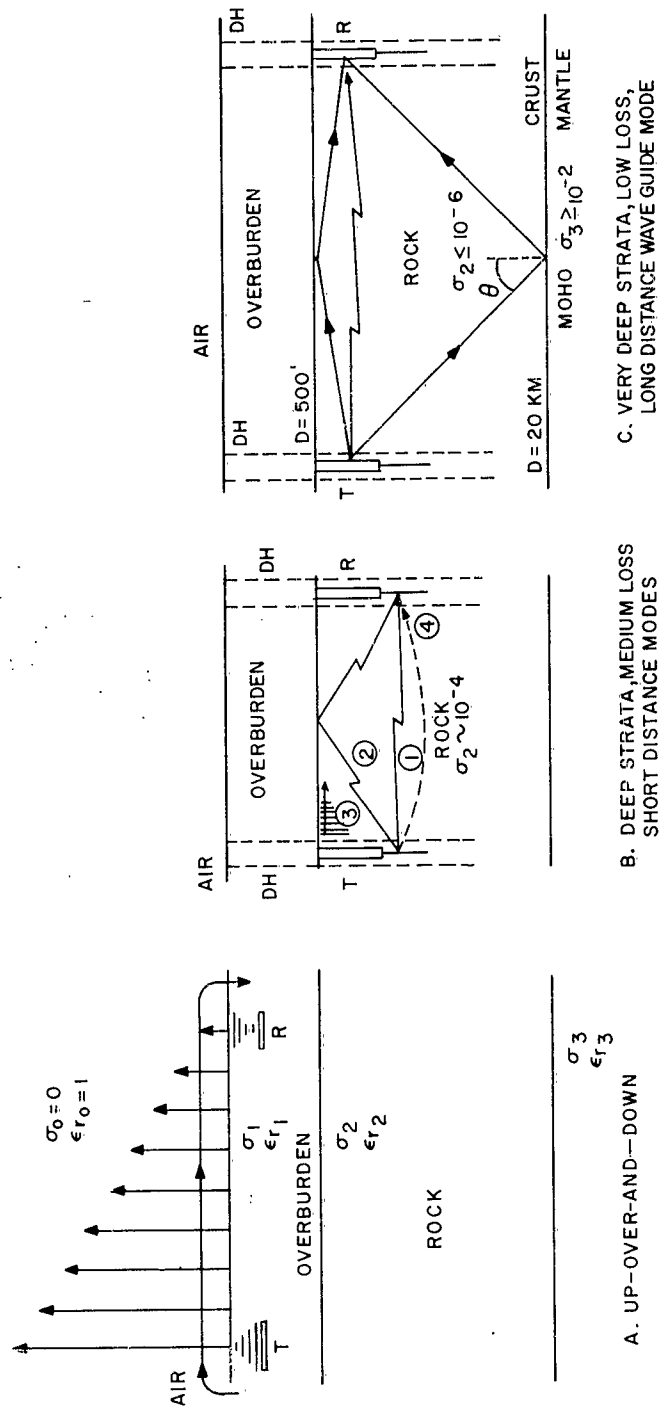
Figure I. 4.   Subsurface propagation modes – simplified sketch

with antennas in ground soils have been carried out by Guy and Hasserjian[43,45] among others.

Horizontal antennas are buried just below the earth's surface, perhaps a few tens of feet. The antennas are arranged axially, i.e., "end-fire" for maximum received field (A of Figure I.4). Energy travels vertically upward towards the air boundary, dampening exponentially. At the surface, the wave suffers refraction loss and the major component in air is the vertically polarized electric field,as though there were a pseudo vertically polarized emitter just above the buried transmitting antenna T. The wave propagates along the surface with the characteristics of a ground wave. Recent modifications to the simpler theory take into account the mode theory of propagation in the cavity between the earth and ionosphere. As the wave propagates along the surface, energy leaks into the ground; in the vicinity of the receiving antenna R, one may imagine the wave "bending over" after undergoing refraction loss to become a horizontally polarized wave, with further exponential damping towards R.

With antennas buried not too deep (a few meters) to minimize exponential damping, distances of hundreds of miles are potentially feasible. The influence of external noise on the received signal, which is also attenuated into the earth, gives rise to useful frequencies in the VLF region. There are various trade-offs regarding depth and optimum frequency for best signal-to-noise ratio at the receiver.[60,61]

This mode has an advantage where antennas must be buried for protection, but the depths cannot be too great. However, the signals can be readily detected in air and can cause interference; vice versa, VLF signals

from other stations can cause interference to the desired received signal.

The theory assumes a soil thickness so great that there is no appreciable "reflection" effect from the overburden-rock boundary, because of exponential damping in the soil. It further assumes that the "direct" signal through the overburden from T to R is negligible, a reasonable assumption for larger distances in highly conducting soils and sea water.

2. Deep-Strata, Medium Loss, Short Distance Mode

Deep strata modes, represented in B of Figure I. 4 and C of Figure I. 4, differ from the UOD mode in A of Figure I. 4 in two principal ways. First, rather deep drill holes (DH) must be available to afford access from the earth's surface to the lower loss rock lying beneath the overburden. Second, and as a consequence of the geometry of drill holes, vertically polarized radiators appear more favorable from a practical point of view. We have principally considered vertical linear radiators, insulated and bare, and fed by means of coaxial lines. The theory for and experiments with such antennas are discussed in Section IV and in Appendices D and E.

When the conductivity of the rock σ_2 is somewhat lower than that of the overburden but not as low as that of such igneous rocks of Figure I. 3, the situation of B of Figure I. 4 pertains. The theory assumes first that the rock is a simple medium of infinite extend; this is developed in Section IIG. The result is applicable to the direct ray for great depths shown in ① in B of Figure I. 4. The next approximation takes into account the effect of the overburden-rock boundary; it further assumes that the thickness

of the rock down to the next major discontinuity such as the Moho, is so great

that the effect of reflections at such discontinuities is negligible due to expo-

nential and spreading losses. This assumption appears to be valid if σ_2 is

of the order to 10^{-4} mhos/m or greater.

The theory of the effect of the overburden-rock boundary is

given in Appendix C and summarized in Section IIG. Besides the direct ray

(1) , there is a wave reflected from the overburden-rock interface as (2) ,

and a wave component (3) guided along that interface. This wave component

notation parallels the "ground wave" treatment for antennas in air above

ground with the rock replacing the air as the "propagation" medium. The

resulting effect of waves (2) and (3) depends upon the propagation constants

of the overburden and the rock and upon their ratio, which gives the relative

refractive index of the two media.

Estimates for communication range may be made for various

assumptions of the propagation model, the constants of the media, electrical

length of antennas, and noise. The calculations have been done in Section IIF

for the rather simplified model of a direct ray between T and R in a homo-

geneous rock medium, which calculations would apply for antennas at several

skin depths below an overburden boundary. The antennas were assumed to be

identical and electrically short, and results are given for insulated antennas

which were short circuited. For an allowed total transmission loss of 205 db

and a conductivity $\sigma_2 = 10^{-4}$ mhos/m, the range is 5 miles at 10 kc and

about 12 miles at 1 kc. If the conductivity σ_2 varies, the ranges will vary

roughly proportional to $\sqrt{1/\sigma_2}$ at a given frequency and for such ranges.
Greater ranges can be achieved by using resonant insulated antennas if hole
depths are sufficiently great. If the allowed transmission loss is based upon
a receiver limited by its own internal noise, then the ranges will decrease if
atmospheric noise fields are not sufficiently attenuated by the overburden.

There is the possibility of the UOD mode of propagation. For
vertical electric dipoles immersed in the overburden or sea water, as for
the model sketched in A of Figure I. 4, Moore[60,61] has shown that the verti-
cal electric field in air at large distances is negligible compared with the
horizontal component, which is itself weak. The theory for such mode has
not been worked out completely for vertical electrical antennas in the rock.
However, if values of relative refractive index of the overburden with respect
to the rock are not too great, the potential UOD modes would be expected to
be much weaker than those for similar antennas nearer the surface but
immersed in the overburden.

A further potentially attractive mode is the downward refracted
wave shown as ④ in B of Figure I. 4. Such a mode can occur if the con-
ductivity decreases to low values with increasing depth, causing a decrease
in refractive index with depth compared with that nearer the overburden.
The situation is roughly analogous to ionospheric propagation from air into
an ionized medium of lesser refractive index causing ray refraction and
return to earth. In the rock, the bending depends upon the initial values of
refractive index at transmitter and receiver and the gradient of refractive

I-18

index with depth. This mode is being studied further with several assumed gradients of refractive index with depth, with a view of utilizing digital computation.

3. Very Deep Strata, Low Loss, Waveguide Mode

This mode is shown sketched in idealized form in C of Figure I.4. It assumes that the rock conductivity σ_2 is at least two orders of magnitude less than that for rays (1), (2), and (3) in B of Figure I.4 and that the gradient of refractive index with depth is very sharp at the rock-overburden boundary and also at the lower discontinuity (say the Moho shown sketched in the Figure at 20-km depth). Rather larger antenna depths may be required to excite this mode. The simple picture is that of waves propagated in rock of very low loss tangent and guided between parallel planes (or spherical sections) of much larger conductivity. The theory is given in Appendix B and is discussed below.

Some examples were used to typify the theory. The cases chosen were those for which a 10-kc wave was excited by a dipole near the upper wall and the field was calculated at a point near that wall at a distance ρ. The upper and lower plane walls were assumed separated a distance d = 20 km. The dielectric in between was assumed to have a relative dielectric constant ϵ_{r_2} = 4. Two cases for the conductivity σ_2 were considered: (a) for σ_2 = 0 (loss-less dielectric) and (b) for σ_2 = 10^{-6} mhos/m (a rather low value, and such that the loss tangent p_2 = 0.45). The resulting electric field E_z was normalized to the same dipole moment

Ids = 16,900 amp-meter for the two cases, the value chosen being that which gives a field of 300 mv/m at ρ = 1 km for 1 kw radiated from a short loss-less dipole over a perfect ground plane for waves in a loss-less dielectric with ϵ_{r2} = 4. The results are shown plotted in Figure I.5, in which values of E_z in db above 1 mv/m are plotted vs horizontal distance ρ on a log scale for the two assumed values of σ_2. There are three modes excited: m = 0, 1, 2; the solid curves are the resultant field; the dashed curves are those for the TEM mode (m = 0). The departure of the solid and dashed curves is the quantity $|W|$ given in Appendix B.

The values of E_z for $\sigma_2 = 10^{-6}$ are relatively lower than those for $\sigma_2 = 0$, due first to the exponential damping exp $(-\alpha_2 \rho)$ in the former. Also, at ρ = 50 km, the relative enhancement of E_z for $\sigma_2 = 10^{-6}$ above E_o' e$^{-\alpha_2 \rho}$ is smaller than that enhancement of E_z for $\sigma_2 = 0$ above E_o'.

For the example cited, there does not appear to be much theoretical advantage in considering the waveguide mode over the TEM mode when a conductivity as small as 10^{-6} mhos/m exists. If such a waveguide mode existed over great distances in the earth, the presence of a lower boundary may cause weaker fields than those due to the TEM mode, but not much stronger. This appears due to the greater attenuation of the higher order modes. Further calculations for different frequencies, plane separations, and conductivity are needed to generalize the relative behavior of E_z found for this example.
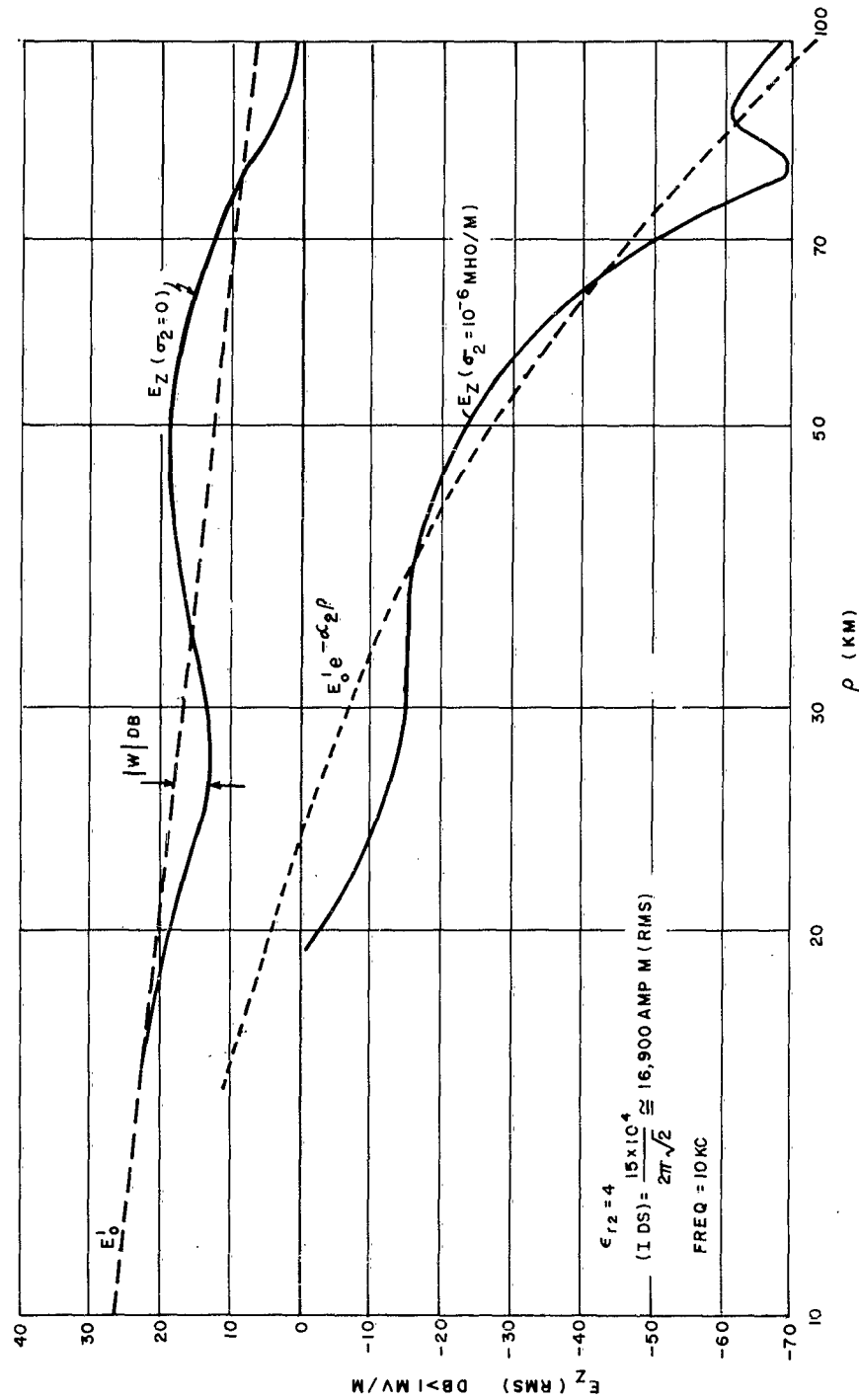
Figure I.5. Vertically polarized field (E_z) vs distance ρ for guided waves, perfectly conducting plane walls. $f = 10\,kc$, $d = 20\,km$, $\epsilon_{r_2} = 4$

$$(Ids) = \frac{15 \times 10^{-4}}{2\pi\sqrt{2}} = 16,900 \text{ amp. m. (rms)}$$

C. History of the Program

Basic consideration of the problem of underground communications was undertaken in a study for project Minuteman, sponsored by Boeing Aircraft Company. It resolved into a program of electrical measurements of rock and boundary media in the laboratory and field, antenna design and measurements, propagation and path attenuation measurements in the field, consideration of the subterranean noise levels to be encountered, and a theoretical study and analysis effort.

Raytheon Company sponsorship was then used to initiate one phase of immediate interest, based upon some of the results of the previous study. This was the use of layers of rock salt as a potential transmission medium. These salt layers, of varying thickness, are reached at drilling depths of 100 feet to 2000 feet depending on location. The three major salt basin areas in the United States cover areas of 50,000 to 150,000 square miles. The low conductivity of this medium offered attractive possibilities for underground communications, though the thickness of the salt layers placed a lower limit of 3 to 4 mc on the frequency to be used when assuming a waveguide mode.

Experiments were conducted in the Retsof salt mine at Geneseo, New York, during the latter part of 1959. This mine is approximately 1000 feet underground, the depth minimizing the limitations on signal-to-noise due to surface noise and interference. It was intended to use test holes drilled 100 feet into the floor of the mine as antenna holes for simple propagation tests. These holes, supposedly dry, were filled with brine and

totally unsatisfactory for the intended use. Cracks and fissures in the layers under the mine floor allowed water infiltration reducing the effectiveness as a transmission medium.

Further measurements in salt layers were attempted in early 1960 at Honeoye, New York. This is a site of natural gas drilling, with hole depths 1500 feet and deeper usual in the area. The wells selected were approximately 4 miles apart, and the corings indicated a layer of salt 75 feet thick centered at 1500 feet. These holes were supposed to be dry. The water used in drilling had, as at the Retsof salt mine, infiltrated the salt layers encountered in drilling, and the insides of the holes were soaked with brine. Tubular dipole antennas were used, resonant at about 6 mc. These antennas were wrapped in polyethylene sheeting to prevent their being shorted out electrically by the brine coating the inside of the holes.

These unsuccessful experiments in a watery salt medium indicated the need for a more favorable area for experimentation. They pointed out the need for controlled conditions in drilling, which are not always feasible when using holes drilled for other purposes.

Work was initiated in New Hampshire where low-conductivity granite is common and reached easily through relatively thin layers of overburden. Sites were selected at Concord, Goffstown, and Bedford where drilled holes already existed at each location. Various antenna and propagation measurements were conducted at these sites. The propagation tests pointed up a problem. The small amount of overburden in this area complicated an

accurate assessment of the transmission path between the sites: i.e., was the signal propagated principally through the rock or via the up-over-and-down mode?

The AFCRL sponsored a continuation of the work under the present USAF contract, effective in the Spring of 1961. Following some preliminary measurements of phase on signals between Goffstown and Bedford, the phase measurements were repeated in an attempt to differentiate between rock-propagated and air-propagated signals. Results were not conclusive in proving that the principal mode was rock-propagated. Attention was then concentrated on measurements of the drill hole water, and first definitive measurements were made on insulated antennas.

Field model measurements were made in early 1961 at Weston, Massachusetts, where 40-mc air-resonant dipoles were used from 1 to 25 mc over a path length of several hundred feet to arrive at vertical directivity patterns for this type of antenna. Antenna impedance measurements were taken over this spectrum.

A study of balanced dipoles and J antennas was made at Swenson's Quarry in Concord, N.H., these antennas being lowered horizontally into cracks cut in the granite. It was hoped that the variation in impedance of the standard dipole antenna when in close contact with the granite would allow a better understanding of an antenna in intimate contact with a low-conductivity medium.

Later phases of the work were commenced on Cape Cod in early 1962. Seismic and magnetic surveys were performed over several areas, and sites were then chosen for drill holes, one in Harwich and ultimately two in Brewster. The holes were 1000 feet deep and overburden thickness, an important consideration for attenuation of atmospheric noise, varied from 400 to 450 feet.

It is with the work since early 1961 that the technical aspects of the report are concerned.

D. Structure of This Report

The work to be reported consists of the work done under the contract since its inception over a year ago. The various wave propagation constants to be employed are defined in Section II. Particular attention is given to effects of large vs small loss tangents of the propagating media on the various coefficients used.

Section III contains a description of the various facilities, equipment, and test equipment employed, with several photographs.

In Section IV the theory and experimental results for bare and insulated antennas are given. The theoretical discussions draw on more detailed treatments given in the Appendix. The measurements refer to full scale tests in New Hampshire and Cape Cod drill holes.

Section V contains a review of techniques employed for measuring electrical properties of dissipative media. Almost all have been employed,

the major exception being that surface resistivity type techniques have not been employed directly. Emphasis was placed on techniques involving measurement of resonant frequencies of insulated antennas and those involving measurement of attenuation with depth.

Section VI contains results of transmission path measurements, principally those made on Cape Cod.

Section VII includes discussion, conclusions, and recommendations based on the work to date.

Personnel involved are listed in Section VIII; acknowledgements are made in Section IX; an extensive bibliography is given in Section X.

The Appendices include a discussion and tabulation of the f(p) and g(p) functions, the theory of the very deep strata waveguide mode, theoretical treatments of the performance of bare and insulated antennas, the theory of the short distance "ground wave" type of mode of propagation, and the theory of attenuation of atmospheric noise through overburden.

Section II. WAVE PROPAGATION IN CONDUCTING MEDIA

A. Definitions of Electrical Constants - Notation

We shall be concerned with radio wave propagation in simple media.

A simple medium is homogeneous and isotropic, the electrical constants (in

general complex) of which are proportionality constants between density

functions and electromagnetic field vectors, as given for example by King.[5]

Various complex amplitudes assume a periodic dependence upon time (t) of

the form $\epsilon^{j\omega t}$, where $j = \sqrt{-1}$, and $\omega = 2\pi f$ where f = frequency of the

variation.

We employ the mks system of units. There are two universal con-

stants ϵ_o and ν_o: ϵ_o is the fundamental electric constant, called the

dielectric constant or permittivity of free space; ν_o is the fundamental

magnetic constant, called the diamagnetic constant or reluctivity of free space.

The reciprocal of the latter is μ_o, called the permeability of free space,

which we shall use for convenience and familiarity in preference to ν_o,

although ν_o is the more fundamental.[5] Numerical values are

$$\epsilon_o = 8.854 \times 10^{-12} \text{ farad/meter} = 10^{-9}/36\pi \text{ farad/meter}$$

(II. 1)

$$\mu_o = \frac{1}{\nu_o} = 4\pi \times 10^{-7} \text{ henry/meter}$$

1. Dielectric Constant $(\underset{\sim}{\epsilon})$*

The complex quantity

$$\underset{\sim}{\epsilon} = \epsilon_o \; \underset{\sim}{\epsilon}_r \qquad\qquad\text{(II. 2)}$$

is called the absolute permittivity or absolute dielectric constant. The dimensionless complex quantity $\underset{\sim}{\epsilon}_r$ is called the complex relative permittivity or complex relative dielectric constant and

$$\underset{\sim}{\epsilon}_r = \epsilon_r' - j \; \epsilon_r'' \qquad\qquad\text{(II. 3)}$$

2. Permeability $(\underset{\sim}{\mu})$

The complex quantity

$$\underset{\sim}{\nu} = \nu_o \; \underset{\sim}{\nu}_r \qquad\qquad\text{(II. 4)}$$

is called the absolute reluctivity of the medium and

$$\underset{\sim}{\nu}_r = \nu_r' - j \; \nu_r'' \qquad\qquad\text{(II. 5)}$$

is called the relative reluctivity (dimensionless) of that medium. In the conducting dielectric media of interest, we assume (see below) that $\underset{\sim}{\nu}_r$ is real. In this case,

$$\underset{\sim}{\mu} = \mu_o \; \underset{\sim}{\mu}_r = \mu_o \; \mu_r' \qquad\qquad\text{(II. 6)}$$

is called the permeability and μ_r the relative permeability (dimensionless) with $\underset{\sim}{\mu}_r = \mu_r' = 1/ \nu_r'$.

---

* The tilde sign under a quantity is used to indicate a complex quantity, temporarily.

II-2

3. Conductivity ($\underset{\sim}{\sigma}$)

The constant

$$\underset{\sim}{\sigma} = \sigma' - j \; \sigma'' \tag{II.7}$$

is the complex conductivity of the medium, measured in mhos/meter (variously designated $(\Omega\,m)^{-1}$ or $(\mho/m)$).

4. Dielectric Factor ($\underset{\sim}{\xi}$)

The quantities $\underset{\sim}{\sigma}$, $\underset{\sim}{\epsilon}$, and ω often occur in combination and the quantity

$$j \omega \underset{\sim}{\xi} = \underset{\sim}{\sigma} + j \omega \underset{\sim}{\epsilon} \tag{II.8a}$$

can be written

$$\underset{\sim}{\xi} = \underset{\sim}{\epsilon} - j \; \underset{\sim}{\sigma}/\omega = (\epsilon' - \frac{\sigma''}{\omega}) - j \; \frac{1}{\omega} (\sigma' + \omega \epsilon'') \tag{II.8b}$$

$$= (\epsilon_e) - j \; \frac{1}{\omega} (\sigma_e)$$

and $\underset{\sim}{\xi}$ is called the <u>complex dielectric factor</u>.

The real part

$$\epsilon_e = \epsilon' - \sigma''/\omega = \epsilon_o \, \epsilon_{er} = \epsilon_o (\epsilon_r' - \sigma''/\omega \, \epsilon_o) \tag{II.9a}$$

is called the <u>real effective</u> permittivity or <u>dielectric constant</u> ϵ_e, and ϵ_{er} is the <u>real effective relative</u> permittivity or relative <u>dielectric constant</u>. In the imaginary part of equation (II.8b), the quantity

$$\sigma_e = \sigma' + \omega \epsilon'' \tag{II.9b}$$

is called the <u>real effective conductivity</u>.

In most measurements, it is ϵ_e (or ϵ_{er}) and σ_e that are determined. A frequency variation in ϵ_e is oftened attributed to the presence

of the imaginary part σ'' of $\underset{\sim}{\sigma}$. Similarly, a frequency variation in σ_e

is often attributed to the imaginary part ϵ'' of $\underset{\sim}{\epsilon}$.

We shall drop the subscript "e" and the primes and henceforth

let

σ = real effective conductivity

ϵ = real effective absolute dielectric constant

but will keep in mind the respective definitions of equations (II. 9b) and

(II. 9a) for these quantities.

B. The f(p) and g(p) Functions for Evaluating $\sqrt{1 \pm jp}$

The complex factors used in propagation of waves in dissipative

media involve the complex radical $\sqrt{1 \pm jp}$. As shown in Appendix A, the

real and imaginary parts are the functions f(p) and g(p), respectively; i. e.,

$$S = \sqrt{1 \pm jp} \; = \; f(p) \pm j \, g(p) \qquad\qquad \text{(II. 10)}$$

In polar form, the complex square root may be written as

$$\sqrt{1 \pm jp} \; = \; |S| \; e^{\pm j\theta} \qquad\qquad \text{(II. 11)}$$

The f(p) and g(p) functions were first computed by G. W. Pierce[64]

and have been published by King.* Appendix A contains more extensives

tables of f(p), g(p), g(p)/f(p), $|S|$ and θ; the values were obtained using a

digital computer.

Values of these functions and the important ratio $\dfrac{g(p)}{f(p)}$ are shown

plotted on the curves of Figure II. 1 and Figure II. 2 as functions of p. In

---

* See Reference 4, Appendix II.
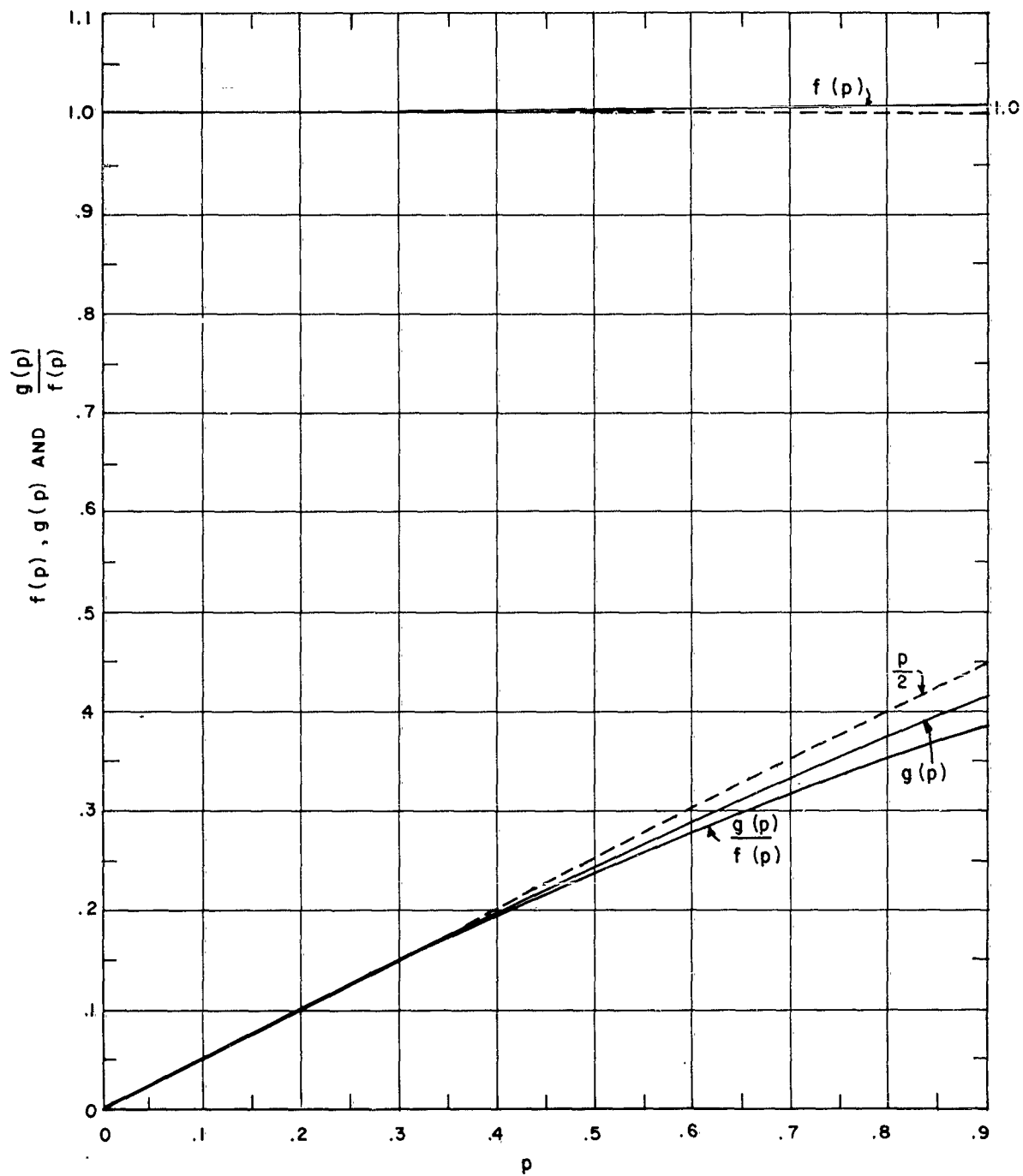
Figure II. 1.   The functions f(p) and g(p) used in evaluating $\sqrt{1 \pm j\ p} = f(p) \pm j\ g(p)$.   Also shown is ratio $g(p)/f(p)$.   Range of $p < 1.0$
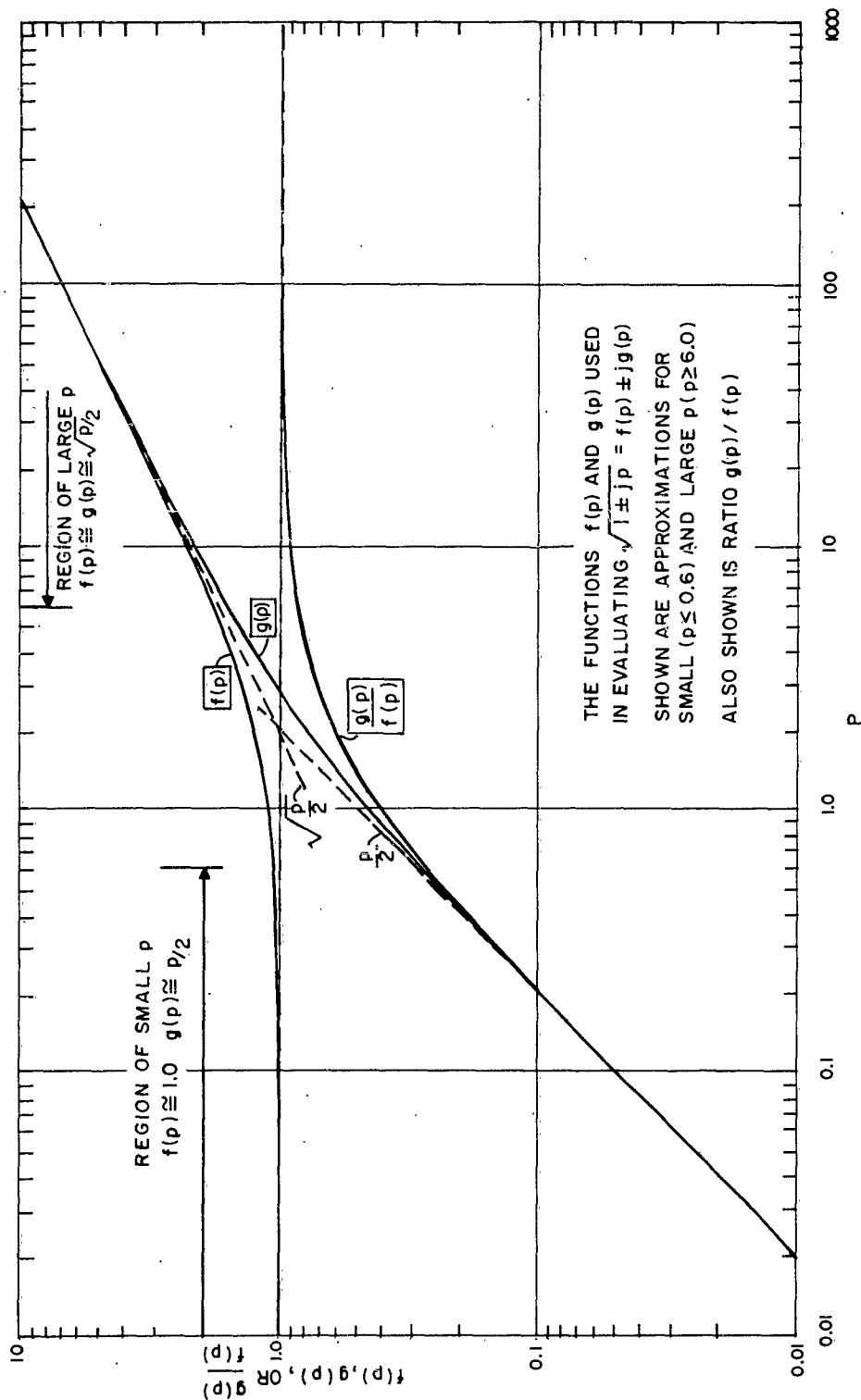
Figure II. 2. The functions f(p) and g(p) used in evaluating $\sqrt{1 \pm jp} = f(p) \pm j\, g(p)$. Also shown is ratio $g(p)/f(p)$. Shown are approxima.. tions for small p $(p < 0.6)$ and large p $(p \geq 6.0)$.

Figure II.1, the range of p is $p \lesssim 0.9$, and the plots are linear. In Figure II.2, the range of p is $0.01 \leq p \lesssim 200$, and the curves are plotted on log-log scales.

Of importance are limiting ranges of p, for which simplified approximate expressions for these functions can be used.

1. Small p $(p^2 << 1)$

In this case

$$f(p) \cong 1 + p^2/8 - - - \tag{II.12a}$$

$$\cong 1, \quad (p^2/8 << 1) \tag{II.12b}$$

$$g(p) \cong \frac{p}{2} (1 - p^2 - - -) \tag{II.13a}$$

$$\cong \frac{p}{2}, \quad (\frac{p^2}{8} << 1) \tag{II.13b}$$

$$\frac{g(p)}{f(p)} \cong \frac{p}{2} (1 - \frac{p^2}{4} - - - -) \tag{II.14a}$$

$$\cong \frac{p}{2}, \quad (\frac{p^2}{4} << 1) \tag{II.14b}$$

If $p \lesssim 0.6$, first approximation accuracies are

$$\left.\begin{array}{ll} f(p) \cong 1, & \text{too low by 4\% or less} \\ g(p) \cong p/2, & \text{too high by 4\% or less} \\ \dfrac{g(p)}{f(p)} \cong p/2, & \text{too high by 8\% or less} \end{array}\right\} \tag{II.15}$$

If $p \lesssim 0.6$, second approximation accuracies are

$$f(p) \cong 1 + p^2/8, \quad \text{too high by 0.4\% or less}$$

$$g(p) \cong \frac{p}{2} (1 - \frac{p^2}{8}), \quad \text{too low by 0.6\% or less} \tag{II.16}$$

$$\frac{g(p)}{f(p)} \cong \frac{p}{2} \left(1 - \frac{p^2}{4}\right) , \text{ too low by 1.0\% or less} \qquad \text{(II. 16)}$$

In the range $0 \leq 1 \leq 0.6$, we use first approximations for simplicity and reasonable accuracy, the expressions being those of equations (II. 12b), (II. 13b), and (II. 14b) for $f(p)$, $g(p)$ and $g(p)/f(p)$, respectively, with accuracies indicated in equation (II. 15).

2. Large p ($p^2 \gg 1$)

$$f(p) \cong \sqrt{\frac{p}{2}} \left(1 + \frac{1}{2p} + \cdots\right) \qquad \text{(II. 17a)}$$

$$\cong \sqrt{\frac{p}{2}} , \quad \left(\frac{1}{2p} \ll 1\right) \qquad \text{(II. 17b)}$$

$$g(p) \cong \sqrt{\frac{p}{2}} \left(1 - \frac{1}{2p} + \cdots\right) \qquad \text{(II. 18a)}$$

$$\cong \sqrt{\frac{p}{2}} , \quad \left(\frac{1}{2p} \ll 1\right) \qquad \text{(II. 18b)}$$

$$\frac{g(p)}{f(p)} \cong 1 - \frac{1}{p} + \cdots \qquad \text{(II. 19a)}$$

$$\cong 1 \qquad \text{(II. 19b)}$$

If $p \geq 6$, first approximation accuracies are

$$f(p) = \sqrt{\frac{p}{2}} , \quad \text{too low by 8\% or less}$$

$$g(p) = \sqrt{\frac{p}{2}} , \quad \text{too high by 9\% or less} \qquad \text{(II. 20)}$$

$$\frac{g(p)}{f(p)} = 1 , \quad \text{too high by 18\% or less}$$

If $p \geq 6$, second approximation accuracies are

$$f(p) \cong \sqrt{\frac{p}{2}} \left(1 + \frac{1}{2p}\right) , \quad \text{too low by 0. 3\% or less}$$

$$g(p) \cong \sqrt{\frac{p}{2}} \left(1 - \frac{1}{2p}\right), \quad \text{too low by 0.4\% or less}$$

$$\frac{g(p)}{f(p)} \cong 1 - \frac{1}{p}, \qquad \text{too low by 0.1\% or less} \tag{II.21}$$

If $p \gtrsim 10$, first approximation accuracies are

$$f(p) \cong \sqrt{\frac{p}{2}}, \quad \text{too low by 5\% or less}$$

$$g(p) \cong \sqrt{\frac{p}{2}}, \quad \text{too high by 5\% or less} \tag{II.22}$$

$$\frac{g(p)}{f(p)} \cong 1, \quad \text{too high by 10\% or less}$$

If $p \gtrsim 10$, second approximation accuracies are

$$f(p) \cong \sqrt{\frac{p}{2}} \left(1 + \frac{1}{2p}\right), \quad \text{too low by 0.1\% or less}$$

$$g(p) \cong \sqrt{\frac{p}{2}} \left(1 - \frac{1}{2p}\right), \quad \text{too low by 0.2\% or less} \tag{II.23}$$

$$\frac{g(p)}{f(p)} \cong 1 - \frac{1}{p}, \quad \text{too low by 0.1\% or less}$$

For simplicity and reasonable accuracy, the first approximation forms are employed, given by equations (II. 17b), (II. 18b), and (II. 19b) for $f(p)$, $g(p)$, and $g(p)/f(p)$, respectively. The accuracy is quite adequate for $p \gtrsim 10$ as indicated in equation (II. 22) and is somewhat poorer if $p \gtrsim 6$, particularly for $g(p)/f(p)$, as indicated in equation (II. 20).

The departure of the first approximations from the true values of the functions are also shown graphically in the curves of Figure II. 1 and Figure II. 2 for the small range of p ($p \leq 0.6$) and large range of p ($p \gtrsim 6$).

C. Loss Tangent (p)

The loss tangent p is the ratio of conduction current to displacement current components. This ratio may be obtained from the dielectric factor, equation (II. 8b), as the ratio of imaginary to real part, i. e.

$$p = \frac{\sigma_e}{\omega \epsilon_e} \qquad \text{(II. 24)}$$

or dropping the subscript "e" as discussed

$$p = \frac{\sigma}{\omega \epsilon} = \frac{\sigma}{\omega \epsilon_o \epsilon_r} \qquad \text{(II. 25)}$$

where by σ we mean the real effective conductivity, by ϵ the real effective dielectric constant, and by ϵ_r the real effective relative dielectric constant, as discussed in Section IIA.

We may write equation (II. 25) as

$$p = \frac{60 \sigma \lambda_o}{\epsilon_r} \qquad \text{(II. 26a)}$$

$$= \frac{1.8 \times 10^{10} \sigma}{f \epsilon_r} \qquad \text{(II. 26b)}$$

$$= \frac{1.8 \times 10^4 \sigma \ (10^{-3} \ \text{mhos/m})}{f_{kc} \ \epsilon_r} \qquad \text{(II. 26c)}$$

in which

$$\left. \begin{aligned} &\lambda_o = \text{free space wavelength (meter)} \\[6pt] &f \quad = \text{wave frequency (cps)} \\[6pt] &f_{kc} = \text{wave frequency (kc)} \\[6pt] &\sigma \quad = \text{conductivity (mhos/meter)} \\[6pt] &\sigma \ (10^{-3} \ \text{mhos/m}) = \text{conductivity in millimhos/meter} \end{aligned} \right\} \text{(II. 27)}$$

Values of loss tangent p are plotted as functions of frequency f_{kc} on the curves of Figure II.3 with σ and ε_r as parameters. Two values of ε_r of 5 and 25 should bracket values encountered for a large variety of rocks and soils. Two ranges of p are plotted (note scales of p and f_{kc}) for small p (p $\leq$ 0.6) and large p (p $\geq$ 10), these limits being shown in heavy horizontal lines.

Thus, for small p, if ε_r = 5 and σ = 10^{-4} mhos/meter, the frequency must <u>exceed</u> 600 kc, while if ε_r = 25 for that same σ, the frequency must <u>exceed</u> 120 kc. Again, for large p (p $\geq$ 10), if ε_r = 5 and σ = 10^{-4} mhos/m, the frequency must be <u>less</u> than 36 kc, while if ε_r = 25 for that same conductivity, the frequency must be <u>less</u> than 7.2 kc.

For sea water, with σ = 4 mhos/m and ε_r = 81, the loss tangent is p = 8.89 x $10^5/f_{kc}$ and will be large (p $\geq$ 10) at all frequencies less than about 90 mc.

D. Propagation Constant or Complex Phase Constant ($\underset{\sim}{k}$)

The complex phase constant $\underset{\sim}{k}$ is found from the general relation

$$\underset{\sim}{k}^2 = \omega^2 \underset{\sim}{\mu} \underset{\sim}{\varepsilon} \qquad (II.28)$$

where $\omega = 2\pi f$, f = frequency, $\underset{\sim}{\mu}$ is the permeability and $\underset{\sim}{\varepsilon}$ the dielectric factor, discussed in Section IIA. We assume $\underset{\sim}{\mu}$ is real and that $\underset{\sim}{\mu}_r$ is unity so that $\underset{\sim}{\mu} = \underset{\sim}{\mu}_o = 4\pi \times 10^{-7}$ h/m.
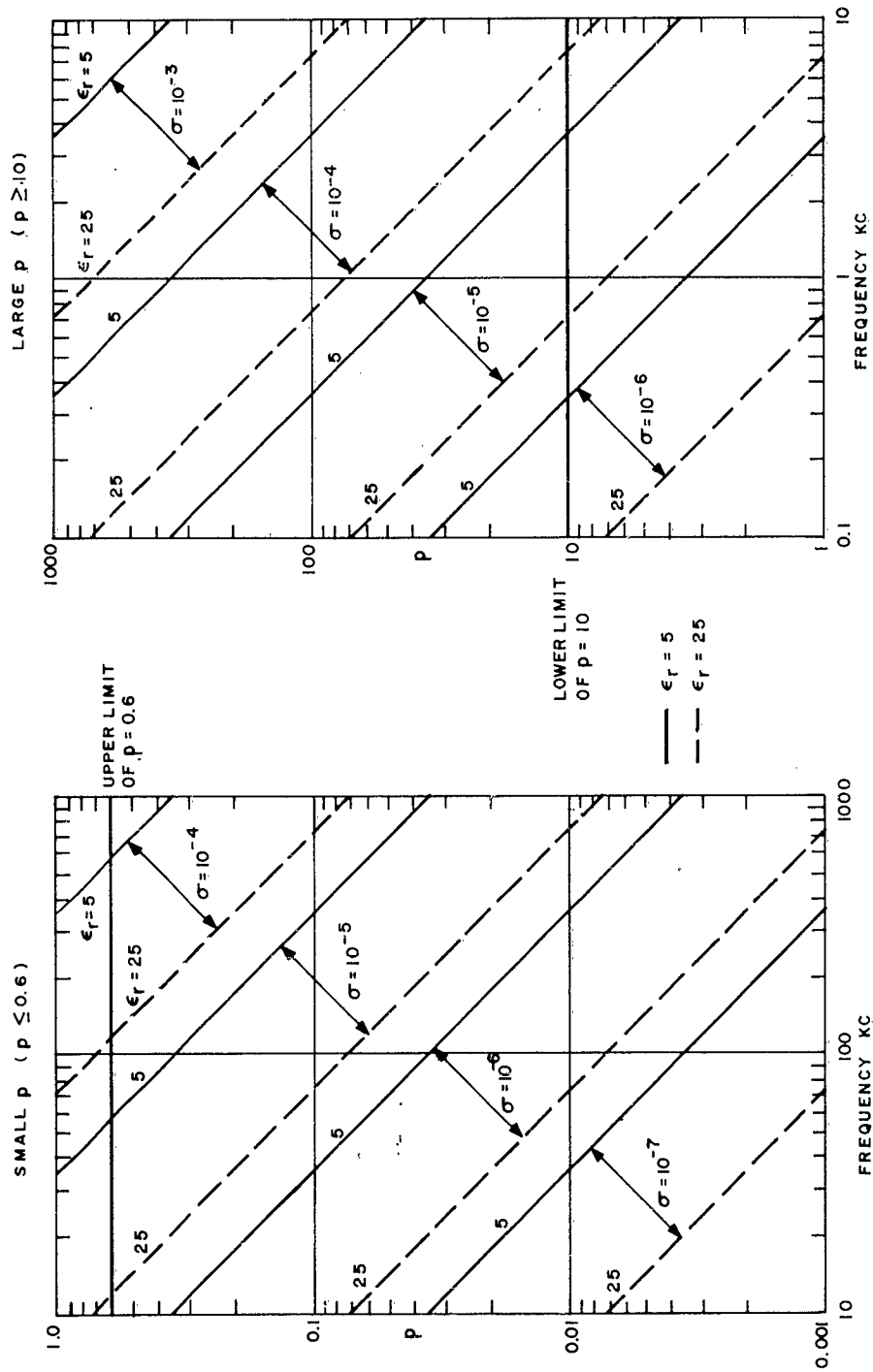
Figure II.3. Loss tangent (p) vs frequency, σ and ϵ_r parameters

(a) Small p (p $\leq$ 0.6)
(b) Large p (p $\geq$ 6.0)

σ = effective conductivity (real) in mhos/meter

We let*

$$\underset{\sim}{k} = \beta - j \propto = \beta (1 - j \frac{\propto}{\beta})$$ (II. 29)

where β is the <u>phase constant</u> and $\propto$ the <u>attenuation constant</u> measured in radians (or nepers) per meter, and both are real.

With equation (II. 8b) without subscript "e", plus the relations in Section IIB and equation (II. 29), we may write equation (II. 28) as

$$\underset{\sim}{k} = \omega \sqrt{\mu_o \underset{\sim}{\xi}} = \omega \sqrt{\mu_o \epsilon_o} \sqrt{\epsilon_r} \sqrt{1 - jp}$$ (II. 30a)

$$= \beta_o \sqrt{\epsilon_r} \left[f(p) - j \, g(p) \right]$$ (II. 30b)

1. Phase Constant (β) and Wavelength in the Medium (λ)

From equation (II. 30b) with equation (II. 29)

$$\beta = \beta_o \sqrt{\epsilon_r} \, f(p)$$ (II. 31)

and with

$$\beta = 2\pi / \lambda$$
$$\beta_o = 2\pi / \lambda_o$$ (II. 32)

where λ_o is the wavelength in free space

$$\frac{\lambda}{\lambda_o} = \frac{1}{\sqrt{\epsilon_r} \, f(p)} = \frac{v_p}{v_o}$$ (II. 33)

where v_p = phase velocity and v_o = velocity of light in vacuo. ** The effect of the magnitude of p on this ratio is discussed below.

---

* In some texts, the notation $\gamma = \propto + j\beta = -jk$ is sometimes used for the propagation constant.
** The phase velocity is given by

$$v_p = \frac{\omega}{\beta} = \frac{\omega}{\beta_o} \left[\frac{1}{\sqrt{\epsilon_r} \, f(p)} \right] = \frac{v_o}{\sqrt{\epsilon_r} \, f(p)}$$ (II. 33a)

2. Attenuation Constant (α)

From equation (II. 30b) with equation (II. 29)

$$\alpha = \beta_0 \sqrt{\epsilon_r} \; g(p)$$

$$= \frac{2\pi}{\lambda_0} \sqrt{\epsilon_r} \; g(p) \tag{II. 34}$$

$$= \frac{2\pi}{\lambda} \; g(p)$$

The effect of the magnitude of p on α is discussed below.

Occasionally, confusion in expressing attenuation losses arises because of the various units assigned to α in practice. The far-zone fields attenuate or vary exponentially with distance, according to $e^{-\alpha R}$. For simple media, an exponential attenuation (power) <u>loss</u> A may be ascribed to this variation, which is the square of the reciprocal of $e^{-\alpha R}$; i.e.,

$$A = e^{2\alpha R} \tag{II. 34a}$$

where the units are <u>nepers/meter</u> for α and <u>meters</u> for R, for consistency. In practice, it is most convenient to express A as a logarithm of a power ratio, and the usual form is the decibel rather than the neper. Thus, the exponential attenuation loss A in decibels is

$$A(db) = 10 \log_{10} A = 8.686 \; \alpha \; (\text{nepers/meter}) \; R \; (\text{meter}) \tag{II. 34b}$$

The relations for α and R will be expressed in subsequent sections in units other than nepers/m and meters. One has

$$\alpha \; (\text{nepers/meter}) = \frac{1}{8.686} \; \alpha \; (db/m) = \frac{3.281}{8.686} = \alpha \; (db/ft)$$

$$= \frac{3.281}{8.686 \times 5280} \; (db/mi) \tag{II. 34c}$$

$$R(\text{meter}) = \frac{1}{3.281} \ R(\text{ft}) = \frac{5280}{3.281} \ R(\text{mi}) \qquad \text{(II. 34d)}$$

Hence,

$$
\begin{aligned}
A \ (\text{db}) &= \propto \ (\text{db/m}) \quad R \ (\text{meter}) \\
&= \propto \ (\text{db/ft}) \quad R \ (\text{ft}) \qquad\qquad \text{(II. 34e)} \\
&= \propto \ (\text{db/mi}) \quad R \ (\text{mi})
\end{aligned}
$$

To express A in equation (II. 34a) as a dimensionless power ratio, the logarithmic unit in $\propto$ must be the neper and the length unit in $\propto$ must be the same as that for R.

3. **Effect of Magnitude of Loss Tangent (p) on Relations for** $\propto$, β **and** λ

   a. Small loss tangent (p $\leq$ 0. 6)

   When p is sufficiently small, first approximations for f(p) and g(p) are used, whence

$$f(p) \ \cong \ 1 \qquad\qquad \text{(II. 12b)}$$

$$g(p) \ \cong \ \frac{p}{2} = \frac{\sigma}{2\omega\epsilon} \qquad\qquad \text{(II. 13b)}$$

$$\frac{g(p)}{f(p)} \ \cong \ \frac{p}{2} = \frac{\sigma}{2\omega\epsilon} \qquad\qquad \text{(II. 14b)}$$

In this case of small loss tangent, several useful relations result.

   (1) Phase constant, phase velocity and wavelength

$$\beta \cong \beta_{o} \ \sqrt{\epsilon_r} \qquad\qquad \text{(II. 35a)}$$

$$\frac{\lambda}{\lambda_o} = \frac{1}{\sqrt{\epsilon_r}} = \frac{v_p}{v_o} \qquad\qquad \text{(II. 35b)}$$

When $p \cong 0$ as in air (for which $\sigma \cong 0$), $\lambda \cong \lambda_o$, $v_p \cong v_o$.

In dielectrics, such as polyethylene in coaxial cables,

$\sigma \cong 0 \cong p$ and with $\epsilon_r = 2.25$

$$\frac{\lambda}{\lambda_o} = \frac{v_p}{v_o} = \frac{1}{1.5} = 0.67$$

giving rise to the "fore-shortened wavelength."

(2) Attenuation constant

In this case

$$\alpha \cong \beta_o \sqrt{\epsilon_r} \frac{p}{2} = \frac{60 \pi \sigma}{\sqrt{\epsilon_r}} \quad \text{neper/meter} \qquad \text{(II. 36a)}$$

$$= 1.637 \times 10^3 \frac{\sigma}{\sqrt{\epsilon_r}} \quad \text{db/meter} \qquad \text{(II. 36b)}$$

$$= 4.990 \times 10^2 \frac{\sigma}{\sqrt{\epsilon_r}} \quad \text{db/ft.} \qquad \text{(II. 36c)}$$

$$= 2.635 \times 10^6 \frac{\sigma}{\sqrt{\epsilon_r}} \quad \text{db/mile (statute)} \qquad \text{(II. 36d)}$$

Less used is the relation of attenuation per wavelength

$$\alpha' = 1637.3 \frac{\sigma}{\epsilon_r} \lambda_o \quad \text{(db/medium wavelength)} \qquad \text{(II. 37a)}$$

$$= 1637.3 \frac{\sigma}{\sqrt{\epsilon_r}} \lambda_o \quad \text{(db/free-space wavelength)} \qquad \text{(II. 37b)}$$

in which λ_o is the free space wavelength in meters.

It must be emphasized that relations of equation (II. 36) are valid only for small loss tangents (p $\leqq$ 0.6) of the medium. Such relations cannot be used for sea water at frequencies less than 150 mc, for example.

From the relations of equation (II. 36) one sees that α is

independent of frequency as long as σ and ϵ_r are constant with frequency. The remarks in Section IIA must be recalled to the effect that σ and ϵ_r as used here are the <u>real effective</u> conductivity and <u>real effective</u> relative dielectric constant, respectively, and thus may be functions of frequency (low) if imaginary parts of complex $\underset{\sim}{\sigma}$ and $\underset{\sim}{\epsilon_r}$ are important.

b. Large loss tangent (p $\gtrsim$ 10) - metallic skin depth (τ)

When p is sufficiently large(say p $\gtrsim$ 10), first approximations give

$$f(p) \cong \sqrt{p/2}$$

$$g(p) \cong \sqrt{p/2} \qquad\qquad\qquad \text{(II. 22)}$$

$$\frac{g(p)}{f(p)} \cong 1$$

Accordingly, the following relations develop.

(1) Phase constant, phase velocity and wavelength

From equation (II. 31) with equation (II. 17b)

$$\beta \cong \beta_o \sqrt{\epsilon_r} \sqrt{\frac{p}{2}} = \sqrt{\frac{\omega \mu_o \sigma}{2}} \quad \text{(rad/m)} \qquad \text{(II. 38)}$$

$$\lambda \cong 2\pi \sqrt{\frac{2}{\omega \mu_o \sigma}} \quad \text{(meter)} \qquad\qquad \text{(II. 39)}$$

$$v_p = \frac{\omega}{\beta} \cong \sqrt{\frac{2\omega}{\mu_o \sigma}} \quad \text{(meter/sec)} \qquad\qquad \text{(II. 40)}$$

(2) Attenuation constant - skin depth (τ)

The skin depth (τ) is reciprocal of attenuation constant (α) and when the loss tangent is large (p $\gtrsim$ 10), one speaks of the "metallic

skin" depth. From equation (II. 34) and equation (II. 18b)

$$\tau = \frac{1}{\alpha} \cong \sqrt{\frac{2}{\omega \mu_o \sigma}} \quad \text{nepers/meter} \tag{II. 41}$$

Upon comparing equation (II. 41) with equation (II. 38), one notes

$$\alpha \cong \beta \cong \frac{1}{\tau} \tag{II. 42}$$

$$\alpha/\beta = g(p)/f(p) \cong 1 \tag{II. 43}$$

whence the complex propagation constant $\underset{\sim}{k}$ becomes

$$\underset{\sim}{k} = \beta - j\alpha \cong \beta(1-j) \cong \frac{1-j}{\tau} \tag{II. 44}$$

For non-magnetic media ($\mu_r = 1$), the expression for τ can

be written variously as

$$\tau = \frac{503.2}{\sqrt{f\,\sigma}} \quad \text{(meter)} \tag{II. 45a}$$

$$= \frac{15.92}{\sqrt{f_{kc}\sigma}} \quad \text{(meter)} \tag{II. 45b}$$

$$= \frac{1651}{\sqrt{f\,\sigma}} \quad \text{(feet)} \tag{II. 45c}$$

$$= \frac{522.2}{\sqrt{f_{kc}\sigma}} \quad \text{(feet)} \tag{II. 45d}$$

Accordingly,

$$\alpha \cong 1.987 \times 10^{-3} \sqrt{f\,\sigma} \quad \text{nepers/meter} \tag{II. 46a}$$

$$= 6.283 \times 10^{-2} \sqrt{f_{kc}\sigma} \quad \text{nepers/meter} \tag{II. 46b}$$

$$= 0.5458 \sqrt{f_{kc}\sigma} \quad \text{db/meter} \tag{II. 46c}$$

$$= 0.1663 \sqrt{f_{kc}\sigma} \quad \text{db/foot} \tag{II. 46d}$$

$$= 16.63 \sqrt{f_{kc}\sigma} \quad \text{db/100 feet} \tag{II. 46e}$$

$$= 878.3 \quad \sqrt{f_{kc}\sigma} \qquad db/mile \text{ (statute)} \qquad (II.46f)$$

One may express the attenuation per skin depth or per wavelength in the medium as

$$\alpha' = 8.686 \ db/skin \ depth \qquad (II.47a)$$

$$= 54.58 \ db/medium \ wavelength \qquad (II.47b)$$

One further comment on attenuation: the attenuation α is the result of <u>exponential</u> damping of the electromagnetic fields in a dissipative medium. The fields vary with distance not only according to $e^{-\alpha R}$ but also according to other distance dependent functions (e.g., $1/R$).

4. Example

As an example of calculations for various propagation constants, consider an unbounded simple medium[5] with

$$\sigma = 2 \times 10^{-4} \ mhos/meter$$

$$\epsilon_r = 9$$

which are independent of frequency and somewhat typical for rock. In this case

$$p = loss \ tangent = \frac{400}{f_{kc}} \qquad (II.48a)$$

$$\lambda_o = free\text{-}space \ wavelength = \frac{300}{f_{kc}} \ , (kilometers) \qquad (II.48b)$$

$$\alpha = 6.2832 \times 10^{-2} \ g(p) \ f_{kc}, \quad (nepers/kilometer) \qquad (II.48c)$$

$$= 0.8783 \ g(p) \ f_{kc} \ , \quad (db/statute \ mile) \qquad (II.48d)$$

$$\beta = 6.2832 \times 10^{-2} \ f(p) \ f_{kc} \ , \quad (radians/kilometer) \qquad (II.48e)$$

$$\lambda = \text{medium wavelength} = \frac{100}{f_{kc} \, f(p)} \quad \text{(kilometers)} \qquad \text{(II.48f)}$$

$$= \frac{3.281 \times 10^5}{f_{kc} \, f(p)} \quad \text{(feet)} \qquad \text{(II.48g)}$$

$$\frac{\lambda}{\lambda_o} = \frac{v_p}{v_o} = \frac{0.333}{f(p)} \qquad \text{(II.48h)}$$

$$\tau = \frac{5.222 \times 10^4}{f_{kc} \, g(p)} \quad \text{(feet)} = \text{skin depth} \qquad \text{(II.48i)}$$

The pertinent calculations of the above quantities are tabulated in Table II.1 for $1 \leqq f_{kc} \leqq 1000$.

The dimensionless quantities p and λ / λ_o and the values of λ_o (km), β (rad/km) and α (neper/km) are plotted in the curves of Figure II.4. The values of α (db/mile), λ (feet) and τ (feet) are shown plotted on the curves of Figure II.5.

In Figure II.4 it is seen that loss tangent p and free-space wavelength vary inversely with first power of frequency. Small loss tangents are encountered ($p \leqq 0.6$) at frequencies exceeding 667 kc; large loss tangents are encountered for frequencies less than 66.7 kc ($p \geqq 6$); and for the more accurate limit $p \geqq 10$, the frequencies must be less than 40 kc. The attenuation constant (α) and phase constant (β) are about equal and increase with frequency proportional to $(f_{kc})^{1/2}$, up to the 40 to 67 kc region. At frequencies exceeding 667 kc, α approaches the constant value given for the small loss tangent case of 4π nepers/kilometer, and β approaches the loss-less values $\beta_o \sqrt{\varepsilon_r}$ or $2\pi \times 10^{-2} f_{kc}$ rad/km and thus increases as f_{kc} increases.

TABLE II.1

Calculations of Pertinent Propagation Constants

$$\sigma = 2 \times 10^{-4} \text{ mhos/meter}$$
$$\epsilon_r = 9$$

f_{kc}	p	$f(p)$	$g(p)$	λ_o (km)	α (n/km)	α (db/mi)	β (rad/km)	λ/λ_o	τ (ft)	λ (ft)
1	400	14.141	14.141	300	0.888	12.42	0.888	.0236	3693	23204
2	200	10.003	9.993	150	1.256	17.55	1.257	.0333	2613	16400
5	80	6.364	6.284	60	1.974	27.60	1.999	.0524	1662	10311
10	40	4.528	4.416	30	2.775	38.78	2.845	.0736	1183	7246
20	20	3.243	3.085	15	3.877	54.19	4.075	.1028	846.4	5059
50	8	2.128	1.878	6	5.900	82.47	6.685	.1566	556.1	3084
100	4	1.601	1.261	.3	7.923	110.75	10.059	.2082	414.1	2049
200	2	1.272	0.786	1.5	9.877	138.06	15.984	.2621	332.2	1289.7
500	0.8	1.068	0.3745	0.6	11.765	164.46	33.552	.3121	278.9	614.4
1000	0.4	1.019	0.1962	0.3	12.328	172.32	64.026	.3271	266.2	322.0
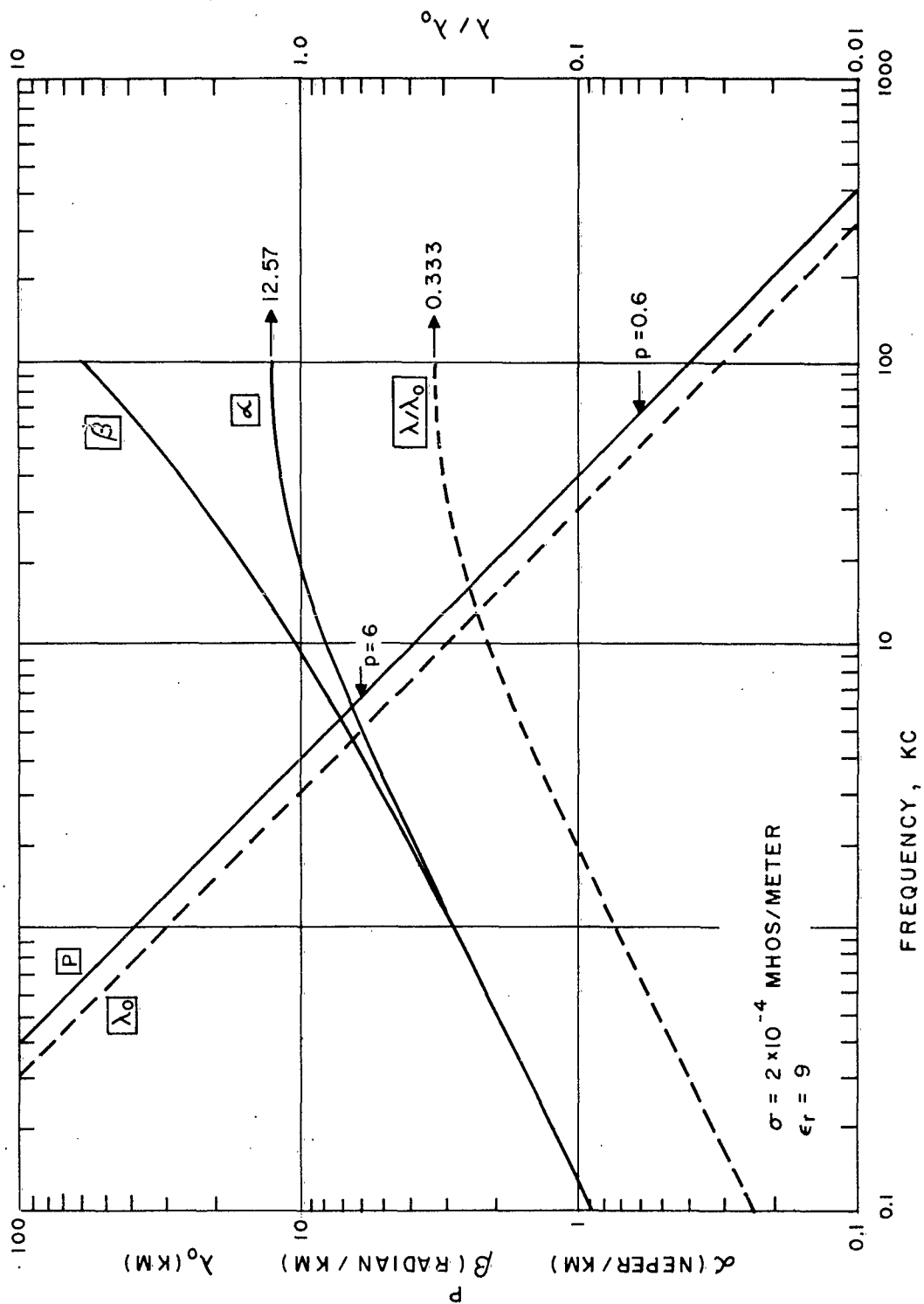
Figure II.4. Propagation constants for infinite homogeneous medium

$\sigma = 2 \times 10^{-4}$ mhos/meter
$\epsilon_r = 9$
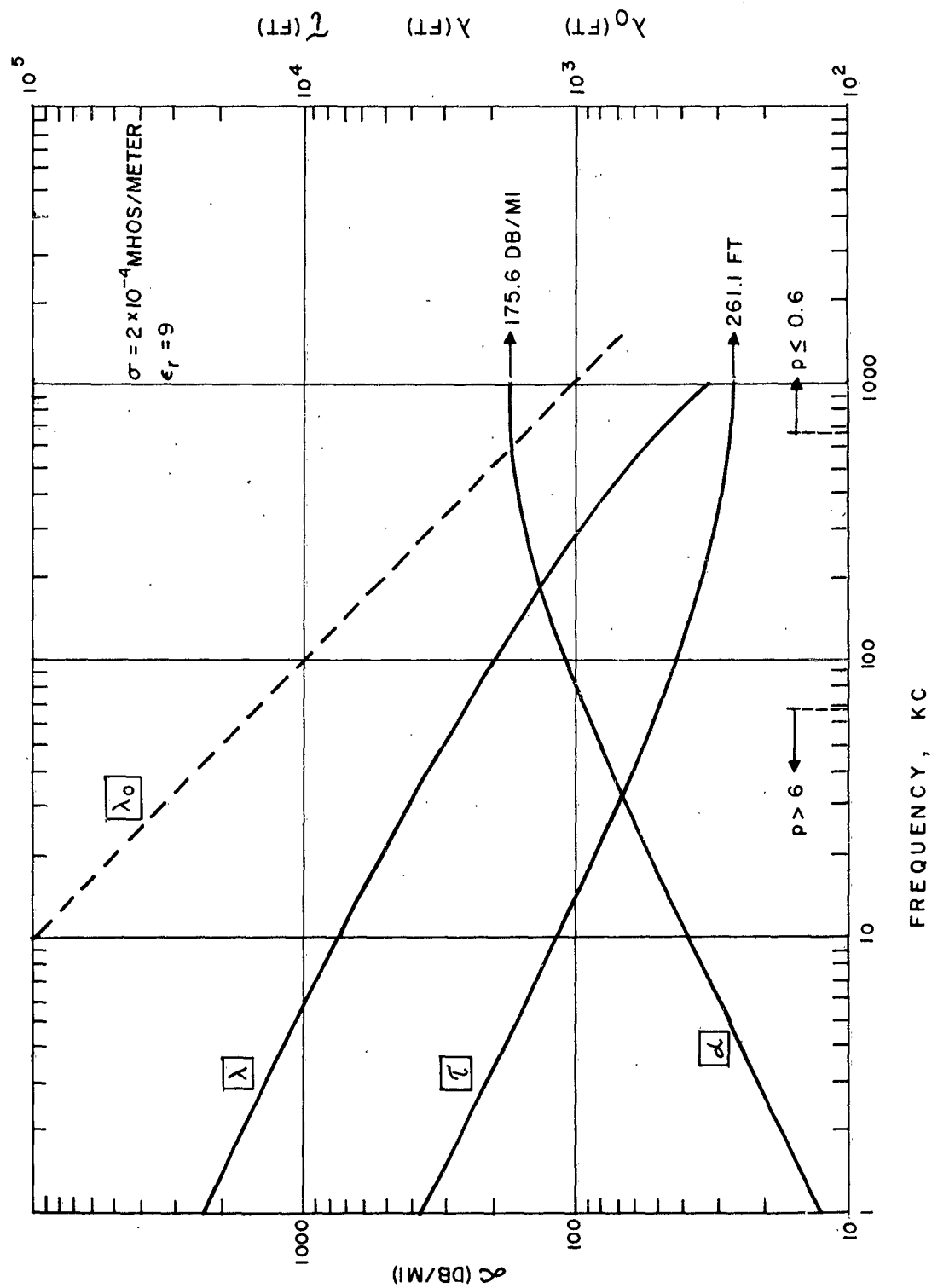
Figure II.5. Variations of α, λ_0, λ and τ with frequency

$\sigma = 2 \times 10^{-4}$ mhos/meter

$\epsilon_r = 9$.

In Figure II.5 in the large loss tangent region $(p > 6)$, α increases as $(f_{kc})^{1/2}$ and in the small loss region $(p \leq 0.6)$ approaches the constant value 175.6 db/statute mile. The skin depth varies as $(f_{kc})^{-1/2}$ in the large loss region according to equation (II.45d) and tapers off to the constant value for low loss tangents given by the reciprocal of equation (II.36a) as $\frac{1}{4\pi}$ km or 261.1 feet. The wavelength in the medium (λ) varies as $(f_{kc})^{-1/2}$, like τ in the low-frequency, large loss-tangent, region; at the higher frequency, low loss-tangent, region, λ approaches $\lambda_o/\sqrt{\epsilon_r}$ and thus varies here as $3.281 \times 10^5/f_{kc}$ (feet).

E. Characteristic Impedance $(\mathcal{Z})$ of the Medium

The characteristic impedance of the medium is given by

$$\mathcal{Z} = \frac{\omega \mu_o}{k} = \sqrt{\frac{\mu_o}{\epsilon}} \quad \text{(ohm)} \tag{II.49}$$

$$= \frac{\omega \mu_o}{\beta(1 - j \, \alpha/\beta)} = \frac{\mathcal{Z}_e}{1 - j \, \alpha/\beta} \quad \text{(ohm)} \tag{II.50}$$

in which the effective impedance $\mathcal{Z}_e$ is

$$\mathcal{Z}_e = \frac{\omega \mu_o}{\beta} \quad \text{(ohm)} \tag{II.51}$$

Using equation (II.31)

$$\mathcal{Z}_e = \frac{\omega \mu_o}{\beta_o} \frac{1}{\sqrt{\epsilon_r} \, f(p)} = \frac{\mathcal{Z}_o}{\sqrt{\epsilon_r} \, f(p)} \quad \text{(ohm)} \tag{II.52}$$

in which $\mathcal{Z}_o$ is the impedance of free space

$$\mathcal{Z}_o = \frac{\omega \mu_o}{\beta_o} \cong 120\pi \cong 377.0 \text{ ohms} \tag{II.53}$$

From the above, a useful general relation is

$$\omega \mu_o = k \frac{\xi}{2} = \beta \xi_e = \beta_o \xi_o \qquad (II.54)$$

F. Transmission Equation

1. General Expression

In Appendix F, the transmission loss L_t associated with the

power transferred between parallel linear antennas in dissipative media was

developed. The antennas were assumed to be loss-less and situated in the

far-zone of each other. For antennas of length 2h, the conditions for the

latter assumption are that

$$h << R \qquad (II.55a)$$

$$\left| k_3 R \right|^2 >> 1 \qquad (II.55b)$$

where R is the distance between the centers of the antennas and k_3 is the

complex phase constant of the medium.* The transmission loss L_t is the

ratio of the power P_T into the transmitting antenna terminals to that power

P_R available from the receiving antenna terminals, when the antennas are

loss-less. When the far-zone conditions in equations (II.55) prevail, mutual

impedance effects on antenna impedances are neglected and the impedances

at the antenna terminals are the self-impedances of the antennas. In such

---

* We use the numerical subscripts appropriate to the 3 coaxial region nota-
tion for insulated antennas. Thus subscript "1" denotes the inner conductor,
subscript "2" denotes the insulation which is absent in bare antennas, and
subscript "3" denotes the dissipative region in which the antennas are im-
mersed.

From the above, a useful general relation is

$$\omega \mu_0 = k \frac{\zeta}{2} = \beta \zeta_e = \beta_0 \zeta_0 \qquad\qquad \text{(II. 54)}$$

F. Transmission Equation

    1. General Expression

        In Appendix F, the transmission loss L_t associated with the power transferred between parallel linear antennas in dissipative media was developed. The antennas were assumed to be loss-less and situated in the far-zone of each other. For antennas of length 2h, the conditions for the latter assumption are that

$$h << R \qquad\qquad \text{(II. 55a)}$$

$$\left| k_3 R \right|^2 >> 1 \qquad\qquad \text{(II. 55b)}$$

where R is the distance between the centers of the antennas and k_3 is the complex phase constant of the medium.* The transmission loss L_t is the ratio of the power P_T into the transmitting antenna terminals to that power P_R available from the receiving antenna terminals, when the antennas are loss-less. When the far-zone conditions in equations (II. 55) prevail, mutual impedance effects on antenna impedances are neglected and the impedances at the antenna terminals are the self-impedances of the antennas. In such

---

* We use the numerical subscripts appropriate to the 3 coaxial region notation for insulated antennas. Thus subscript "1" denotes the inner conductor, subscript "2" denotes the insulation which is absent in bare antennas, and subscript "3" denotes the dissipative region in which the antennas are immersed.

case, it is shown in Appendix F that the far-zone transmission loss may be written as

$$L_t = L_S A \frac{1}{G_T G_R} \qquad \text{(II. 56)}$$

where

$$L_S = \text{"spreading loss"} = \left(\frac{4\pi R}{\lambda_3}\right)^2 = (2 \beta_3 R)^2$$

$$A = \text{"exponential damping loss"} = e^{2 \alpha_3 R}$$

$$G_T, G_R = \text{"modified power gains" for loss-less transmitting and receiving antennas, respectively.}$$

In the above, β_3 is the phase constant, α_3 the attenuation constant, and λ_3 the wavelength of the dissipative medium, discussed in Section IID.

The "modified power gain G" for a loss-less antenna is given by equation (F.24) in Appendix F for the far-zone as

$$G = \frac{\zeta_{e3}}{\pi R_o} \left| \frac{\beta_3 F_o (\theta, kh, k_3 h)}{k_3} \right|^2 \qquad \text{(F. 24)}$$

where

ζ_{e3} = effective characteristic impedance (real) of the dissipative medium

$$= \frac{\omega \mu_o}{\beta_3} \quad \text{for non-magnetic media}$$

ω = radian frequency = $2\pi f$

μ_o = permeability of free space = $4\pi \times 10^{-7}$ henry/m.

R_o = self "radiation resistance" referred to the input terminals (Appendix F. III)

case, it is shown in Appendix F that the far-zone transmission loss may be written as

$$L_t = L_S A \frac{1}{G_T G_R} \qquad \text{(II. 56)}$$

where

$$L_S = \text{"spreading loss"} = \left(\frac{4\pi R}{\lambda_3}\right)^2 = (2\beta_3 R)^2$$

$$A = \text{"exponential damping loss"} = e^{2\alpha_3 R}$$

$G_T, G_R =$ "modified power gains" for loss-less transmitting and receiving antennas, respectively.

In the above, β_3 is the phase constant, α_3 the attenuation constant, and λ_3 the wavelength of the dissipative medium, discussed in Section IID.

The "modified power gain G" for a loss-less antenna is given by equation (F.24) in Appendix F for the far-zone as

$$G = \frac{\mathcal{Z}_{e3}}{\pi R_o} \left| \frac{\beta_3 F_o(\theta, kh, k_3 h)}{k_3} \right|^2 \qquad \text{(F. 24)}$$

where

$\mathcal{Z}_{e3} =$ effective characteristic impedance (real) of the dissipative medium

$= \dfrac{\omega \mu_o}{\beta_3}$ for non-magnetic media

$\omega =$ radian frequency $= 2\pi f$

$\mu_o =$ permeability of free space $= 4\pi \times 10^{-7}$ henry/m.

$R_o =$ self "radiation resistance" referred to the input terminals (Appendix F. III)

case, it is shown in Appendix F that the far-zone transmission loss may be written as

$$L_t = L_S \, A \, \frac{1}{G_T G_R} \tag{II.56}$$

where

$$L_S = \text{"spreading loss"} = \left(\frac{4\pi R}{\lambda_3}\right)^2 = (2\beta_3 R)^2$$

$$A = \text{"exponential damping loss"} = e^{2\alpha_3 R}$$

$G_T, G_R = $ "modified power gains" for loss-less transmitting and receiving antennas, respectively.

In the above, β_3 is the phase constant, α_3 the attenuation constant, and λ_3 the wavelength of the dissipative medium, discussed in Section IID.

The "modified power gain G" for a loss-less antenna is given by equation (F.24) in Appendix F for the far-zone as

$$G = \frac{\zeta_{e3}}{\pi R_o} \left| \frac{\beta_3 F_o (\theta, kh, k_3 h)}{k_3} \right|^2 \tag{F.24}$$

where

$\zeta_{e3} = $ effective characteristic impedance (real) of the dissipative medium

$$= \frac{\omega \mu_o}{\beta_3} \quad \text{for non-magnetic media}$$

$\omega = $ radian frequency $= 2\pi f$

$\mu_o = $ permeability of free space $= 4\pi \times 10^{-7}$ henry/m.

$R_o = $ self "radiation resistance" referred to the input terminals (Appendix F.III)

In equation (F. 24) of Appendix F, the function $F_o(\theta, kh, k_3h)$ is the far-zone pattern factor (complex) given by equation (F.5) in Appendix F as

$$F_o(\theta, kh, k_3h) = \frac{k_3}{2} \sin \theta \int_{-h}^{h} \frac{I(z') e^{jk_3 z' \cos \theta}}{I(0)} dz' \qquad (F.5)$$

and is the pattern factor referred to the input current $I(0)$, with $I(z')$ being the current distribution for an antenna lying along the z-axis and z' the coordinate along the antenna. The angle θ is the "stagger angle" between the axis of an antenna and the line drawn between the centers of the antennas. The complex phase constant k is that of the current distribution; k is the same as k_3 for bare antennas but is generally smaller than k_3 for insulated antennas (Section IV, Appendices D, E, and F).

In practice, the transmission loss in equation (II. 56) is modified by two effects: one being that the antennas are not loss-less and the other being due to the use of necessarily low frequencies. The consequences of first may be accounted for by an "antenna efficiency factor" η. At very low frequencies, the antennas may be in the "near-zone" of one another. Also, because of finite hole depths into the rock strata, the electrical lengths of the antennas are small. One is then concerned with the mutual impedance effects between electrically short antennas.

The "antenna efficiency factor" η may be defined as the ratio of the resistance R_o when there are no losses to that including losses R_{in} referred to the input terminals. The loss resistances are the so-called

"non-radiating" or "dead-loss" resistances and include ohmic losses in the wires and, in the case of insulated antennas, the resistances of input and output electrodes. Hence

$$R_{in} = R_o + R_{ohmic} + R_{electrodes}$$
$$= R_o + R_{DL} \tag{II.57}$$

where R_{DL} is the dead-loss resistance. The "input radiation resistance" R_o is used in the sense that

$$\frac{|I(0)|^2 R_o}{2}$$

represents the power input to the terminals of a loss-less transmitting antenna and hence the power that "leaves" such an antenna to be dissipated in the medium surrour 'ing the antenna. Hence

$$\eta = \frac{R_o}{R_{in}} = \frac{R_{in} - R_{DL}}{R_{in}} = \frac{R_o}{R_o + R_{DL}} \tag{II.58}$$

To account for losses, Norton[63] uses the term "system loss" to describe the power transferred between antennas. We shall use the symbol L_T to describe the "total system losses." In the far-zone, L_T differs from L_t in equation (II.56) by antenna efficiency factors η_T and η_R for transmitting and receiving antennas, respectively. Thus

$$L_T = L_t \ \frac{1}{\eta_T \eta_R} = L_S A \left(\frac{1}{\eta_T G_T} \right) \left(\frac{1}{\eta_R G_R} \right) \tag{II.59}$$

where the other symbols have the meanings described before.

II-28

The mutual impedance effects may be treated by circuit theory wherein the coupled antennas are represented by a T-network. The development was published by Wait[80] and shortly thereafter by Norton[63] with more general expressions. For antennas in the far-zone, the results lead to the same expressions for L_t in equation (II. 55) and for L_T in equation (II. 59). Digressing momentarily to use the notation of Norton,[63] the accessible terminals of the transmitting antenna a are AA and those of the receiving antenna b are the terminals BB in the T-network. The central member of the T-network is the mutual impedance Z_m between the two antennas while Z_a and Z_b are the self-impedances of the two antennas. The series arm of the T from the transmitter terminals is $Z_a - Z_m$ and that from the receiver terminals is $Z_b - Z_m$. Thus, the impedance at AA with BB open-circuited is Z_a while the impedance at BB, with AA open-circuited, is Z_b. The receiver load impedance connected across BB is Z_L. The transmitter source imped-ance is Z_S. The input impedance at the transmitter terminal AA of the net-work with Z_L connected is Z_{in}; the output impedance at the receiver terminal BB looking towards the T is Z_{out}. The mesh currents are I_a and I_b and the mesh currents flow in the same direction through Z_m. The network equations with no source voltages in the mesh in which I_b is flowing may be written as

$$Z_{in} = Z_a - \frac{Z_m^2}{Z_b + Z_L} \qquad \text{(II. 60a)}$$

$$Z_{out} = Z_b - \frac{Z_m^2}{Z_a + Z_S} \qquad \text{(II. 60b)}$$

$$-I_b(Z_b + Z_L) + I_a Z_m = 0 \qquad \text{(II. 60c)}$$

The ratio of the power P_T into the input terminals AA to the power P_L delivered to the load is

$$\frac{P_T}{P_L} = \frac{|I_a|^2}{|I_b|^2} \frac{\text{Re } Z_{in}}{\text{Re } Z_L} = \left| \frac{Z_b + Z_L}{Z_m} \right|^2 \frac{\text{Re } Z_{in}}{\text{Re } Z_L} \qquad \text{(II. 61)}$$

For a constant power input P_T, this ratio will be minimized when Z_L is the complex conjugate Z_{out}^* of the output impedance. In this case $P_L = P_L \text{(max)}$ = P_R where P_R is the <u>available</u> power from the receiving terminals.

Now except in closely spaced arrays, $|Z_m|^2 << |Z_a| \, |Z_a + Z_S|$. (Z_m is defined[8,9] as the ratio of the open-circuit voltage V_R(OC) induced in the receiver antenna at its terminals to the current $I_T(0)$ at the terminals of the transmitting antenna. An example in a propagation test is described in Section VI where on a 1-mile path V_R(OC) was of the order of 200 microvolts at 1 kc for an antenna current of 1 ampere with the transmitter approximately matched to the transmitter antenna input impedance of 100 ohms. The receiver self-impedance was roughly the same value. Hence with $|Z_m|$ about 2×10^{-4} ohms, the inequality was satisfied.) Hence $Z_{out} \doteq Z_b$ and the matching condition is $Z_L = Z_{out}^* \doteq Z_b^*$. If we write $Z_m = Z_m \, e^{j\emptyset}$, then the total system loss, $Z_L = Z_b^*$, is

$$L_T = \frac{P_T}{P_R} = \frac{4(R_{in})_T \, (R_{in})_R}{Z_m^2} - 2 \cos 2\emptyset \qquad \text{(II. 62)}$$

For the practical case in deep-strata propagation, the first term on the right in equation (II.62) is larger than the second and

$$L_T = \frac{4\,(R_{in})_T\,(R_{in})_R}{|Z_m|^2} = \frac{4\,R_{oT}\,R_{oR}}{\eta_T\,\eta_R\,|Z_m|^2} \tag{II.63}$$

In the far-zone, governed by equation (II.55), the electric field in spherical coordinates has only a θ-component for a transmitting antenna lying along the z-axis. At the receiver antenna this field may be written as in Appendix F, equation (F.4); the use of the effective length $\mathscr{l}_e$ from equation (F.28) is convenient whence

$$E_{\theta_T} = j\,\frac{\omega\mu_o\,e^{-j\,k_3 R}}{4\pi R}\,I_T(0)\,\mathscr{l}_{e_T} \tag{II.64}$$

The open-circuit voltage $V_R(OC)$ induced in the receiver antenna at its terminals due to E_{θ_T} is

$$V_R(OC) = E_{\theta_T}\,\mathscr{l}_{e_R} \tag{II.65}$$

where $\mathscr{l}_{e_R}$ is the effective length of the receiver antenna. Hence

$$Z_m = |Z_m|\,e^{j\phi} = \frac{V_R(OC)}{I_T(0)} = j\,\frac{\omega\mu_o\,e^{-\alpha_3 R}\,\mathscr{l}_{e_T}\,\mathscr{l}_{e_R}}{4\pi R}\,e^{-j\,\beta_3 R} \tag{II.66a}$$

$$|Z_m| = \frac{\omega\mu_o\,e^{-\alpha_3 R}\,|\mathscr{l}_{e_R}|\,|\mathscr{l}_{e_T}|}{4\pi R} \tag{II.66b}$$

$$\phi = \pi/2 - \beta_3 R - \phi_{e_R} - \phi_{e_T} \tag{II.66c}$$

where we have written the complex effective length $\ell_e = |\ell_e| e^{-j\phi_e}$ with subscript T and R to denote transmitter and receiver antennas, respectively.

With equation (II.66b) in equation (II.63)

$$L_T = \frac{4 R_{o_T} R_{o_R}}{\eta_T \eta_R} \left\{ \frac{\omega \mu_o e^{-\alpha_3 R} |\ell_{e_R}||\ell_{e_T}|}{4\pi R} \right\} \qquad (II.67)$$

Recalling, from equation (F.28) in Appendix F, the expression for ℓ_e is deduced from the reciprocal theorem for the far-zone and is given by

$$\ell_e = \frac{2}{k_3} F_o(\theta, kh, k_3 h) \qquad (II.68)$$

the modified power gain in equation (F.24), Appendix F, becomes

$$G = \frac{\mathcal{J}_{e3} |\beta_3 \ell_e|^2}{4\pi R_o} \qquad (II.69)$$

Substituting equation (II.69) for the appropriate antenna into equation (II.67), the total system loss L_T reduces to that form given in equation (II.59) for the far-zone.

In the far-zone, the calculation of the pattern factor F_o^b and modified power gain G^b for bare dipoles is reasonably straightforward, as indicated in Appendices D and F. For insulated dipoles, the far-field expressions reduce to simpler forms if the assumption is made, which is valid in practice, that the insulation radius a_2 is small compared with the wavelength λ_3 in the dissipative medium (Appendix E). The far-zone pattern factors F_o^{OC} and F_o^{SC} and modified power gains G^{OC} and G^{SC} then are developed readily in Appendix F for insulated dipoles which are terminated in an open

circuit (OC) and short circuit (SC), respectively.

In the near-zone region of the antennas, the behavior of the electromagnetic fields for bare dipoles differs formally from that for insulated dipoles. We shall illustrate the effect of the mutual impedance on L_T by reference to bare antennas. Also, since in practice the frequencies will be low, the antennas are electrically short ($\beta_3 h \lesssim 0.3$, $\alpha_3 \lesssim \beta_3$). The current distribution in such a case has the triangular form

$$I(z) = I(0) \left(1 - \frac{|z|}{h}\right) \tag{II.70}$$

for both transmitting and receiving antennas. The additional assumption is that

$$\frac{h^2}{R^2} \ll 1 \tag{II.71}$$

which is less of a restriction than the far-zone conditions (II.55) and is called the "quasi-far zone" condition by King.[5] The electric field of the transmitting dipole then has components in spherical coordinates[51] given by

$$E_{\theta_T} = j \frac{\omega \mu_o I_T(0)}{4 \pi} h_T \frac{e^{-j k_3 R}}{R} \left(1 - j \frac{1}{k_3 R} - \frac{1}{k_3^2 R^2}\right) \sin \theta \tag{II.72a}$$

$$E_{R_T} = \frac{\omega \mu_o I_T(0)}{2 \pi k_3 R} h_T \frac{e^{-j k_3 R}}{R} \left(1 - j \frac{1}{k_3 R}\right) \cos \theta \tag{II.72b}$$

Note that E_{θ_T} has essentially far-zone form except for the quantity in parentheses. This follows from the far-zone pattern factor F_o^b for electrically short bare dipoles which is the value given by equation (F.5) when $\left| k_3 h \right|$ is small and is then given by equation (F.13a) in Appendix F as

$$F_o^b = \frac{k_3 h}{2} \sin \theta \qquad\qquad (F.13a)$$

One then may write equation (II.72a) as

$$E_{\theta_T} \text{(near-zone)} = E_{\theta_T} \text{(far-zone)} \left(1 - j \frac{1}{k_3 R} - \frac{1}{k_3^2 R^2}\right) \qquad (II.73)$$

where E_{θ_T} (far-zone) is given by equation (II.64) with $\ell_{e_T} = \frac{2}{k_3} F_o^b = h_T \sin \theta$. Inspection of equations (F.13a) and (II.72a) shows that as θ is varied, maximum values of F_o^b and E_{θ_T} occur when $\theta = 90^\circ$, at which the losses L_T and L_t should have minimum values.

To evaluate L_T and L_t, consider that the electrically short, bare dipoles are perpendicular to the line joining their centers. The open-circuit voltage induced in the receiver antenna at its terminals is[8,9]

$$V_R(OC) = - \int_{-h_R}^{h_R} \frac{E_{z_T} I_R(z) \, dz}{I_R(0)} \qquad\qquad (II.74)$$

where E_{z_T} is the component of the field due to the transmitting dipole along the axis (z-axis) of the receiving dipole of length $2h_R$ and $I_R(z)$ is the current distribution along the receiving antenna as though it were transmitting with input current $I_R(0)$. Now for θ near 90°,

$$E_{z_T} = - E_{\theta_T} \sin \theta + E_{R_T} \cos \theta = - E_{\theta_T} \sin \theta \left(1 - \frac{E_{R_T} \cos \theta}{E_{\theta_T} \sin \theta}\right)$$
$$(II.75)$$

As long as h_R satisfies equation (II.71), the second term in the parentheses is small compared with unity, and $E_{z_T} \doteq - E_{\theta_T} \sin \theta \doteq - E_{\theta_T}$. Hence

$$V_R(OC) = E_{\theta_T} (\theta = 90^\circ) \, \ell_{e_R} \text{ where } \ell_{e_R} = \int_{-h_R}^{h_R} \frac{I_R(z) \, dz}{I_R(0)} = h_R. \text{ For}$$

$\theta = 90^\circ$, ℓ_{e_T} has its maximum value $\ell_{e_T} = h_T$ and the pattern factors have maximum values $(F_o^b)_{max} = k_3 h/2$. As in equation (II.66), the mutual impedance Z_m is

$$Z_m = Z_m \text{ (near-zone)} = \frac{j \, \omega \mu_o e^{-\alpha_3 R}}{4 \pi R} (\ell_{e_T})_M (\ell_{e_R})_M (A - j B) e^{-j \beta_3 R}$$

(II.76a)

$$|Z_m| \text{ (near-zone)} = |Z_m| \text{ (far-zone)} \sqrt{A^2 + B^2}$$

(II.76b)

$$\emptyset = \pi/2 - \beta_3 R - \tan^{-1} B/A$$

(II.76c)

in which

$$A - j B = \left(1 - j \, \frac{1}{k_3 R} - \frac{1}{k_3^2 R^2} \right)$$

(II.77)

$$|Z_m| \text{ (far-zone)} = \frac{\omega \mu_o e^{-\alpha_3 R} (\ell_{e_T})_M (\ell_{e_R})_M}{4 \pi R}$$

(II.78a)

$$= \frac{\omega \mu_o e^{-\alpha_3 R} h_T h_R}{4 \pi R}$$

(II.78b)

Subject to the conditions for deducing L_T in equations (II.62) and (II.63), plus the conditions on dipole length in equation (II.71), the total system loss for electrically short bare dipoles may be written for $\theta = 90^\circ$ in a form like equation (II.67)

$$L_T = \frac{4 R_{o_T} R_{o_R}}{\eta_T \eta_R} \left\{ \frac{\omega \mu_o e^{-\alpha_3 R} (\ell_{e_T})_M (\ell_{e_R})_M}{4 \pi R} \sqrt{A^2 + B^2} \right\}^{-2}$$

(II.79)

or in the form like equation (II. 56)

$$L_T = \frac{L_S\,A}{G^N} \left[\frac{1}{\eta_R\,G_R^b} \right]_M \left[\frac{1}{\eta_T\,G_T^b} \right]_M \qquad\qquad \text{(II. 80)}$$

where the subscript "M" indicates a maximum value at $\theta = 90^\circ$. In the last

equation we have introduced the symbol G^N to indicate the "near-zone enhance-

ment gain." For bare dipoles, subject to equation (II. 71), which are electri-

cally short, $G^N = A^2 + B^2$ where $A - jB$ is given by equation (II. 77). G^N may

be considered as the enhancement of the electric field (magnitude squared)

over and above that field which would be calculated by using far-zone formula-

tions, for parallel dipoles.* For bare dipoles which are electrically longer

and perpendicular to a line joining their centers, the mutual impedance could

be calculated as for antennas in air.[3] The exponential sine and cosine inte-

grals of complex argument are involved in the formulation for Z_m.

For insulated dipoles, an equation for L_T could be written which

is formally like equation (II. 80) with appropriate modified power gains G for

the antennas, but the evaluation of G^N would differ from $A^2 + B^2$ where A and

B are given in equation (II. 77). This is because the cylindrical components

E_z and E_ρ vary with the radial distance ρ according to a zero-order Hankel

function of the second kind of complex argument $k_3\rho$, as shown in Appendix E.

For purposes of calculation, we shall assume that the dipoles

are identical and perpendicular to the line joining their centers spaced a

---

* For bare dipoles which are arranged coaxially so that $\theta = 0^\circ$, equation (II. 72b)
would be used. Such arrangement was used in the depth attenuation method
described in Section VF. Calculation of L_T for coaxial dipoles in air is given
by Norton.[63]

distance R, that the dipoles are electrically short and that the dipoles are immersed in an unbounded, homogeneous, isotropic dissipative medium. Further, we assume that input impedances of the antennas are their self-impedances, i.e., their mutual impedance has negligible effect on their input impedances. Then the total system loss L_T in equation (II.80) may be written

$$L_T = \frac{L_S\,A}{G^N}\left(\frac{1}{\gamma\,G_M}\right)^2 \quad (\theta = 90^\circ,\ \beta h \lesssim .3,\ h^2 << R^2) \quad \text{(II.81)}$$

where G_M is the maximum modified power gain for the loss-less dipole occurring at $\theta = 90^\circ$.

It is convenient to consider L_T in equation (II.81) as the product of two terms: the first containing terms which depend upon the distance R and called the "propagation loss L_P" and the second consisting of terms which do not depend upon R and called the "antenna coupling loss L_A." Accordingly

$$L_T = L_P\,L_A \quad \text{(II.82)}$$

where

$$L_P = L_S\,A\,\frac{1}{G^N} \quad \text{(II.83a)}$$

$$L_A = \left(\frac{1}{\gamma\,G_M}\right)^2 \quad \text{(II.83b)}$$

It is common to use decibel notation so that in decibels

$$L_T(db) = 10\log L_T = L_P(db) + L_A(db) \quad \text{(II.84)}$$

where

$$L_P(db) = 10\log L_P = L_S(db) + A(db) - G^N(db) \quad \text{(II.85a)}$$

$$L_A(db) = 10 \log L_A = -20 \log (\eta \, G_M) = -2 \left[\eta G_M, db \right] \qquad \text{(II. 85b)}$$

and

$$L_S(db) = 20 \log \left(\frac{4\pi R}{\lambda_3} \right) = 21.98 + 20 \log \frac{R}{\lambda_3} \qquad \text{(II. 86a)}$$

$$= 6.02 + 20 \log \left(\beta_3 R \right)$$

$$A(db) = 10 \log e^{2 \, \alpha_3 R} = 8.69 \, \alpha_3 R \qquad \text{(II. 86b)}$$

$$G^N(db) = 10 \log G^N \qquad \text{(II. 86c)}$$

The types of antennas being discussed are sketched in Figure
II. 6. The electrically short dipoles have current distributions which are
triangular for the bare dipole, in A of Figure II. 6, and the insulated dipole
which is terminated in an open-circuit, in B of Figure II. 6. For the insulated
dipole which is terminated in a short-circuit, in C of Figure II. 6, the current
amplitude is practically constant along the dipole.

The antenna coupling loss L_A will be evaluated first. After a
discussion and calculation of the propagation loss L_p, the total system loss
L_T will be evaluated and discussed. The calculations will be limited prin-
cipally to the case where the loss tangent $p_3 \gtrless 10$, i. e., for given values of
σ_3 and ϵ_{r_3} of the medium, the frequency f_{kc} in kc is limited to

$$f_{kc} \lessgtr 18 \times 10^5 \quad \sigma_3 / \epsilon_{r_3}$$

$$\lessgtr 2 \times 10^5 \quad \sigma_3 (\epsilon_{r_3} = 9)$$

2. Antenna Coupling Losses L_A - Electrically Short Antennas

We shall use superscripts on quantities to denote values of those
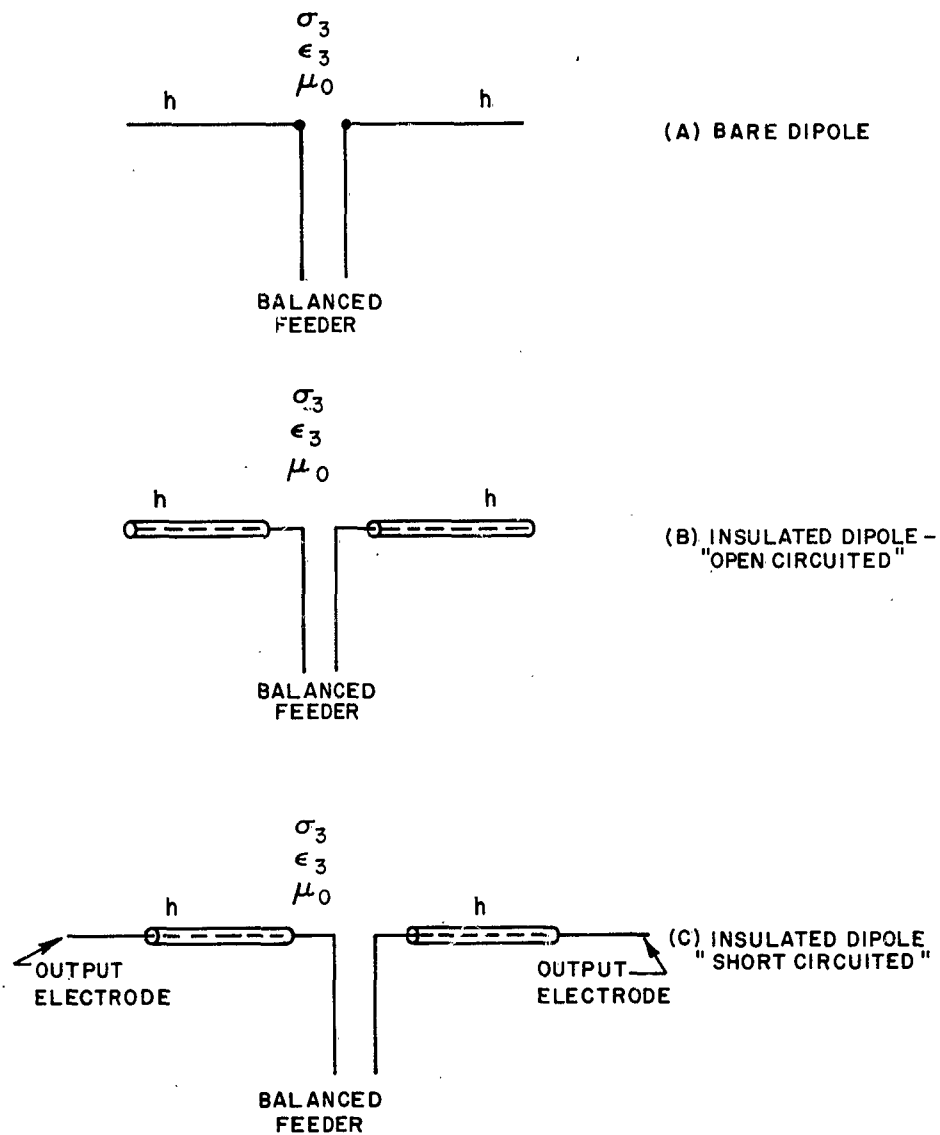
Figure II. 6.   Bare and insulated dipoles in infinite simple medium
   A.   Bare dipole
   B.   Insulated dipole, open-circuited
   C.   Insulated dipole, short-circuited

quantities for three types of antennas; "b" designates the bare dipole, and "OC" or "SC" apply to insulated dipoles terminated in an open-circuit or short-circuit, respectively.

a. Modified Power Gain

The various maximum modified power gains G_M become (Appendix F)

$$G_M^b = \frac{\zeta_{e_3}}{4\pi R_o^b} \beta_3^2 h^2 \qquad (II.87a)$$

$$G_M^{OC} = \frac{\zeta_{e_3}}{4\pi R_o^{OC}} \beta_3^2 h^2 \qquad (II.87b)$$

$$G_M^{SC} = \frac{\zeta_{e_3}}{4\pi R_o^{SC}} \beta_3^2 h^2 \qquad (II.87c)$$

where $\zeta_{e_3} = \dfrac{\omega \mu_o}{\beta_3}$ is the effective characteristic impedance (a real quantity) of the medium. The resistances R_o are the input resistances of the antenna with no ohmic losses. From Appendices D and E, for a medium with large loss tangent,

$$R_o^b = \frac{\zeta_{e_3} \psi}{4\pi \beta_3 h} \qquad (II.88a)$$

$$R_o^{OC} = 2 \times \frac{\omega \mu_o h}{24} = \frac{\omega \mu_o h}{12} \qquad (II.88b)$$

$$R_o^{SC} = 2 \times \frac{\omega \mu_o h}{8} = \frac{\omega \mu_o h}{4} \qquad (II.88c)$$

in which ψ is King's expansion parameter[51] given by $\psi = \Omega - 3.386$ and

Λ is the thickness parameter $\Lambda = 2 \ln \dfrac{2h}{a}$. With equation (II. 88) in equation (II. 87)

$$G_M^b = \frac{(\beta_3 h)^3}{\psi} \tag{II. 89a}$$

$$G_M^{OC} = \frac{3}{\pi} (\beta_3 h) \tag{II. 89b}$$

$$G_M^{SC} = \frac{4}{\pi} (\beta_3 h) \tag{II. 89c}$$

Let us compare the gains G_M for the same length h such that $\beta_3 h \lesssim .3$. The short-circuited insulated antenna has small theoretical advantage over the open-circuited form according to the ratio $4/3 = 1.2$ db. The open-circuited coaxial antenna is superior to the bare antenna according to

$$\frac{G_M^{OC}}{G_M^b} = \frac{3 \, \psi}{\pi \, (\beta_3 h)^2} \geq \frac{100 \, \psi}{3 \, \pi} \geq 10.6 \tag{II. 90}$$

For modestly thin antennas, with $\Lambda \doteq 13$ for example, this means G_M^{OC} exceeds G_M^b by more than 20 db.

Moreover, while the formulas for the bare antenna assume $\beta_3 h \lesssim .3$, those for the electrically short coaxial antennas assume that $\beta h \lesssim .3$ where β is the phase constant of the current and is typically smaller than β_3. This means a larger length of coaxial antenna can be tolerated and still be subject to the condition $\beta h \lesssim .3$ Consequently, the insulated antenna for the same small electrical length of antenna can have an advantage over the

bare antenna even larger than the 20 db just cited as an example.

Calculations were made to illustrate the comparisons of G_M given by equations (II. 89). The dissipative medium is assumed to have $\sigma_3 = 2 \times 10^{-4}$ mhos/m and values of G_M were calculated for frequencies $f \leq 10$ kc, for which $p_3 > 10$. The half-length of the antennas is h and is assumed to be 100 m, and thus the conditions $\beta_3 h \leq .3$ and $\beta h \leq .3$ are fulfilled. The antenna conductor radius a_1 is assumed to be 10^{-3} m, approximately that for #12 wire. Accordingly, $\Omega = 24.411$. For the insulated antenna, the RG-8/U type was assumed with ϵ_{r_2} (polyethylene) = 2.25, and $a_2/a_1 = 3.49$. The results of the calculations are shown in the curves of G_M(db) vs frequency (log scale) from 0.1 to 10 kc in Figure II.7. The gains for the dipoles in the medium are all less than unity, and the relative advantages of each type discussed above can be seen graphically.

b. Antenna Efficiency

The antenna efficiency η was given in equation (II. 58) with the input self-resistance given in equation (II. 57) as the sum of R_o, R_{ohmic} and $R_{electrodes}$. In most cases, the values of $R_{electrode}$ exceed those of the radiation and ohmic loss terms. The evaluation of these terms depends upon the current distributions in the appropriate part of the antenna circuit. We have found linear conducting cylinders as practical forms of terminating electrodes for insulated monopole antennas (see Sections III and IV). In computing the gains of insulated antennas, we neglect radiation from such electrodes. A crude idea of relative radiation may be seen in comparing

II-42
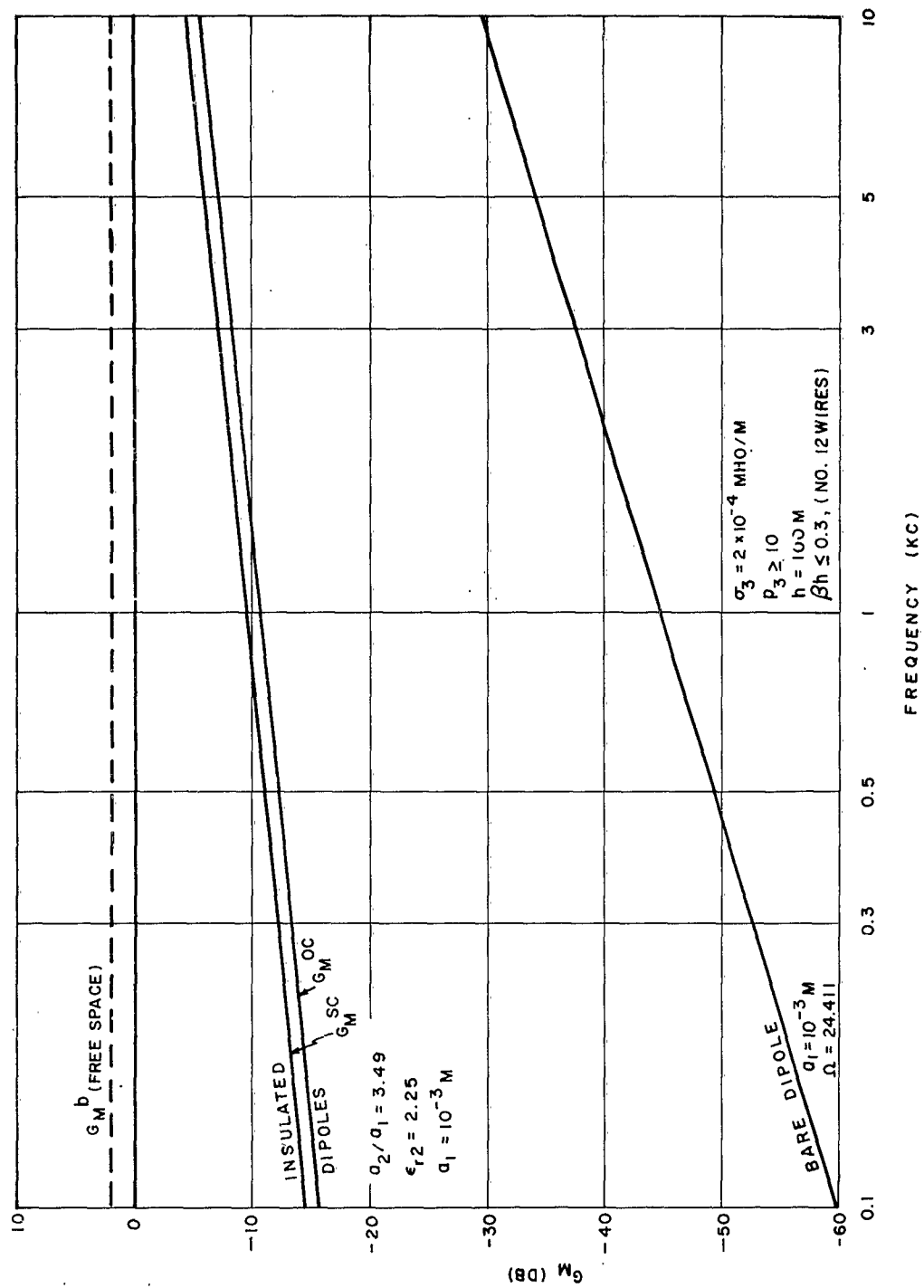
Figure II.7. Maximum power gain (modified G_M for loss-less, center fed dipoles, electrical short (h = 100 m, $\beta h \leq 0.3$, and #12 wires) $\sigma_3 = 2 \times 10^{-4}$ mhos/m, $p_3 \geq 10$.

$G_M^{\ b}$ with $G_M^{\ SC}$ in Figure II.7, for example, for the conditions assumed there.

As an illustration, consider the antennas used for Figure II.7, i.e., $h = 100$ m, $a_1 = 10^{-3}$ m (#12 wire). For the ohmic loss in the wire, we assume the internal resistance per unit length r^i to be its d.c. value r_o, which for #12 copper wire is

$$r^i \cong r_o = \frac{1}{\pi a_1^2 \sigma_1} = 5.49 \times 10^{-3} \text{ ohm/m} \qquad (II.91)$$

which is valid for frequency less than 3 kc and approximately so for frequencies less than 10 kc.

The ohmic loss R_{ohmic} depends on current distributions. For the electrically short antennas one obtains

$$(R_{ohmic})^b = \frac{2}{3} h r^i \qquad (II.92a)$$

$$(R_{ohmic})^{OC} = \frac{2}{3} h r^i \qquad (II.92b)$$

$$(R_{ohmic})^{SC} = 2 h r^i \qquad (II.92c)$$

With R_o given by equation (II.88) and R_{ohmic} given by equation (II.92) the efficiencies given by equation (II.58) were calculated over the range $0.1 \lessapprox f_{kc} \lessapprox 10$. For the short-circuited case the terminating electrodes were assumed to have zero resistance and to be non-radiating. Other values of terminating electrode resistance R_T for the dipole were assumed at $R_T = 10, 20,$ and 167.3 ohms. (The last value of R_T assumed would be that for electrode terminations each made of 100 m of #12 wire.) The calculated values of η are shown plotted in the curves of Figure II.8, with η given in db ($= 10 \log_{10} \eta$).
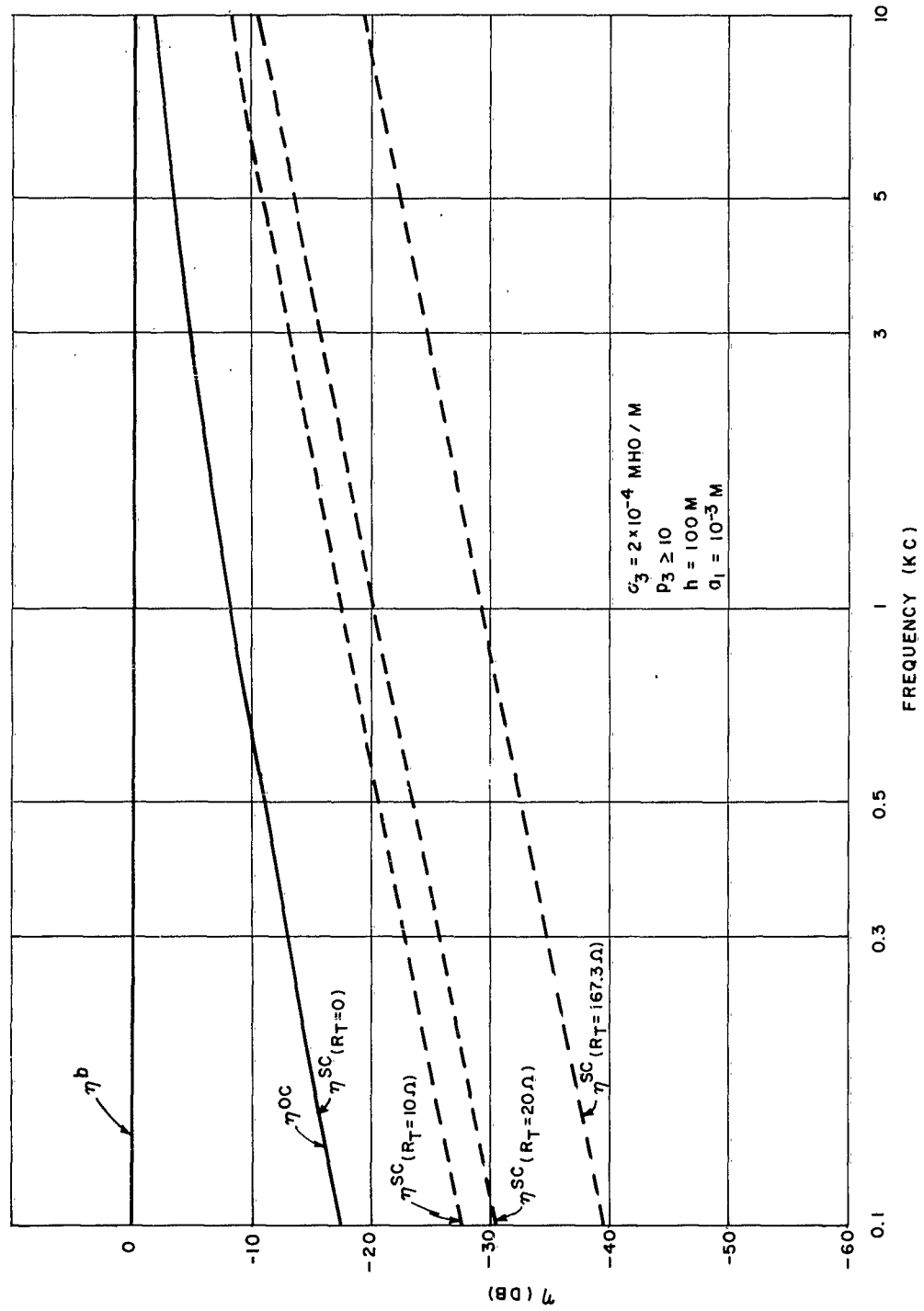
Figure II. 8.   Efficiency η of various electrically short dipoles, $\sigma_3 =$
2×10^{-4} mhos/m, $p_3 > 10$, h = 100 m, $a_1 = 10^{-3}$ m.

The efficiency-gain product $(\eta\, G_M)$ was next obtained from the curves of Figure II. 7 and Figure II. 8, and resulting values of $\eta\, G_M$ in db were plotted on the curves of Figure II. 9. It is seen that for the conditions assumed, values of (ηG_M) for the insulated antennas exceed those for the bare wire dipole. The slight advantage for the short-circuited insulated dipole for $R_T = 0$ over that for the open-circuited insulated dipole disappears when R_T has a small finite value (e. g., $R_T = 10$ ohms). $(\eta\, G_M)^{SC}$ becomes much less than $(\eta G_M)^{OC}$ as R_T increases.

The advantage of open-circuited insulated dipoles, indicated by $(\eta\, G_M)^{OC}$ over that for short-circuited dipoles, indicated by $(\eta\, G_M)^{SC}$ when $R_T > 0$, again disappears when there are mismatch losses between the dipole and feeder. These losses occur because the input impedance of the open-circuited dipole is a very large capacitative impedance when electrically short, whereas the short-circuited dipole presents a better match to the feeder. In the open-circuited case, insertion of a low-loss inductor matched to the antenna capacitative reactance at the operating frequency should preserve the advantage of the insulated dipole with open-circuit termination.

3. Propagation Losses L_P

a. Near-Zone Enhancement Gain G^N

The value of G^N to be used in equation (II. 81) for the total system loss L_T depends upon the type of antenna. For illustration, we compute G^N for an electrically short, bare, dipole using equation (II. 77), subject
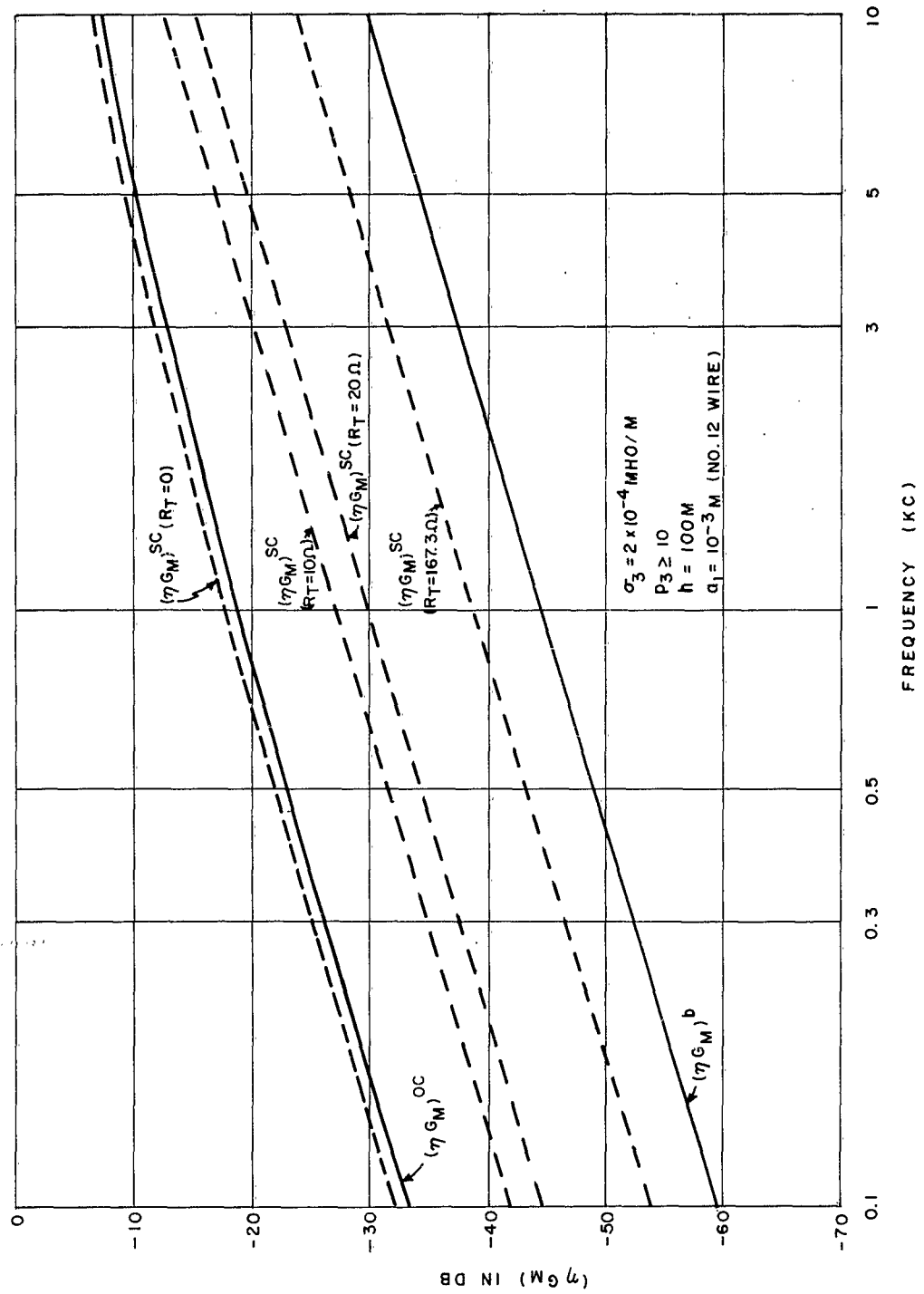
Figure II.9. Efficiency-Gain Product (ηG_M) for electrically short dipoles, $\sigma_3 = 2 \times 10^{-4}$ mhos/m, $p_3 \geq 10$, $h = 100$ m, $a_1 = 10^{-3}$ m(#12 wire).

to the condition $h^2 << R^2$ and $\beta_3 h \lesssim .3$. Let us write $k_3 R = \beta_3 R (1 - j \frac{\alpha_3}{\beta_3})$

$= v(1 - j u)$. Then with equation (II.77)

$$G^N = \left| A - j B \right|^2 = \left| 1 - j \frac{1}{k_3 R} - \frac{1}{k_3^2 R^2} \right|^2 = A^2 + B^2$$

$$A = 1 + \frac{u}{v(1 + u^2)} - \frac{1 - u^2}{v^2(1 + u^2)^2}$$

$$B = \frac{1}{v(1 + u^2)} \left[1 + \frac{2u}{v(1 + u^2)} \right]$$

$$u = \alpha_3 / \beta_3, \qquad v = \beta_3 R$$

$$\left. \right\} \quad \text{(II.93)}$$

When the loss tangent of the medium is large ($p_3 \geq 10$), then $\alpha_3 \doteq \beta_3$ and

$u \doteq 1$. With $u = 1$, then

$$A = 1 + \frac{1}{2v} \quad ; \quad B = \frac{1}{2v}(1 + \frac{1}{v}) \qquad \text{(II.94)}$$

Calculations of G^N were made first for $f = 1$ kc and $\epsilon_{r_3} = 9$,

and for $\sigma_3 = 10^{-5}$, 10^{-4} and 10^{-3} mhos/m. At such a frequency $p_3 \geq 20$ for

$\sigma_3 \geq 10^{-5}$ mhos/m, and the relations in equation (II.94) apply. A plot of

G^N(db) vs $\beta_3 R$ (= v) results in the single curve shown in Figure II.10. Cor-

responding plots of G^N vs R are shown in the three curves of Figure II.11 for

the three assumed values of σ_3.

The condition $h^2/R^2 << 1$ for which the field expressions were

developed may be written

$$h \leq R/4, \quad R \geq 4h, \quad \beta_3 R \geq 4 \beta_3 h \qquad \text{(II.95a)}$$
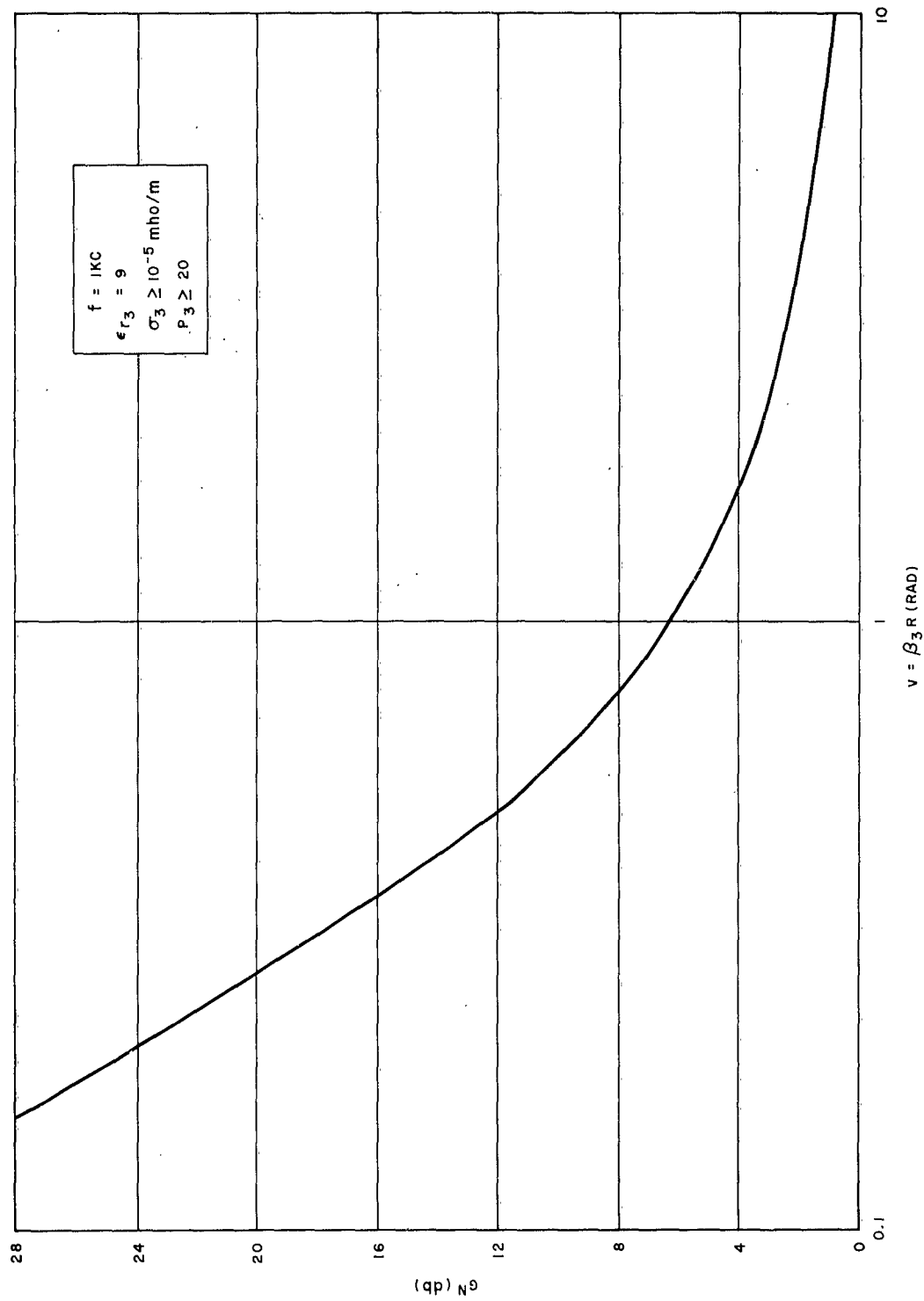
Figure II. 10. Near-zone enhancement gain (G^N) vs $\beta_3 R$. Center fed dipole $(\beta_3 h \leq .3)$, $f = 1\,kc$, $\epsilon_{r_3} = 9$.
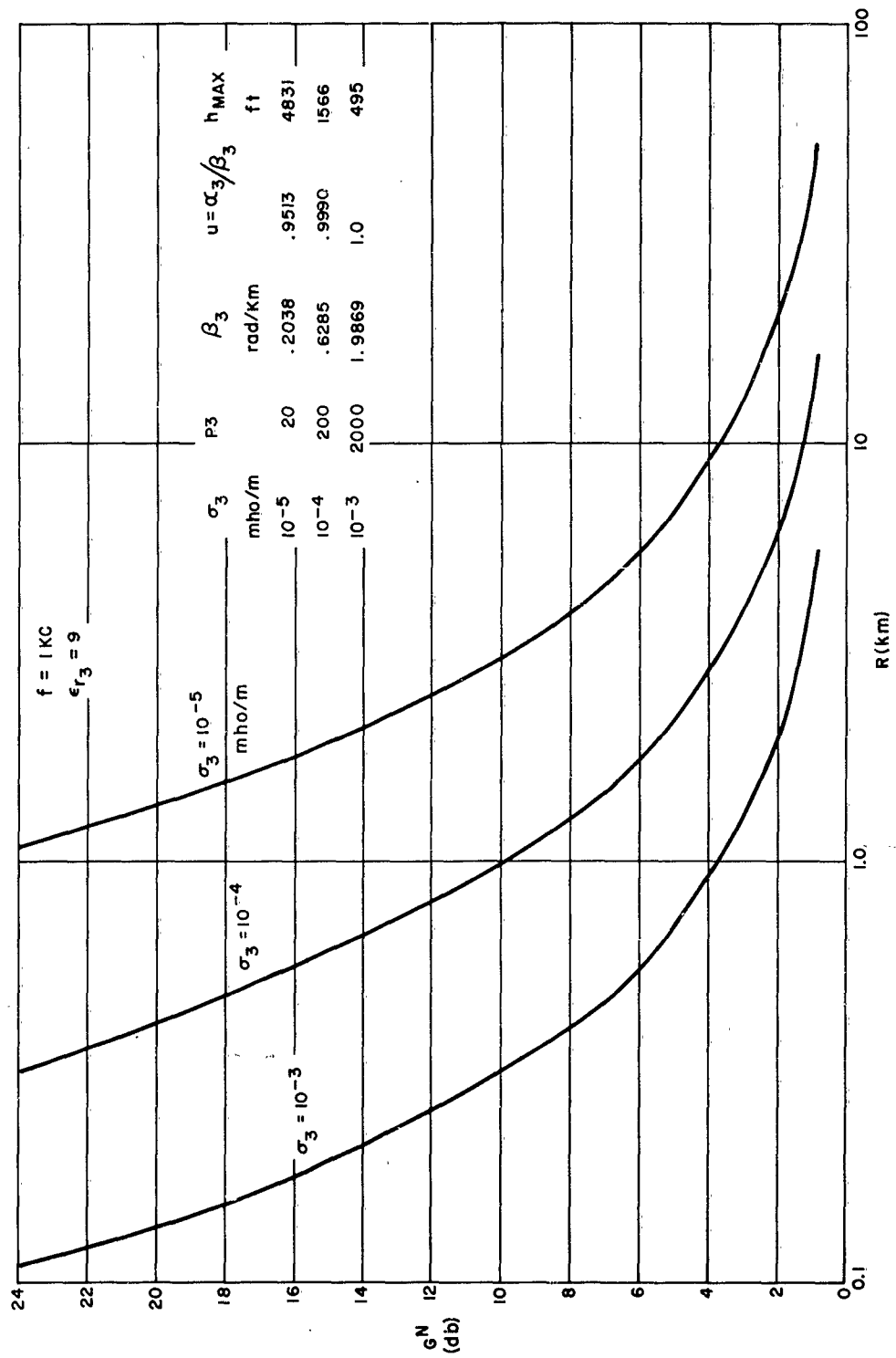
Figure II.11. Near-zone enhancement gain (G^N) vs R. Center fed dipole $(\beta_3 h \leq .3)$, $f = 1$ kc, $\epsilon_{r_3} = 9$.

The condition for the antenna to be considered electrically short is

$$\beta_3 h \le 0.3 , \quad h \le \frac{0.3}{\beta_3} \qquad\qquad (II.95b)$$

The far-zone condition may be written

$$\left| k_3 R \right|^2 >> 1 , \quad \left| k_3 R \right| \ge 4 , \quad \beta_3 R = \frac{4}{\sqrt{1 + u^2}} \qquad (II.95c)$$

Conditions (II.95a) and (II.95b) govern the ranges of $\beta_3 R$ or R which may be used to determine G^N. For Figure II.10 where $u = \alpha_3/\beta_3 \doteq 1$, if $\beta_3 R \ge 3.0$, far-zone conditions prevail and G^N is only 2 db or less. For smaller values of $\beta_3 R$, near-zone conditions prevail, but subject to condition (II.95a). If $\beta_3 h = 0.3$, the curve in Figure II.10 may be used for G^N if $\beta_3 R \ge 1.2$, according to condition (II.95a). Values of G^N at still smaller values of $\beta_3 R$ can be used only if $\beta_3 h$ is smaller than 0.3. In Figure II.11, the insert contains tabular values of loss tangent p_3, phase constant β_3, the ratio $\alpha_3/\beta_3 = u$ and maximum values of h for the three values of σ_3 assumed. (The tables in Appendix A were used for calculations.) The maximum value of h is that for which the antenna may be considered electrically short, condition (II.95b). Thus, for $\sigma_3 = 10^{-5}$ mhos/m, $p_3 = 20$, $u = \alpha_3/\beta_3 = .9513 \doteq 1.0$, $\beta_3 = 0.2038$ rad/km. For the antenna to be electrically short, the maximum value of h is $0.3/\beta_3 = 1472$ m $= 4831$ ft. Distances R less than 20 km are in the near-zone. If h = 4831 ft, values of G^N on the curve may be used if $R \ge 5.9$ km. However, if h = 1200 ft, values of G^N on the curve may be used where $R \ge 1.5$ km and $G^N \le 18$ db.

Similar calculations were made but for a frequency of 10 kc.

The results are shown in the curves of G^N vs $\beta_3 R$ in Figure II. 12 and G^N vs

R in Figure II. 13. In one case of conductivity, $\sigma_3 = 10^{-5}$ mhos/m, the loss

tangent is smaller than 10 ($p_3 = 2$) so that α_3 is less than β_3 ($u = \alpha_3 / \beta_3$

$= .6179$). The curve of G^N vs $\beta_3 R$ for $\sigma_3 = 10^{-5}$ mhos/m in Figure II. 12

differs from those for $\sigma_3 = 10^{-4}$ and 10^{-3} mhos/m where $u = \alpha_3 / \beta_3 \doteq 1$.

There is one other restriction on the inclusion of G^N in the

expression for total system loss L_T. In the simpler expression for L_T,

equation (II. 63), it is assumed that $\left| Z_m \right|^2 << 4 R_{o_T} R_{o_R} / \eta_T \eta_R$, which for

identical antennas means $\left| Z_m \right|^2 << 4 R_o^2 / \eta^2$. Now the effect of G^N is included

in $\left| Z_m \right|^2$, and let us call the resulting total loss L_T (near-zone), meaning

that we have included G^N in the calculation of L_T. One form of L_T (near-

zone) is given in equation (II. 79). For identical antennas perpendicular to a

line joining their centers, another form is given in equation (II. 81) in terms

of maximum antenna gains. Let us interpret the limitation on $\left| Z_m \right|^2$ as

$$\left| Z_m \right|^2 \leq 10^{-2} \left[4 R_o^2 / \eta^2 \right] \tag{II. 96}$$

This means that L_T (near-zone) itself in equation (II. 82) must exceed 20 db or

$$G^N \leq 10^{-2} \left(\frac{L_S A}{\eta^2 G_M^2} \right) \tag{II. 97}$$

The quantity in parentheses is the value of L_T assuming that far-zone con-

ditions prevailed, for which we may use the symbol L_T (far-zone). Suppose

for a given path that a calculation of L_T (far-zone) had been made and yielded

a value of 30 db. If re-examination indicates that near-zone conditions did
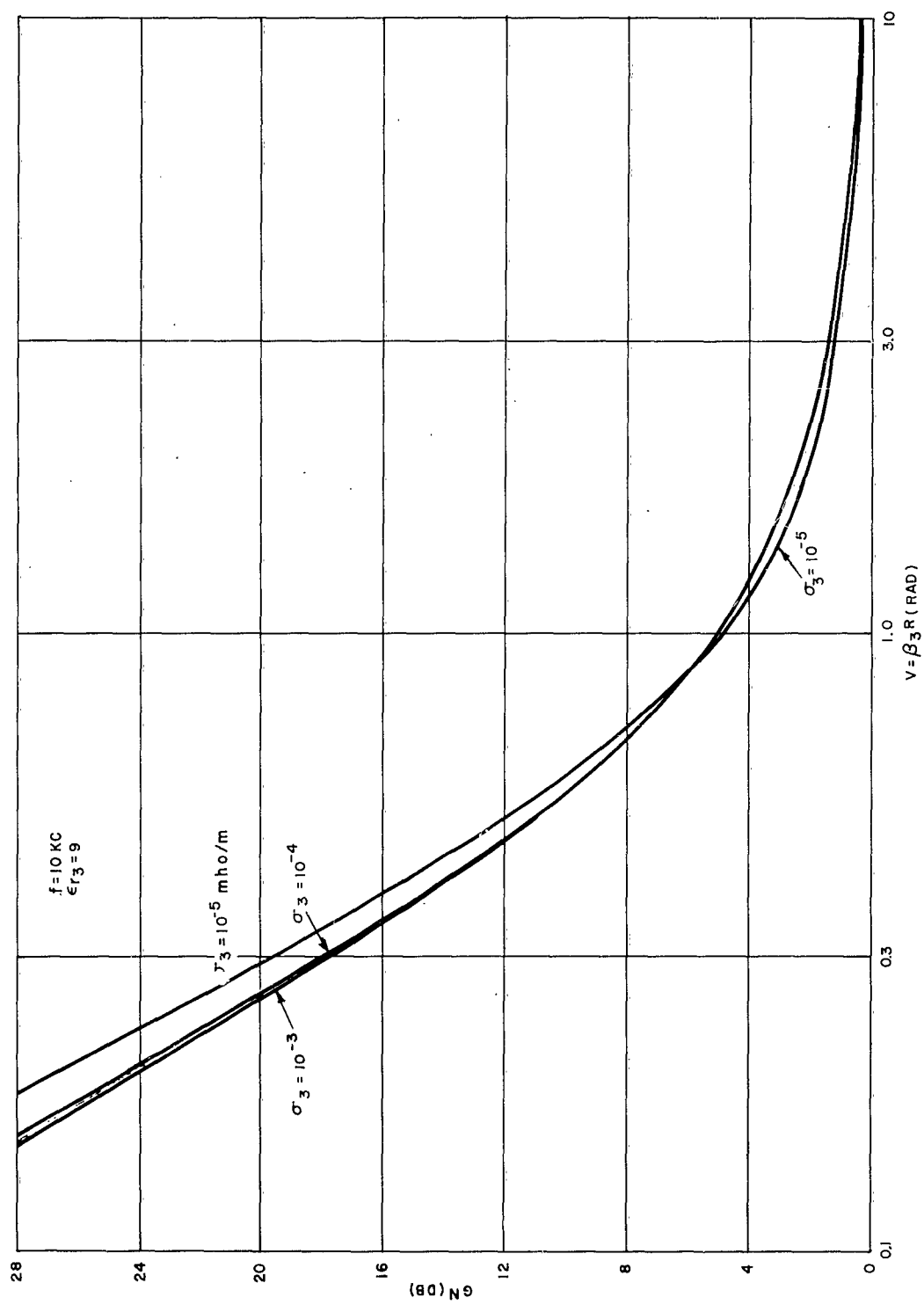
Figure II.12. Near-zone enhancement gain (G^N) vs $\beta_3 R$. Short dipole $(\beta_3 h \leq .3)$, $f = 10$ kc, $\epsilon_{r_3} = 9$.
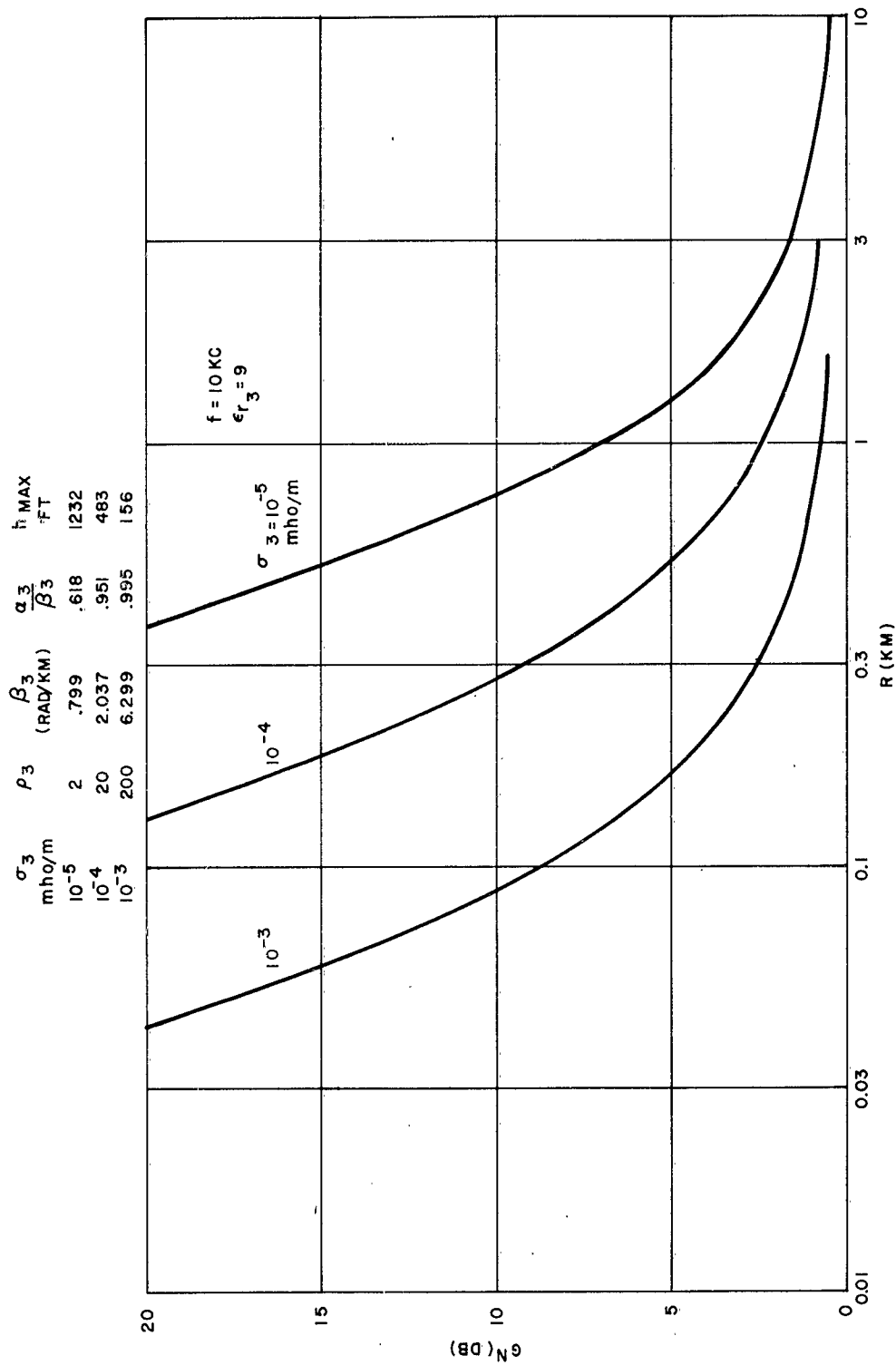
Figure II. 13. Near-zone enhancement gain (G^N) vs R. Short dipole $(\beta_3 h \leq .3)$, $f = 10$ kc, $\epsilon_{r_3} = 9$.

exist, then a calculation of G^N would be made and included to obtain L_T (near-zone) provided $G^N \le 10$ db, if the limitation given by condition (II.96) is applied. We shall soon see that the calculation of L_T for practical cases of interest will be sufficiently large that the restriction on G^N in equation (II.97) is not serious. It will turn out that for many cases, far-field conditions do exist for bare or insulated dipoles and that G^N may be neglected.

      b. Exponential Damping Loss A

      In decibels, the exponential damping loss, using equation (II.86b), may be written

$$A(db) = 8.69 \, \alpha_3 R = 8.69 \, uv \qquad (II.98)$$

where u and v are given by equation (II.93) and v is expressed in radians. Typical calculations are given in the next subsection.

      c. Spreading Loss L_S

      The spreading loss in decibels, using equation (II.86a), may be written

$$L_S(db) = 20 \log \left(\frac{4\pi R}{\lambda_3} \right) = 6.02 + 20 \log v \qquad (II.99)$$

with v given by equation (II.93) in radians. Typical calculations are given in the next subsection.

      4. Example of Calculations

      Consider transmission between two parallel identical dipoles, for which R = 5800' = 1.768 km. The antennas are short-circuited insulated dipoles, of length 2h = 950 feet, h = 144.8 m, with inner conductor made of

#12 wire ($a_1 = 10^{-3}$ m) and polyethylene insulation ($\epsilon_{r_2} = 2.25$) with radius $a_2 \cong 3.5 \times 10^{-3}$ m. It is assumed that the total input resistance $R_{in} = R_{rad} + R_{ohmic} + R_T = 100$ ohms, and is constant with frequency.

It is further assumed that the antennas have common equatorial planes so that $\theta = 90^\circ$ and that any feeder and mismatch losses may be neglected. We desire to compute L_T as a function of frequency with medium conductivity as a parameter. The value of ϵ_{r_3} is assumed to be 9, although for the range of frequencies of interest the loss tangent p_3 will be large even for greater values of ϵ_{r_3}.

It is noted that $\dfrac{R}{h} = \dfrac{5800}{475} = 12.21$ so that the radiation condition $R \gtrsim 4h$ of (II.95a) is satisfied. We have, using Appendices E and F,

$$p_3 = \frac{2 \times 10^6}{f_{kc}} \sigma_3 \qquad\qquad R_{rad} = 2 \times \frac{\omega \mu_0 h}{2\pi} \left[\pi/2 - \theta_u \right]$$

$$\beta_3 = 2\pi \times 10^{-5} f_{kc} \, f(p_3) \qquad\qquad = 0.3639 \, f_{kc} \left(\frac{\pi}{2} - \theta_u \right)$$

$$\beta_3 h = 9.098 \times 10^{-3} f_{kc} \, f(p_3) \qquad \theta_u = \tan^{-1} u$$

$$v = \beta_3 R = 0.11109 \, f_{kc} \, f(p_3) \qquad \eta = R_{rad}/100$$

$$u = \alpha_3 / \beta_3 = g(p_3)/f(p_3) \qquad \eta \text{ (db)} = -24.39 + 10 \log \left[f_{kc} \left(\frac{\pi}{2} - \theta_u \right) \right]$$

$$(\eta \, G_M)^{SC} = \frac{3 \, e_3}{\pi \, R_{in}} \, \beta_3^2 h^2 \left(1 + \frac{2}{3} \beta^2 h^2 \right), \quad \beta h \leqslant .4$$

$$\cong \frac{0.40}{f(p_3)} \, \beta_3^2 h^2, \quad \beta h \leqslant .3$$

G^N (See equation II.93)

$L_S(db) = 6.02 + 20 \log v$

$A(db) = 8.686 \, u \, v$

Calculations of the component losses of the total system loss were made for values of $\sigma_3 = 10^{-4}$, 5×10^{-4}, and 10^{-3} mhos/m. Resulting values of losses $A(db)$ and $L_S(db)$ are shown plotted on the curves of Figure II.14. The various "gain" quantities are shown in the curves of Figure II.15. In these figures "losses" and "gains" are plotted in decibels vs frequency on a linear scale.

Values of $L_P(db)$ and $L_A(db)$, with $\theta = 90^\circ$ and no feeder losses, are plotted on the curves of Figure II.16. Finally, the values of $L_T(db)$ vs frequency are plotted on the curves of Figure II.17.

An optimum value of $L_T(db)$ is noted for $\sigma_3 = 10^{-4}$ mhos/m at about 2 kc. This and the shape of all the curves is the result of the interplay between propagation losses $L_P(db)$ and antenna losses (or gains) $L_A(db)$. For the assumed values, at very low frequencies, the reverse is true due principally to the larger and larger values of the exponential loss $A(db)$.

These curves were used as the basis for predictions of expected losses and signal-to-noise ratio at the receiver for propagation tests on Cape Cod, one path being 5800 feet long. Insulated monopoles with $h = 475$ feet long, of the RG-8/U type, were used with short-circuit terminations. (The results are discussed later, with reference to the relative effects of using monopoles instead of dipoles, total input antenna resistance and apparent
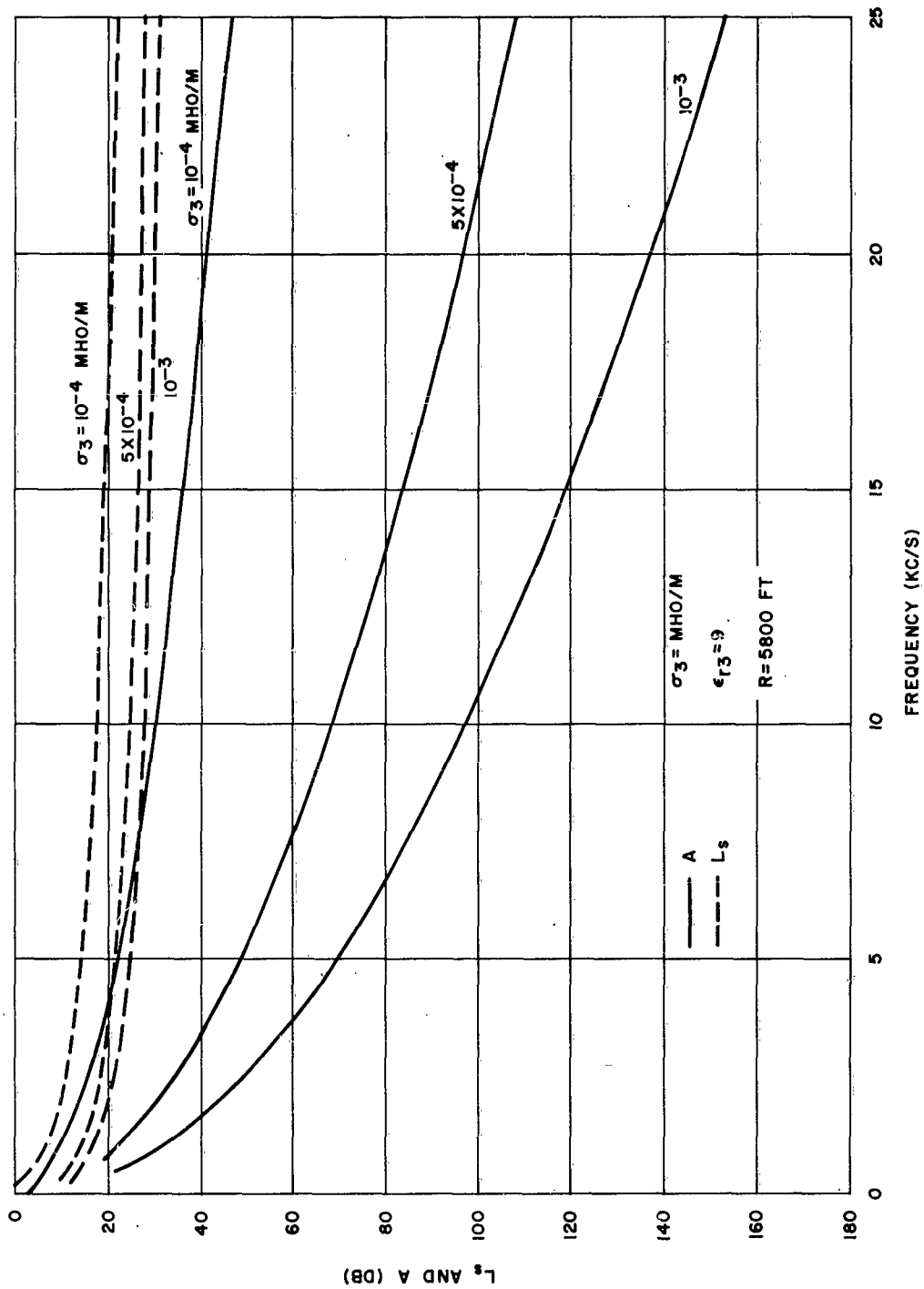
Figure II.14.   Spreading loss (L_S) and exponential attenuation (A) vs frequency.
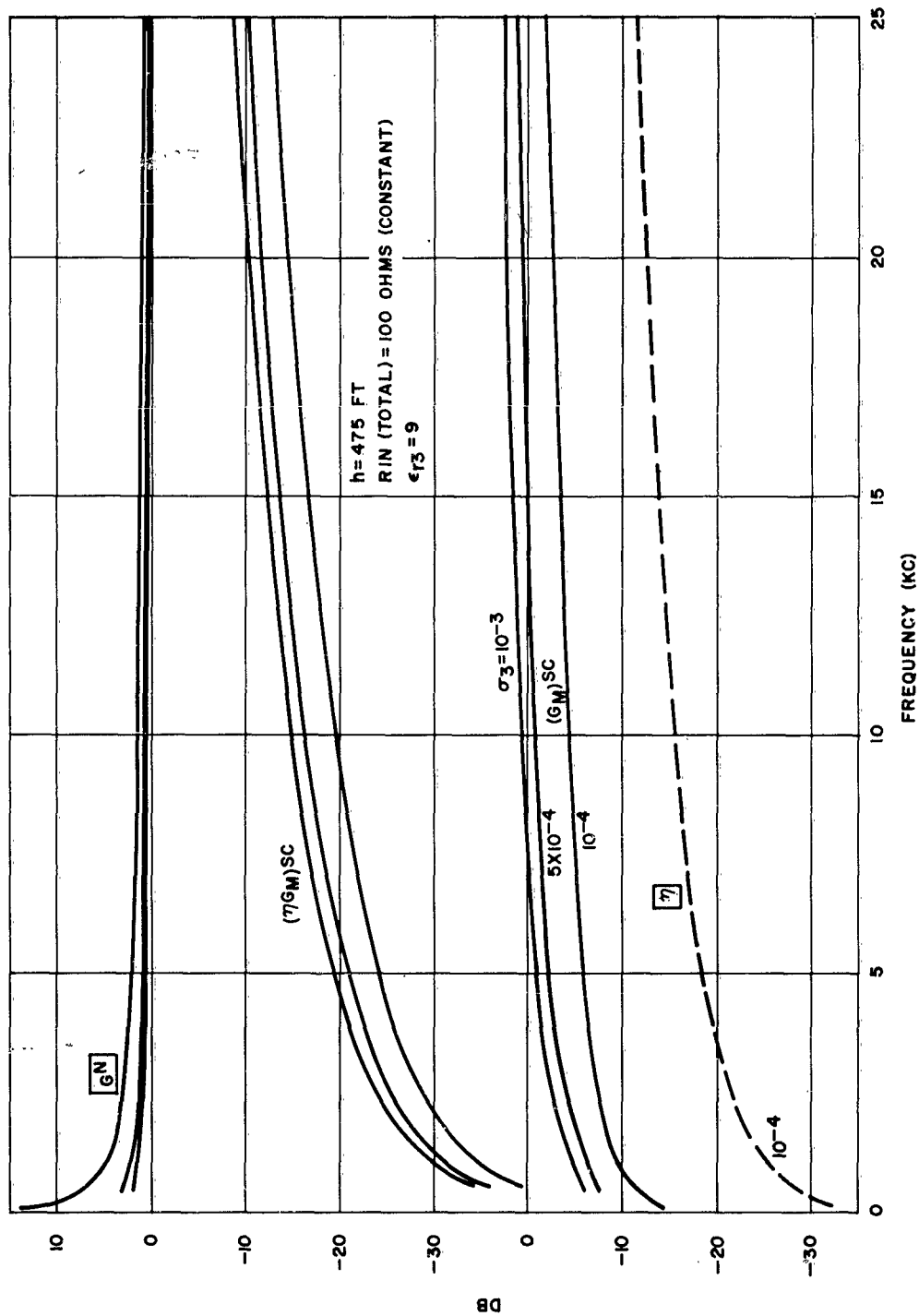
Figure II. 15. Near-zone enhancement gain (G^N), antenna modified power gain (loss-less) (G_M)SC, and radiation efficiency ηSC for center-fed, insulated dipole, short-circuit termination. $h = 475$ ft, R_{in} (total) = 100 ohms (constant), $\epsilon_{r_3} = 9$.
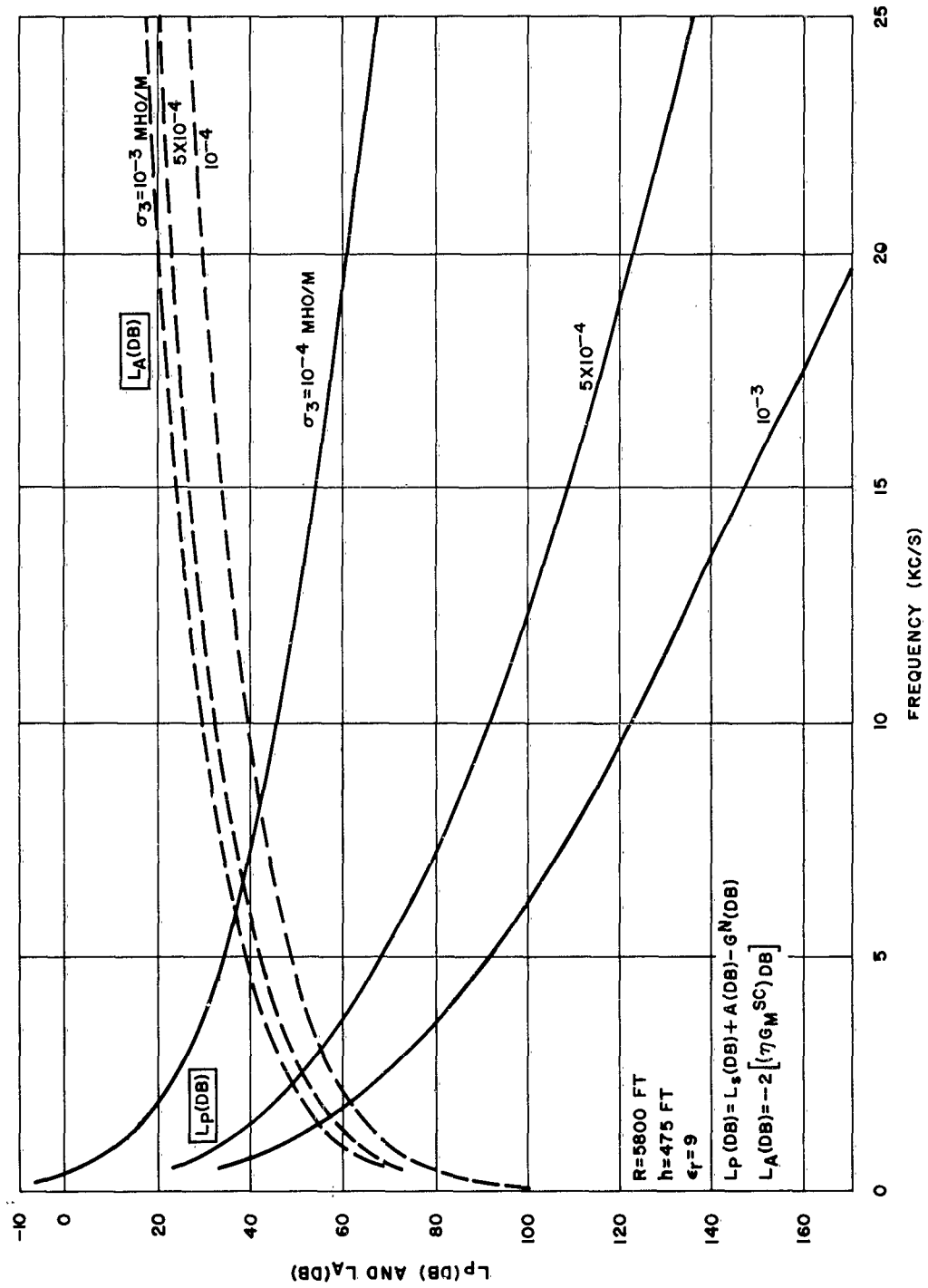
Figure II.16.   Propagation losses (L_P) and antenna coupling losses L_A for center fed electrically short, insulated dipole, short-circuit termination. $R = 5800$ ft, $\epsilon_{r_3} = 9$, $h = 475$ ft.
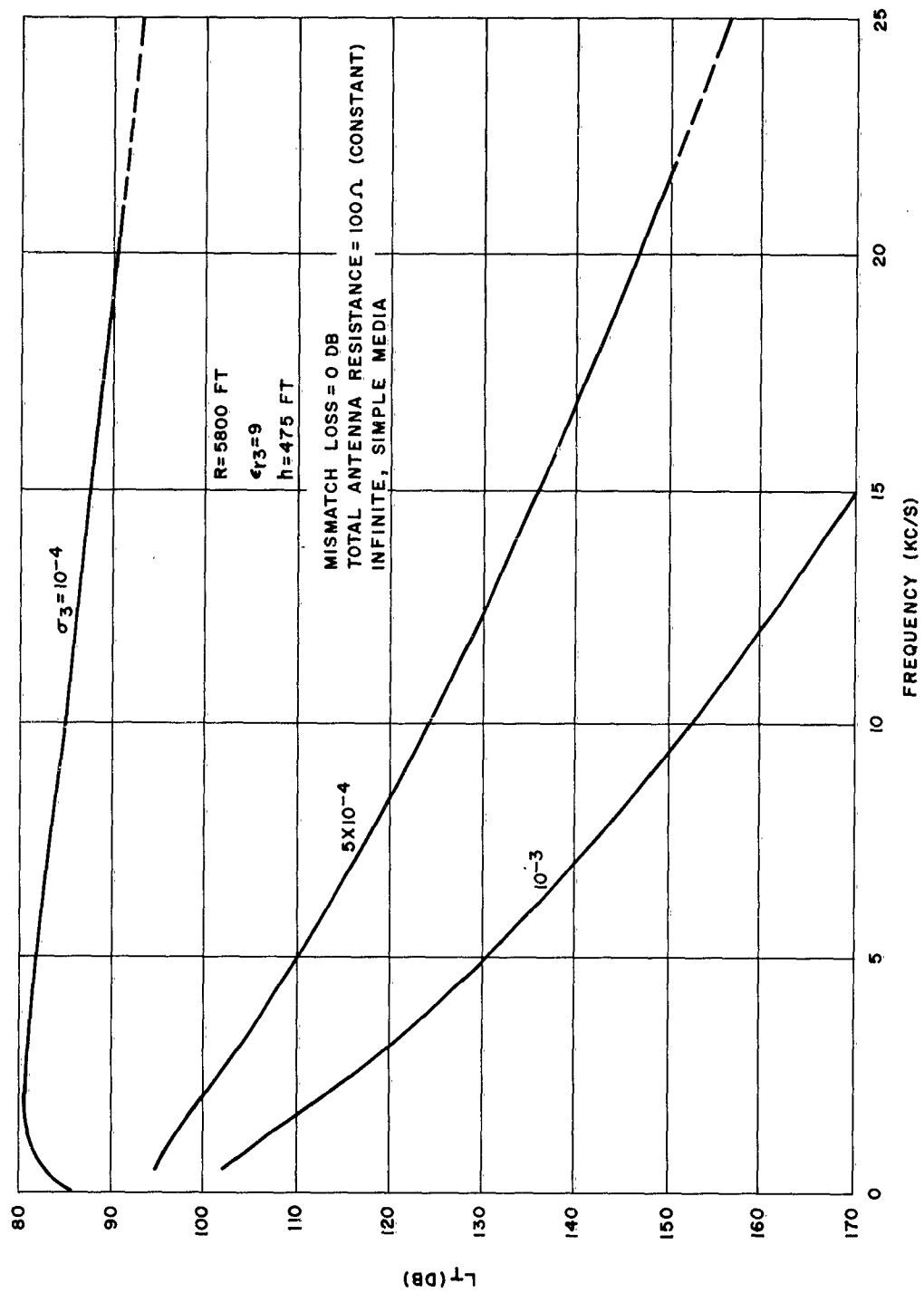
Figure II.17. Total system loss between center fed, parallel, insulated dipoles with short-circuit termina-tions. $R = 5800$ ft, $\varepsilon_{r_3} = 9$, $h = 475$ ft.

values of σ_3.) Thus, if one assumes an antenna power input P_T and values of $P_{R_{min}}$ for the receiver, one calculates the maximum allowable total transmission loss $L_T(max)$. For example, assume P_T = 100 w = 20 dbw. For the receiver, assume noise figure $\overline{NF}$ = 14 db and a noise bandwidth B = 1 kc. The available noise power P_n, in dbw, is $P_n(dbw)$ = 14 - 204 + 30 = -160 dbw. If the required carrier-to-noise ratio at the receiver is 15 db, then the minimum detectable receiver signal power $P_{R_{min}}$ must be -145 dbw. Hence $L_T(db)_{max}$ = 20 - (-145) = 165 db. A readily detectable signal should be found at frequencies much higher than 25 kc if σ_3 = 10^{-4} mhos/m. On the other hand if σ_3 is as high as 10^{-3} mhos/m, frequencies lower than 13 kc must be employed.

Reference to the curves shows that for a given medium environment, the only components of loss under the control of the designer are the antenna system losses, and these are the more important the lower the frequency. For hole dpeths which limit the antenna lengths to electrically short values ($\beta h \leq .4$, say), not a great deal can be done to improve G_M^{SC} itself. Outside of the obvious minimizing of mismatch losses (L_m), this leaves only the improvement in the low "radiation efficiency (γ^{SC})", which means lowering the dead-loss resistance $R_{ohmic} + R_{terminations}$. This parallels the problem of VLF antenna systems in air, but here the worst offender seems to be the resistance of terminating electrodes. For monopoles, there appears to be advantage in considering open-circuit insulated types depending upon electrical length because the dead-loss resistance is

smaller than short-circuited types; however, their input impedance is higher and mismatch to coaxial feeders must be reduced by low-loss matching circuits if this advantage is to be realized.

The previous curves can be used for predictions for other ranges for the same antenna configurations. One observes the behavior of the distance-dependent propagation loss terms individually that combine to make up L_P(db). The "spreading loss" L_S varies as R^2 and thus L_S(db) varies as 20 log R. The exponential attenuation in decibels varies directly with R, i.e., A(db) varies with R (for the same frequency and medium characteristics). The near field enhancement G^N at greater distances becomes much less than the values at 5800 feet used in the curves, and as an approximation we may neglect G^N. Suppose we consider the cases for $\sigma_3 = 10^{-4}$, 5×10^{-4} and 10^{-3} mhos/m. Further it is assumed that the antenna is the same as previously used, so that total antenna coupling losses L_A(db) $= -2 \left[(\eta G_M)^{SC} db \right]$ are those on the curves of Figure II. 16. The propagation losses, neglecting G^N, are values given on the curves of Figures II. 18, II. 20, and II. 22 for $\sigma_3 = 10^{-4}$, 5×10^{-4}, and 10^{-3} mhos/m, respectively. The final values of transmission loss L_T are those on the curves of Figures II. 19, II. 21, and II. 23, respectively, where it is assumed that mismatch losses $L_m = 0$ db. For the previously assumed experimental system $L_T \leq 165$ db, if the receiver sensitivity is limited by "receiver noise" and not by "attenuated atmospheric noise." Thus, for a three-mile path, frequencies less than 2 kc must be employed if $\sigma_3 = 5 \times 10^{-4}$ mhos/m.
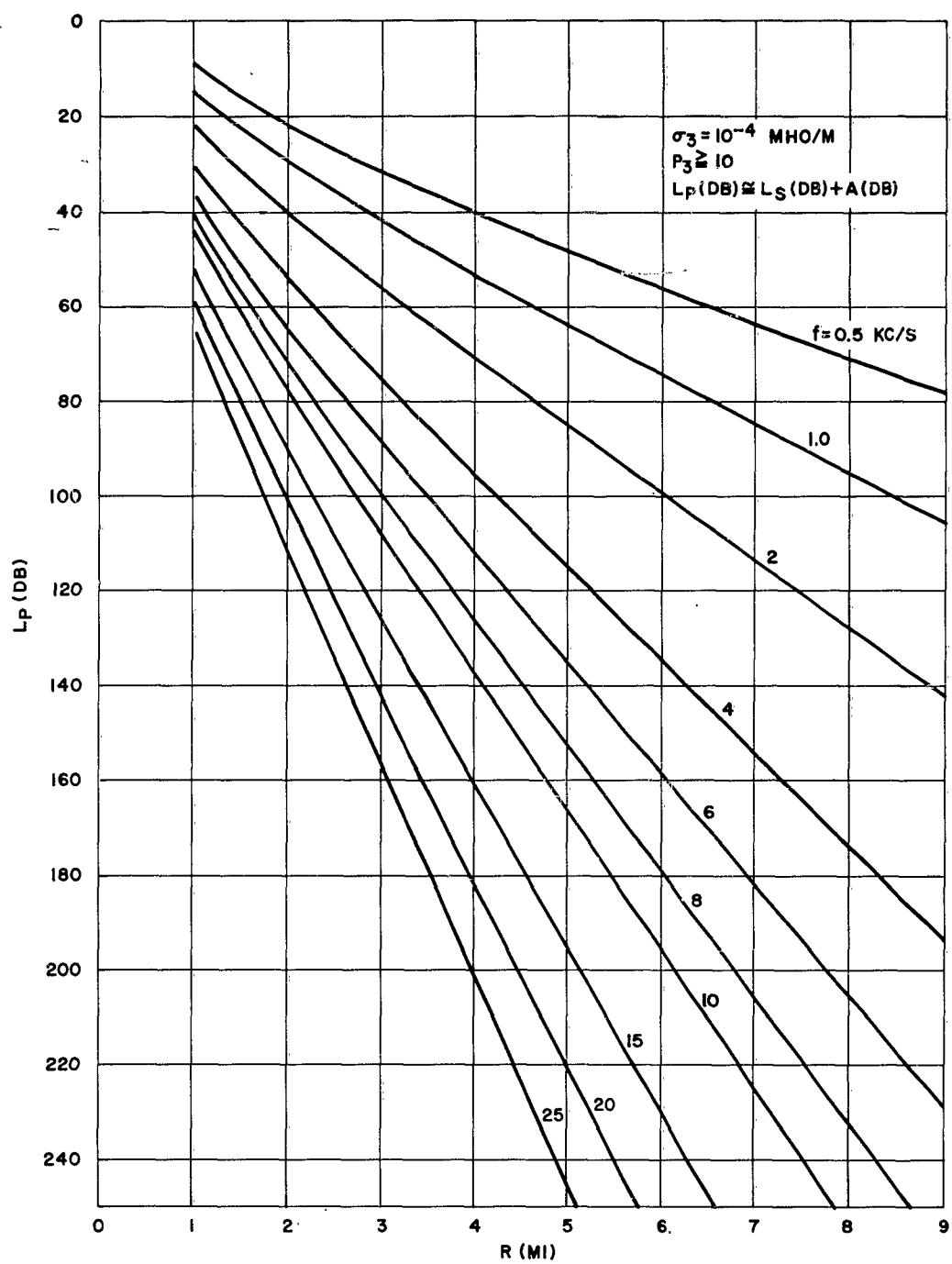
Figure II. 18. L_P(db) vs R for various frequencies (G^N neglected). $\sigma_3 = 10^{-4}$ mh0/m.
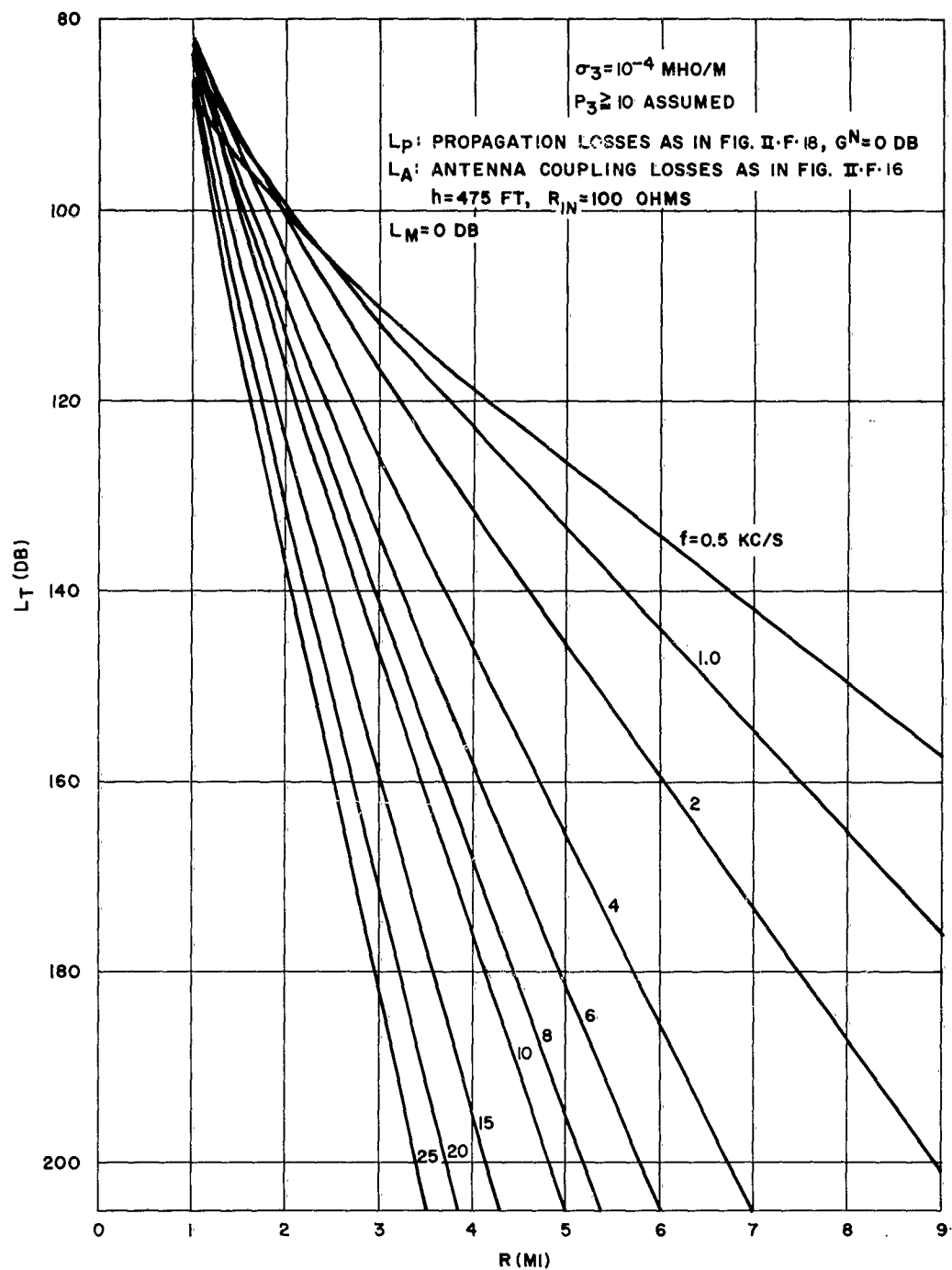
Figure II.19.   Total system loss L_T vs distance R for various
frequencies. $\sigma_3 = 10^{-4}$ mho/m.
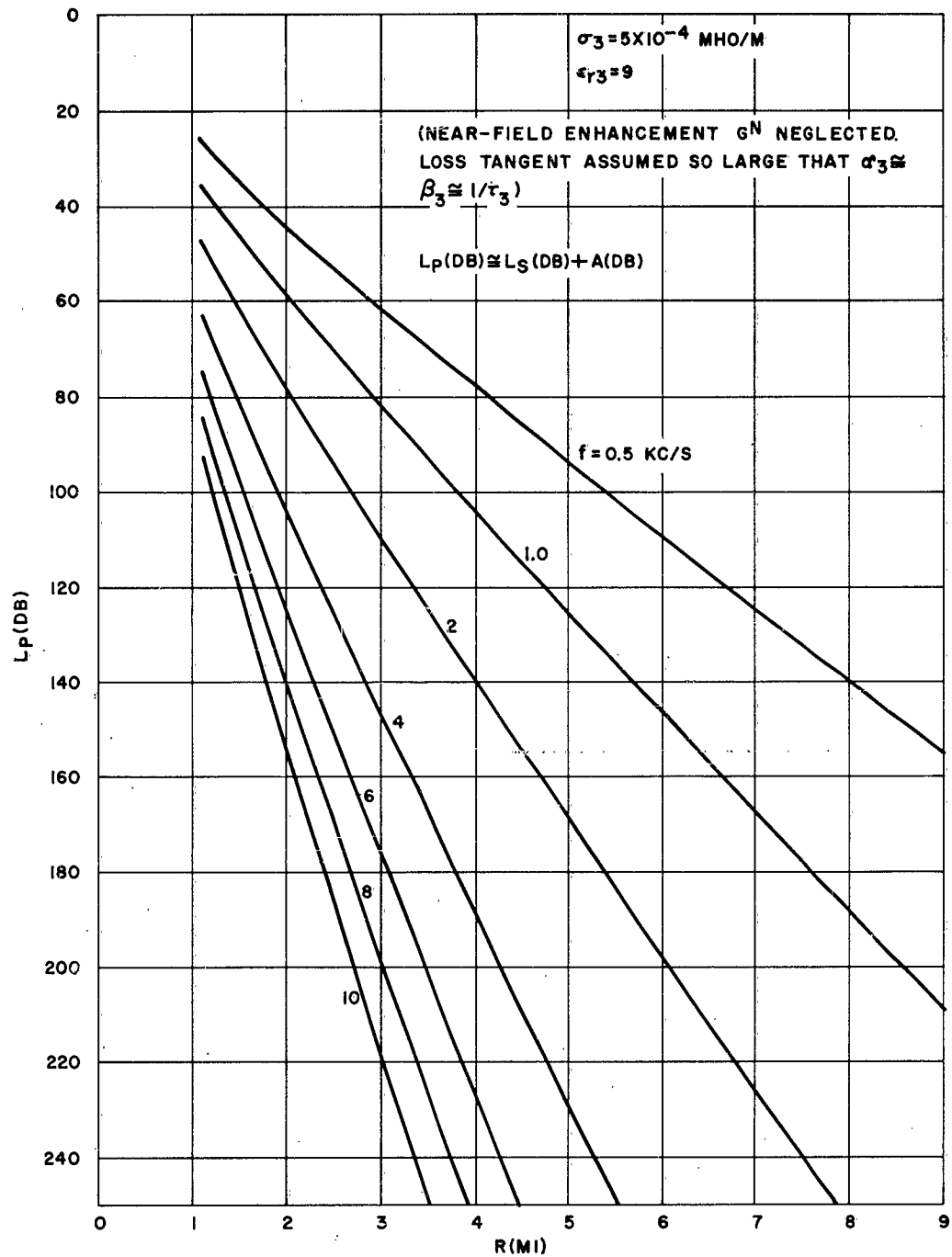
Figure II. 20.   Propagation losses L_P(db) vs distance
R(mi) at various frequencies.

$\sigma_3 = 5 \times 10^{-4}$ mho/m, $\varepsilon_{r_3} = 9$.
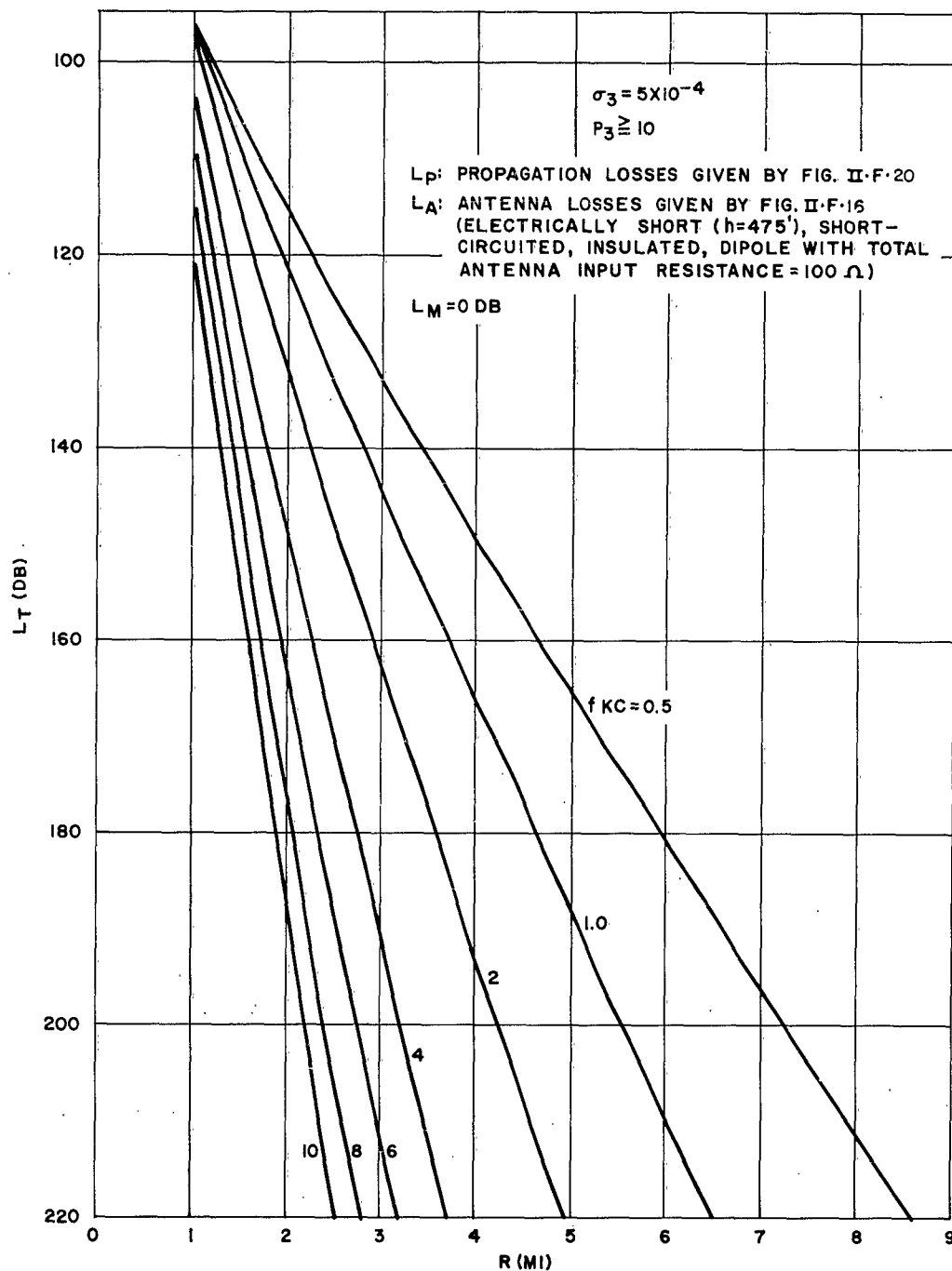
Figure II. 21.   Total system loss L_T vs distance R at various frequencies. $\sigma_3 = 5 \times 10^{-4}$, $p_3 = 10$.
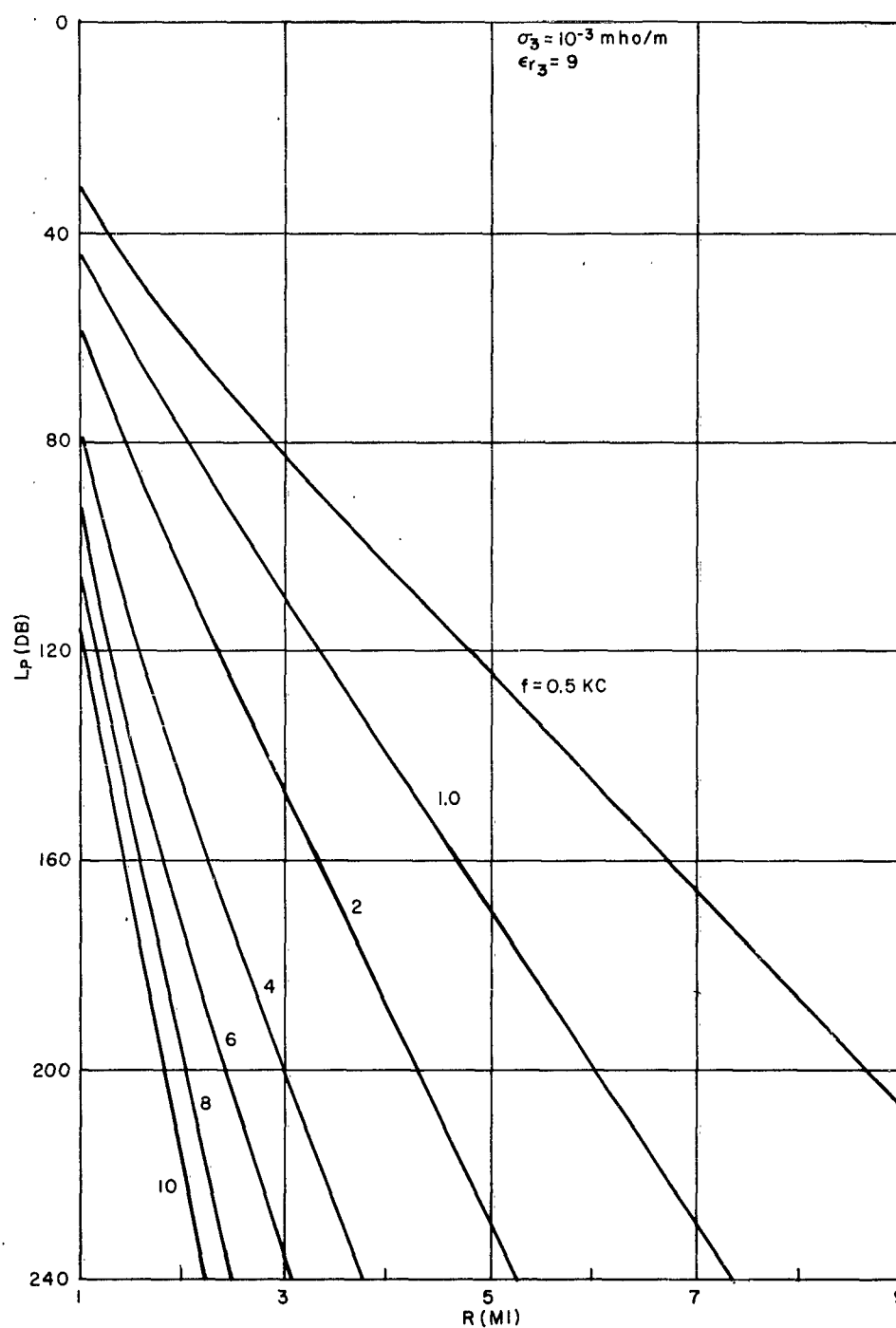
Figure II. 22.   Propagation losses L_P vs distance R at various frequencies. $\sigma_3 = 10^{-3}$ mho/m, $\varepsilon_{r_3} = 9$.
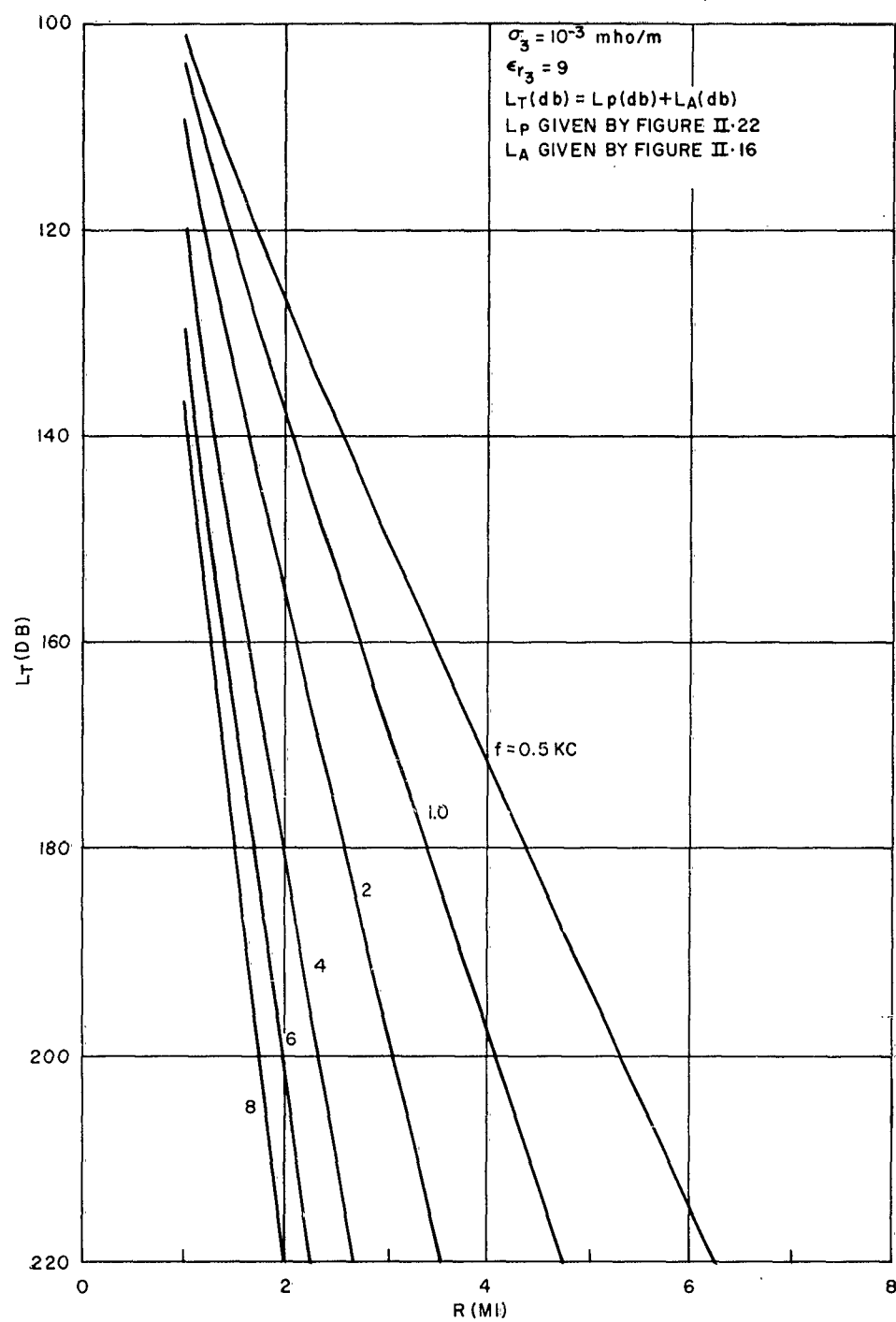
Figure II. 23.   Total system loss L_T vs distance R at various frequencies. $\sigma_3 = 10^{-3}$ mho/m, $\varepsilon_{r_3} = 9$.

Similarly, if the rock has five times lower conductivity than that assumed above so that $\sigma_3 = 10^{-4}$, much higher frequencies could be used than those when $\sigma_3 = 5 \times 10^{-4}$, for the same path length. Conversely, somewhat greater distances can be achieved at the same frequency for the lower conductivity.

It should be emphasized that we have used as an illustrative example an electrically short insulated antenna having a length which was limited by the amount of penetration into the rocks expected for the drill holes on Cape Cod. The obvious areas of improvement possible in antenna performance have been mentioned. For other lengths of antennas, antenna types, frequencies, and conductivities, similar calculations would be made.

Calculations have been given earlier elsewhere for bare antennas[32] where conductivities and loss tangents were assumed to have much lower values than assumed here. Those calculations resulted, of course, in larger ranges and higher limiting frequencies, anticipated in practical circumstances only in a few geological areas at best.

Attenuation of atmospheric noise by an overburden as it affects signal detection is considered later on. The theory is discussed in Appendix G where it is shown that atmospheric noise at VLF may limit the signal-to-noise ratio at the receiver unless the overburden is sufficiently thick and highly conducting.

G. Effect of Other Modes

We consider a simplified two-layer, three region model to approximate the case of rock propagation in practice. An oversimplified sketch is shown in Figure II.24 with each region being a simple medium; region 0 is air with propagation constant $\underset{\sim}{k}_o = \beta_o$; region 1 is lossy overburden with $\underset{\sim}{k}_1^2 \cong -j \, \omega\mu_o \, \sigma_1$ and $k_o^2 \ll k_1^2$; and region 2 is rock with loss tangent p_2 and with $k_2^2 < k_1^2$. A vertical electric dipole is immersed in rock.

To illustrate simple refracted and reflected rays, suppose that all media are loss-less dielectrics so that $\underset{\sim}{k}_o = \beta_o$, $\underset{\sim}{k}_1 = \beta_1 = \beta_o \sqrt{\epsilon_{r_1}}$, and $\underset{\sim}{k}_2 = \beta_2 = \beta_o \sqrt{\epsilon_{r_2}}$ and further that

$$k_1^2 \gg k_o^2 \qquad \epsilon_{r_1} > 1$$

$$k_1^2 \gg k_2^2 \qquad \epsilon_{r_2} < \epsilon_{r_1} \qquad \epsilon_{r_2} < \epsilon_{r_1} \tag{II.100}$$

that is

$$1 < \epsilon_{r_2} < \epsilon_{r_1} \tag{II.101}$$

Then the wave from a dipole in region 2 following the ray path ① would be refracted at the boundary between regions 2 and 1 and the transmitted ray would be bent towards the normal in region 1. This ray, at the boundary between region 1 and 0 would be bent away from the normal in air.

A ray such as ② from the dipole would suffer total internal reflection at the boundary between region 1 and air. A ray such as ③ would suffer total internal reflection at the boundary between regions 2 and 1.

REGION 0   AIR $(K_0 = \beta_0)$

REGION I   OVERBURDEN (K_1)

REGION 2   ROCK (K_2)
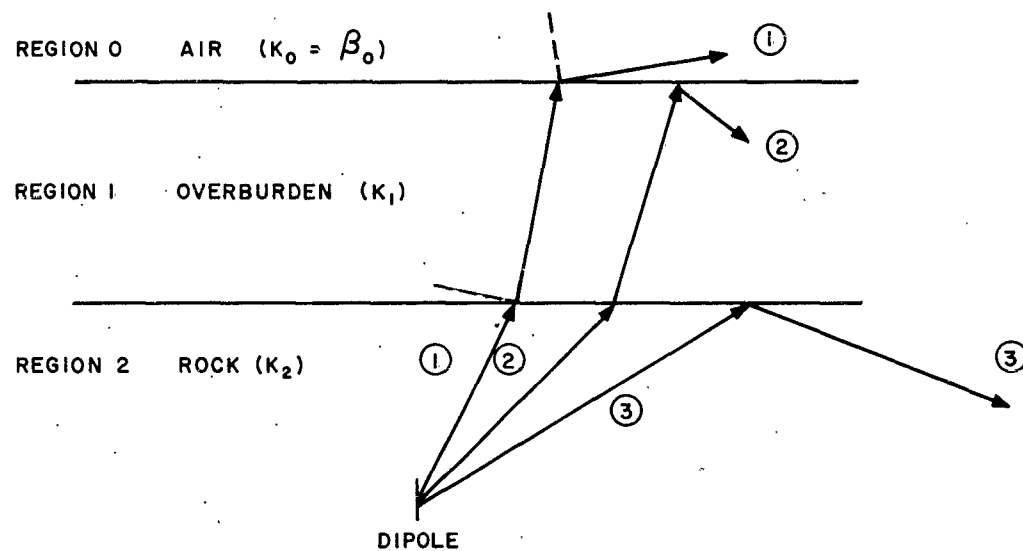
DIPOLE

Figure II. 24.   Oversimplified sketch of two-layer, three medium propagation modes from vertical dipole in rock.

In a situation approaching that in practice, regions 1 and 2 have large loss tangents so that

$$k_1^2 \cong - j \omega \mu_o \; \sigma_1$$

$$k_2^2 \cong - j \omega \mu_o \; \sigma_2$$

$$\left. \right\} \qquad \text{(II. 102)}$$

whence

$$\sigma_1 > \sigma_2 \qquad \text{(II. 103)}$$

one has

$$|k_1| > |k_2| > \beta_o \qquad \text{(II. 104)}$$

The complete analysis of the three medium problem is complicated. For the two medium problem such as air above sea water (or lossy ground) with antennas immersed in the latter, an analysis has been carried out by Moore[60] and Banos and Wesley,[21] the latter for horizontal dipoles. For dipoles not buried too deeply, the principal propagation mode is the up-over-and-down mode launched like "ray ① " and discussed in Section IB. For great distances, the vertical field in air due to a buried vertical dipole is very small and is neglected compared with the horizontal field in air, at the earth's surface. The direct wave is likewise negligible.

The analysis of the three medium problem corresponding to conditions (II. 104) has not been carried out completely. However, if we assume that region 1 in Figure II. 24 is highly conducting and sufficiently thick, then any energy refracted into region 1 is highly attenuated therein. Accordingly, the field in air for a potential UOD mode would be weak and neglibible upon

passing through region 1 to a receiver antenna in region 2.

An analysis has been carried out in Appendix C which takes into account the propagation between vertical electric dipoles at varying distances into the rock medium 2 below the overburden-rock boundary. The analysis takes into account

—— a direct wave between T and R dipoles

—— wave reflection at the rock-overburden boundary, and

—— a wave guided along the interface between rock and overburden.

If the dipole moment is constant with depth, and with plausible values of rock and overburden electrical constants, it is shown that at frequencies exceeding 1 kc the field at the receiver increases with antenna depth, the increase being more marked the higher the frequency. This phenomenon affords one means of distinguishing between a predominantly up-over-and-down mode from a predominantly rock mode signal in that the former the field should decrease as the antenna depths increase below the overburden.

The theory in Appendix C indicates that as the dipole depths increase below the rock-overburden boundary the field intensity at the receiver point approaches the value of the direct wave between T and R. The direct wave, for a given dipole moment, has an intensity at the receiver point which is the same as that in an unbounded medium. It is thus inferred that the transmission loss equation in the previous section may be applied to antennas well below the overburden-rock boundary and that for antennas near that boundary

a small correction is needed which depends upon the conductivity contrast σ_2 / σ_1 and frequency.

Another possible transmission mode makes use of horizontal polarization and, in concept, would be useful at ELF and lower frequencies. The idea is based upon certain concepts used in surface measurements of deep resistivity using four electrodes (see Section V). Instead of two vertical drill holes separated a transmission distance R, there would be four shallower drill holes into the rock at the corners of a long, thin rectangle (of length R). Electrodes would be inserted into the first pair of holes, insulated from the overburden but contacting the rock. These would be connected to a transmitter on the surface and serve as the "current electrodes." A similar pair on the opposite side of the rectangle would be connected to the receiver and act as the "potential electrodes." For an overburden of negligibly small electrical thickness (as at ELF and lower frequencies), the polarization would be horizontal. Conceivably larger dipole moments with two pairs of holes could be achieved at less cost than for two single, very deep holes having the same dipole (vertical) moment. Further studies are needed to evaluate the fields in air as well as in the rock in order to assess the merits of the scheme.

Section III. EQUIPMENT AND FACILITIES

This Section is devoted to a brief description of site facilities and equipment used in the experiments on electrical characteristics of media near drill holes and on limited propagation tests between antennas in pairs of holes.

A. Site Facilities

Four sites were used in New Hampshire (see map in Figure III. 1) in the very early phases of the program which followed that being conducted under Raytheon Company sponsorship. Three of these were at existing drill holes and the fourth was a granite quarry. Three holes were drilled on Cape Cod following an analysis of the results of seismic and magnetic surveys, and the locations are shown on the map of Figure III. 2.

1. Concord (N. H.) Drill Hole

An existing drill hole, 1000 ft. depth, was supplied by the city of Concord with permission to use the site. A view is shown in the photograph of Figure III. 3 showing the 10' x 10' maintenance building housing equipment. Due to some geologic faults, the full hole depth was not usable. Commercial power, 220/110 v. 60 cycle AC, single phase, was made available plus a telephone. The site was used principally for signal transmissions from the AN/GRN-6 on loan from the Department of the Army.

2. Bedford (N. H.) Drill Hole

Use of an existing drill hole 400 ft. deep and site was arranged under a lease with Silverberg Bros. of Bedford. A photographic view is

CONCORD

ROUTE 202

4

1— CONCORD
2— BEDFORD
3— GOFFSTOWN
4— SWANSON'S QUARRY

13 MI.

18 MI.

ROUTE 3

N

3 GOFFSTOWN

ROUTE 114

WALLACE ROAD

MANCHESTER

6 MI.

ROUTE 101

2 BEDFORD
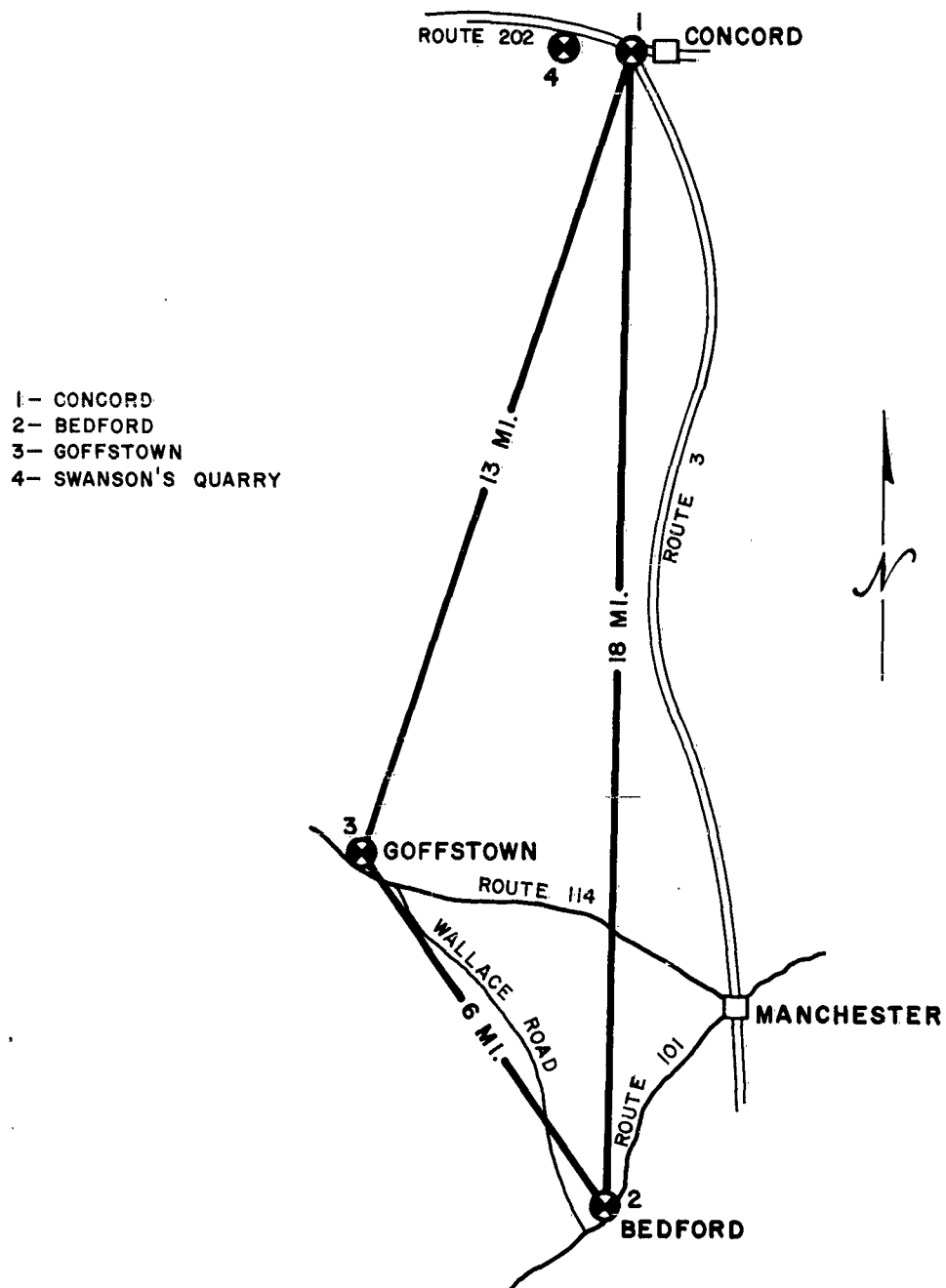
Figure III. 1.   New Hampshire - Location of Drill Hole Sites

Figure III. 2.   Cape Cod - Location of Drill Hole Sites
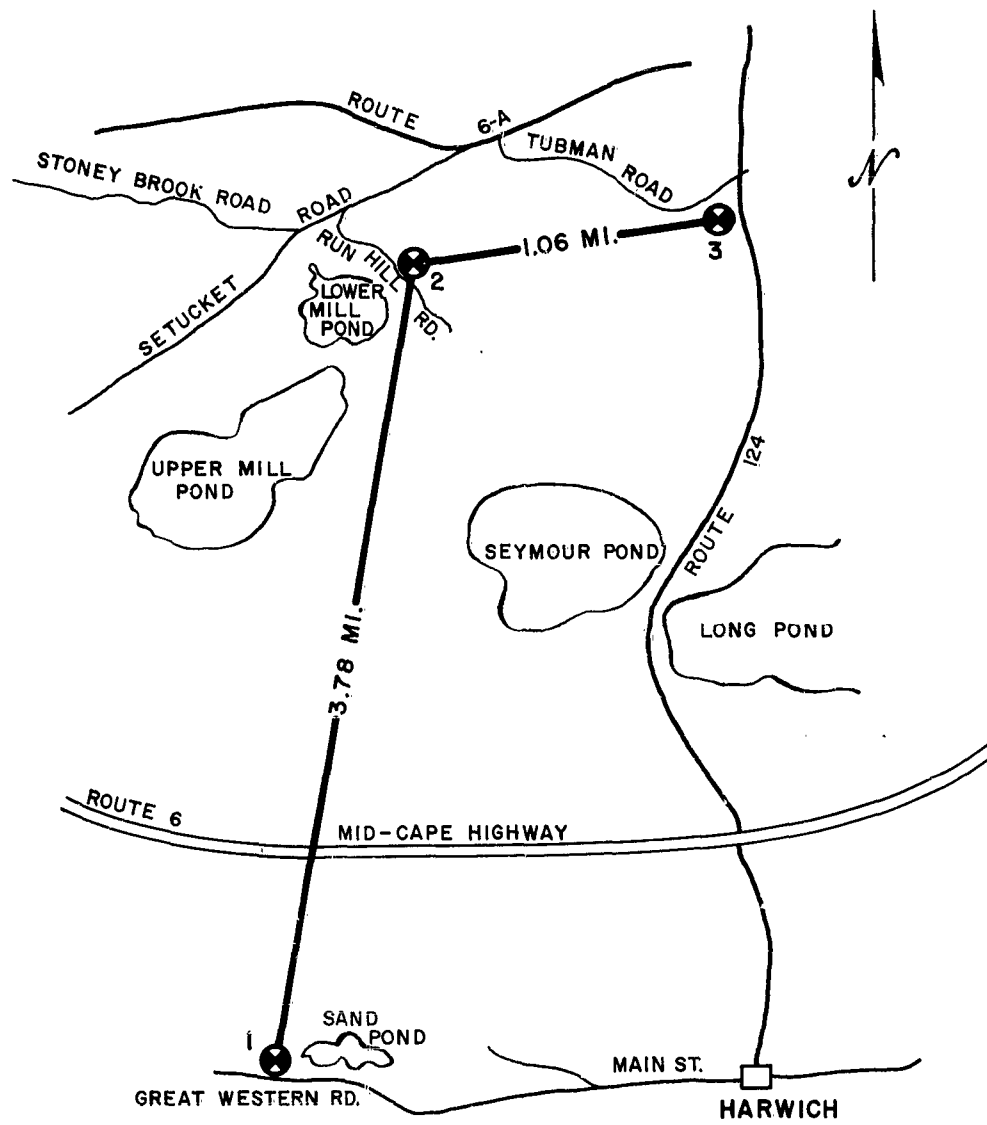
1 - HARWICH
2 - BREWSTER
3 - TUBMAN
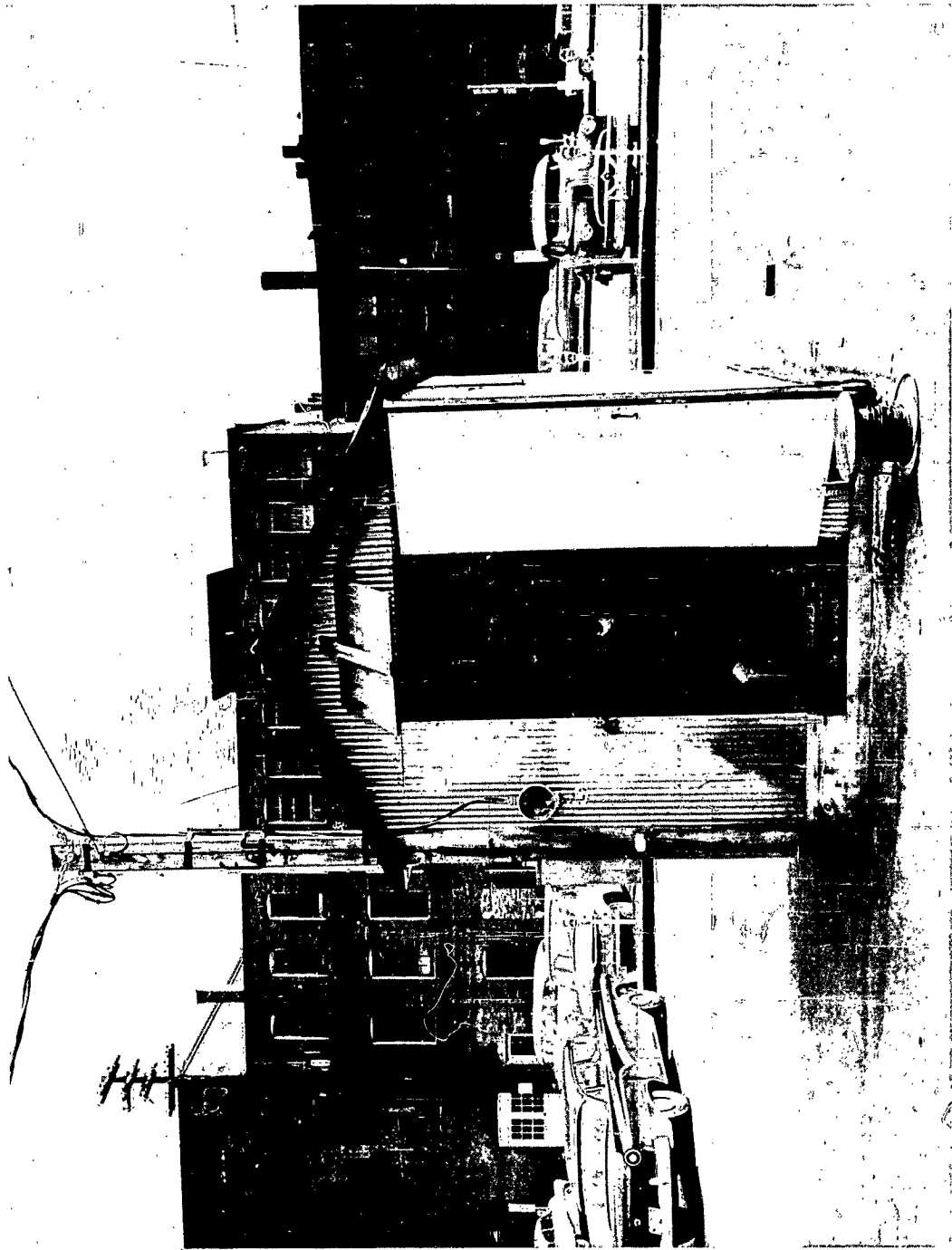
Figure III.3. Concord, New Hampshire Site

shown in Figure III.4. The prefabricated building was about 12' x 12' with a modest attempt at shielding made by stapling copper around the inside of the building. The site was about 18 miles due south of the Concord site. Commercial power, 220/110 v. 60 cycle, single phase, was made available plus a telephone. The site was used for signal reception and for signal transmission using the ART-13 transmitter.

3. Goffstown (N. H.) Drill Hole

About 6 miles north northwest of Bedford and 13 miles south southwest from Concord was located a 400-ft. drill hole in Goffstown. The use of the hole and site was arranged under a lease with Karanikis Brothers, Goffstown. A photograph of the site is shown in Figure III.5, showing the 12' x 12' prefabricated building. The site was used for signal reception and for signal transmissions using a second GRN-6 transmitter on loan from the Department of the Army. Preliminary path transmission tests were made between here and the other sites, prior to more extensive work on Cape Cod. Early impedance measurements on bare and insulated antennas were also made here, the holes being water-filled.

4. Swenson's Quarry (Concord, N. H.)

This granite quarry is operational and located west of Concord. Permission to use the site was arranged with Mr. Swenson. The quarry was used for antenna measurements imbedded in slots in granite, see photograph Figure III.6.
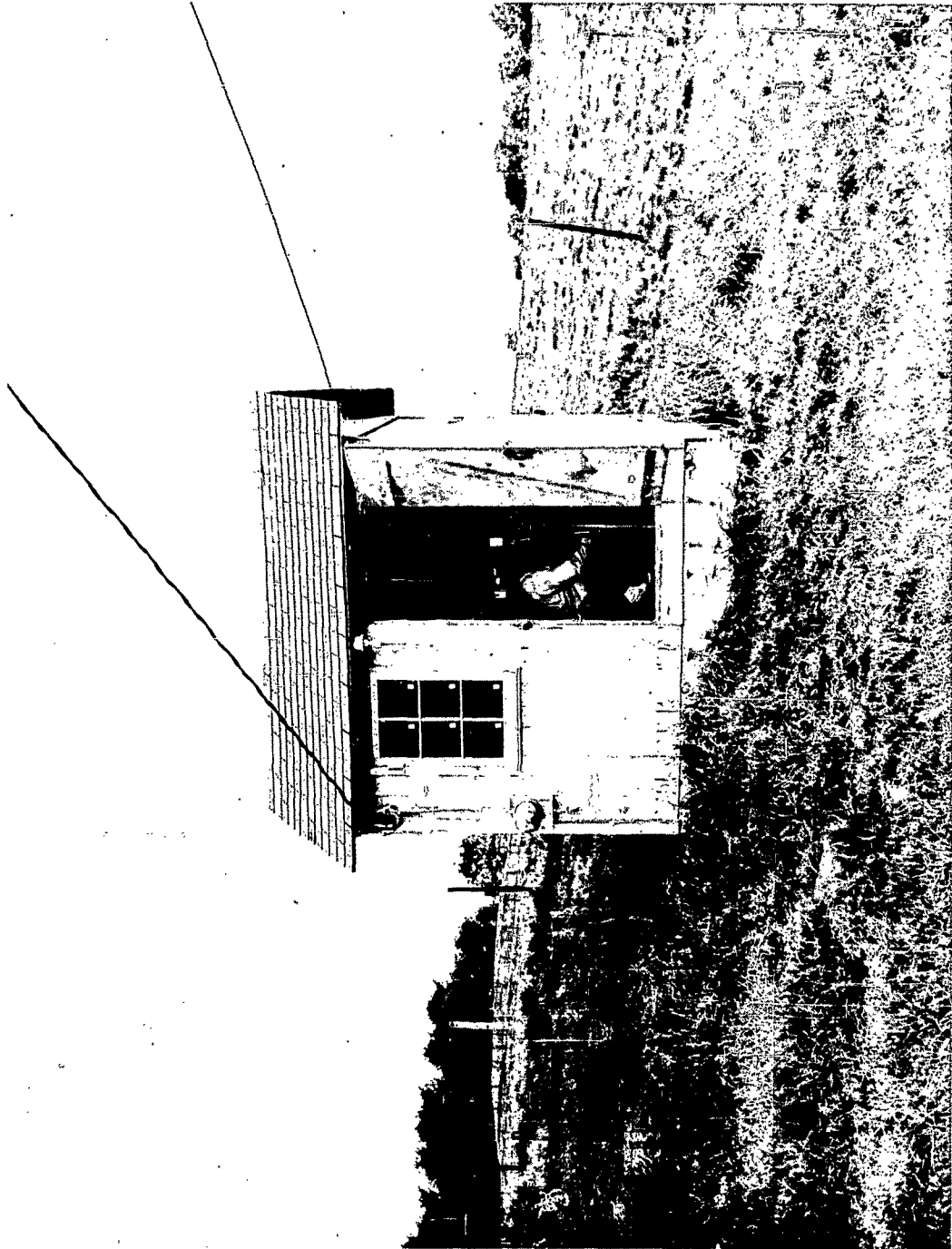
Figure III. 4.   Bedford, New Hampshire Site
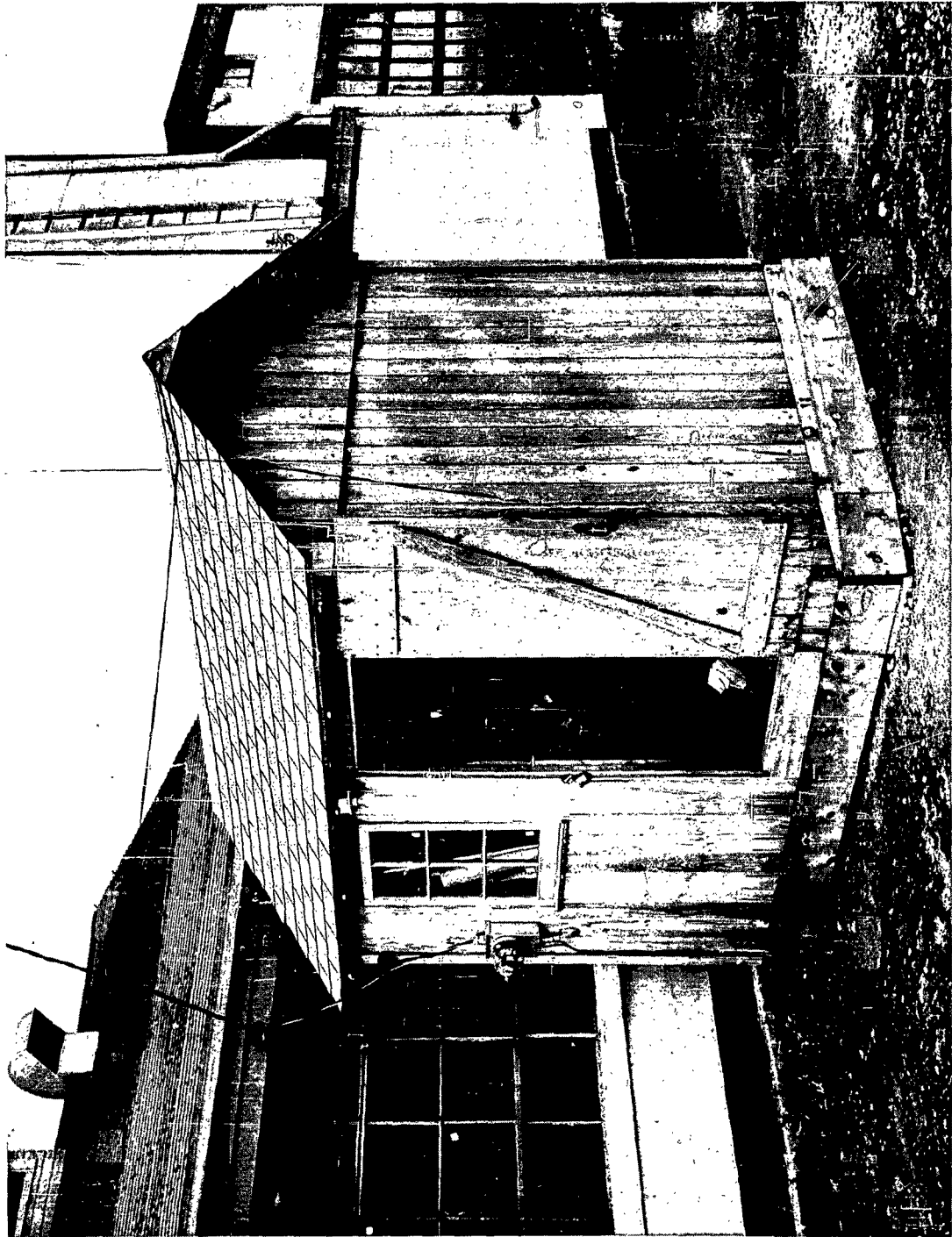
Figure III. 5.   Goffstown, New Hampshire Site
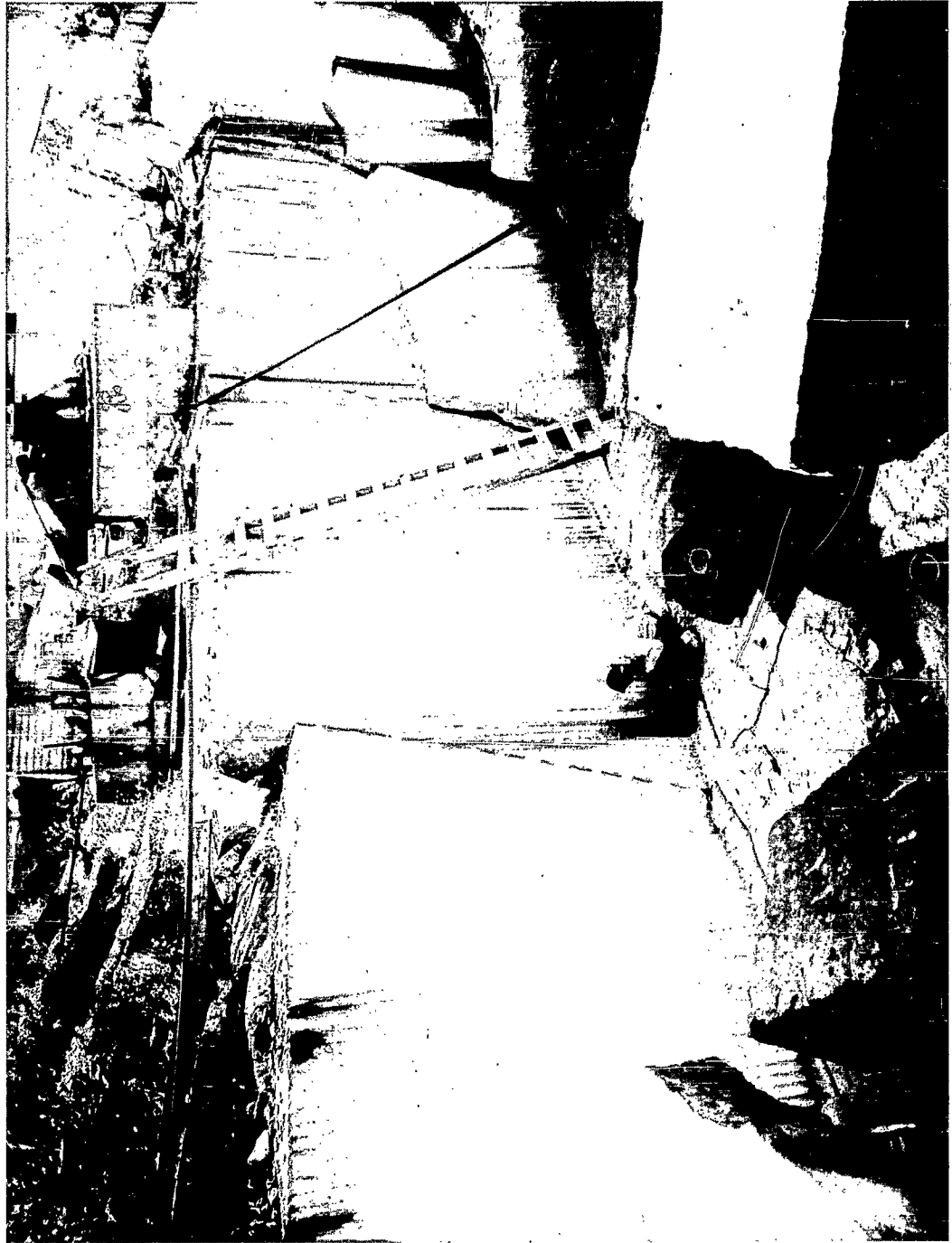
Figure III. 6.   Swenson's Quarry, Concord, N. H.

5. Harwich (Mass.) Drill Hole Site

The location of three drill holes on Cape Cod is shown in the map of Figure III. 2. Seismic,[97] magnetic,[97] and gravity surveys were conducted over the area (see Section V). All holes were 1000 feet in depth; the first two being larger in diameter (7 1/2 inches) and drilled at Harwich and Brewster by R. E. Chapman and Company, Oakdale, Massachusetts. Various views of the drilling operation at the Harwich site are shown in the photographs of Figures III.7, III.8, and III.9. The holes penetrated through 400 to 450 feet of overburden, thence into rock. The overburden portions were lined with iron casings extending into the rock about 25 to 30 feet and sealed off to prevent overburden soils from filling the rest of the hole. The pipe also served as a "ground return" for excitation of various antennas.

Views of the completed Harwich site are shown in the photographs of Figures III. 10, III. 11, III. 12, and III. 13. The site was used through permission of the Harwich Board of Selectman. A prefabricated 14' x 18' building (see Figure III. 10) housed a standard Ace Engineering Company screen room and a Gar Wood/H-24 Beebe cable winch located outside the screen room (see Figure III. 11). The coaxial feedline with an antenna at the bottom was raised and lowered by this winch, the feedline being passed through an aluminum shield connected physically to a pulley arrangement over the casing (Figure III. 10). Connection from the cable on the winch to feed-through cables on the equipment in the screen room was made by a coaxial rotary joint (Scientific-Atlanta Company).
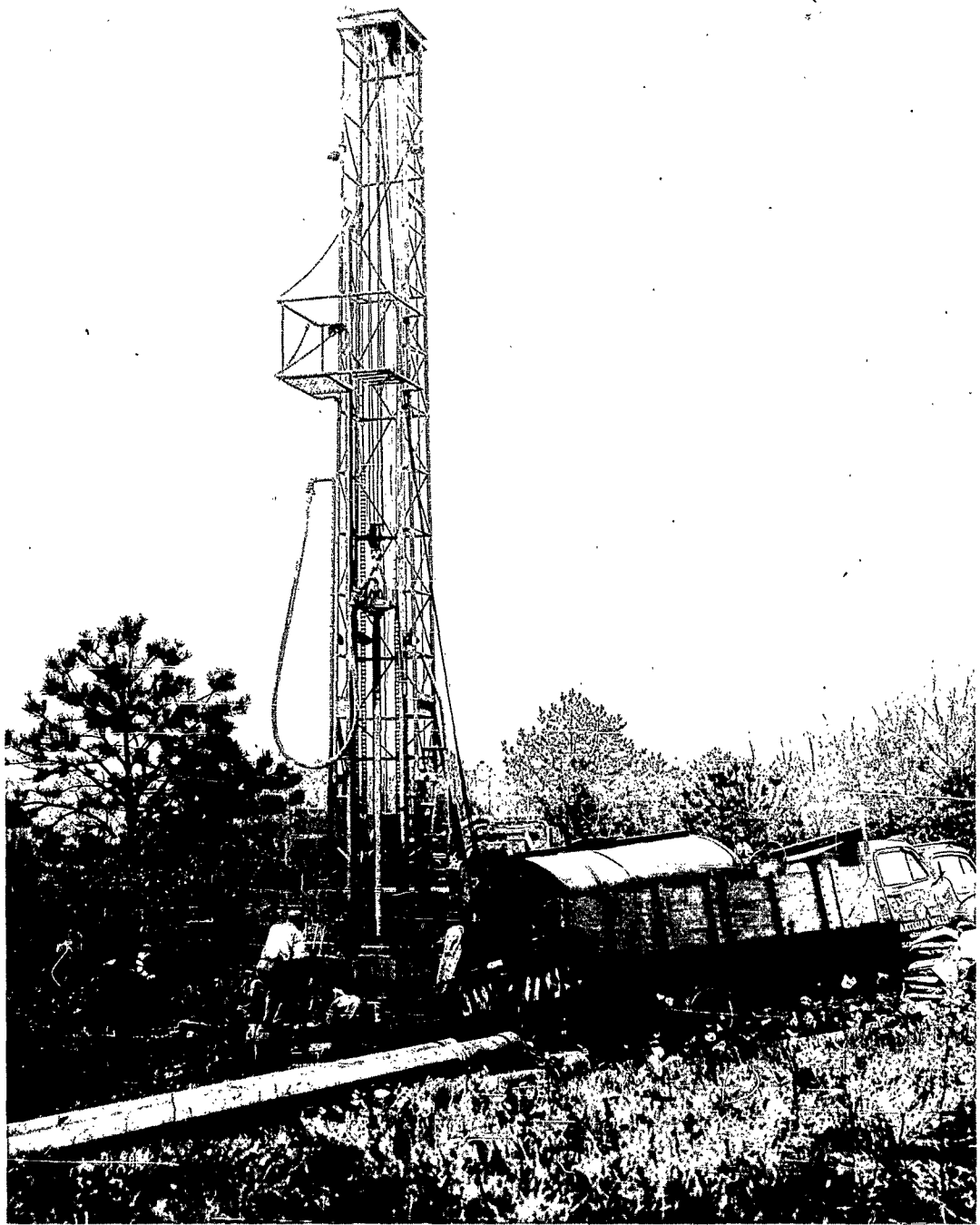
Figure III. 7.   Drilling - Harwich Site
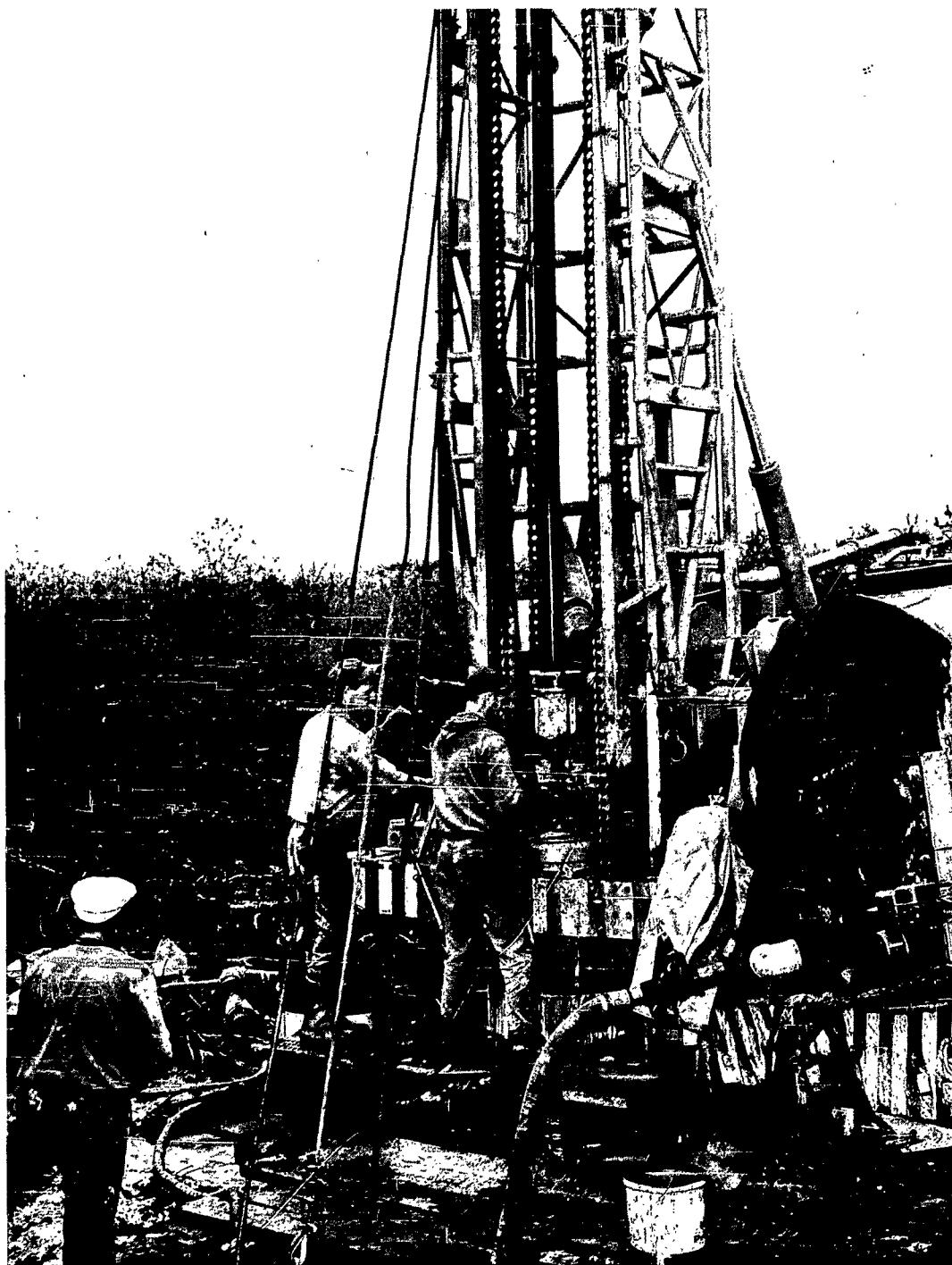
Figure III. 8.   Drilling - Harwich Site

Figure III.9.   Drilling – Harwich Site
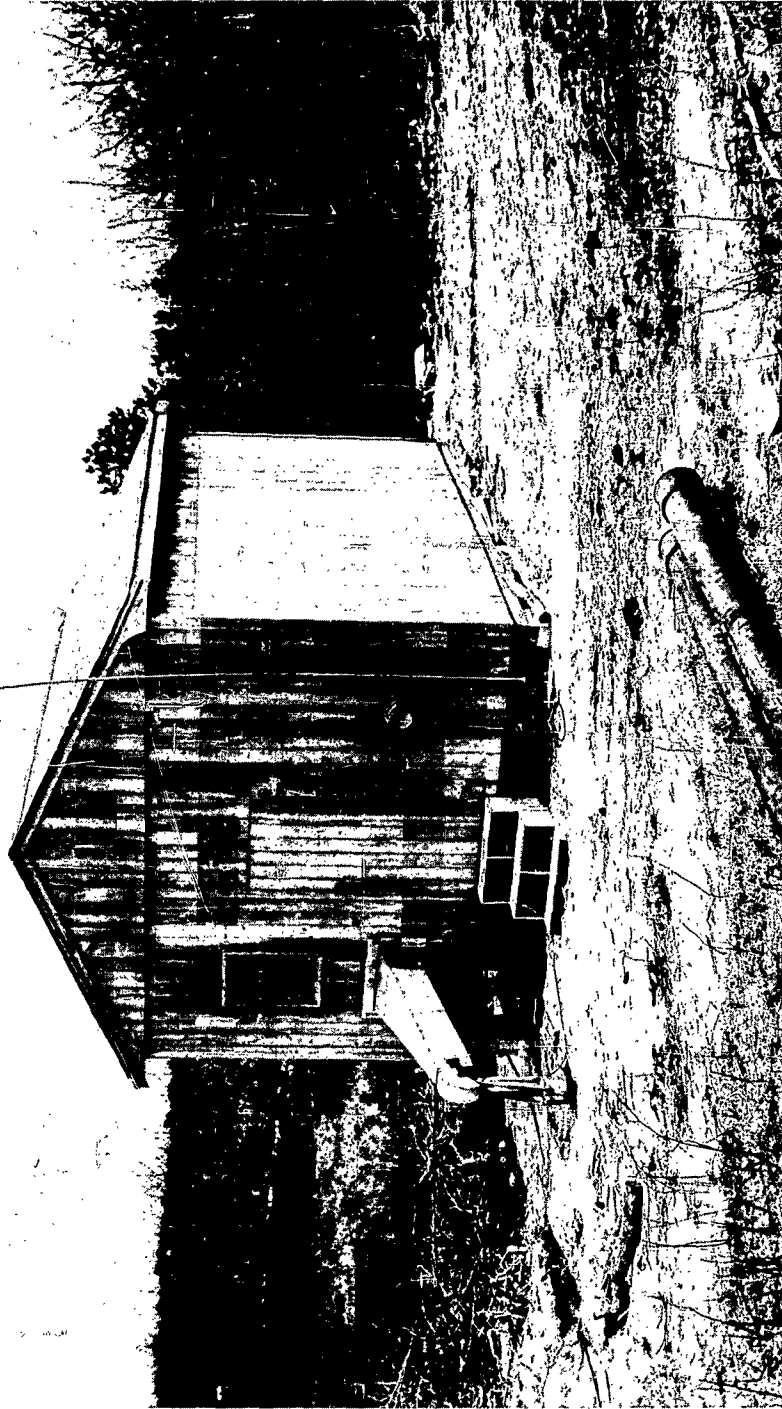
Figure III.10. Harwich
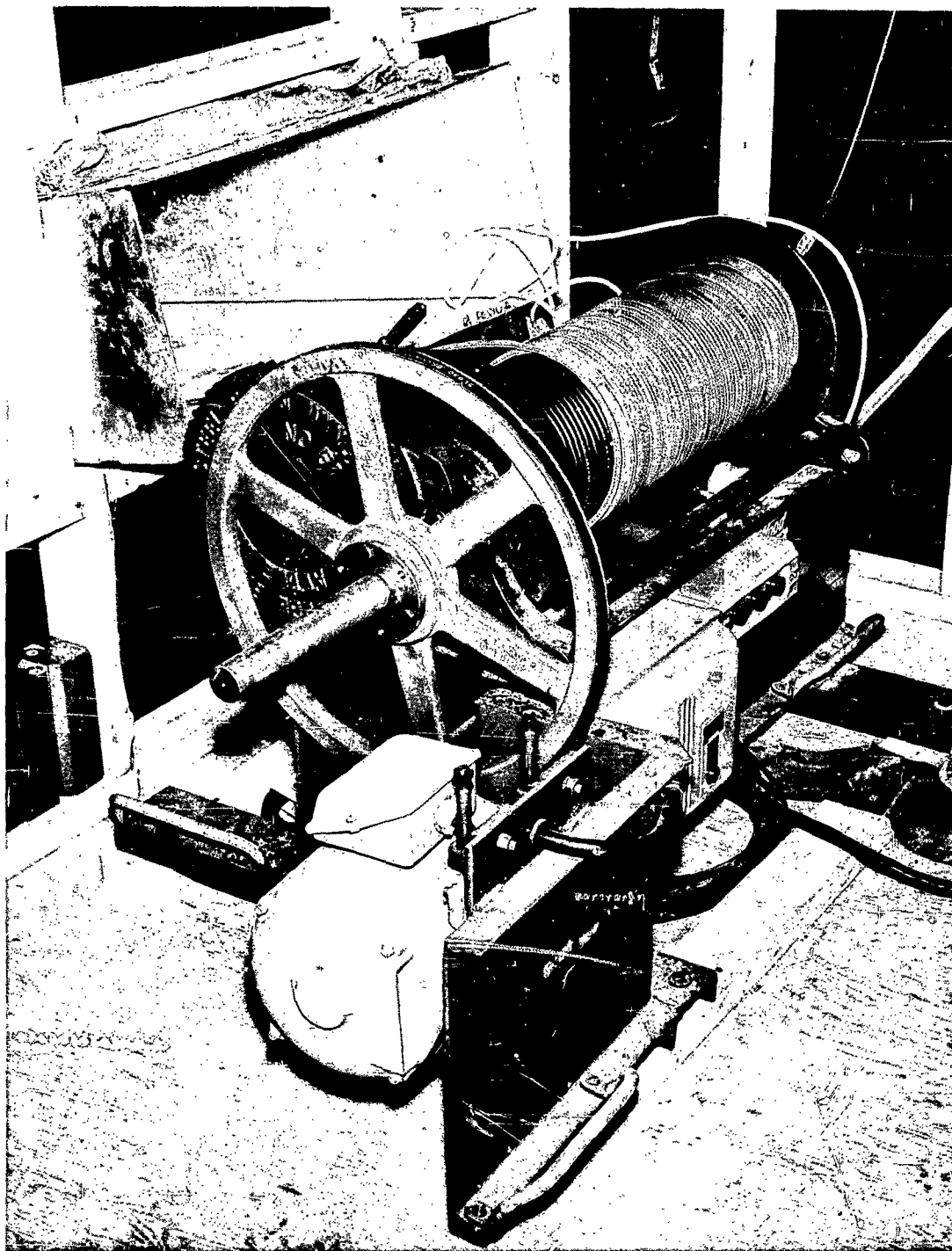
Figure III. 11. Cable Winch
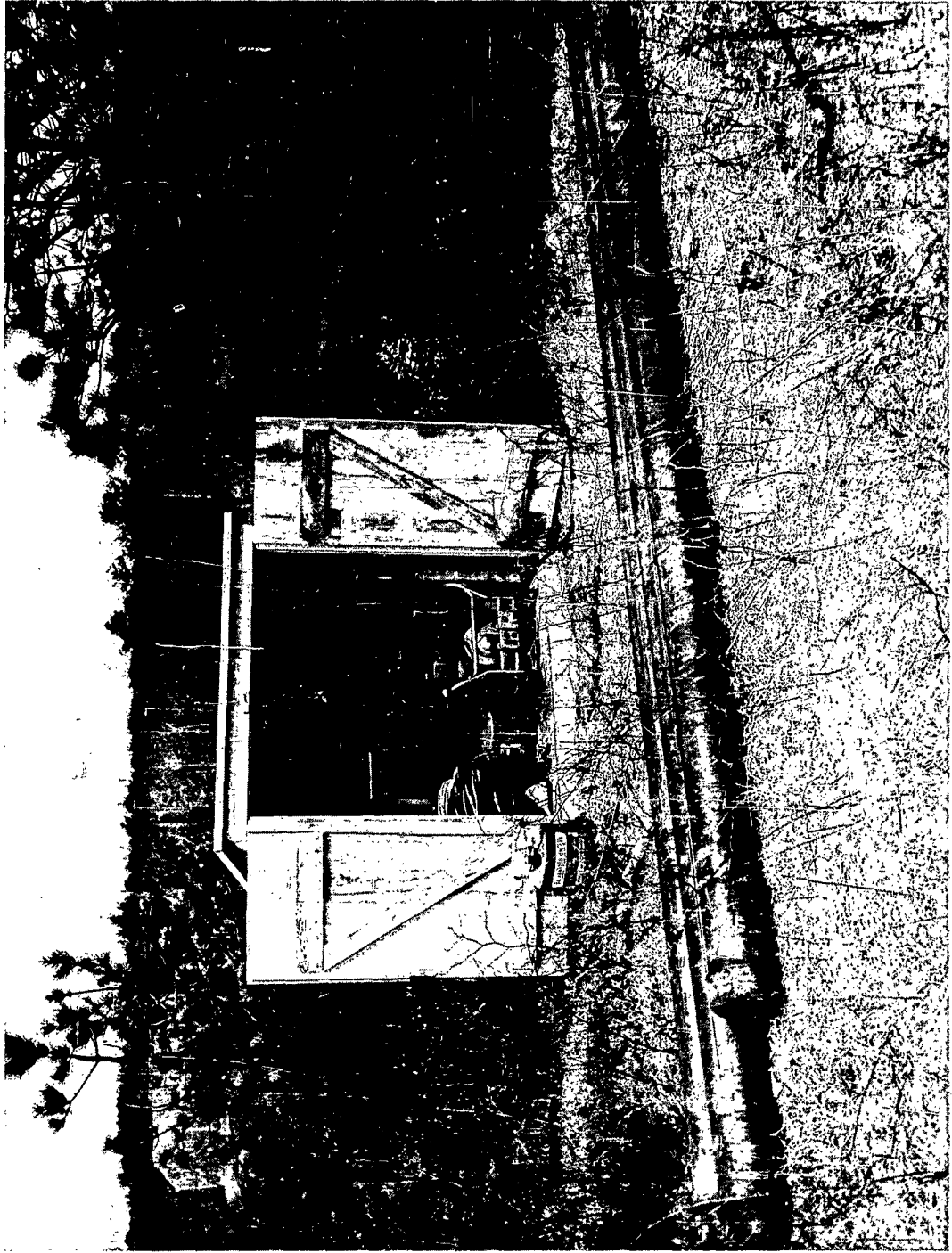
Figure III.12. Power Source – Harwich
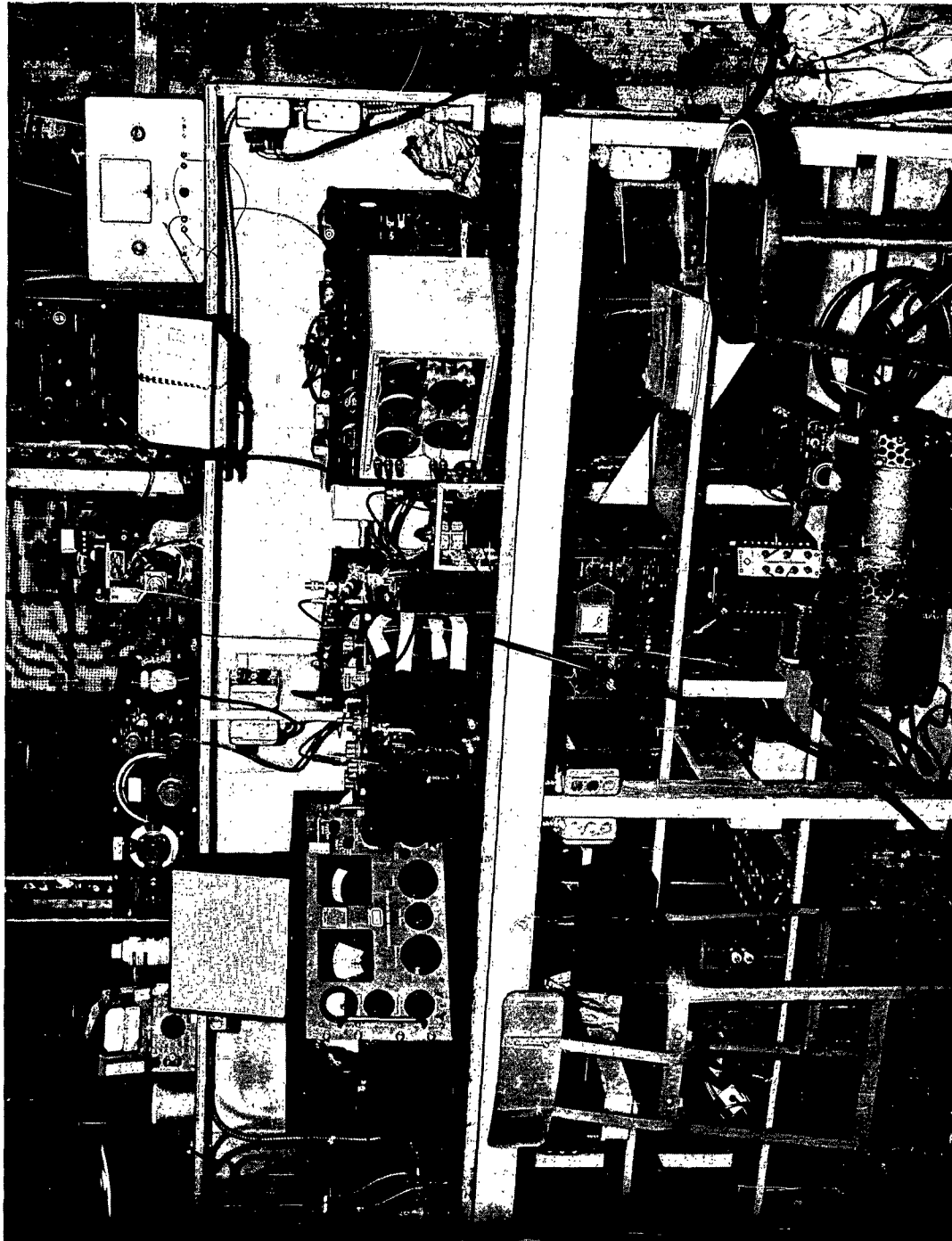
Figure III. 13.   Test Area – Harwich

Power was supplied by an external Onan 5 kw, 220/110 v. 60 cycle, single phase, gasoline driven generator installed in a prefabricated 4' x 6' shelter (see photograph in Figure III. 12).

The site was used extensively for antenna testing, signal and noise reception and for transmission and propagation measurements. For the latter an ART-13 transmitter permitted measurements at frequencies 200 to 500 kc and 2 to 18 mc. A view inside the screen room is shown in the photograph in Figure III. 13, made during antenna impedance tests. On the top shelf, to the left, is a bridge oscillator (General Radio) and to the right, a surplus BC-221 Frequency Meter. On the middle shelf, to the left, is a receiver (Hammarlund) being used as a bridge detector, and centrally located is an impedance bridge (General Radio). To the right are components of a "substitution box," parts of which were constructed by the Raytheon Company, CADPO Labs and others by the USAF CRL Communication Sciences Lab. To the rear is the ART-13 transmitter. On the floors are various power supplies for the ART-13.

6. Brewster (Mass.) Drill Hole Site at Town Dump

A view of the second site, at Brewster near the town dump, is shown in the photograph of Figure III. 14. A prefabricated 14' x 18' building houses a somewhat larger screen room than that at Harwich, the screen room being furnished as GFP. Shielding arrangements were improved in that the cable winch was installed inside the screen room and the complete feeder system was shielded by very thick copper piping and boxing around

Figure III.14.   Brewster

the pulley over the casing (not shown in Figure III. 14).

The site was used extensively for signal propagation, depth attenuation of the field, reception and antenna impedance tests. One transmitter is shown in the interior view in the photograph of Figure III. 15. This was one of the two GRN-6 transmitters on loan from the Signal Corps and moved from New Hampshire. Other transmitters used were a self-excited, 60 cps modulated, oscillator and a high power AF amplifier arrangement used in the successful propagation tests to the Tubman Road site described below.

The work was phased so that results of antenna measurements being conducted at Harwich could be applied to experiments at other sites which required a knowledge of antenna performance, e. g., attenuation with depth measurements at Brewster and transmission tests between Brewster and Tubman Road. Surface measurements of the azimuthal field patterns of buried antennas and variation of such patterns with range were performed at Brewster.

The site was used under permission of the Brewster Town authorities, and supplied with commercial 220/110 v. 60 cycle, single phase power, plus a telephone. Intercommunication with all sites and field personnel was accomplished here and at other sites via PRC-6 and PRC-10 radio sets loaned and maintained by AFCRL Communication Sciences Lab.

7. Tubman (Brewster, Mass.) Drill Hole Site

This site was located on Tubman Road (formerly Poverty Lane)
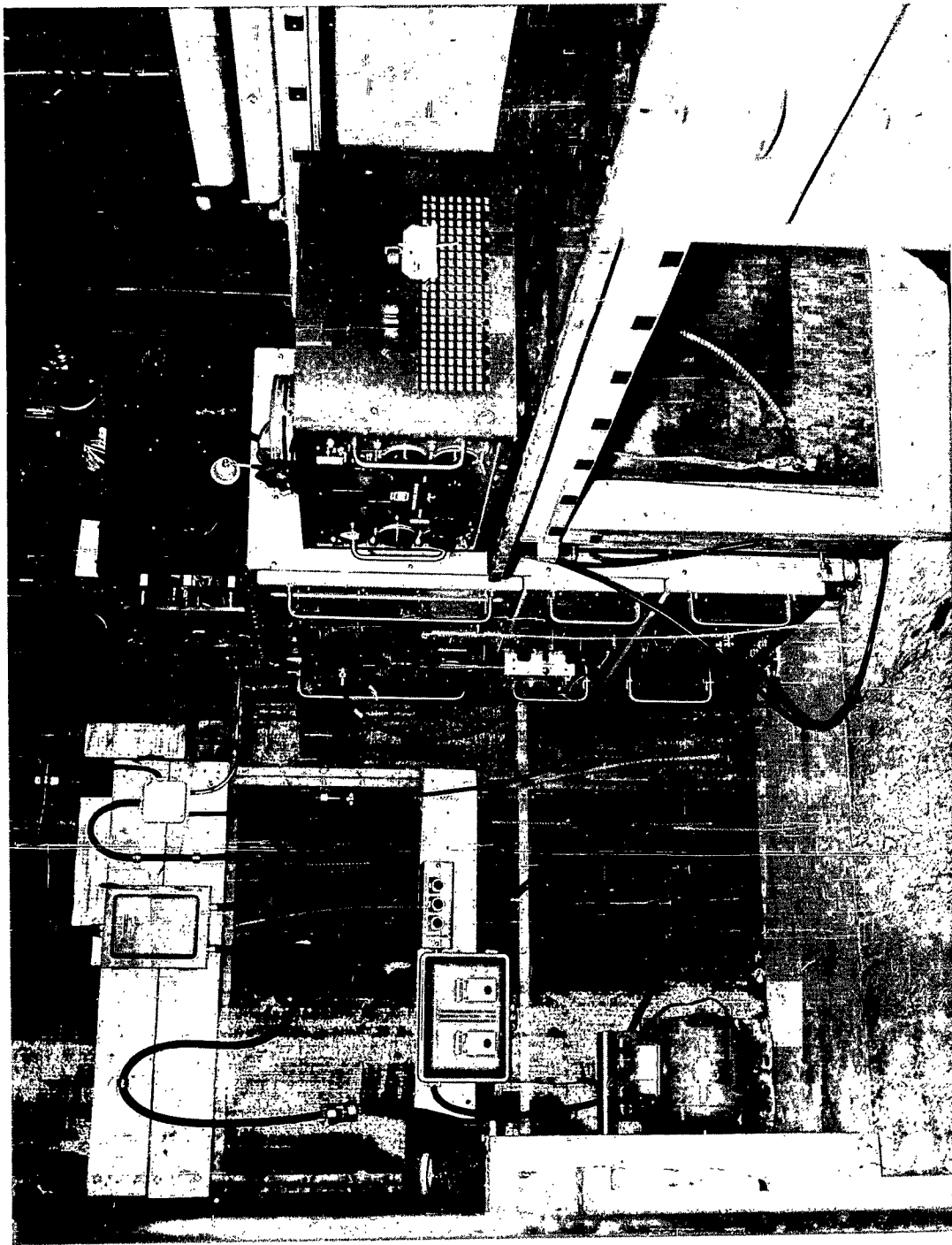
Figure III.15. Shielded room and facilities – Brewster

in Brewster and its use was arranged under a lease with R. Tubman, Brewster. The smaller diameter hole, about 2 3/8 inches in the rock, and again 1000 ft. deep was drilled under contract with E. J. Longyear Company, Minneapolis, Minn.

This last site is equipped with a large aluminum trailer with added arrangements for shielding. Power is supplied by external gasoline driven generators. The trailer and other site facilities, maintenance, and operation were furnished by AFCRL Communication Sciences Lab.

This site was used principally for signal reception measurements on transmissions from the previous site, conducted principally at lower VLF frequencies. Some depth attenuation measurements were also made. Measurements on core samples from the drill hole were made by M. I. T. (Professor Cantwell) as well as ourselves. Deep resistivity measurements on the surface between Tubman and Town Dump sites were made by Geoscience, Inc., for AFCRL.

There were various other locations used for very brief periods for special tests, descriptions of which are not given here.

B. Antennas

1. General Description

The antennas used for tests in vertical drill holes have been of the linear type. Designs for loop antennas have been made but tests have not been accomplished with this type of antenna.

Linear antennas made of <u>bare</u> wires or aluminum tubes were used initially a couple of years ago but since most holes contained water and the surrounding rock media were conducting dielectrics, <u>insulated</u> (or coaxial) types were studied more extensively (see Appendices D, E, and F).

Insulated linear monopoles with open-circuit termination at the "output end" were used extensively more than a year ago in the New Hampshire drill holes. The effect of the "ground" plane (overburden) is discussed in the next subsection.

As better information developed about the electrical character-istics of the rock, principally on Cape Cod, it became theoretically obvious (Section IIF) that operation at frequencies in the lower VLF range would be required to obtain a useful signal. For limited hole depth into the rock (500 feet) and frequencies lower than 20 kc, coaxial antennas of practical types, such as that made by stripping RG-8/U cable, would be electrically short. For electrically-short, coaxial antennas with open-circuit termination, the input impedance is highly capacitative and presents a large mismatch loss to a typical coaxial feeder (Appendix E). Electrically-short, coaxial antennas with short-circuit termination were then studied and employed since their

III-22

input impedance presented a better match to the feeder cable over a wider range of frequencies. The short circuit usually consisted of a piece of bare wire, #12 or #14 AWG, 20 to 50 feet long, connected electrically to the inner conductor of the coaxial element at its output end. A rough estimate of the terminating impedance would be that of the bare wire in the dissipative medium (Appendix D) and was generally much lower than the "characteristic impedance" of the coaxial insulated antenna (Section IV).

The theory of the performance of bare antennas is given in Appendices D and F, and measurements are discussed in Section IV. The theory of the performance of insulated antennas is given in Appendices E and F and measurements are discussed in Section IV. The insulated antennas used were mostly of the RG-8/U type, with the outer neoprene jacket and outer braid stripped off for the length of antenna desired. Some measurements were made of the impedance of vinyl covered wires. Teflon covered wires were purchased or furnished but have not been tested. (Teflon insulation has the advantage in that it has less water absorption than the polyethylene of RG-8/U cable.)

2. The Input "Ground Cage" and "Input Electrodes"

The problem of the "ground plane" arises when using a coaxial feeder connected to a vertical linear antenna, the latter being immersed in the rock medium situated below a more highly conducting overburden. For excitation or detection of waves travelling in the rock, an idealized "ground plane" would be a large, horizontal sheet of metal or ground screen located

along the rock-overburden interface at the antenna. This idealized arrangement was not feasible in practice. The effect of the overburden can be viewed as that of a somewhat lossy ground plane for antennas immersed in the rock if there is an appropriate connection to the feeder. For monopole antennas connected to the bottom end of the inner conductor of the coaxial feeder, then the bottom end of the outer conductor of the feeder should be connected to the overburden, particularly for HF measurements. In drill holes, a casing pipe penetrates through the overburden and the outer braid of the feeder may be connected to the casing pipe. This is accomplished by stripping off the outer neoprene jacket or covering of the feeder cable for a convenient length from the bottom end and relying on friction contact between the exposed braid of the cable and the casing pipe.

To ensure more positive contact between the outer braid conductor of the feeder and the casing, a "ground cage" was devised which clamped over the exposed outer braid of the feeder and provided several positive sliding contacts with the inner surface of the casing. The "ground cage" was positioned on the feeder near the bottom of the casing when using a monopole antenna whose input feed point was just flush with the bottom of the casing. The driving voltage from the coaxial feeder is then applied between the "base" or input point of the monopole (connected to the inner conductor) and the overburden via the casing and "ground cage" (connected to the outer braid conductor).

For monopole antennas having their "base" or input point flush with the casing, the antenna input impedance may be determined from a measurement of the input impedance of the feeder or by a substitution method. The former requires an accurate knowledge of the transmision line constants; the latter method may be used under many conditions, as discussed in the next subsection. If the overburden were perfectly conducting, the measured monopole impedance would be half of that of a dipole in an unbounded rock medium (the correction for coaxial line terminal zone effects is assumed negligibly small[*]). For an overburden of finite but high conductivity compared with the rock, the input impedance of the monopole would include terms attributable to losses in the overburden which would depend presumably upon antenna type, i.e., bare or insulated wires.

If the antenna is lowered into the drill hole to greater depths below the overburden, i.e., below the casing, analytical difficulty is encountered in interpreting measured impedances because of the effect of the extended coaxial feeder. For studying the effects of variation of antenna depth upon antenna impedance and radiated field, it would be desirable to carry a "ground plane" along with the antenna. This was not feasible. A compromise may be achieved by stripping off the outer neoprene jacket of the feeder cable and having the exposed braid outer conductor in contact with the medium (via the conducting water in the drill hole). Antenna currents flow on the outside of this exposed braid back from the "monopole" input

---

[*] See Reference 6, Chapter V, Section 22.

point at the end of the feeder. At HF, but where the loss tangent is still large, such currents attenuate rapidly with the distance d back from the end of the feeder because the skin-depth is small. At a distance d slightly greater than 2 skin-depths, the antenna current amplitude has fallen to 0.1 of the value at the end of the feeder. Considering the driving voltage to be that at the end of the coaxial feeder, the antenna system may be considered to be crudely that of an asymmetrically driven dipole; the driving-point impedance is then the sum of two components, one the impedance looking down of the antenna proper considered as a monopole and the other that of the "input electrode," i.e., the exposed outer braid of the feeder, looking up. As d is further increased, the impedance of the latter should not change markedly (Appendix D and Section IV). The situation at LF and VLF needs further examination because there the braid input electrode, if grounded to the casing, would be more nearly at the same potential as the overburden and questions arise as to what type of antenna is a proper probe at such frequencies for measurement of the variation of field intensities and properties of the medium with depth.

Photographs of the "ground cage" device are shown in the disassembled view of Figure III. 16 and the assembled view of Figure III. 17. In the figures an insulated monopole antenna is shown at the extreme right, connected to the inner conductor of the feeder (RG-8/U here) which has the neoprene cover jacket peeled off to leave the braid exposed. The cage device was fabricated from beryllium copper spring stock screwed to copper collars
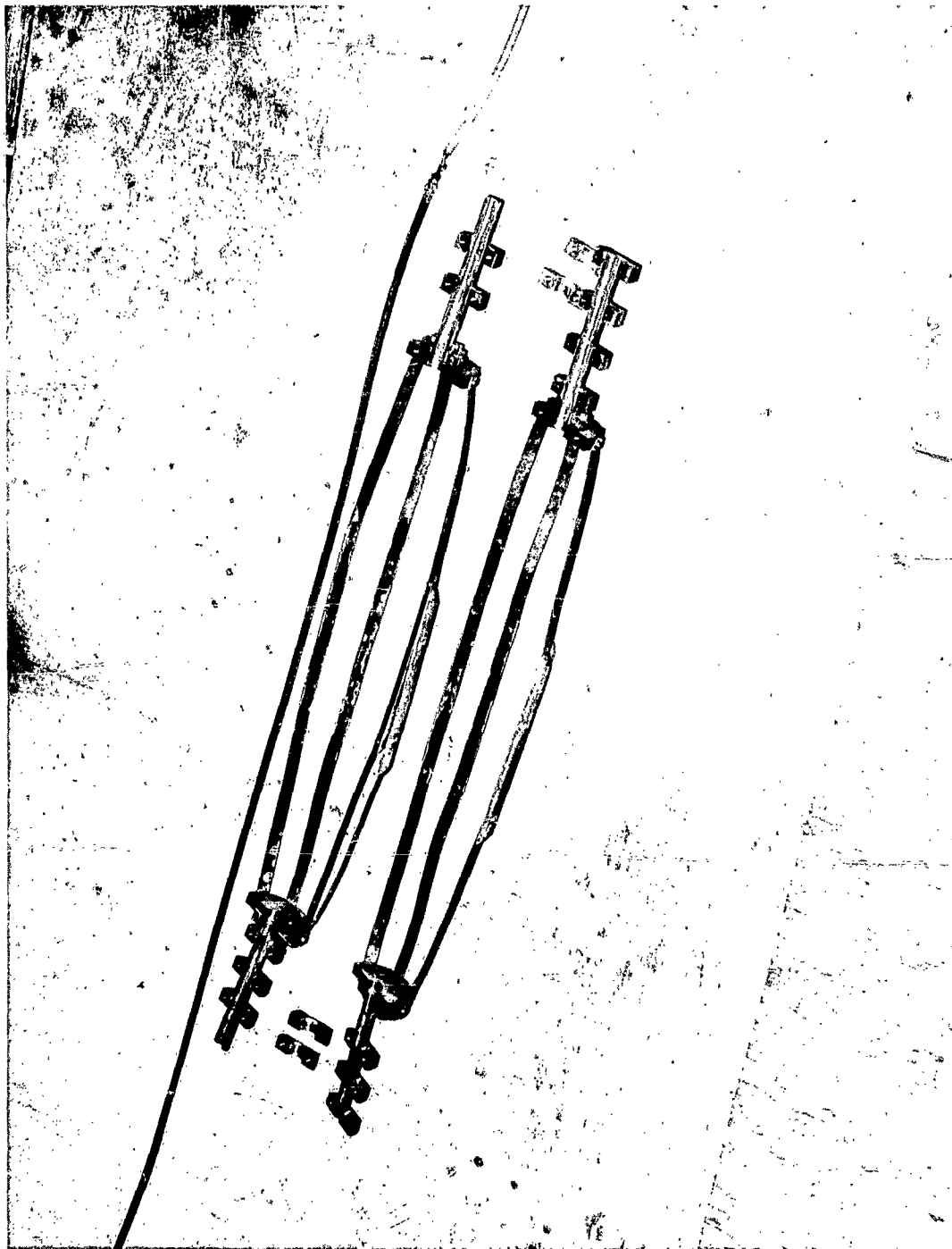
Figure III. 16.   Ground Cage - Unassembled
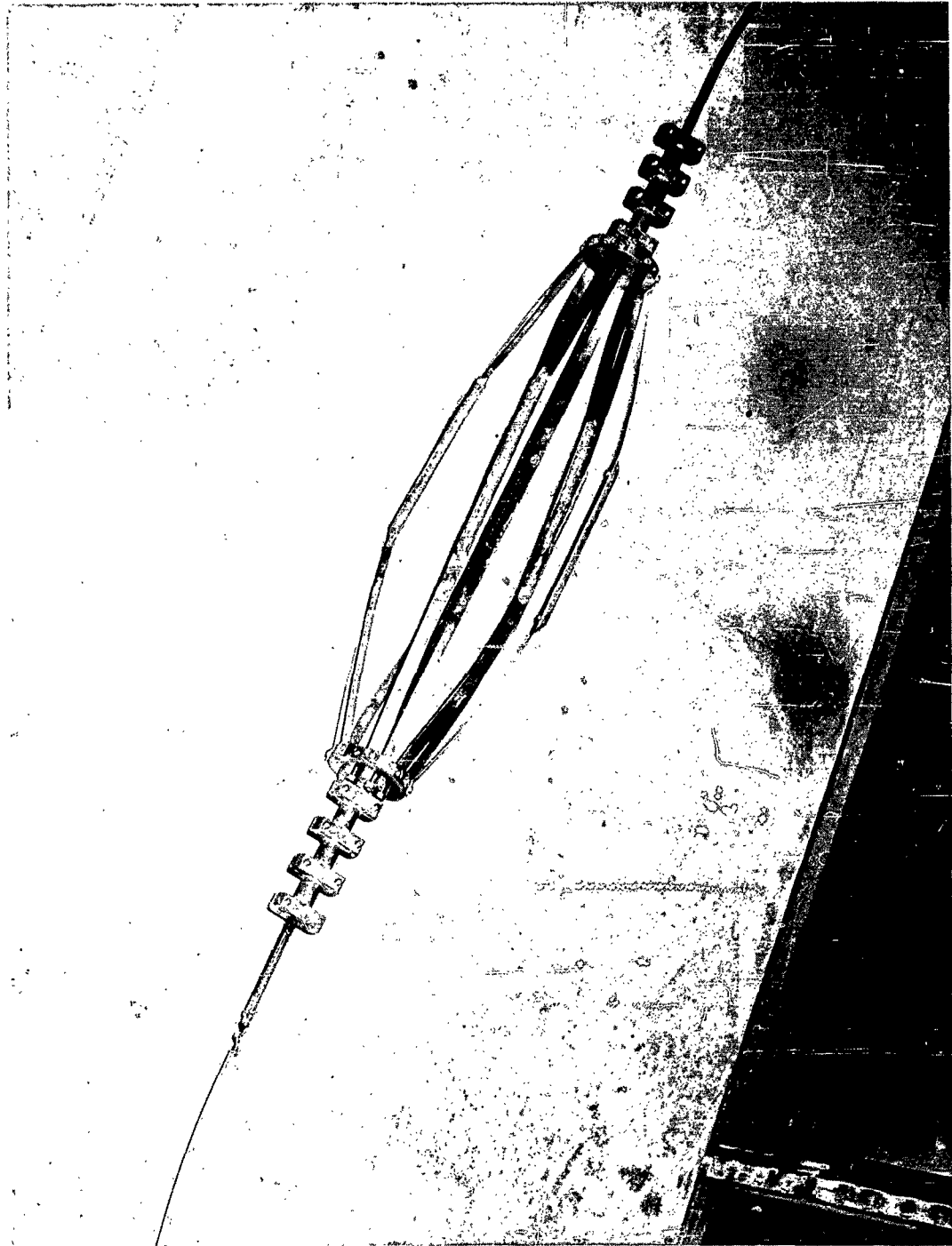
Figure III.17.   Ground Cage Mount - Assembled

and sleeves. Rubbing contactors of brass were soldered to the spring stock. The whole assembly was split in two down the middle to afford ease of assembly and disassembly. The assembled view is shown in Figure III. 17 for measurements of antennas whose input was flush with the bottom of the casing. Adjusting the tension on the springs by spacing the collars contacting the feeder braid varied the amount of friction contact as desired. Adjustments were necessary in each hole due to variations in casing pipe diameters and were required after every assembly-disassembly operation.

All antennas were weighted with counterweights of lead or iron principally cylindrical in form, such as window sash weights.

3. The "Substitution Box" for Impedance Substitution Method

It was necessary to use long feedlines to the antennas when the antennas were immersed in rock deep below the surface. If one knows accurately the electrical characteristics of the feeder (characteristic impedance, total attenuation and total phase shift), one can obtain in principle the antenna impedance terminating the transmission line from a measurement of the input impedance of the line. A useful device for such purposes is the Smith Chart transmission line calculator. When making a series of measurements over a wide range of frequencies on various antennas, the Smith Chart can reduce the time required to obtain antenna impedances. However, from many measurements made earlier in New Hampshire the accuracy of the result leaves much to be desired, particularly when trying to locate resonant and anti-resonant frequencies and the impedances at such frequencies. This

is because the antenna impedances very often were very large, and exact

knowledge of line parameters was not available. The points on the calculator

were then in high standing wave ratio, less accurate, areas.

A substitution method was devised for measurements in

New Hampshire in the Spring of 1961. The method and the "substitution box"

are described here rather than in Section IV on antennas, to round out the

description of equipment employed. The "box" was simply a series or par-

allel arrangement of variable R, L, and C components. The description of

the method employed follows. The input impedance of the line was measured

noting carefully bridge dial settings. The antenna was removed and the "sub-

stitution box" connected in its place at the end of the transmission line. The

components of the "box" were varied to give the same input impedance as

obtained with the antenna was affixed. Then the impedance of the sub box

was measured and called the "antenna impedance." In practice, full fre-

quency runs would be made with the antenna in the hole, measuring line input

impedances throughout and noting carefully all pertinent bridge dial settings.

Then the antenna and line would be removed from the hole, the antenna dis-

connected and "substitution box" connected in its place. Then all data for

the run would be obtained as antenna impedance vs frequency for example

for a given antenna configuration.

A photograph, showing a closer view of the equipment at Harwich

mentioned earlier, is shown in Figure III. 18. The substitution box (not con-

nected in the photo) is shown on the right to the front in a metal box with its
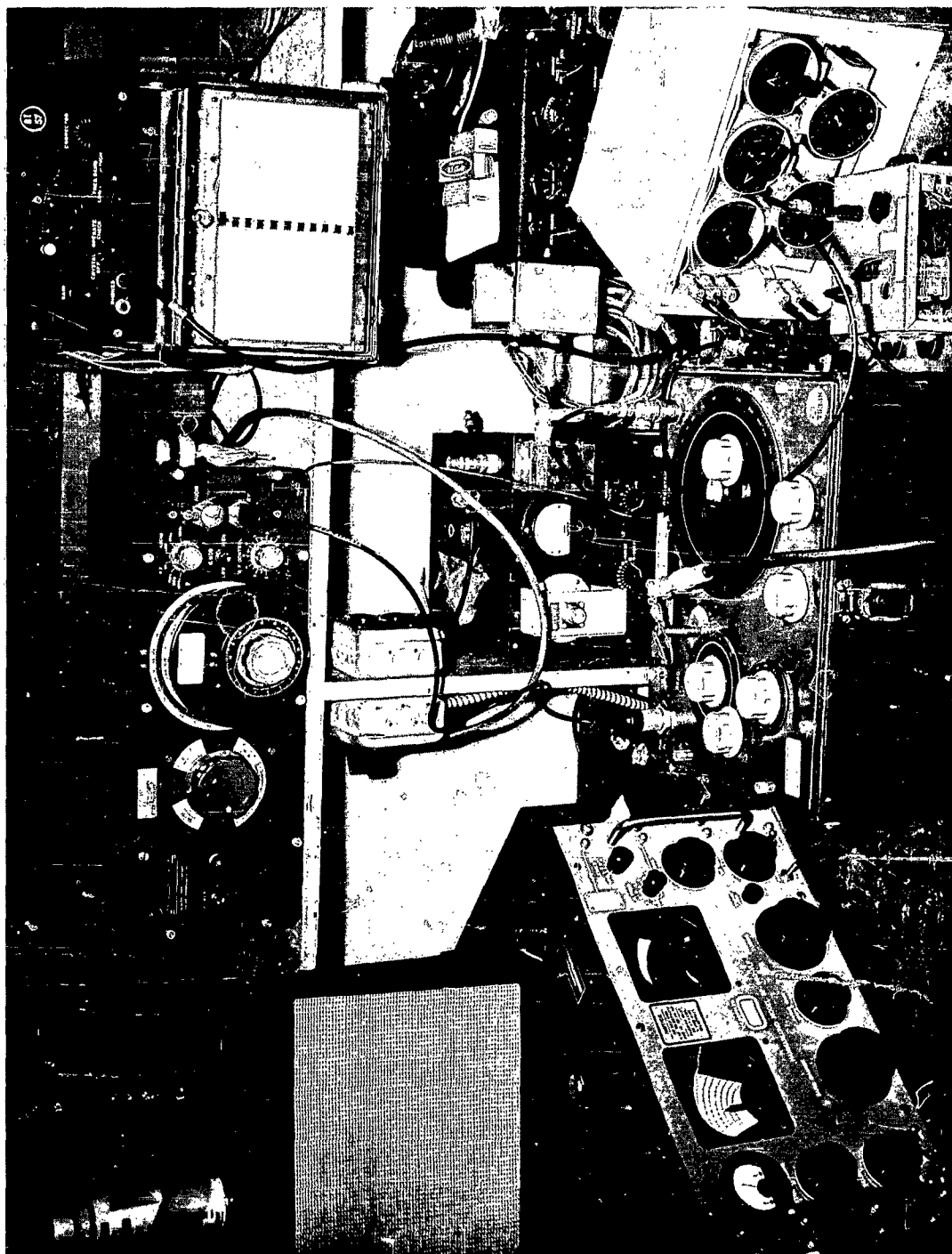
Figure III.18.   Measurement system with sub-box components

cover removed. Auxiliary, step-variable R and C components are in a larger

box just to the rear. The bridge on the same shelf here was the General

Radio Company Type 916-A, with General Radio Company Bridge Oscillator

on the top shelf. The BC-221 Frequency Meter was used to set initial line

impedance measuring frequency and to reset the oscillator for substitution

measurements. The detector in use here is the Hammarlund SP-600 VLF

shown to the left of the RF Bridge.

An example of antenna impedance obtained by Smith Chart

calculator and substitution box methods is shown in Figure III.19. Measure-

ments were made in the Spring of 1961 at Goffstown, N.H., on a 123-foot,

insulated (RG-8/U type), open-circuited, monopole. Results are shown on

the complex plane (X-R) spiral plot, which shows up rather sensitively the

frequency dependent parameters. The plot with substitution box data is

smoother, more accurate and locates resonances reasonably quickly (of

course, plots of X vs f are the better for the determination of resonance but

a smooth X-R spiral plot indicates useful data will result).

Another example of the comparison of more recent data is

shown in Figure III. 20 for an antenna in the Harwich drill hole. A 475-foot,

open-circuited, insulated monopole (RG-8/U) terminated a 759-foot length

of coaxial feeder of the RG-9/U type. Better knowledge of the RG-9/U feeder

characteristics was obtained, but still the phase shift seems to be off a bit

(note anti-resonance at f slightly greater than 250 kc by sub box data vs

slightly less than 235 kc via Smith Chart data).
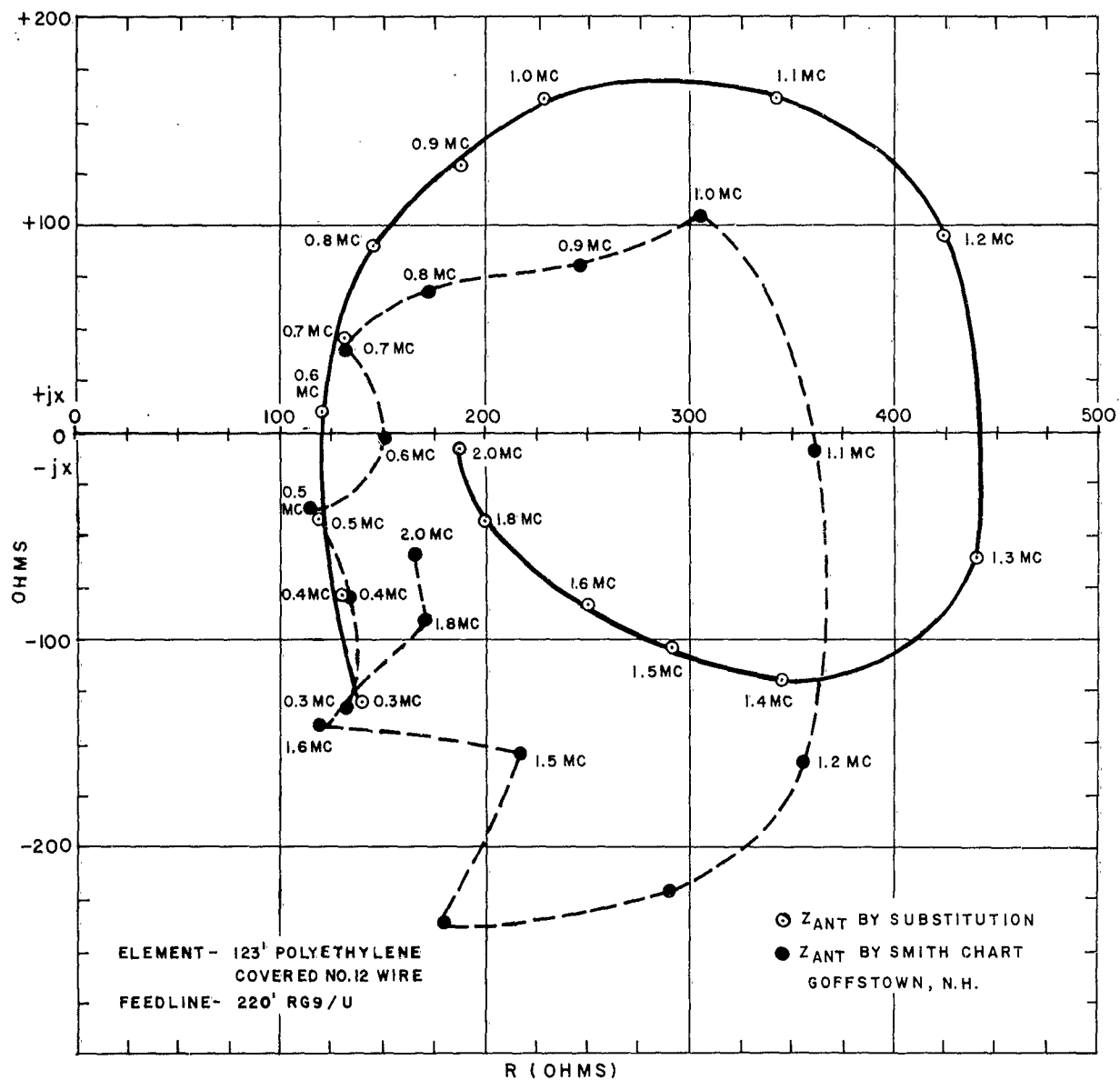
Figure III. 19a.   Antenna Z plot (X vs R) - Goffstown
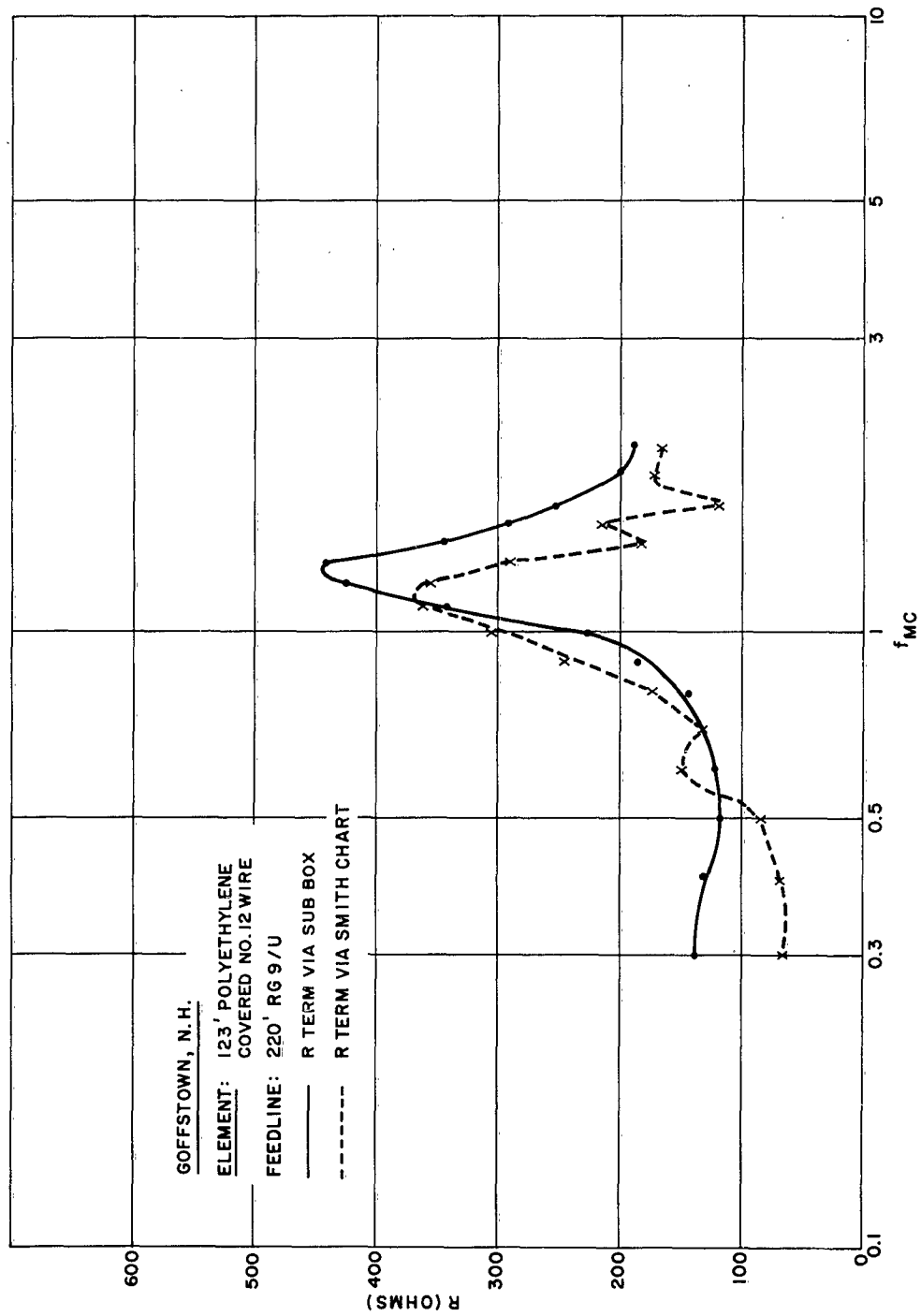
Figure III. 19b.   Antenna input impedance (R vs f) - Goffstown
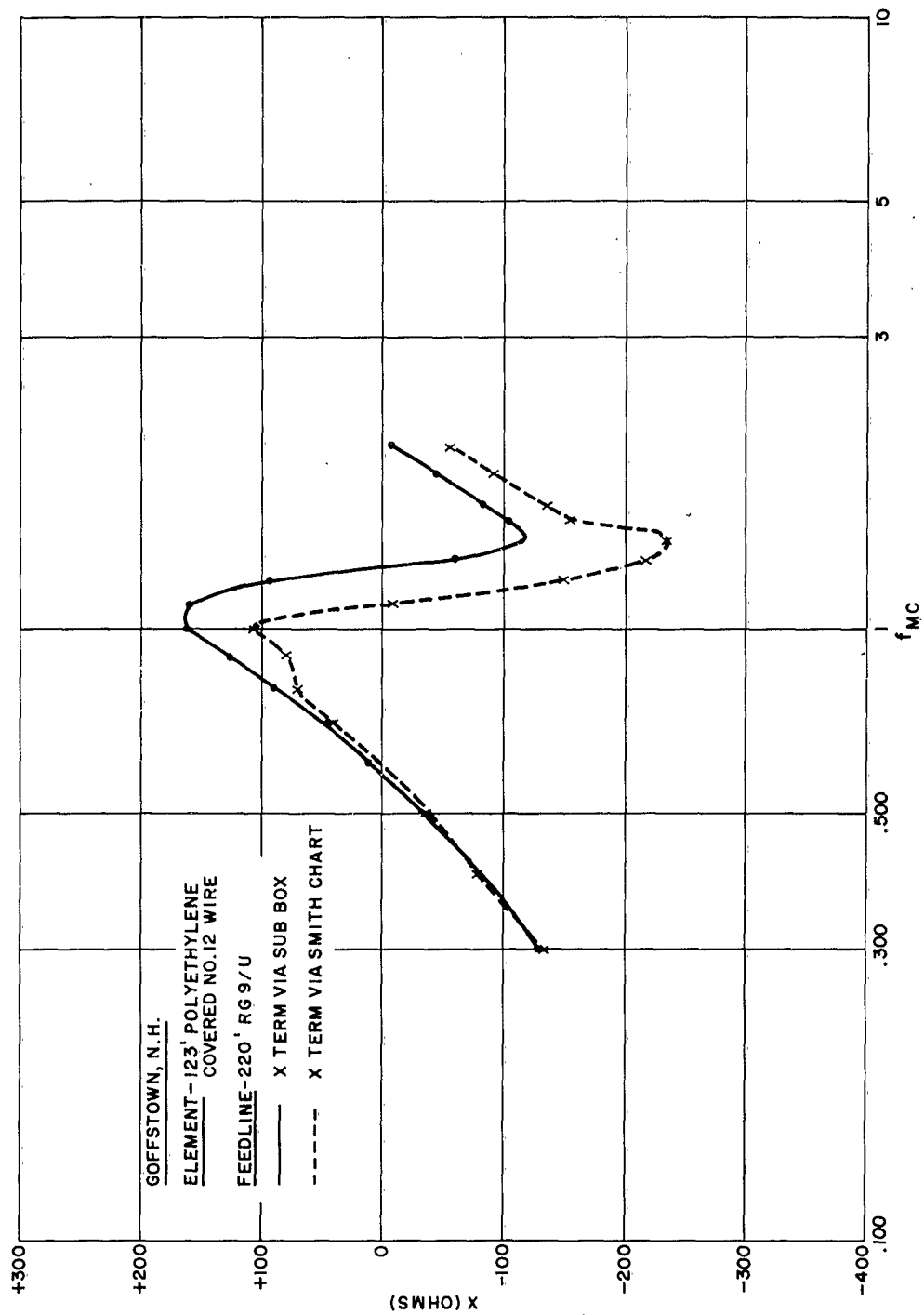
Figure III. 19c.   Antenna input impedance (X vs f) – Goffstown
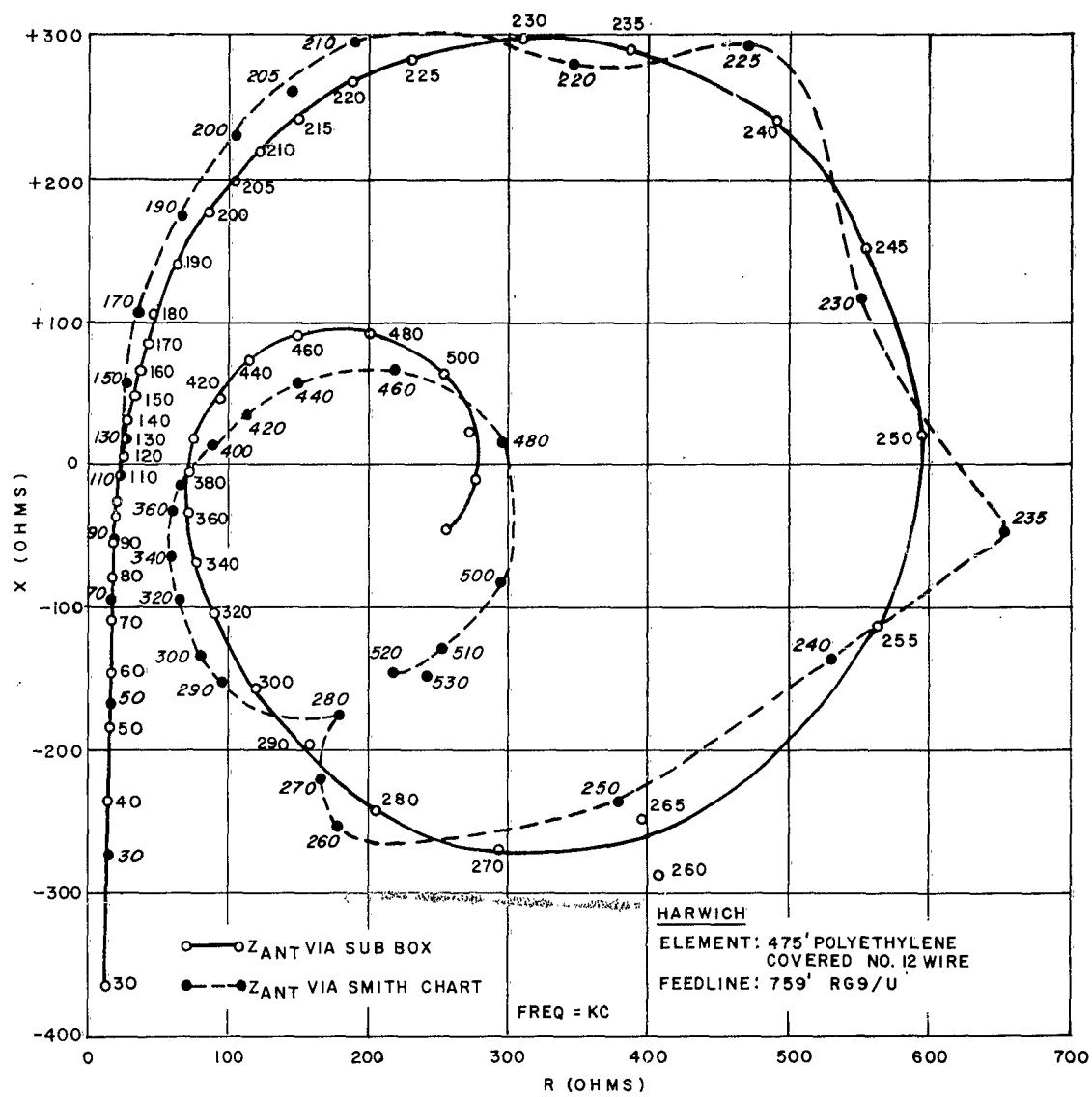
Figure III. 20a.   Antenna impedance (X vs R) - Harwich
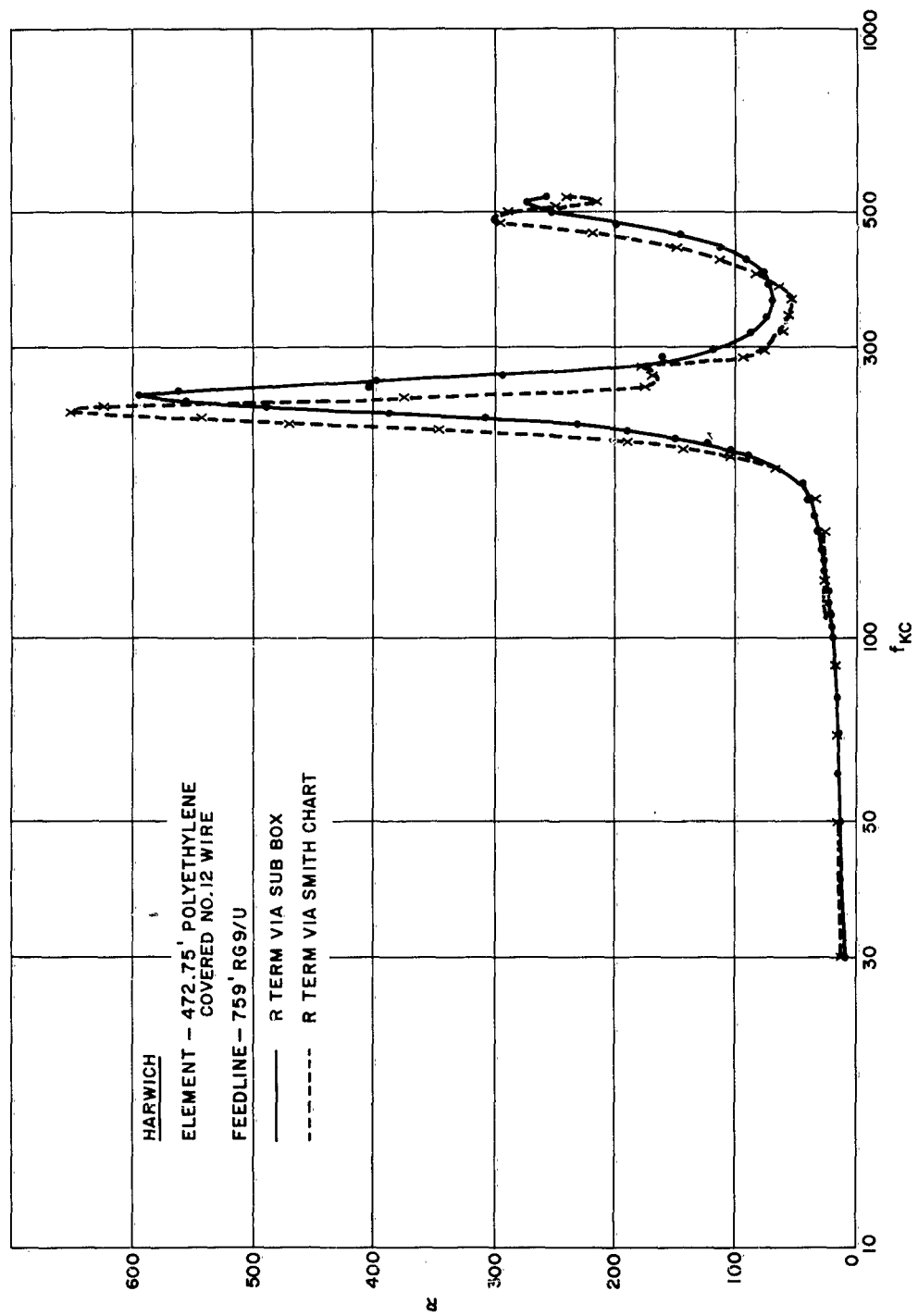
Figure III. 20b. Antenna impedance (R vs f) - Harwich
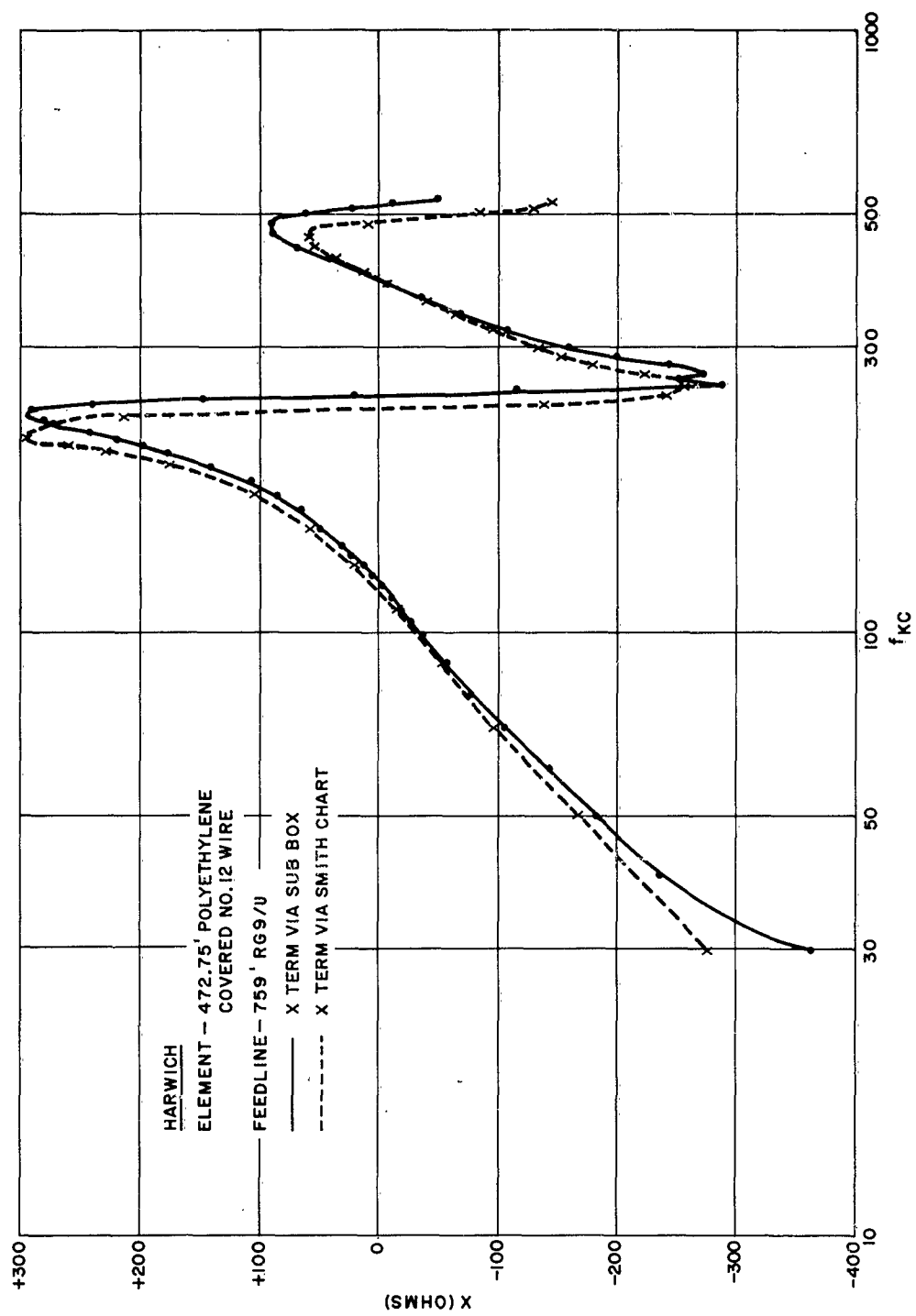
Figure III. 20c. Antenna impedance (X vs f) – Harwich

The substitution box method appears to be well suited for determining the impedance characteristics of the antennas vs frequency at MF and HF. However, there is another limitation at ELF over and above that mentioned regarding the "input electrode" (Section IIIB 2). The assumption is that the electrical characteristics of the feedline when immersed in the hole do not change when substitution methods are being used, e.g., when the feeder is wound up on the winch. The difficulty has shown up when measuring high antenna impedances at frequencies less than 20 kc when using RG-8/U feedlines. This is attributed in part to the fact that at such low frequencies the skin depth of outer conductor of the feeder is comparable with or may exceed the thickness of that conductor. Then the effective characteristic impedance for the line down in the hole will depend upon rock characteristics and will differ from that when the line is wound up on the winch for substitution box measurements. This effect was uncovered most recently upon comparing line parameters computed from "open" and "short" circuit impedance measurements with the coaxial feeder cable wound on the winch with similar computations from measurements with the feeder down the hole. Then a further comparison was made of feeder characteristics computed from measurements using known resistance terminations of 10 and 1000 ohms. The line input impedances with these terminations were measured with the feeder wound up on the winch and then with the feeder down the hole. The resistors were heavily shielded by thick, cylindrical shield containers, epoxied, and measured alone on the bridge. Line impedances with 10-ohm

terminations were practically the same under all conditions at frequencies from 1 kc and higher indicating the series impedance of the cable per unit length (1000 foot length of RG-8/U) remained unchanged. The input impedance with 1000-ohm terminations varied markedly from that obtained with the cable on the winch from that obtained with the terminated cable at various depths in the hole and the input impedance of the terminated line differed markedly at different depths, particularly at frequencies lower VLF and ELF ranges. This indicated that the shunt admittance per unit length varied with surrounding environment and accordingly both Smith Chart and sub box methods for obtaining antenna impedances for the greater depths were limited in utility.

The full effect has not been analyzed but there are obvious remedies such as employing jackets or braids of magnetic material on the cable, or using triaxial cables. Some lengths of the latter type of cables are now on hand but have not been tested or used. Also, from the standpoint of probe antennas to measure depth variations of fields there may be merit in using shielded twin conductor cable like RG-22/U with each conductor connected to the electrode ends of the probe antenna. A reel of this cable is on hand, to be tested first for any variations of line parameters with depth with known resistance terminations and then for use with probe antennas (separated linear electrodes or loops).

C. Transmitters

The following transmitting units have been used for various phases

of the project.

— ART-13 surplus transmitter, frequency range
200-500 kc and 2-18 mc, nominal 100 w output,
CW, MCW or voice.

— GRN-6 beacon transmitters (2) on loan from Signal
Corps to Raytheon Company, nominal 190-500 kc
(operational down to 150 kc, and down to 100 kc with
minor modification), power 300-400 watts, CW, MCW
or voice.

— Self-excited oscillator, Ultrasonic Industries, Inc.,
"Disontegrator System" 320. Half-sine wave 60 cps
pulses, nominally at 75 kc carrier frequency.

— Audio amplifier, constructed by AFCRL (Comm. Lab),
frequencies up to 30 kc nominal 75 watts maximum.

— Audio frequency generator, Comm. Measurements
Lab 1420B, power 300 watts up to 30 kc, reduced
power at frequencies 30 to 50 kc.

The ART-13 and GRN-6 units are shown and identified in various

photographs of Section IIIA. The last three units were employed in the latest

phases of the project, particularly for rock propagated signals on Cape Cod,

which were not detected until frequencies lower than 15 kc were used.

D. Receiver and Pre-amplifier

1. Noise Figure of Hammarlund SP-600-VLF Receiver

Preliminary work on deep strata signal reception measurements

was done entirely with the Hammarlund SP-600 VLF receiver covering the

range of 10-530 kc. Early communication attempts were done in the range

of 200 kc and up, 200 kc being the lower limit of the ART-13 transmitter used
as a source of reasonable power, i.e., 100 watts. Ordinarily the atmospheric
noise at these frequencies obviates any necessity for extremely low noise
figure values of the receiving equipment. However, for rock propagated
signals and vertical antennas immersed below the earth's surface, and with
the receiver equipment located in a well shielded room plus other additional
shielding safeguards, internal receiver noise may be the limiting factor for
detecting the signals. Preliminary tests at the Cape Cod Brewster site
indicated that at frequencies less than 50 kc the less effective overburden
"shielding" allowed attenuated atmospheric noise to be detected on the antenna
deep in the hole. (Any reduction in effectiveness of the screen room and
other shielding safeguards on the surface at the lower frequencies is disre-
garded at this point.)

Later work was done with a GRN-6 beacon transmitter which
allowed operation on frequencies as low as 150 kc and with minor modifica-
tions to 100 kc. The pre-amplifier evolved for use with the SP-600 VLF
receiver could be operated over the range of 200-500 kc, a later modification
reducing its lower frequency capability to 100 kc.

Preliminary noise measurements were made on the SP-600
VLF receiver over its frequency range and at several bandwidths to determine
its capabilities. Measurements were conducted with a Rohde and Schwarz
type SUF noise generator (see Figure III. 21 for block diagram). The noise
figure of the receiver under test, in decibels, was derived from the standard
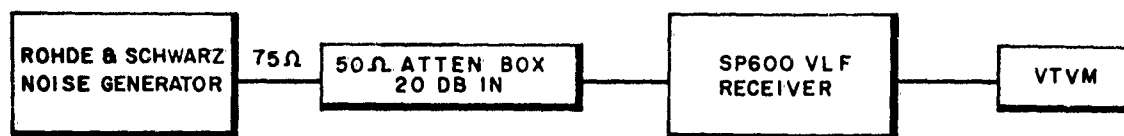
Figure III. 21   Noise Figure Measurement Setup

noise level KTB of -204 dbw/cps minus the output noise voltage of the noise

generator (E_o^2) x receiver bandwidth x SUF calibrate number corresponding

to the noise bandwidth output of the unit.   A noise bandwidth spectrum of

30 cps to 600 kc was used as the output of the noise generator, requiring a

correction multiplying factor of 22 x 10^{-9} w/cps.   Image rejection of the

receiver in question was sufficient to disregard any possible increase in

apparent noise figure due to this factor.   The results of measurements are

shown in Table III. 1.

TABLE III. 1

Noise Measurements on VLF Receiver (SP-600 VLF)

f kc	Noise figure at SP-600 VLF IF bandwidth equal to	
	1. 3 kc	6. 0 kc
15	6. 9 db	7. 0 db
50	11. 0 *	9. 0 *
100	6. 5	6. 2
200	6. 2	6. 0
350	8. 9 *	12. 0 *
500	6. 0	6. 5

*Differences with bandwidth unresolved

These noise figure measurements were taken in an open laboratory area. The same measurements conducted in a shielded room gave lower values of noise figure by approximately 1 db. The shielding of the input circuits of the receiver itself was considered adequate as noise measurements in the test area using a Stoddart NM10-A noise and field intensity meter with a short vertical whip gave noise levels of 20 db > 1 μv at 500 kc to 56 db > 1 μv at the lower frequencies of 150 to 200 kc.

2. Transistorized and Tube Pre-amplifier

Consideration was given to use of solid-state circuitry, its potential small size and the feasibility of battery operation being attractive for contemplated installation at antennas in drill holes as well as on the surface. None of the configurations tried some time ago improved the noise figure of the overall receiving system. The problem at the time was primarily one of state of the art for the components. Some transistors investigated had adequate noise figure ratings but with a degradation of 6 db/octave at frequencies higher than $f = f_\alpha \sqrt{1 - \alpha_o}$ where f_α is the α cut-off frequency and α_o is the low-frequency current gain. In general, there was conflict between the necessity of low current to satisfy the low noise requirement and the high frequency requirement where the α cut-off frequency is inversely proportional to the emitter current, in general being lower at low emitter currents than the typical data sheets would indicate. The best transistor tried had a noise figure rating of 3 db with adequate high frequency performance but results were not satisfactory. None of the circuits tried

resulted in any improvement in the overall receiver noise figure.

Tube circuits were investigated with more satisfactory results. One suitable configuration is the conventional cascode circuit where the first stage functions as a conventional grounded-cathode amplifier in turn feeding a grounded-grid amplifier. This circuit allows maximum power gain from the first stage with resulting maximum reduction of second-stage noise. The grounded-grid second stage presents a high conductance to the plate of the first stage and this heavy loading severely reduces any tendency toward oscillation. The following basic approximations indicate the approach employed for obtaining the circuit parameters:

$$\text{Noise figure} \cong 1 + R_{equiv} \, G_s$$

where R_{equiv} is the equivalent grid-noise resistance in ohms of the tube selected and G_s is the source admittance in mhos. This formula assumes $G_1 >> G_s$ where G_1 is the input admittance of the stage. Also,

$$R_{equiv} = \frac{2.5}{g_m} \quad \text{(for triode amplifiers), ohms}$$

where g_m is the transconductance in mhos.

A triode with a high value of g_m is necessary for low noise applications. Accordingly, a 417A was used as the input amplifier of the unit. The 417A has a g_m = 30,000 micro-mhos, whence R_{equiv} is about 75 ohms which would indicate that noise figures below 2 db could be achieved for expected values of G_s. The low impedance of some of the antennas employed in deep strata reception would require coupling circuitry to establish G_s at a suitable value.

Figure III. 22 is a schematic of the unit evolved which performed

satisfactorily.

Noise figure measurements were made on this unit using the

same technique outlined earlier and results are given in Table III. 2.

TABLE III. 2

Tube Pre-amplifier Noise Figure vs Frequency

$\dfrac{f}{kc}$	Noise figure (db) SP-600 VLF B.W. = 1.3 kc
500	2.56
400	1.72
300	1.58
200	1.40

The pre-amplifier input impedance Z_{in} was measured using a

916AL impedance bridge and results are given in Table III. 3.

TABLE III. 3

Tube Pre-amplifier Input Impedance Z_{in} vs Frequency

$\dfrac{f}{kc}$	Z_{in} (ohms)
500	15.5 + j 65
400	20.5 - j 10
300	20 - j 35
200	18.4 - j 12.5

(All reactances could be tuned
out)
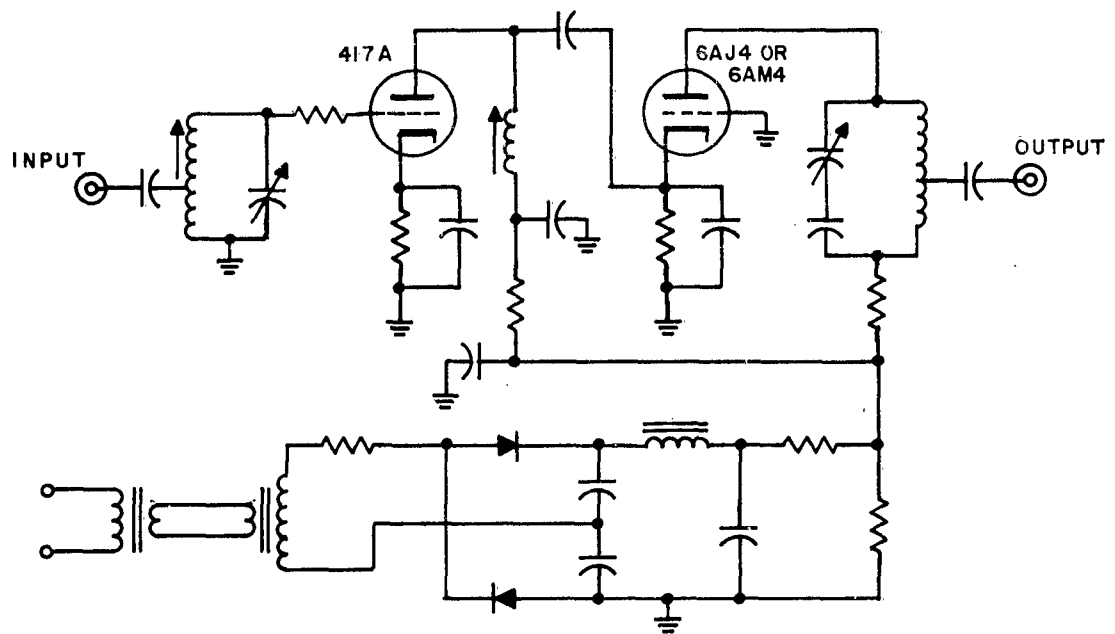
Figure III. 22.   Low noise preamplifier
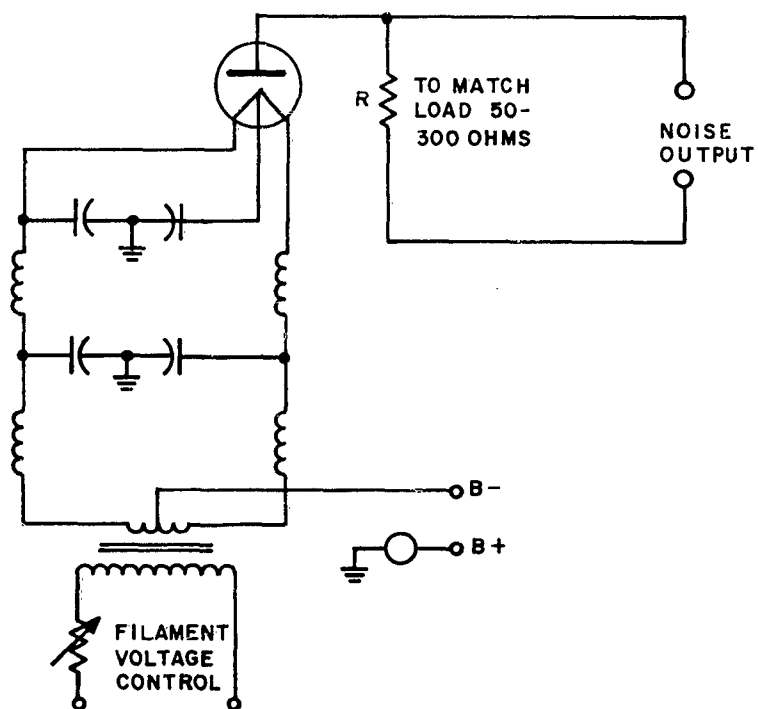
Figure III. 23.   Diode noise source

Noise figure measurements were also made with a conventional noise diode generator; its primary advantage being that the calculation of the noise figure does not require knowledge of the noise bandwidth of the noise source and that of the receiver, which data are required when using the Rohde & Schwarz noise generator. With this noise diode

$$N.F. \ (db) = 10 \log (20 \ IR)$$

R being the generator resistance in ohms and I the diode plate current in amperes. The circuit diagram of the diode noise generator used is shown as Figure III. 23. Results of noise figure measurements of the tube pre-amplifier with the diode noise generator are given in Table III. 4.

TABLE III. 4

Tube Pre-amplifier Noise Figure vs Frequency (Diode Noise Generator)

f_{kc}	Noise figure (db) SP-600 VLF B. W. = 1.3 kc
500	2.55
400	1.76
300	1.76
200	1.46
100	2.55*

*After modification of pre-amplifier to allow operation on 100 kc.

In the frequency range 200-500 kc, comparison of Tables III. 2 and III. 4 shows that either noise generator can be employed.

Figure III.24 shows a comparison of the calibration of the receiver alone with that of the receiver plus pre-amplifier, the original data being obtained by engineers at AFCRL. The calibration is that of IF output voltage as a function of RF signal input voltage.

3. HP-302A Wave Analyzer

This instrument which is basically a highly selective tuned voltmeter, bandwidth ± 3.5 cycles, was used as a VLF receiver from 20 cycles to 50 kc. Sensitivity is in the order of 0.5 microvolt. The unit is transistorized with provision for AC or battery operation. The input imped-ance is very high, the resistance component being approximately 100,000 ohms.

The wave analyzer was the only device used for signal reception measurements at frequencies below 10 kc.

E. Recorders

Esterline-Angus, Brush recorders - Used for instrumentation experi-ments with the receiving equipment, preparatory to continuous recording of atmospheric noise field intensity. The recorders with d.c. amplifiers were not used extensively up to present.

F. Bridges

1. G/R 916A - Used primarily for antenna impedance measurements above 400 kc (range of bridge 400 kc - 60 mc). Also used for measurement of impedance of test cell dielectric sample holders, such as Balsbough 2TN50 and 100T3 liquid test cells.
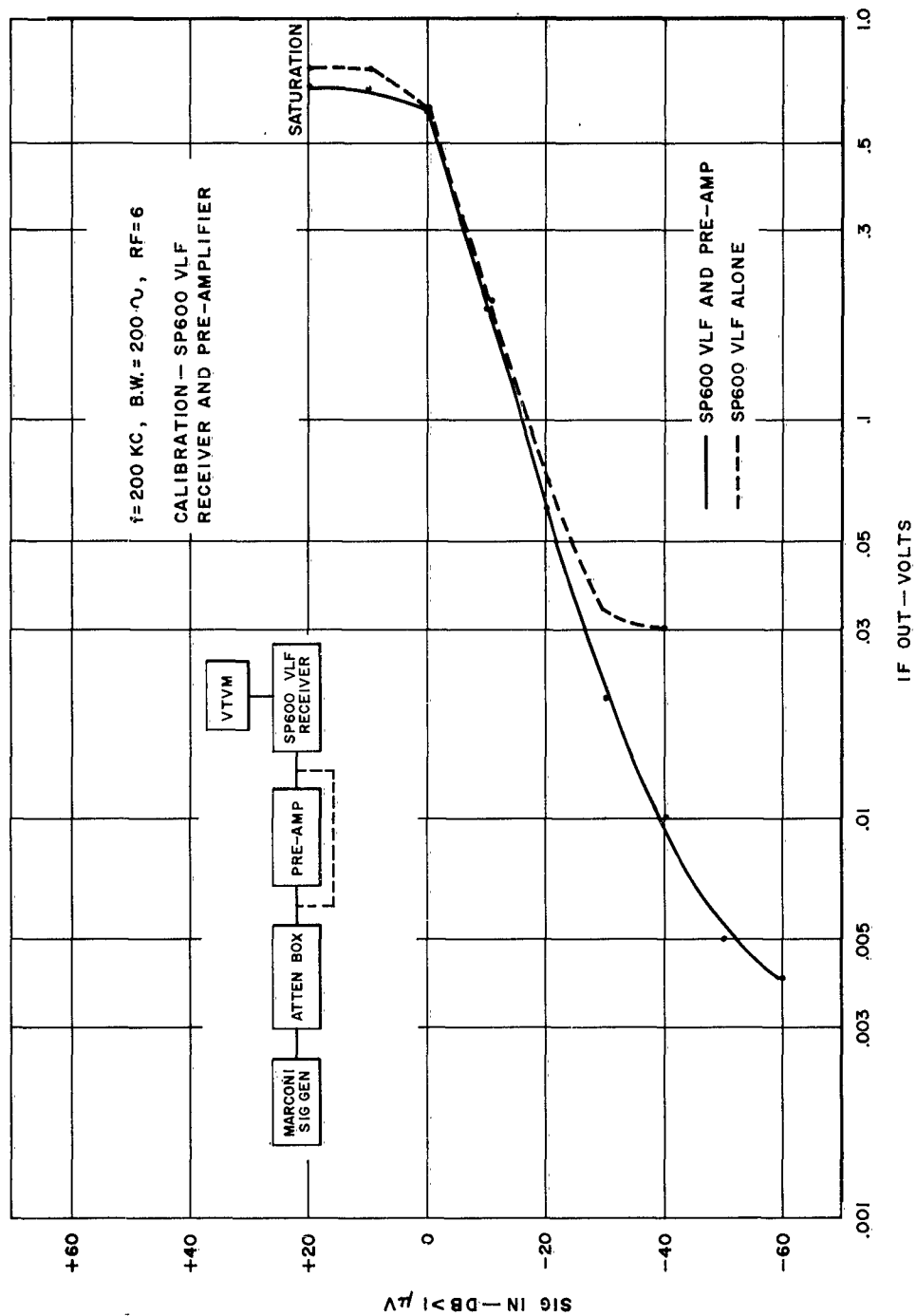
Figure III. 24.   Calibration of SP-600 VLF receiver and preamplifier f = 200 kc

2. G/R 916AL - Used primarily for antenna impedance measure-
ments below 400 kc (range of bridge 50 kc - 5 mc) and for dielectric sample
measurements.

3. G/R 1650A - Used for antenna impedance measurements below
50 kc and measurements on solid dielectric samples.

4. G/R 716C Capacitance Bridge, G/R 716P4 Guard Circuit, and
G/R 1960A Dielectric Sample Holder - These three units were used as one
system for the measurement of solid and liquid dielectric samples.

5. G/R 1603A Z-Y Bridge - Used principally for feedline and
antenna impedance measurements in the frequency range of 20 cps to 30 kc.

6. Boonton 160A Q-Meter - Used to obtain electric constants of
solid dielectric samples such as rocks by a Q variation technique.

G. Field Intensity Meters

1. Stoddart   20B (150 kc - 25 mc) - Used for field strength
measurements and surveys within its frequency spectrum.

2. Stoddart NM-10A (14 kc - 250 kc) - Same application as NM-20B.

3. Hewlett Packard 302A Wave Analyzer plus loop or whips - Used
in combination particularly at ELF and lower VLF. Required calibration
for antenna impedance loading mismatch at ELF and VLF.

Section IV. ANTENNAS

A. Introduction

Because of the physical confines of vertical drill holes used for access

from the earth's surface into the rock media below, the antennas studied for

the research conducted to date were single linear radiators, bare or insulated.

The theory used for obtaining the impedance properties of bare an-

tennas immersed in a dissipative medium is given in Appendix D and that for

insulated antennas in Appendix E. The radiation properties of these types of

antennas may be compared by comparing their "modified power gains G,"

the theory for which is given in Appendix F. The comparison of theoretical

values of G was given in Section IIF.

This Section considers the impedance properties of bare and linear

antennas including the use of antennas as probes to obtain the electrical con-

stants of the surrounding dissipative medium. A comparison of theory with

experiment is given where feasible.

In comparing the performance of bare wire with insulated wire an-

tennas, we use the three coaxial region notation applicable to the latter. Thus,

region 1 is the inner conductor; region 2, the insulation; and region 3, the

surrounding dissipative region. The region is indicated by a subscript. For

bare wires, subscript 2 is omitted.

B. Bare Antennas

1. Review of Theory

a. General

The first assumption in the theory given in Appendix D is that the conductivity of the metal cylindrical conductor is so great that the complex phase constant k of the current is extremely close to that value k_3 for the dissipative medium for media of interest.

The solution for input impedance is based upon variational methods used for antennas in free space, but where k_3 is substituted for the real phase constant β_o for space and the complex characteristic impedance ζ_3 of the medium is substituted for the real value $\zeta_o \doteq 120\pi$ ohms for space. For reasons of convenience discussed in Appendix D, our treatment follows the development of Tai[70] rather than that of Storer.[68]

The calculations of the input impedance Z_o and of the constant A which appears in the current distribution depend upon evaluation of three factors $\mathcal{V}_{11}$, $\mathcal{V}_{12}$, and $\mathcal{V}_{22}$ each of which are long expressions involving sine and modified cosine integrals of complex argument z = k h = $\beta h - j\alpha h$ where h is the half-length of the center driven antenna. Because we lacked tables of these functions, we had to resort to series expansions for the exponential integral of complex argument to obtain approximate values. Corrington[30] has shown how the sine integral Si(z) and the cosine integral Ci(z) may be obtained from tabular values of the exponential integral $E_1(z)$ which exist.[19] The function desired in evaluating $\mathcal{V}_{11}$, $\mathcal{V}_{12}$, and $\mathcal{V}_{22}$ is the function L(z) given by

$$L(z) = \text{Cin}(z) + j \, \text{Si}(z) \qquad \qquad (\text{IV. 1})$$

where

$$Cin(z) = \ln \gamma z - Ci(z) = .5772 + \ln(z) - Ci(z) \qquad (IV.2)$$

and where $\ln(z)$ means the natural logarithm of z.

Writing $z = x - jy$ where $y \leq x$, the values of $L(z)$ deduced from the series expansion for small z give good agreement with values of $L(z)$ deduced from tabular values when the series use but two terms and $x \leq .6$. The asymptotic expansion for large z may be used when $z \geq 3$; the error in approximate values of $L(z)$ is small, being the larger for $y = 0$ than for $y = x = 3$, and reduces as x increases further. Since the factors based upon Tai's expressions[70] involve $L(2z)$ and $L(4z)$ but not $L(z)$, the impedance for the interesting case for the half-wave antenna where $\beta h = \pi/2 = x$ may be well approximated by using the asymptotic series for complex argument, for the whole range of loss tangent such that $\alpha \leq \beta$.

b. Input Impedance Z_0 and Admittance Y_0

Values of Z_0 and Y_0 derived from the zero-order variational method, or the so-called EMF solution, are denoted by Z_{00} and Y_{00}. They are based upon an assumed sinusoidal distribution of current

$$I(z') = I(0) \frac{\sin k (h - |z'|)}{\sin kh} \qquad (IV.3)$$

where z' is the position coordinate for an antenna centered and lying along the z-axis and $I(0)$ is the input current.

For an antenna having a total length equal to a half-wavelength in a loss-less dielectric, $\beta h = \pi/2$. The values of Z_{01} and Y_{01} deduced by

the variational method for $p = \alpha = 0$ agree very well with the King-Middleton

second order values[5] and thus agree well with experiment. Values deduced

by King using a simplification to his iterative procedure[52,51] differ but

slightly more. The values Z_{oo} and Y_{oo} differ greatly from Z_{o1} and Y_{o1} for

antennas with modest thickness (see Table D. 2 of Appendix D).

For the half-wave antenna immersed in a medium of small

loss tangent with $p \leq .4$, King[51] and King and Harrison[53] have obtained values

of Z_o and Y_o for $\Omega = 10$. Values of Y_{o1} using the approximate relations

aforementioned may be seen in Figure IV. 1 together with King-Harrison values

in the region $p \leq .4$. The conductances agree very well and there are small

differences in susceptance.

When the loss tangent is so large that $\alpha = \beta$ and the antenna

length is still a half-wavelength in the medium, an interesting new result

occurs. It is that for practical purposes the input impedance may be calculated

using the sinusoidal current distribution (EMF method). The values of Y_{o1}

differ but little from Y_{oo} for practical purposes. This is due to the fact that

when the loss tangent is very large, the current amplitude $|I(z')|$ decreases

rapidly with distance along the antenna so that contributions near the ends

become less significant. This also results from the sinusoidal distribution,

equation (IV. 3), used to obtain the values of Z_{oo} and Y_{oo}.

When the antennas are electrically short so that $\beta h \leq .3$ and

$\alpha = \beta$, a parameter Ψ used by King[51] is convenient to use, where

$$\Psi = \Omega - 2 - 2 \ln 2 = \Omega - 3.386 \qquad \text{(IV. 4)}$$
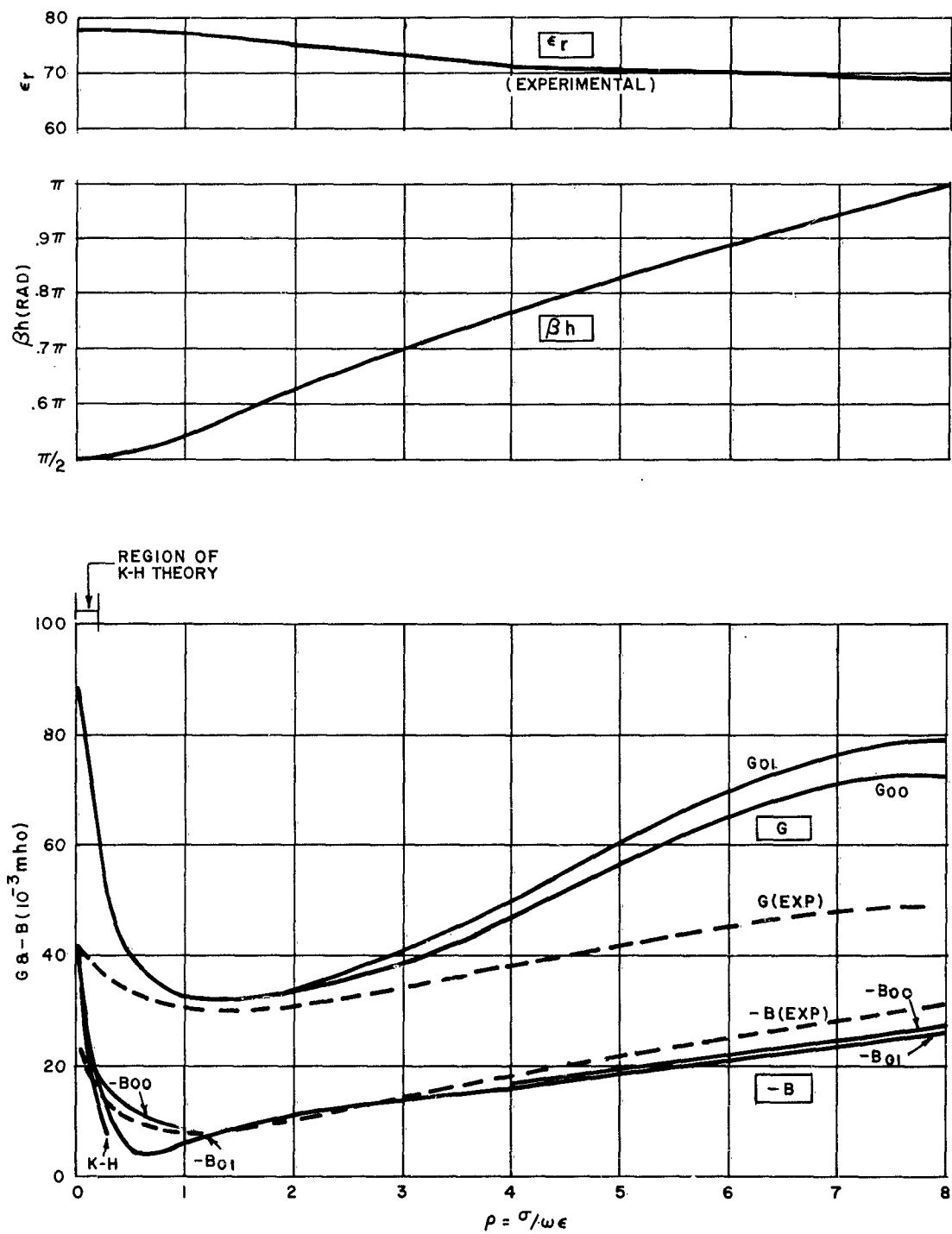
Figure IV. 1. Bare antennas - comparison of theory with
experimental data of Iizuka and King.
f = 114 mc, Ω = 10

and Ω is the thickness parameter. The current distribution used for the trial current in the first-order variational method reduces to the simple triangular distribution

$$I(z') = I(0) \left[1 - \frac{|z'|}{h} \right] \tag{IV.5}$$

which is the same as that deduced from the sinusoidal distribution in equation (IV.3). Hence for kh sufficiently small $Z_{o1} = Z_{oo}$ and $Y_{o1} = Y_{oo}$. The normalized admittance is given by equation (D.36) of Appendix D; and resulting expressions for G_{o1} (G_{oo}) and B_{o1} (or B_{oo}) for any value of loss tangent (or α/β) are quite long. Rather simple expressions result for $\alpha = 0$ and $\alpha = \beta$. These are

$$\mathcal{Z}_e G_{o1} = \frac{2\pi \beta^4 h^4}{3 \psi} \left(\frac{1}{\psi} \right) \quad , \quad \alpha = 0 \tag{IV.6a}$$

$$\mathcal{Z}_e B_{o1} = + \frac{2\pi \beta h}{\psi} \quad , \quad \alpha = 0 \tag{IV.6b}$$

and

$$\mathcal{Z}_e G_{o1} = \frac{4\pi \beta h}{\psi} \quad , \quad \alpha = \beta \tag{IV.7a}$$

$$\mathcal{Z}_e B_{o1} = - \frac{8\pi \beta^3 h^3}{3 \psi} F' \quad , \quad \alpha = \beta \tag{IV.7b}$$

Equations (IV.6b) and (IV.7a) are identical to corresponding expressions of King.[51] In equation (IV.6a), King has the factor $\left(\frac{1}{\Omega - 3} \right)$ in place of our factor $\left(\frac{1}{\psi} \right) = \left(\frac{1}{\Omega - 3.386} \right)$. In equation (IV.7b), we have a factor F' and King has the factor F where

$$F' = 1 + \frac{2}{3\psi} \quad , \qquad F' = 1 + \frac{1.081}{\Omega - 3} \tag{IV.8}$$

IV-6

and thus equation (IV.6a) and equation (IV.7b) agree well with King's results

for thin antennas, the agreement being the better the thinner the antenna.

The significance is that, for practical purposes, the input impedance and ad-

mittance for a thin, electrically short, bare antenna may be derived from the

simpler EMF method, for any loss tangent of the medium, using series ex-

pansions of the exponential integral if tabular values are not available.

2. Comparison of Theory with Experimental Measurements
of Admittance at VHF of Iizuka and King

There are experimental data for the input admittance of an an-

tenna immersed in a lossy dielectric of known electrical constants which

afford a comparison of theory with experiment. The experimental data are

those obtained at VHF (114 mc) by Iizuka and King[48] for a monopole driven

over a large ground plane in contact with a liquid solution housed in a rec-

tangular container, the monopole being immersed in the liquid. The relative

dielectric constant ϵ_r and conductivity σ of the solution were varied and

measured, from which the loss tangent p was calculated. The monopole had

a fixed length such that $\Lambda = 10$ and electrical length $\beta h = \pi/2$ when p was

very small (p = .0356). The resulting dipole values of conductance G and

susceptance B were determined as p varied up to values of p = 8.8 in several

steps. The susceptance was negative (inductive reactance) and the experi-

mental dipole values of G and (-B), read from the curves,[48] are shown on

the curves of Figure IV.1 as functions of loss tangent p. The values were

determined from coaxial line measuring methods and included any terminal

zone reactive effects, the effects of the step discontinuity at the base of the

antenna which had to be "clipped on" the larger diameter inner conductor of

the measuring coaxial line, and possible effects of reflection from the walls

of the finite sized tank.

The experimental values of ϵ_r read from the curves of Iizuka

and King[48] are also shown on the curve labeled " ϵ_r (experimental)" in

Figure IV. 1. An important feature is the variation of electrical (half) length

βh as p varies. Knowing ϵ_r and p of the medium and half-length h of the

antenna, it is a simple matter to compute βh if one has tables of f(p), as in

Appendix A, and uses the relations of Section II. Thus

$$\beta h = \beta_o h \sqrt{\epsilon_r} \; f(p) \tag{IV. 9}$$

The known fixed value of h may be used in equation (IV. 9). But it was known

that h was such that $\beta h = \pi/2$ when p was so small that $f(p) \doteq 1$, and that

$\epsilon_r = 78$ for such low values of p. Hence equation (IV. 9) may be rewritten

for this case as

$$\beta h = \frac{\pi}{2} \sqrt{\frac{\epsilon_r}{78}} \; f(p) \tag{IV. 10}$$

where the value of ϵ_r to be used is that corresponding to p according to the

curve " ϵ_r " in Figure IV. 1. Using equation (IV 10), we calculated βh as a

function of p and the results are shown in the curve labeled "βh" in Figure

IV. 1. Note that βh increases from $\pi/2$ (half-wave antenna) to values ex-

ceeding π (full-wave antenna) as p increases from 0 to 9. It is important to

realize then that G and (-B) are not the values for a half-wave antenna,

$\beta h = \pi/2$, except for those values where p is small. Note that, for the

experiments, βh increases with p slowly at first and then almost linearly with p. Note also that βh differs from $\pi/2$ by 2% or less for $0 \lesssim p \lesssim 0.5$ for the experiments. These observations result from the experimental variation of $\sqrt{\epsilon_r}$ and f(p) with p in equation (IV. 10).

Knowing ϵ_r and βh as functions of p, the theoretical input impedance and admittance may be calculated according to the variational methods given in Appendix D. Our calculations assumed the validity of asymptotic expansions for βh $\gtrsim \pi/2$, the accuracy of which is discussed above and illustrated in Appendix D. The resulting approximate zero-order (EMF) values G_{oo} and $(-B_{oo})$ and first order values G_{o1} and $(-B_{o1})$ so calculated are shown plotted in Figure IV. 1.

For large loss tangents, with βh near π, the zero and first order susceptance differ but slightly and the conductances differ by about 10%. This is in accordance with the observation above and in Appendix D, for large loss tangent p where $\alpha \doteq \beta$, that zero-order (EMF) methods are adequate for practical purposes for such electrical lengths.

For small loss tangents, $p \lesssim 0.4$ say, the first order values agree with the King-Harrison values[51,53] particularly for the conductance. When p = 0.5 the susceptance (-B) for the zero-order method is twice the first order value.

There are differences between the theoretical values Y_{o1} and experimental values for large loss tangents near p = 8 and small loss tangents near p = 0. For large loss tangents the experimental values of G are quite

a bit lower than the theoretical values; experimental values of (-B) are but slightly larger than the theoretical ones. When p = 0, it is known that the first-order theoretical values agree well with experimental data for antennas in air. The error in the experimental values in Figure IV. 1 for the smallest loss tangent used (p = .0356) may be attributed to a combination of effects due to reflection from the walls of the tank, the step discontinuity at the base of the antenna, and the reactive end effect on the transmission line, all of which are included in the experimental values plotted. Reflection effects due to walls become negligible, for the tanks used, for large loss tangents due to increased exponential damping in the media. Some difference is expected for any value of p due to the effect of the step-discontinuity discussed by Iizuka and King. [48] The trends of theoretical and experimental values with increasing p are generally in good agreement, in that the conductance and the (negative) susceptance decrease with p quite sharply for low values of p, reach minima, and then increase. *

3. VLF and LF Measurements in Drill Holes Into Rock

Measurements were made on bare wires in an attempt to ascertain the electric constants of the surrounding medium when using the wires as probes and values of input impedance for such wires when used on insulated

---

* We have just received a copy of a report by Iizuka and King [49] on more extensive measurements following their previous work. [48] Time has not permitted comparing the new measurements with theory under the present contract, but will be reported upon at some future date.

antennas as terminating, short-circuiting, electrodes.

While data were obtained for wires immersed in the Brewster hole, the more consistent set of data was that for the measurements at Harwich. Various lengths of #12 wire were connected to the end of a coaxial feeder (RG-8/U) about 564 feet long; about 150 feet of the neoprene jacket were removed from the feeder back from the point to which the bare wire was connected, exposing the braid outer conductor for contact with the casing pipe. The "ground cage" (Section IIIB) used for antenna measurements at a later date was not yet available. The substitution method described in Section IIIB was used to obtain the antenna input impedance. The wire antenna with counterweight and coaxial feeder was lowered into the drill hole so that the wire was exposed to the rock but the feeder was not (antenna input flush with the bottom of the casing). The feeder was connected to an RF bridge and the feeder impedance was measured as a function of frequency, carefully noting all pertinent bridge dial settings, for a given wire length. The assembly was withdrawn from the hole, the wire removed, and the effective antenna input impedance obtained by the substitution box method. The process was repeated for other lengths of wire.

The resulting values of input resistance R_{in} and reactance X_{in} are plotted on the curves of Figure IV.2, for lengths ranging from 5 to 200 feet and frequencies 50 to 500 kc. It is seen that X_{in} is positive indicating a large loss tangent. Values of R_{in} at first decrease with length to a minimum, then increase and tend to taper off at large values of h. To date, however,
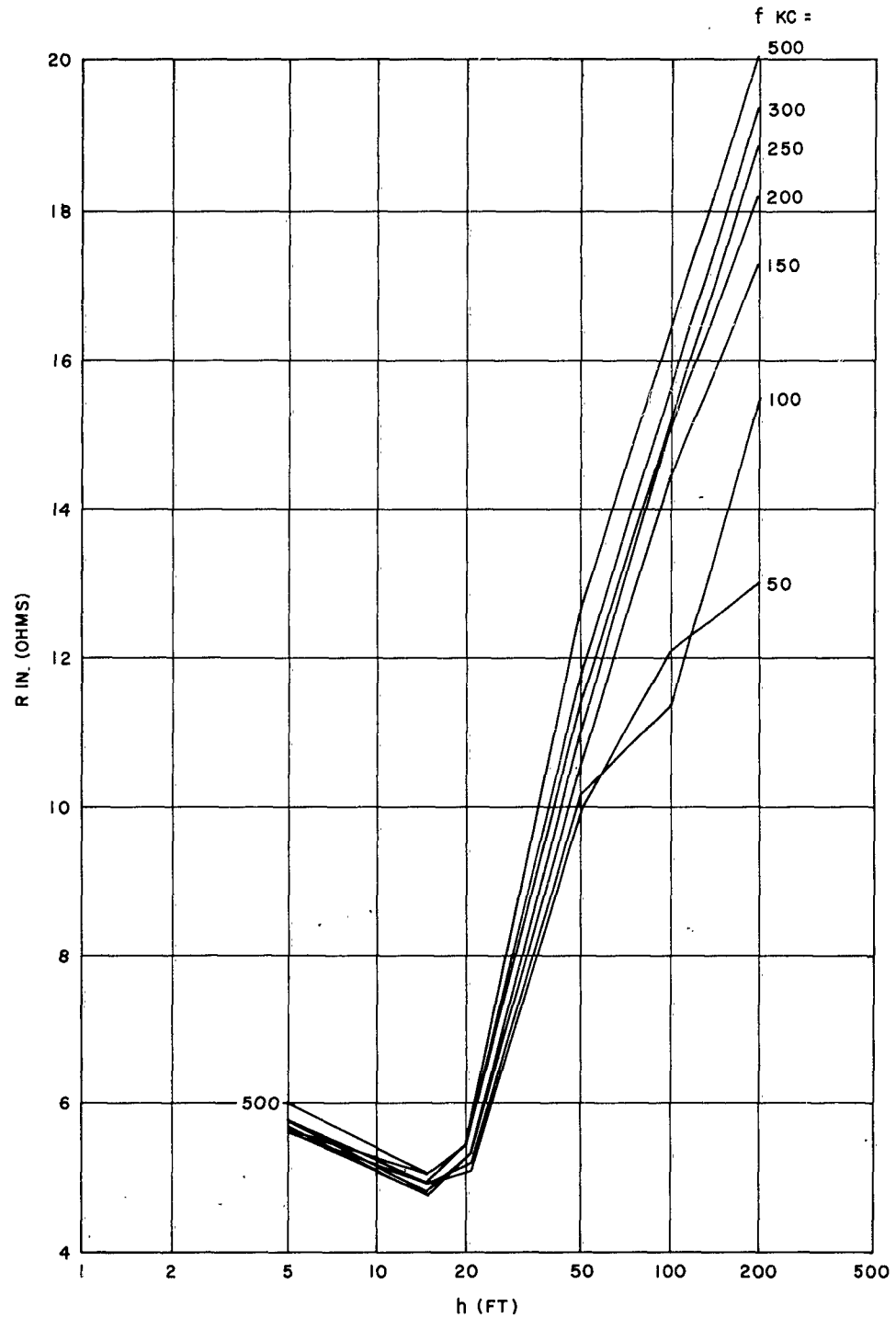
Figure IV. 2a.   Input impedance of bare wire vs length
h of #12 wire - Harwich - R_{in}
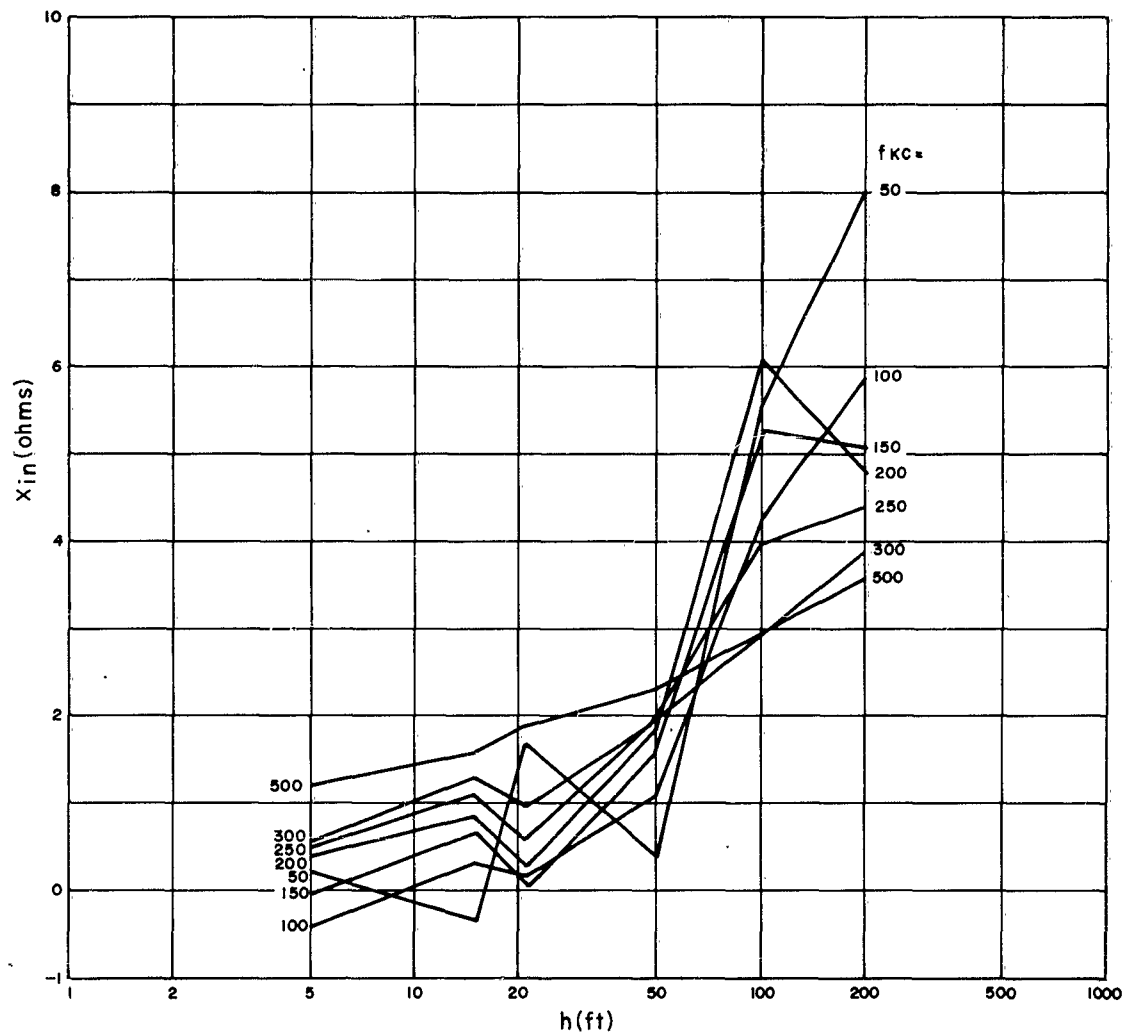
Figure IV. 2b. Input impedance of bare wire vs length
h of #12 wire - Harwich - X_{in}

it has not been possible to analyze these data to determine σ and ϵ_r of the medium surrounding the wire. The difficulty lies in the effect of the "ground plane," in this case the overburden below which is suspended the wire. One might crudely estimate the input impedance Z_{in} to consist of the sum of two components, one being the impedance of the wire considered as a monopole over a perfect ground and the other being the impedance of the pipe immersed in the overburden. If this picture were approximately true, then knowledge of σ for the overburden might help, but we did not know this value.

The data may be used to indicate an upper bound to the values of the impedance when the wire is used as a short-circuit termination for an insulated antenna. Since the characteristic impedances of insulated antennas should be about 150 ohms for the types employed, then wire lengths 50 feet or less should provide a reasonably good (conductive) short-circuit for conditions similar to those for the Harwich drill hole (see next subsection for results of measurements).

Measurements were made at ELF and VLF but difficulties with leakage through the feeder preclude the utility of such data; measurements with a better shielded coaxial (triaxial) feeder or with a balanced feeder plus dipole should be performed.

C. Insulated Antennas

1. Review of Theory

a. General

The theory for insulated antennas immersed in a dissipative medium is given in Appendix E. Assuming radial dimensions are small

IV-14

compared with the wavelength λ_3 of the dissipative medium surrounding the insulation, the complex phase constant k differs markedly from that value k_3 for the dissipative medium for practical antennas, and simpler relations result.

In this Section, the input impedance properties of the insulated antenna are considered. The aspect of "modified power gain G" is considered theoretically in Appendix F and discussed further in Section IIF. Comparison is made between the values of G for the insulated antenna, open- and short-circuited terminations, vs the bare wire. A qualified comparison of G from path transmission measurements is discussed in Section VI where it is shown that G for the bare antenna must be quite low compared with the short-circuited coaxial antenna (by the order of 30 db or so), for the Cape Cod path.

b. Complex Phase Constant k of the Current

An essential result, under the various assumptions which are valid for the antennas employed, is that the phase constant k has a small imaginary component. With $k = \beta - j\alpha = \beta(1 - j\,\alpha/\beta)$, one has

$$\beta \doteq \frac{2}{\sqrt{\ln a_2/a_1}}\;P_{31} \qquad\qquad (IV.11)$$

$$\alpha/\beta = \left(\frac{\pi}{2} - \theta_3 + \frac{\tau_1^2}{a_1^2}\right) \bigg/ P_{31}^2 \quad (VLF\ value) \qquad (IV.12)$$

in which

$$P_{31}^2 = \ln \frac{2}{\gamma\,|k_3|\,a_1} \qquad\qquad (IV.13)$$

and where

$$k_3 = \beta_3 - j \; \alpha_3 = |k_3| \; e^{-j\,\theta_3} \quad\quad\quad\text{(IV. 14a)}$$

$$\theta_3 = \tan^{-1} \frac{g(p_3)}{f(p_3)} = \tan^{-1} \frac{\alpha_3}{\beta_3} \quad\quad\quad\text{(IV. 14b)}$$

$$\beta_2 = \beta_0 \sqrt{\epsilon_{r_2}} \quad\quad\quad\text{(IV. 14c)}$$

    c.   Quarter-Wave Resonant Lengths, h_r, and Estimate of σ_3

The insulated antenna behaves as a coaxial line insofar as the input impedance is concerned, the "outer conductor" of which is the dissipative medium. If the termination is an open circuit, the antenna will be resonant where $(\beta h)_r = \pi/2$. Calculations were given in Appendix E, Section VII showing the effect of varying the radius a_1 of the inner conductor upon the resonant frequency f_r for an antenna of fixed length h (600 feet), air insulation of fixed radius a_2 (6 inches), immersed in a medium of constant conductivity σ_3 (2×10^{-3} mhos/m) and relative dielectric constant ϵ_{r_3} (= 40).

If the loss tangent p_3 is large, then in equation (IV. 14a), $|k_3| = \sqrt{2/\tau_3}$ where τ_3 is the skin depth, and $\theta_3 = \pi/4$. The expression for P_{31}^2 becomes dependent on σ_3 but not ϵ_{r_3}. The effect of σ_3 upon the resonant length h_r as a function of frequency for which $\beta h_r = \pi/2$ is shown in the curves of Figure IV. 3 for an RG-8/U type antenna where h_r is plotted vs frequency on a log-log plot with σ_3 as a parameter. For comparison, curves are shown dashed for the resonant lengths for a wire in air and for the normal RG-8/U cable; the difference is due to the dielectric constant $\epsilon_{r_3} = 2.25$
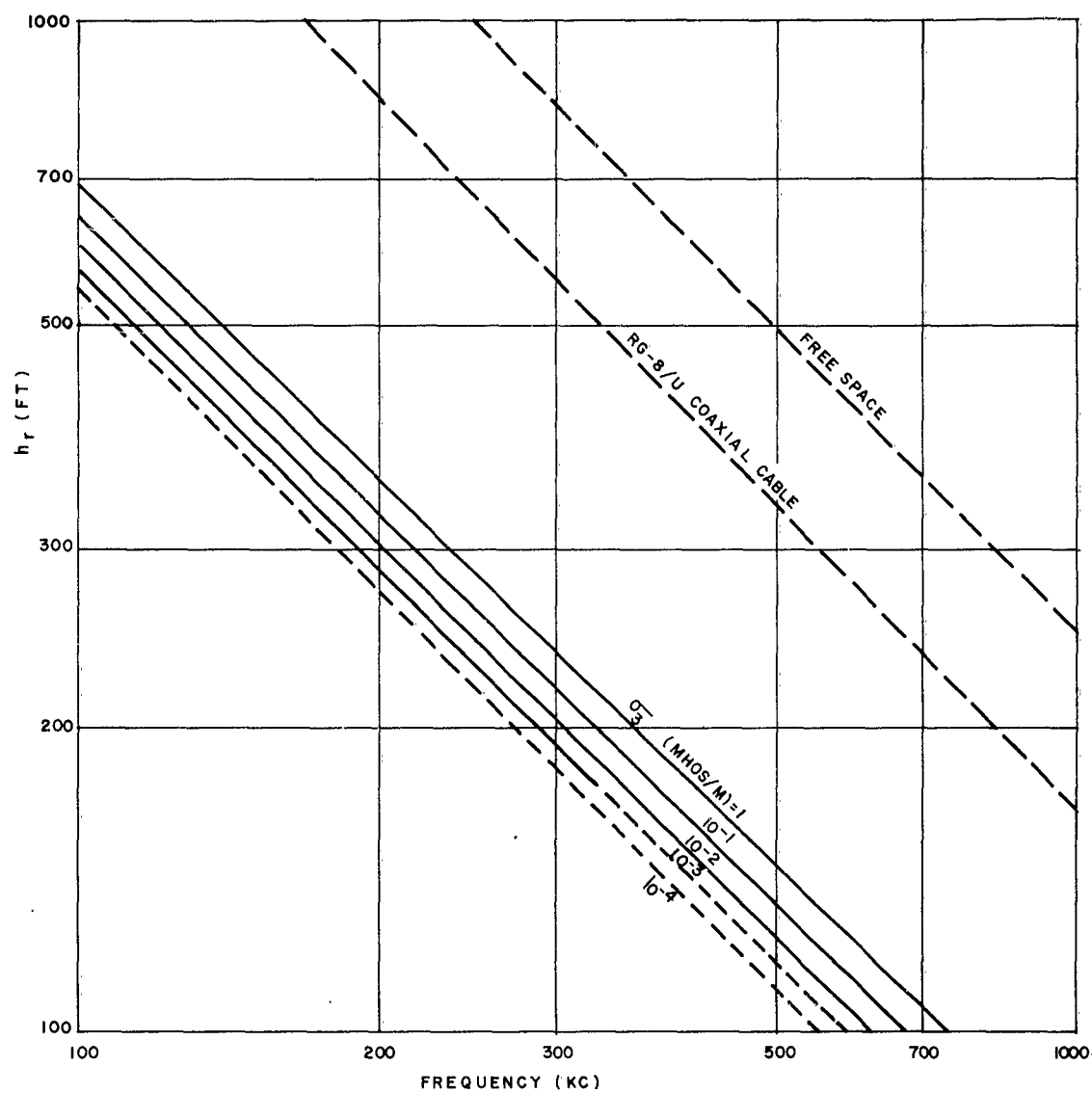
Figure IV. 3. Required quarter-wave resonant lengths h_r for insulated monopole antenna vs frequency. RG-8/U type insulated monopole antenna, open-circuit termination ($2a_2 = 0.285''$, $2a_1 = 0.0816''$, $\varepsilon_{r_2} = 2.25$)

σ_3 = conductivity of surrounding medium, $\varepsilon_{r_3} = 9$

for the polyethylene insulation. Throughout the range of frequency for

$\sigma_3 = 1$, 0.1, and 0.01 mhos/m, the loss tangent is large if ϵ_{r_3} is assumed

to be 9. For $\sigma_3 = 0.001$, the loss tangent is large up to 300 kc and the curve

is shown dashed at higher frequencies. It is shown in Appendix E, Section II

that for a typical coaxial antenna (RG-8/U type) λ/λ_o is of the order of 0.2,

whereas for the usual RG-8/U cable, λ/λ_o is about 0.67. This is attributed

to the logarithmic term P_{31} discussed below; for the media being employed

P_{31} varies as $\left[\ln (1/\sqrt{\sigma_3}) \right]$ and λ/λ_o varies as $1/P_{31}$.

The curves for Figure IV.3 were used to predict resonant

lengths for RG-8/U type insulated antennas in known media and were used for

the earlier measurements made in New Hampshire. The results for input

impedance shown in Figure III.19 are discussed in Sections VG and IVC be-

low with reference to the resonant length predicted. (Curves for vinyl covered

#12 and #14 wire similar to those in Figure IV.3 were prepared for purposes

of predicting resonant lengths for such antennas intended for use in New

Hampshire drill holes; they are not reproduced here but successful results

were also achieved.)

The curves for h_r vs desired resonant frequency in the range

$100 \leq f_{kc} \leq 1000$ do not show great sensitivity to values of σ_3. It was desired

to examine this effect more closely for lower frequencies being contemplated

for use in Cape Cod drill holes, first for predicting h_r and second, having

measured the resonant frequency, for determining the electrical constants of

the medium. Contemplating the use of polyethylene covered wire antenna

(made from RG-8/U coaxial cable), the curves of Figure IV. 4 were prepared

for the range $100 \leq f_{kc} \leq 170$ kc. The curves are plots of σ_3 vs the resonant

frequency f_r with the length h as a parameter on the curves. The curves are

based on the simpler relations for β in equation (IV. 11) when the loss tangent

is large. The lower limit for determining σ_3 assuming $p_3 \geq 6$, $\epsilon_{r_3} = 9$ is

shown. Note that σ_3 is plotted on a log scale.

Figure IV. 4 was used first for predicting h_r for a desired

resonant frequency, assuming a knowledge of σ_3 and f_{kc}, and results are

discussed in Sections VG and IV. C below. Conversely, knowing f_{kc} and h for

resonance the value of σ_3 can be determined. For an estimate of σ_3 of

modest accuracy, accurate measurements of f and h are required.

d. Characteristic Impedance Z_C

The insulated antenna is considered from the impedance point

of view to behave as a coaxial line. It has a "characteristic impedance" Z_C

given in Appendix E as

$$Z_C = R_{C_o} \; \frac{\beta}{\beta_2} \; (1 - j \; \frac{\alpha}{\beta}) = R_C \; (1 - j \frac{\alpha}{\beta}) \tag{IV. 15}$$

where $\frac{\beta}{\beta_2}$ and $\frac{\alpha}{\beta}$ are given in equations (IV. 11) and (IV. 12) and R_{C_o} is the

characteristic resistance of the insulated antenna with metallic outer conduc-

tor, e. g., a normal coaxial line. For a high quality coaxial line of the

RG-8/U type, R_{C_o} is about 52 ohms. For a coaxial antenna made from

RG-8/U cable by stripping off its outer conductor braid and neoprene jacket,

R_C is typically about three times R_{C_o}, i. e., of the order of 150 ohms (for
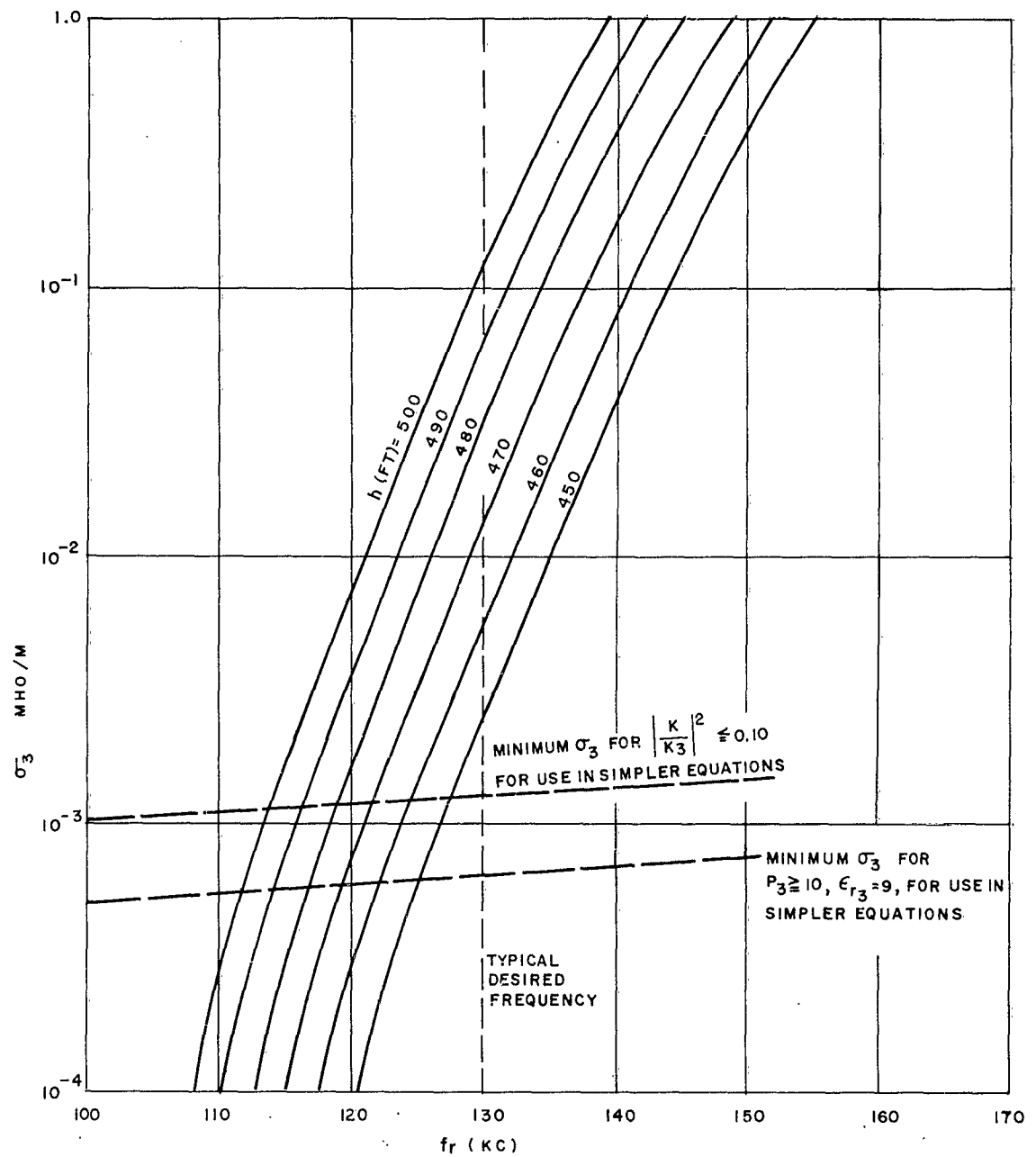
Figure IV. 4. RG-8/U coaxial antenna - effect of conductivity (σ_3) on quarter-wave resonant frequency (f_r) for various monopole lengths (h). $\varepsilon_{r_3} = 9$.

$\sigma_3 = 10^{-4}$ mhos/m, $\epsilon_{r_3} = 9$, f - 10 kc, the ratio is shown in Appendix E, Section II, to be 3. 2).

e. Input Impedance Z_{in} for Antennas of Finite Length h

The input impedance of a coaxial antenna depends upon its complex phase constant k, length h, and the output terminating impedance Z_T. It also depends upon the nature of the "input electrode." If the input electrode is the ideal perfectly conducting ground plane of infinite extent and in intimate contact with the dissipative medium, the input impedance Z_{in} is considered to be that of a monopole driven over a ground plane. The input impedance of a symmetrically driven dipole would be twice that value for the monopole antenna. The values of Z_{in} for a monopole in a dissipative medium driven over a large ground plane of finite conductivity are assumed to be approximately those with a perfect ground plane, if the relative refractive index (conductivity contrast for large loss tangents) of the two media is large, the difference being principally in the addition of a "ground resistance" term.

Expressions for the input impedance of a monopole antenna were developed in Appendix E. Values were calculated for a typical case with open-circuit termination in Appendix E, Section VII, the results showing behavior quite similar to those for an open-circuited coaxial transmission line. At quarter-wave resonance the resistance is small and at anti-resonance the resistance is large. At frequencies below first resonance, Z_{in} is highly capacitative. The effects of varying the ratio of the radii a_2/a_1 for a fixed insulation radius a_2 and length h were illustrated and discussed.

For $Z_T - 0$, the input impedance is like that of a short-circuited coaxial line, denoted by $Z_{in}(SC)$ and given by

$$Z_{in}(SC) = j \, Z_C \tan kh = Z_C \tanh (j kh) \qquad \qquad \text{(IV. 16)}$$

When $Z_T = \infty$, the input impedance is like that of a coaxial line which is terminated in an open circuit, denoted by $Z_{in}(OC)$, and given by

$$Z_{in}(OC) = - j \, Z_C \cot kh = Z_C \coth (j kh) \qquad \qquad \text{(IV. 17)}$$

Here, with $k = \beta (1 - j \, \alpha/\beta)$, β and α/β are given by equations (IV. 11) and (IV. 12), respectively, and Z_C is given by equation (IV. 15). At frequencies for which $\beta h \doteq \pi/2$, $h \doteq \lambda/4$, the short-circuited antenna is anti-resonant and has a high input resistance, the value of which depends inversely upon α/β. When $h \doteq \lambda/2$, the short-circuited antenna is resonant with a small value of input resistance which is proportional to α/β. For frequencies below first anti-resonance, $Z_{in}(SC)$ has an inductive reactance which becomes smaller the lower the frequency. Resonant and anti-resonant frequencies for $Z_{in}(OC)$ correspond to anti-resonant and resonant frequencies, respectively, for $Z_{in}(SC)$. Resonant and anti-resonant frequencies are not harmonically related for the insulated antenna in a dissipative medium due to the logarithmic dependence on frequency of the P_{31} term in the expression for β, equation (IV. 11).

In practice, for "short-circuited" antennas, Z_T is not zero but $\left| Z_T/Z_C \right|^2 \ll 1$, so that a good short circuit may be achieved. The principal effect of a finite but small Z_T on $Z_{in}(SC)$ is to reduce the anti-resonant

resistance; for electrically short antennas, the effect is to add the value of Z_T to the value of $Z_{in}(SC)$ obtained when $Z_T = 0$. Similarly, for "open-circuited" antennas, in practice Z_T is not infinite but is so high that $\left| Z_T / Z_C \right|^2 \gg 1$. The principal effect is to reduce the conductance $G_{in}(OC)$ at resonance; for electrically short antennas, the effect is to add the value of Y_T to the value of the input admittance $Y_{in}(OC)$ obtained when $Y_T = 0$.

2. VLF and LF Measurements in Drill Holes into Rock

a. Apparatus and Techniques

The antenna systems comprising an insulated monopole connected to a coaxial feeder are described in detail in Section IIIB. The connection at the feed point to the monopole was water-proofed. The open-circuit termination was provided by additional polyethylene insulation beyond the end of the inner conductor; the short-circuit termination was usually a length of #12 or #14 wire soldered to the inner conductor. The outer neoprene cover on the coaxial feeder was stripped back from the antenna feed point a distance variously 150 to 450 feet for several different tests. When it became available, the "grounding cage" described in Section IIIB was affixed to the exposed braid portion of the coaxial feeder, assuring more positive contact between the outer conductor of the feeder to the casing pipe in the overburden. The grounding cage was not available for the measurements on antennas in New Hampshire holes and friction contact between the exposed braid and the pipe was relied upon to provide a "ground" connection. For the impedance measurements to be described, the monopole input point was at a depth below

and within a foot of the bottom of the casing (depth referred to as "flush with the casing").

The substitution method described in Section IIIB was used to obtain the impedance observed at the monopole input point.

b. Insulated Antenna, Open-Circuit Termination, Goffstown, N.H.

The earlier measurements were made in New Hampshire at frequencies in the LF to HF spectrum. On one series of tests it was desired to have an antenna resonant at 500 kc. Highly conducting water in the holes (see Section VD) which was expected to be present in the surrounding rock precluded the use of bare antennas. Practical antennas made from RG-8/U cable and vinyl covered wires were suggested. Using the curves of Figure IV.3, a length of RG-8/U type insulated antenna 123 ft. long was estimated to obtain first input resonance for an open-circuited antenna. The resulting impedances are shown plotted in Figure III.19, including spiral plots in the complex X-R plane and rectangular plots of R and X vs frequency. Input resonance occurred near 480 kc, which result is discussed in Section VG.

c. Insulated Antennas, Open-Circuited Termination, in Two Holes on Cape Cod

It was desired to compare input impedances of the same antenna inserted into the rock in two different drill holes on Cape Cod. The sites used were at the Brewster Town Dump and at Harwich which are described in Section IIIA. The antennas were RG-8/U type, 472.75 feet long, with open-circuit termination. The ground cage was employed and the

monopole input was flush with the casing. Frequencies of observation were varied from 30 to 500 kc. The input impedances are plotted on the curves of Figure IV.5 and Figure IV.6. The curves, although differing in detail, show the impedance variation to be smooth and the values to pass through two resonances and two anti-resonances as frequency varies. Resonances and anti-resonances are not harmonically related. Maximum resistances near anti-resonances are larger and minimum resistances near resonances are smaller for the Harwich antenna. Impedances below first resonance becomes the more capacitive the lower the frequency. These observations are in qualitative agreement with theory. Frequencies at resonance are slightly lower for the Brewster antenna.

        d.   Insulated Antenna, Open-vs Short-Termination, Harwich

The input impedances $Z_{in}(SC)$ and $Z_{in}(OC)$ for an RG-8/U type (polyethylene covered #12 wire) insulated monopole 475 feet long were measured in the Harwich drill hole. The input depth was flush with the casing. The open circuit was provided as aforementioned. The short circuit was a 50-foot piece of #12 buss wire. The results may be compared by reference to the curves in Figures IV.7 and IV.8. At frequencies below first anti-resonance, $Z_{in}(SC)$ remains inductive; this is as opposed to the capacitative reactance behavior for $Z_{in}(OC)$ at similar frequencies. The maximum resistance near first anti-resonance (approximately 120 kc) for $Z_{in}(SC)$ is but slightly higher than the maximum resistance near anti-resonance (approximately 250 kc) for $Z_{in}(OC)$, attributed in part to the frequency dependence in

Figure IV.5. Input impedance of an insulated monopole, open-circuit termination. Comparison of impedance for same antenna in two different 1000-ft. drill holes on Cape Cod, and barely inserted into rock below overburden. Frequency in kc is parameter on curves. Complex plane, spiral plot.

INSULATED OPEN-CIRCUIT MONOPOLE INPUT IMPEDANCE

IDENTICAL ANTENNA IN DIFFERENT HOLES

ANTENNA: RG-8/U TYPE, 472.75' LONG

FEEDER: RG-8/U COAX (BREWSTER 1000'
HARWICH 525')

INPUT ELECTRODE: PIPE, $7\frac{5}{8}$" DIAMETER,
ABOUT 450' LONG, CONNECTED AT
BOTTOM TO OUTER CONDUCTOR OF
FEEDER VIA GROUNDING CAGE
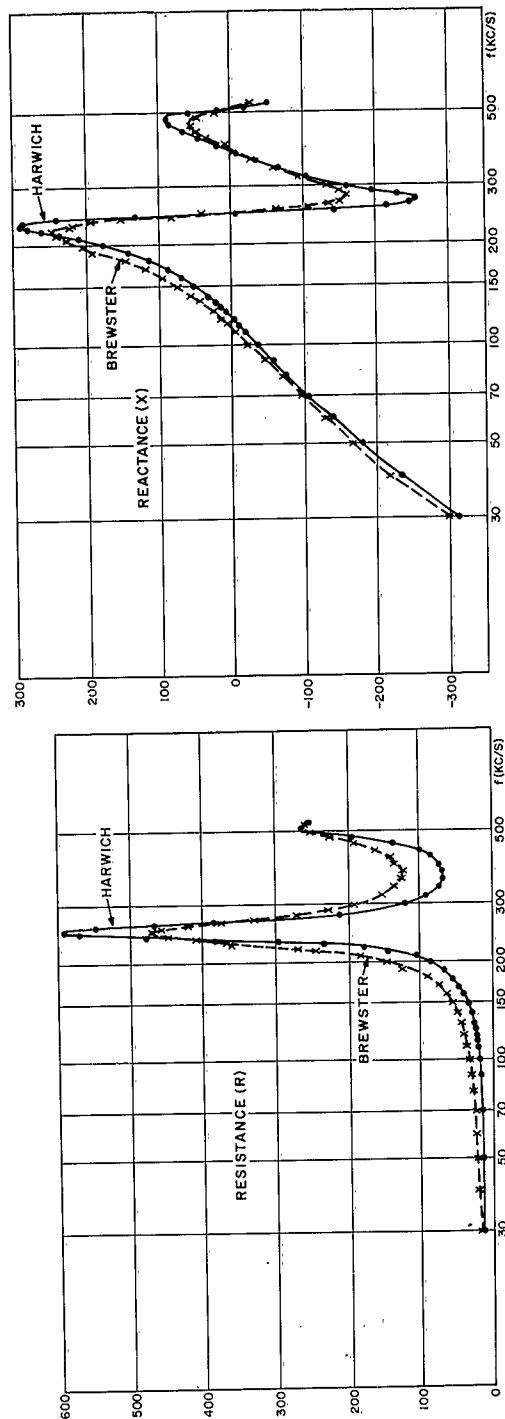
Figure IV. 6. Input resistance (R) and reactance (X) of insulated, open-
circuited monopole vs frequency. Conditions are those
of Figure IV. 5. Solid curves (Harwich), dashed
curves (Brewster)

IV-27
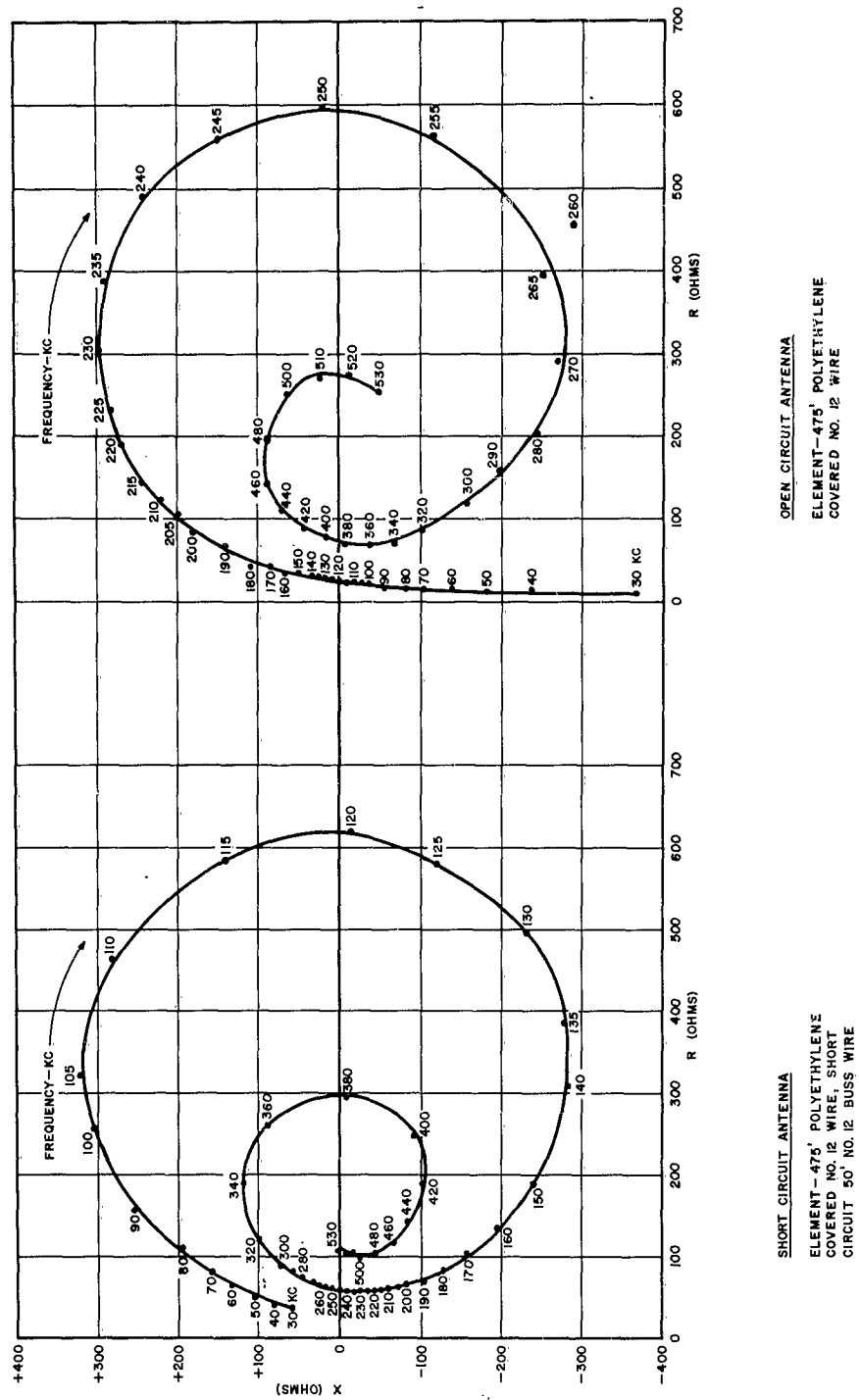
Figure IV. 7. Comparison of input impedances of insulated monopoles with short-circuit or open-circuit terminations (complex impedance plane, spiral plot). Frequency in kc is parameter on curves.

IV-28

HARWICH

———— SHORT CIRCUIT ANTENNA.
ELEMENT 475' POLYETHYLENE
COVERED NO. 12 WIRE. SHORT
CIRCUIT 50' BARE NO. 12 BUSS

——————OPEN CIRCUIT ANTENNA.
ELEMENT 475' POLYETHYLENE
COVERED NO. 12 WIRE
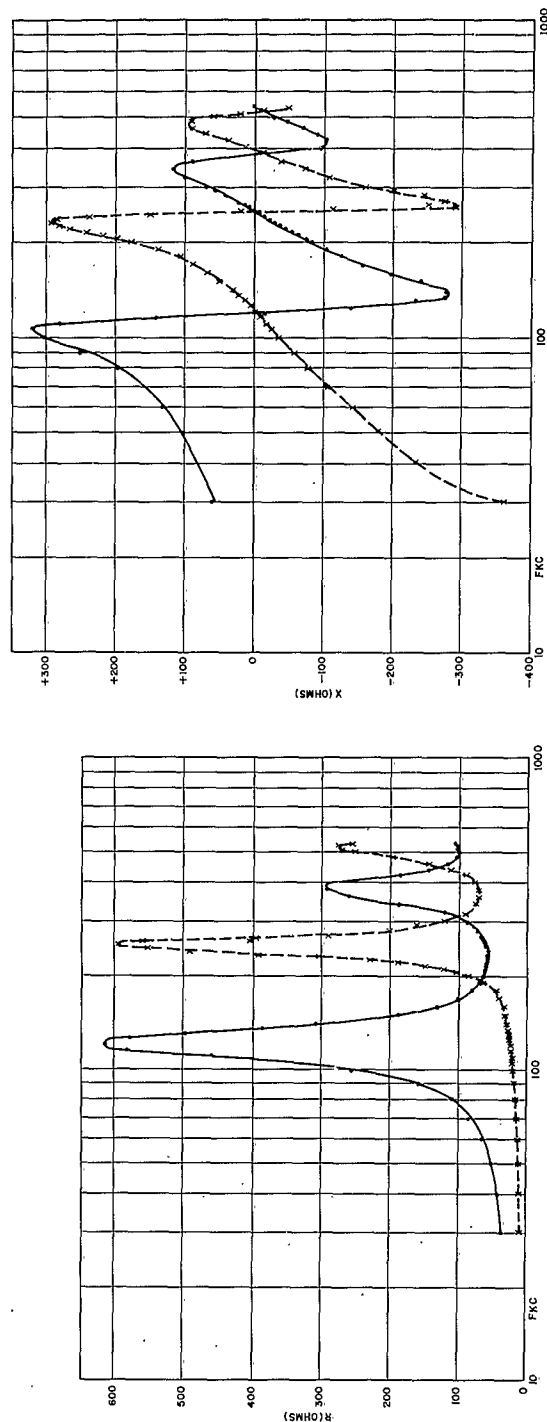
Figure IV.8. Input resistance (R) and reactance (X) of an insulated monopole vs frequency, "open circuit" (dashed curves), and "short-circuit" (solid curves) terminations. Conditions as for Figure IV.7.

α/β in equation (IV. 12). Similar remarks apply to maximum values of

$\left|X_{in}\right|$. The various resonant and anti-resonant frequencies for $Z_{in}(OC)$ agree

quite well with the corresponding anti-resonant and resonant frequencies for

$Z_{in}(SC)$. The input impedance of the short-circuit termination $Z_T \rightarrow 0$ is like

that for a travelling wave along the short-circuiting wire. A crude approxi-

mation of the value of the value of Z_T would be half that of a center-driven

bare dipole. If we assume the values for Figure IV. 2 apply, then

$\left|Z_T\right|^2_{SC} << \left|Z_C\right|^2$ and $Z_{in}(SC)$ should have an anti-resonance occurring at a

frequency near that obtained for a perfect short circuit $Z_T = 0$. The fre-

quency for resonance for $Z_{in}(OC)$ being close to this indicates $\left|Z_T\right|^2_{OC} >> \left|Z_C\right|^2$.

We had no means at the time to measure the impedance Z_T for the "open-

circuit" as used. (A technique was being investigated, with preliminary data,

for obtaining Z_T (open circuit) by use of the input admittances of two electri-

cally short antennas, one having exactly twice the length of the other and each

having the same physical shape of the desired finite open circuit.)

For practical application note that the values of $Z_{in}(SC)$ for

an electrically short antenna, i. e. , for frequencies much lower than those

for anti-resonance, provide a better impedance match to a 50-ohm coaxial

feeder than those for an open-circuit antenna (RG-8/U type antenna).

3. Comparison of Theory with Experimental Data

It would be desirable to have input impedance data for insulated

antennas similar to those for bare wire antennas obtained by Iizuka and King[48,49]

at VHF for antennas immersed in dissipative media of known electrical

constants. It was suggested to Professor King that this might be a useful research using their experimental set-up. The results are being made the subject of a report.[*]

With regard to our full-scale VLF-LF measurements for antennas immersed in the rock below an overburden as in Cape Cod holes, several comments made above indicate agreement in the gross features of the theory with experimental measurements:

— The trend of measured input impedance $Z_{in}(OC)$ and $Z_{in}(SC)$ with frequency is in accord with theory;

— The measured resonant and anti-resonant frequencies for $Z_{in}(OC)$ are in good agreement with corresponding anti-resonant and resonant frequencies for $Z_{in}(SC)$ with $\left| Z_T \right|^2_{SC} << \left| Z_C \right|^2$ and $\left| Z_T \right|^2_{OC} >> \left| Z_C \right|^2$ and in accordance with theory;

— Predicted resonant frequencies for the quarter-wave antenna of fixed length are in good agreement with theory for reasonable assumed values of constants of the medium. Values of f_r are, however, not too critically dependent upon a knowledge of σ_3 for large loss tangents p_3 in the range of constants encountered.

Finally, a curve of $Z_{in}(OC)$ vs frequency was computed for an open-circuited coaxial antenna of the RG-8/U type, 475 feet long. The theoreical curve, assuming $Z_T = \infty$, is shown in Figure IV.9 in which the experimental curve for the Harwich antenna from Figure IV.8 is shown for comparison, for frequency 50 to 300 kc. The frequency range covers first resonant

---

[*] Dr. K. Iizuka, private communication.
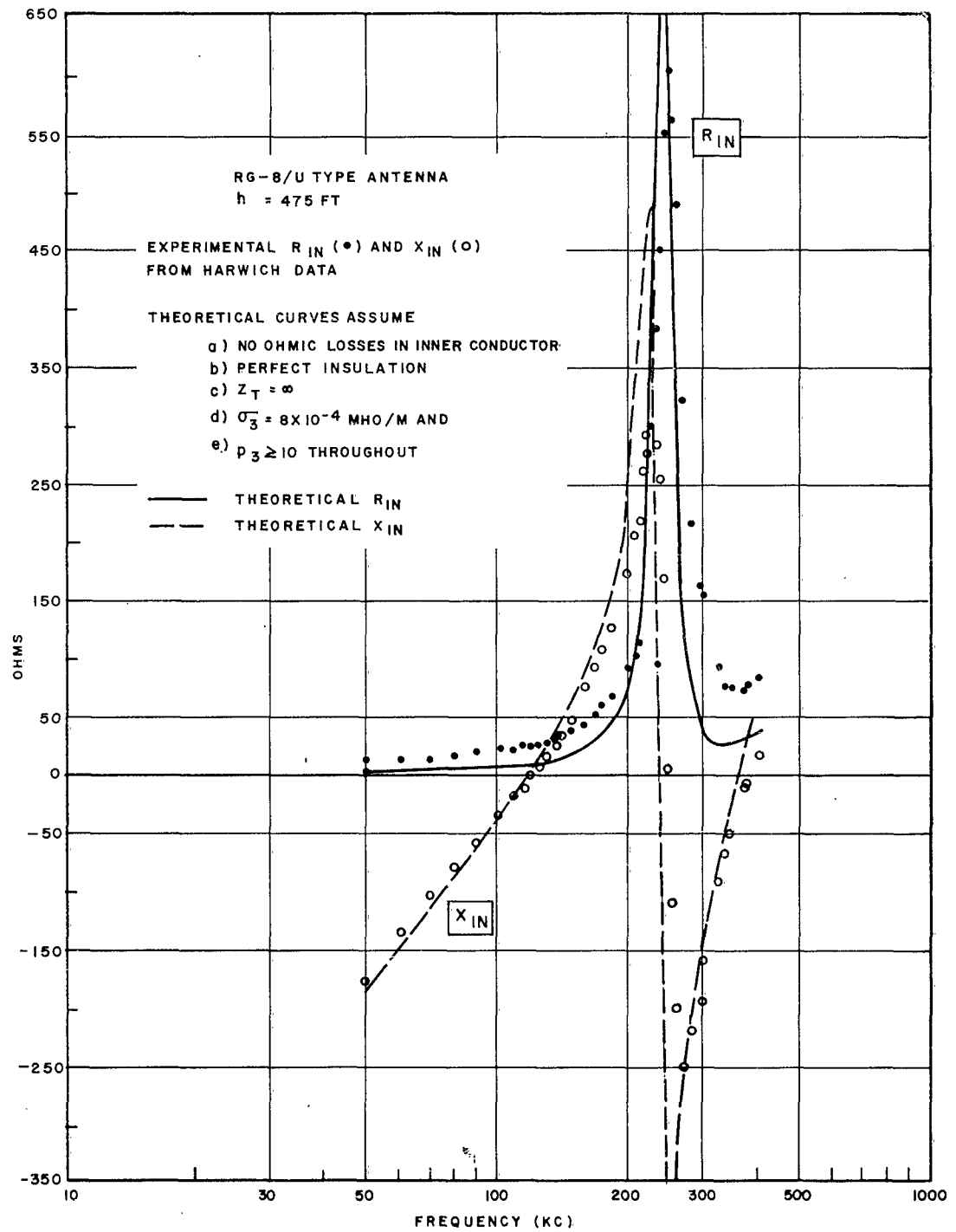
Figure IV. 9. Comparison of theoretical with measured input impedance $Z_{in}(OC)$ for insulated monopole, open circuited.

and anti-resonant impedances. Further assumptions regarding the antenna are that the inner wire was perfectly conducting and of radius $a_1 = 0.0408"$ = 1.036 mm, that $\ln \frac{a_2}{a_1} = 1.250$, and that the insulation was a perfect dielectric with $\mathcal{E}_{r_2} = 2.25$. The medium was assumed to have the electrical constants shown on Figure IV.9. The theoretical and experimental curves agree well in the trends and resonant and anti-resonant frequencies. The theoretical maximum resistance is larger than that measured and is attributed to the simplying assumptions in the theory, namely, a perfectly conducting inner conductor, a loss-less dielectric, $Z_T = \infty$, and a very large, perfectly conducting "ground plane." In practice, these assumptions are not all fulfilled. The finite conductivity of the inner conductor and losses in the water-absorbing polyethylene insulation would affect α / β, to some extent expected to be small. The finite though expected large value of Z_T would also reduce maximum values of input resistance and reactance. It is expected that the finite conductivity of the overburden ground plane would also affect these components of the impedance (maximum values) without affecting seriously the resonant frequency. The measured value also includes the end effect of the coaxial line but this correction (negative capacitance) is expected to be small.

Section V. TECHNIQUES FOR MEASURING ELECTRICAL CONSTANTS OF ROCK STRATA

A. Introduction

For ultimate application to radio transmission through rock strata, it is desirable to make measurements of the radio properties of such media _in situ._ This is because small amounts of pore water can markedly influence the value of conductivity deduced from laboratory measurements on "dry" samples of the rock. The values of conductivity for "dry" granite appear to be more influenced by temperature than pressure, as is the relative dielectric constant. Both σ and ϵ_r for dry granite appear to increase with high temperature and are somewhat frequency sensitive in that σ increases markedly with increased frequency and ϵ_r decreases slightly with increased frequency. Temperature ranges discussed exceed 200° C. and frequency ranges include the ELF and VLF spectra.[*]

Even if the porosity of the rock is small, say less than 1% of the pore space by volume, the conductivity of the "wet" granite is changed markedly by pore water. If the "dry" granite has a conductivity, say 10^{-6} mhos/m, a "wet" granite infiltrated by much higher conductivity water will tend to have a conductivity more nearly that of the pore water. If the rock depths are of the order of 3 to 10 miles ("shallow" to the geologist) and temperatures are of the order of 200° C, free water does not form and very low values of σ are anticipated. Our measurements have been at depths into

---

[*] A. Orange, AFCRL, private communication.

drill holes only 1000 feet deep and the rock encountered is well fractured; correlative surface resistivity measurements of deep resistivity indicate granite conductivity of the order of 10^{-4} mhos/m may be encountered at these and slightly greater depths. Such a value is much larger than typical values for "dry" granite ("dry" in the sense that all free water has been removed).

In addition to the water content problem necessitating measurements in situ (or a reasonable facsimile thereof in the laboratory), there is a second major characteristic of nature requiring such measurements. This is that rock electrical characteristics are anisotropic both with depth and with horizontal extent, at practical depths. Suppose one had drilled two holes A and B deep into the rock, and it was desired to transmit signals between antennas immersed in the rock portion of those two holes, assumed separated many miles. Assuming the most careful measurements of rock constants of samples from each hole under closely simulated in situ conditions, the values deduced represent those for the area immediately around each hole and do not necessarily apply to the rock region in between the holes. Values of the constants for each hole deduced by any of several techniques to be discussed, may be assumed to approximate those important to the performance of antennas immersed in each hole (say radially outward from A or B to a distance of a few skin-depths). As to what the rock properties are between the hole, other techniques must be employed. Drilling costs would prohibit the use of an adequate number of holes to deduce the anisotropic effects, and results would be difficult to analyze except in a gross statistical sense.

From a theoretical point of view for the radio scientist, Wait and Conda[85] have treated the distinction in the anisotropic case between horizontal, vertical, geometric mean, and apparent conductivity for interpreting measurements of ground conductivity, and developed the theory applicable to a two-layer model of the earth (say, overburden layer of finite thickness above a semi-infinite rock medium below).

In Section VB there is a general discussion of techniques which may be used to deduce electrical properties of rock under two categories: the first where drill holes do not exist and the second where drill holes do exist. The measurements in which we have participated and/or actually performed are described in the ensuing Subsections VC through VH. In the last Subsection some proposed measurements employing loops are discussed.

B. General Discussion of Measurement Techniques

It is desired to measure the electrical properties of rock strata in situ, into which antennas are to be immersed and through which radio waves are to be propagated for purposes of communication. The techniques which may be employed may be divided into two categories, (1) those which do not require direct access into the rock by virtue of vertical drill holes or mines, and (2) those which may be employed when such holes or mines exist. Of course, if the drill holes or mines are "clean" electrically ("clean" in the sense that no electrically disturbing structures are present and that the drilling has not affected the rock electrically), then techniques in category (1) to be discussed can be employed whether or not the drill holes exist.

1. Those Not Requiring Direct Access (Drill Holes) Into
   the Rock

   a. Surface Resistivity Methods

   Measurements are made of the mutual impedance between dipoles on the surface of the earth as a function of dipole spacing. The results yield values of apparent resistivity of the earth below and interpretation of conductivity of layers depends upon the model assumed. The technique is discussed further in Subsection VC with reference to measurements made on Cape Cod by others.

   b. Magneto-Telluric Methods

   In magneto-telluric methods the source of the fields to be observed are those such as natural telluric currents. The horizontal electric intensity E_h and magnetic intensity H_h are observed. At the earth's surface the apparent complex impedance of the earth looking downward is

   $$\mathcal{Z}_a = E_h/H_h \qquad\qquad (V.1)$$

   assuming plane waves. The observations are made at fractional cps frequencies at which the loss tangents of the media are large. Then

   $$\mathcal{Z}_a = \sqrt{j\omega\mu_o\sigma_a} \qquad\qquad (V.2)$$

   for non-magnetic media, where σ_a is the apparent conductivity of the earth. If the earth is assumed to be horizontally stratified, values of σ_a in equation (V.2) may be used to determine the characteristics of those horizontal layers, depending upon the model assumed. Thus, for two-layer models (e.g., an overburden of finite thickness above a semi-infinite rock medium) the equations

and curves of Cagniard,[27] Wait[79] and Wait and Conda[85] may be used for
interpretation. For three-layer models, the relations of Cagniard[27] and the
curves of Yungul[93] may be employed.

While we have made no magneto-telluric (M-T) measurements
in our program, the results of others serve to indicate the great depths which
can be obtained. Lahiri and Price[57] and more recently Cantwell and Madden,[28]
using M-T methods, found that at depths of the order of 100 km, the conduc-
tivity increased to values between 0.03 and 1 mho/m, presumably associated
with the Moho. Geophysicists prefer to use active surface measuring methods
rather than M-T methods.

c. Role of Seismic, Magnetic Field and Gravity Surveys

Seismic, magnetic field and gravity surveys are used to
locate and classify various types of rock media and discontinuities. Examples
were those surveys performed on Cape Cod. The results of seismic and
magnetic field measurements and analysis are contained in a report of work
performed by Weston Geophysical Engineers[97] under a subcontract. Gravity
surveys were made by the Geophysical Research Directorate, AFCRL, under
Mr. Gerry Cabaniss. The surveys covered several areas on Cape Cod and
were concentrated on regions near Harwich (where the first hole was drilled)
and Brewster (where the second hole at the Town Dump and the third hole off
Tubman Road were drilled). Seismic soundings were carried out at several
points along lines on the surface. Seismic refraction data were used to locate
a drill hole near Sand Pond in Harwich. Rock media appeared to commence

at depths below 400 to 500 feet from the surface. In the area in Brewster, seismic velocities were about 1700 ft/sec at sea level, about 5000 ft/sec in the overburden, and 14,500 to 18,000 ft/sec in the rock strata below, the higher value probably corresponding to denser and more massive bedrock.

Contours of the earth's magnetic field showed probable anomalous areas in the shape of "fingers." Most probable areas for a good rock propagation path are those where seismic velocities are high and magnetic and gravity contours are relatively free of anomalies. Such surveys do not give directly the electrical properties of the rock strata, but give probable rock formations and extent and areas to be avoided.

These surveys may be used to help interpret measurements of deep resistivity from measurements on the surface (surface resistivity and M-T methods). The rock conductivity data deduced from the latter methods are strictly applicable to the extremely low frequencies employed, usually in the fractional to a few cps range.

There may be phenomena peculiar to a certain area being surveyed which are not typical of areas being explored generally for finding rock strata suitable for radio wave propagation. Thus, for Cape Cod there was concern that the surrounding sea water might infiltrate the area and affect some of the conclusions of survey measurements. A study was made by Rev. J. W. Skeehan, S. J. (Boston College) as a consultant of the possible effect of sea water infiltration. A previous study had been made of the behavior of fresh and salt water mixing on Long Island. After the Harwich hole

had been drilled, Fr. Skeehan noted the salinity was 340 ppm and, using this with the previous correlative behavior on Long Island, concluded that the limited development of clay strata was insufficient to render the underlying deposits impervious to saline contamination. Rock conductivity would then be higher than that were such contamination not present. Saline contamination would not be expected for general inland areas.

2. Techniques Where Drill Holes Exist

A number of techniques have been used for measurements of electrical properties of rock when suitable drill holes exist. Our experience has been with drill holes which are filled with water and the surrounding rock is well fractured and porous. The conductivity of such rock is governed more by that of the water. Techniques which may be used to measure the constants of liquid media or of sample rock extracted in the drilling are described in von Hippel's text. [14]

a. Transmission-line type methods

b. Impedance measurements of samples with RF bridges and Q-meter

These methods, with results, are described in Subsections VD and VE, respectively.

When a single hole exists having an adequate depth of penetration into the rock, a new method was devised which permits one to deduce surrounding rock electrical constants from a measurement of

c. Attenuation vs depth into rock media

This method, known as the "depth attenuation method" is described in Section VF and includes some results of measurements on Cape Cod.

The input impedance of a linear antenna immersed in a dissipative medium depends upon the constants of that medium and type of antenna being employed. One then has the method which is that of obtaining

d. Estimates from antenna impedance measurements

The method and some results using bare and insulated line or antennas are described in Subsection VG.

When two drill holes exist between which a radio signal has been transmitted, it is possible to obtain an estimate of the intervening rock conductivity. The method and results are discussed in Subsection VH. entitled

e. Estimates from path transmission loss data (1 mile - Cape Cod)

Finally we have made some studies of methods using loops which might be employed. Measurements have not been made with these methods and their proposed use is described in the last Subsection entitled

f. Proposed methods using loops.

C. Surface Resistivity Measurements - Discussion of Cape Cod Data (Geoscience, Inc.)

While we have not made measurements ourselves using surface resistivity methods, we have participated in measurements made by others on Cape Cod and described below. Because of the relation of the subject to our

V-8

program and because of some proposed methods which are also discussed below, the topic is treated further here.

1. Four Electrode Arrangements

The usual four electrode schemes with a variation suggested by Wait and Conda[85] are shown from the top schematically in Figure V.1. Current is introduced into the earth through the "current" electrodes P and Q. The potential difference resulting elsewhere is measured between "potential" electrodes p and q. In the Wenner array in A of Figure V.1, P and Q are the outer electrodes, p and q the inner ones. In the Eltran arrangement, B of Figure V.1, the electrodes are also arranged on a line, but P and Q are at one end and p and q are at the other end. In C of Figure V.1 is shown the modification to the Eltran arrangement introduced by Wait and Conda[85] and called the "right-angle" array. An advantage to the last is the absence of mutual inductance term in the mutual impedance between "primary" PQ and "secondary" pq. The usual arrangements have all inter-electrode consecutive spacings equal, shown as a in the figure.

As discussed by Wait and Conda,[85] one measures the mutual resistance R_{12} from the measured "primary" current (I_1) and induced open-circuit voltage in the "secondary" (V_2). From a knowledge of "electrode circuit" length and spacing between primary and secondary electrode circuits, one computes the apparent conductivity σ_a for the scheme used. The final geometric mean conductivity $\bar{\sigma}$ is obtained by curve matching to sets of master curves from data obtained as spacing a is varied. The curves depend
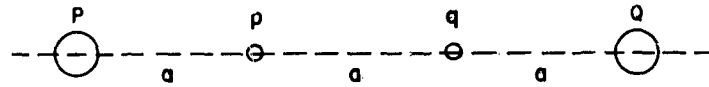
(A) WENNER ARRAY
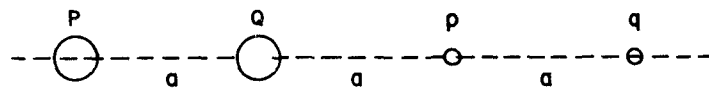
(B) ELTRAN ARRAY
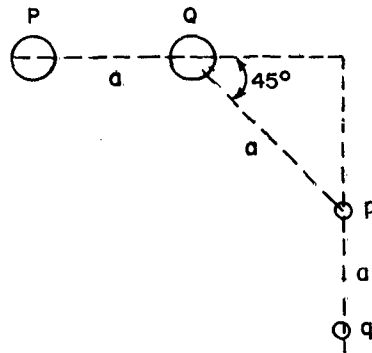
(C) RIGHT ANGLE ARRAY

Figure V. 1.   Four electrode, equispaced, arrays for surface resistivity
measurements (A) Wenner array, (B) Eltran array, (C)
Right angle array.

upon the model assumed and the type of electrode array employed. The curves are plots of $\sigma_a/\overline{\sigma}$ vs a/d_{eff} with reflection coefficient K as a parameter, where d_{eff} is the effective thickness $\propto d$ (of the upper layer of thickness d) and $\propto$ is the anisotropy ratio $\sqrt{\sigma_h/\sigma_v}$ (see Figure V.2). Curves for the two-layer model, Wenner array, were developed some time ago and recently were given for all three arrays in the above notation by Wait and Conda.[85] They show that the Eltran array is more sensitive at smaller spacings than the Wenner array but the latter is better at larger spacings. The right-angle array is somewhat in between the others for showing up sensitively departures of $\sigma_a/\overline{\sigma}$ with a/d_{eff}. Master curves have been computed for a three-layer model by Yungul.[93] For the two-layer case, one computes σ_a from a knowledge of measured mutual resistance R_{12} and array spacing. When a is small, the measured R_{12} is due principally to the upper layer if its conductivity is larger than the lower region. If homogeneous regions are assumed and the upper layer thickness d is known, the curve of "measured" $\sigma_a/\overline{\sigma}$ vs a/d gives the value of K whence the value of σ_2 of the lower region.

Some preliminary measurements were made by Geoscience, Inc.,[94] for AFCRL along a single line through the drill holes at the Brewster Dump site and on Tubman Road on Cape Cod. The technique employed the improved phase detector scheme of Madden, Cantwell et al.[59] Insulated dipoles with special low resistance grounds were employed as the transmitting (current) and receiving (voltage) electrodes. The dipole lengths were mostly 1000 feet. Dipole centers were spaced from 2000 to 8000 feet in 1000 ft. intervals.
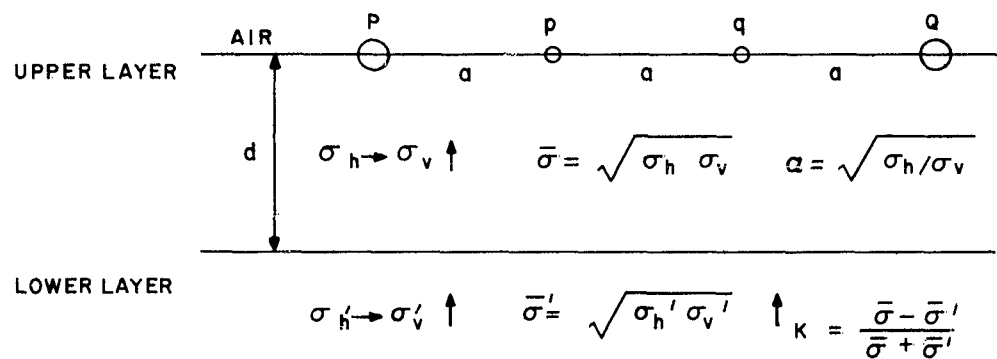
Figure V. 2.   Schematic representation for two-layer ground, each layer anisotropic.   (Sketch shows Wenner type 4-electrode arrangement.)

Because of the anisotropic behavior alluded to earlier, certain care is needed in the analysis of the data. Strictly, for the survey of an area including the desired propagation path, one should make measurements over lines in several directions to ascertain horizontal anisotropy. The results are considered tentative because they are based on measurements along one direction. Even in such case, it is necessary to select data for analysis. By a simple techniuqe of "contouring" the values of apparent conductivity, Geoscience, Inc., was able to deduce the appropriate values for further analysis.

For the spacings so selected, the resistivity of the upper layer was estimated from values for small spacings as 100 to 150 meter-ohms, i.e., conductivity σ_1 of 7 to 10 millimhos/meter for the overburden. Comparing the graph of apparent resistivity vs electrode separation with master curves for a two-layer model, the graph agreed fairly well with master curves; with σ_2 the conductivity of the rock, the conductivity contrast $\frac{\sigma_2}{\sigma_1}$ = $\frac{1}{39}$. If σ_1 is assumed to be 10^{-2} mhos/m, then d works out to be 500 ft. and σ_2 is about 2.6×10^{-4} mhos/m. On the other hand, if σ_1 is assumed as 6.7×10^{-3}, then d works out to be 700 ft. and σ_2 is then 1.7×10^{-4} mhos/m. From seismic soundings the upper layer thickness is more nearly the former value and one deduces σ_1 to be 10^{-2} and σ_2 to be 2.6×10^{-4} mhos/m.

The marked distortion of the apparent conductivity "contours" noted near the Brewster Dump drill hole corroborates qualitatively the variability in earth-rock structure as a possible cause for distortion in surface

field pattern measurements at various ranges from the hole when being used as the location of a transmitting antenna (see Section VI). The overburden was sand, clay, and gravel. Small scale measurements to obtain a good estimate of overburden conductivity are apt to be quite variable. Some of the variability noted near the drill holes may be due to the casing pipe itself.

Following the ideas of Wait and Conda[85] regarding anisotropy, the values of σ deduced above are those for an assumed homogeneous over-burden and rock layers, i.e., α was assumed unity. The resulting value of σ should be corrected to its geometric mean value $\overline{\sigma}$ if α were known.

Measurements should be made along other directions and better estimates of upper layer (overburden) conductivity are needed to obtain more final values of soil and rock constants.

In place of the long electric dipoles, loops placed parallel to and on the ground may be used, as discussed in the last Subsection.

D. Transmission-Line Type Measurements

Sections of parallel wire or coaxial transmission lines may be used for certain types of measurements of the electrical properties of dissipative media. When such lines are electrically short, they may be considered as parallel wire or coaxial "condensers."

An example of the use of parallel wire lines is that reported by Kirkscether[55] for measuring the electrically properties of the ground. Iizuka and King[49] used a coaxial line filled with a dissipative liquid and measured the properties of that liquid by slotted line and impedance techniques at VHF.

A coaxial condenser was also used. (Measurements of the properties of linear radiators immersed in such liquids were being studied and a knowledge of the constants of the liquid was required.) Von Hippel[14] has described such techniques. Concentric cylinder cells are available commercially for measurements on liquids such as the various two- and three-terminal cells of Balsbaugh Company (Braintree, Mass.).

The measurements using short transmission lines are principally affected by the constants of the medium between the wires or cylinders when the spacing is close. Thus, Kirkscether[55] inserted parallel rods into the ground to measure the properties of the ground. In principle, insertion of lines into a rock sample could be employed but the sample would have to be large for measurements at LF. The method is suitable for measurement of drill hole or well water and is described.

As an example of transmission-line methods, a short section of a nominal 300-ohm parallel-wire line was immersed in water in a hole used at Goffstown, N. H. The line was connected through a section of RG-22/U two conductor shielded line to impedance measuring apparatus. The feedline and parallel wire test line characteristics in air were first measured by open- and short-circuit impedance measurements on each line. Because the lines are "balanced" to ground and the bridge employed (916A and 916AL) was not, three-terminal measurements were employed throughout. The parallel-wire line was 70 feet long and the RG-22/U feeder was 40 feet long. Well water characteristics were measured from 100 kc to 10 mc.

The method and analysis is based on extension of relations given in several texts and we used those given in King[6] (Chapter II). The characteristic impedance Z_C for a uniform line is given by

$$Z_C = \sqrt{z/y} = \left| Z_C \right| e^{j\phi_c} \tag{V.1}$$

where

    z = series impedance per unit length of line

    = $r + j x = r + j\omega\ell$

    y = shunt admittance per unit length of line

    = $g + j b = g + j \omega c$

with

$$\tag{V.2}$$

    r = series resistance per unit length of line

    ℓ = series inductance per unit length of line

    g = shunt conductance per unit length of line

    c = shunt capacitance per unit length of line

If the input impedance Z_{SC} be measured when the output of the line is short-circuited, and the input impedance Z_{OC} be that when the output is open-circuited, then

$$Z_C = \sqrt{Z_{SC} Z_{OC}} \tag{V.3}$$

Let us form the ratios

$$\eta = \frac{r}{\omega\ell}$$
$$p = \frac{g}{\omega c} \tag{V.4}$$

V-16

The quantity η is the reciprocal of the series Q of the line and p is the loss tangent of the medium surrounding and in between the conductors, assumed homogeneous. From the definitions of g and c for conductors in a medium, for the parallel-wire line

$$\dot{p} = \frac{g}{\omega c} = \frac{\sigma}{\omega \epsilon_o \epsilon_r} = \frac{60 \sigma \lambda_o}{\epsilon_r} \qquad (V.5)$$

where σ and ϵ_r are the conductivity (mhos/m) and relative dielectric constant (dimensionless) of the medium. The quantity $\epsilon_o \cong 10^{-9}/36\pi$ farads/m and λ_o is the free space wavelength (meters), in equation (V.5). We desire to obtain p and ϵ_r, from which σ can be determined by use of equation (V.5).

Forming the square of equation (V.1) and using equations (V.2) and (V.4), one obtains,

$$Z_C^2 = \left| Z_C^2 \right| e^{j 2 \phi_c} = \sqrt{\frac{\omega^2 \ell^2 + r^2}{\omega^2 c^2 + g^2}} \; e^{j \left[\tan^{-1} p - \tan^{-1} \eta \right]}$$

$$= \frac{\ell}{c} \sqrt{\frac{1 + \eta^2}{1 + p^2}} \; e^{j \tan^{-1} \left(\frac{p - \eta}{1 + \eta p} \right)} \qquad (V.6)$$

and the square of equation (V.3) gives value of Z_C^2 from measured values of Z_{SC} and Z_{OC}.

The parallel line is measured in air. Let this value be Z_o; it is found for a well constructed line with very low loss "spreaders" that ϕ_c is negative. In air, this means that $\eta > p$; for simplicity we assume for the line in air $p \cong 0$. Hence, denoting by η_o the value of η so determined in air,

$$\gamma_o = - \tan \left[2 \, (\emptyset_c)_o \right] \qquad \text{(V.7)}$$

For example, one measurement of the line in air, at 8 mc, gave

$$Z_o = 334 \; \underline{/-0.65^o} = \left| Z_o \right| e^{j \emptyset_{co}}$$

$$\gamma_o = \tan 1.3^o = .023$$

It is assumed that the medium does not change the value of r and $\mathcal{l}$ from its value in air (a major effect would be to change $\mathcal{l}$ if the relative magnetic permeability μ_r greatly exceeded unity). The value of γ for the line in the medium is therefore assumed to be its value in air, whence $\gamma^2 << 1$.

The line is inserted into the well water, connected to the RG-22/U feeder whose values of Z_C and propagation constant were previously measured. The input impedance of the RG-22/U so connected was measured when the parallel wire line was open circuited and then short circuited. These impedances, when inserted into a Smith Chart calculator with known feedline characteristics, gave values of the open- and short-circuited impedances Z_{OC} and Z_{SC} of the immersed test line.

The values of Z_{SC} and Z_{OC}, inserted into equation (V.3), gave values of Z_C for which $\emptyset_c > 0$. This means that $p > \gamma$. It turned out that approximate values of p were so large that the assumptions $p >> \gamma$ and $p\gamma << 1$ appeared justified. With these assumptions, plus $\gamma^2 << 1$, equation (V.6) becomes

$$Z_C^2 = \left| Z_C^2 \right| e^{j 2 \emptyset_c} \simeq \frac{\mathcal{l}}{c} \sqrt{\frac{1}{1 + p^2}} \; e^{j \tan^{-1} p} \qquad \text{(V.8)}$$

whence

$$p \cong \tan 2 \phi_c \tag{V.9}$$

$$\left| Z_C^2 \right| \cong \frac{\left| Z_o^2 \right|}{\epsilon_r} \cos(2 \phi_c)$$

and thus

$$\epsilon_r \cong \frac{\left| Z_o^2 \right|}{\left| Z_C^2 \right|} \cos(2 \phi_c) \tag{V.10}$$

Thus, from measured values of Z_o, $\left| Z_C \right|$ and ϕ_c, values of p and ϵ_r are obtained from equations (V.9) and (V.10), and accordingly, σ from equation (V.5).

Measured values of $\left| Z_C \right|$ and ϕ_c were plotted as a function of frequency and smoothed curves drawn through the points. From "smoothed" values of $\left| Z_C \right|$ and ϕ_c so obtained, ϵ_r, p, and σ were computed and are shown plotted on the curves of Figure V.3.

The results and trends agree reasonably well with some water sample measurements made in the laboratory using a short coaxial condenser and a parallel plate capacitor. Measurements with the latter showed slightly lower values at lower frequencies. Polarization at the electrodes at low frequencies affects the apparent values measured and depends upon electrode size and shape.

The conductivity of the well water would approximate that of well fractured granite around the hole. This assumes that a "dried" sample of the rock would show a conductivity 10^{-5} mhos/m or less and that the well
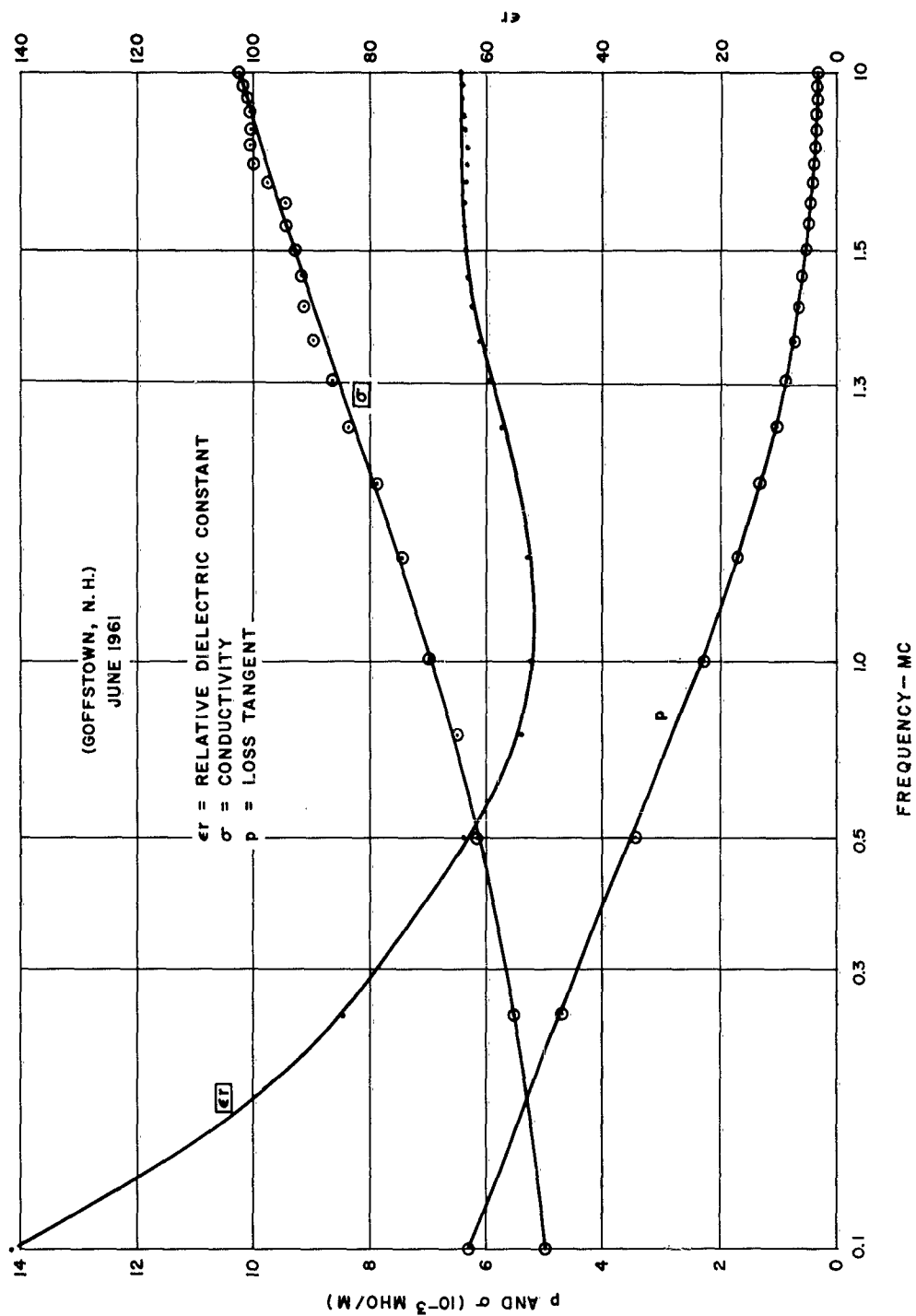
Figure V.3.   Electrical characteristics of drill hole water (Goffstown, N. H.)
June, 1961.   Parallel wire transmission line method.

water is characteristic of the water in the pores and cracks of the well fractured granitic rock.

    E.   Impedance Measurements of Samples by RF Bridges and Q-Meter

       1. Water Samples

Bridge measurements of the impedance of the well water from holes in New Hampshire were made using cells that were either a coaxial condenser or of the parallel plate variety. Results agreed with values using a section of parallel wire line (Subsection VD) except at the lowest frequencies, presumably due to differing "polarization film" effects.

However, we have had less success in such sample measurements on water from drill holes at Harwich and Brewster on Cape Cod. Chemical analysis reveals salinity of 35 ppm for one sample of Harwich drill hole water. The water is quite murky in appearance and gives evidence of some magnetic material, perhaps rust or ion chips from casings. Samples passed through filters showed reasonable values of ϵ_r and σ at high frequencies. A new coaxial condenser was built but not in time for tests.

       2. Rock Samples - Frequency Dependence

Measurements of rock samples were made using a Boonton Type 160A Q-meter for frequencies exceeding 50 kc and a General Radio Type 1650A bridge for lower frequencies.

To approximate in situ conditions, some of the samples were soaked in tap water for a week prior to measurements. (It is appreciated that such "soaking" does not always force water into the pore spaces.) The

resulting data from Q-meter measurements are not considered reliable because of the low value of Q. The data are presented nevertheless, giving ϵ_r, σ and loss tangent p as a function of frequency.

The measurements were an attempt to ascertain the possible frequency dependence of the electrical properties of water-soaked samples. The results are shown plotted on the composite curves of Figure V.4 for relative dielectric constant (ϵ_r), loss tangent (p) and conductivity (σ) for the following four examples

        — Harwich rock sample (slate) - solid curve

        — Brewster rock sample (granite) - long dashes

        — Concord rock sample (granite) - short dashes

        — Weston rock sample (granite) - dash dots

The frequency dependence of σ may be ascertained from log-log plots of the data on the curves of Figure V.5. It appears for these samples so treated that when frequency is low, where loss tangent is high, that σ is relatively independent of frequency. At higher frequencies, where the loss tangent is low, it appears that σ may vary proportional to frequency with an exponent between 0.5 and 1.0, approximately.

The remarks are apropos values of σ deduced for rock samples from surface resistivity measurements at d.c. or fractional cps frequencies.

One should not draw the conclusion from the data that σ in the whole Harwich drill hole area is less than that for the whole Brewster drill hole areas. The data are for random samples only. An example of variability of σ with depth is discussed below.
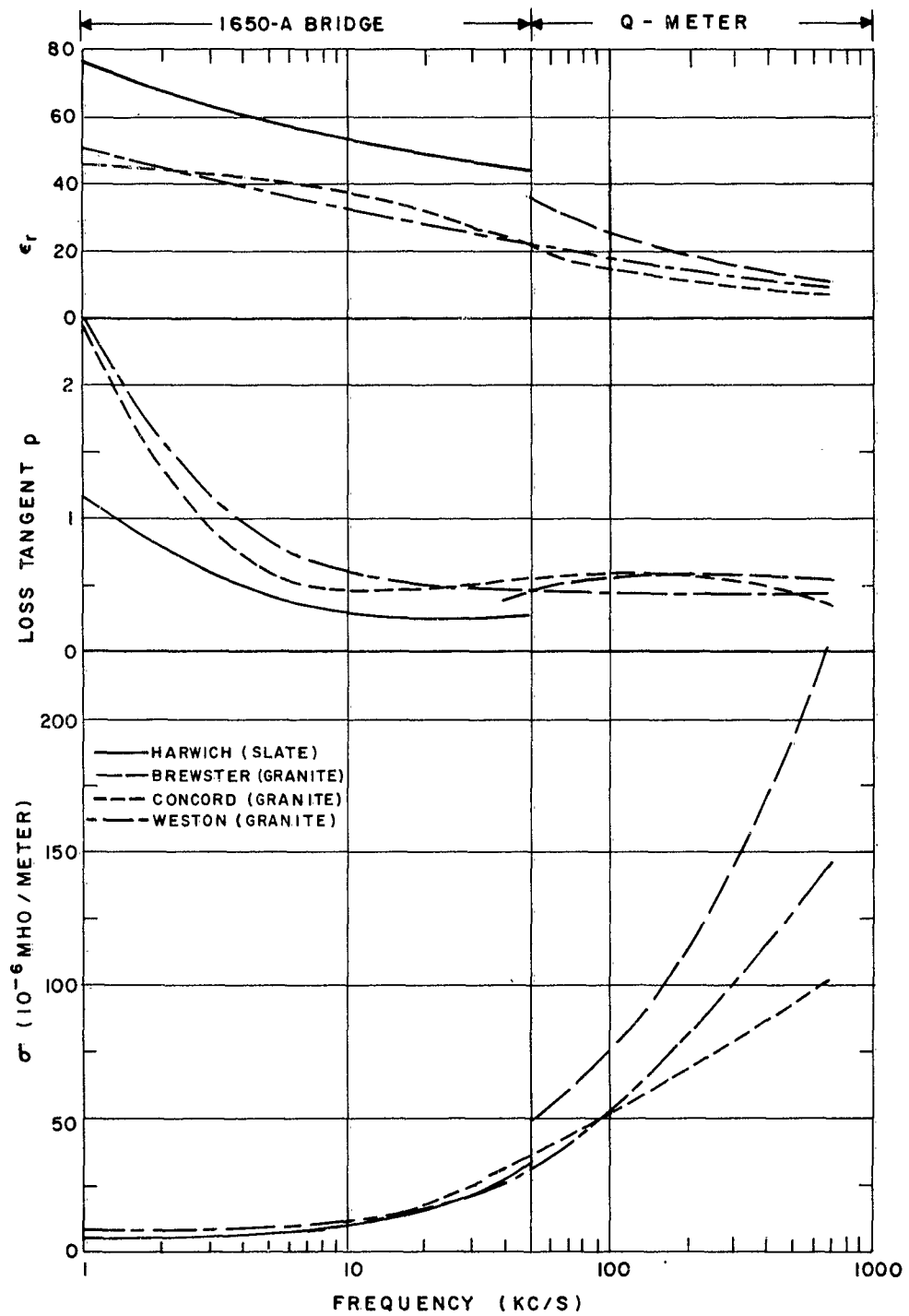
Figure V. 4. Frequency dependence of electrical properties of rock
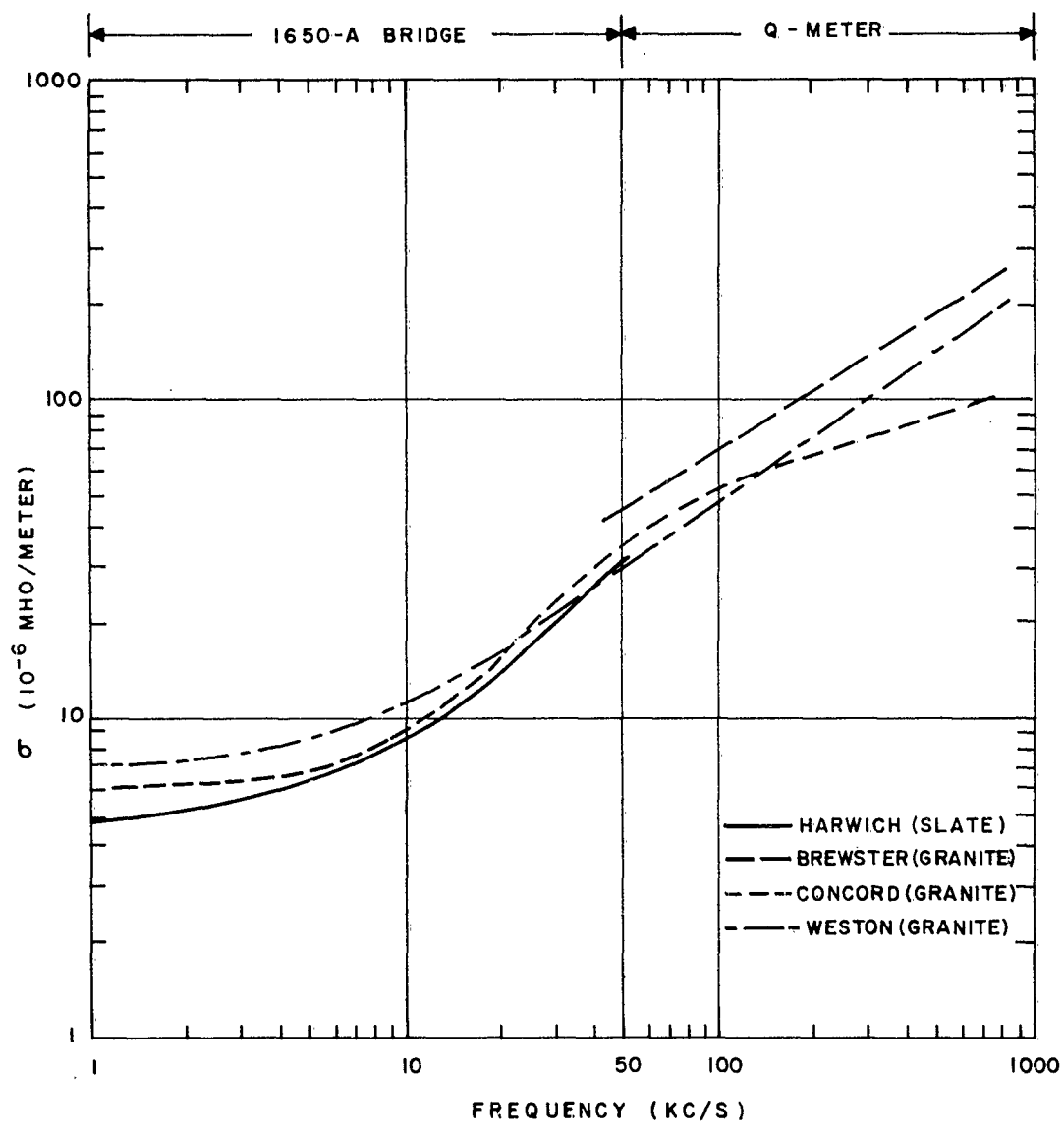
Figure V.5.   Frequency dependence of conductivity (σ)
for water-soaked rock samples

3. Drill Hole Core Samples - Conductivity vs Depth

An example of the variability with depth is that obtained from core samples of the Tubman Road (Cape Cod) drill hole. The cores were measured within a few hours after extraction and care was taken in the handling and treatment of the cores. Because depths were modest, the measurements are believed to represent in situ values at extremely low frequencies (1 to 10 cps). The measurements were made by Cantwell and tabulated by Geoscience, Inc.[94] The results are shown plotted in the semi-log plot of Figure V.6 with identifications of the rock being those tabulated in the report of Geoscience, Inc. An "unweighted average" conductivity of the core samples is about 1.5×10^{-4} mhos/m. This is in fair agreement with the surface resistivity value of 2.6×10^{-4} mhos/m based on the useful data at points a few thousand feet to the west towards the Brewster Dump drill hole site.

Noted on Figure V.6 are the overburden depths of 310 feet based on seismic sounding data of the Weston Geophysical Engineers, Inc.[97] in an easterly direction from the Tubman site and from contour values 1000 ft. to the east of that site. Also noted is the estimate of lower boundary of overburden (395 ft.) and casing depth (410 ft.) from drill log information.

F. Attenuation vs Depth into Rock Media

1. Method and Variation

The depth attenuation method is that of measuring the decay of the field in the rock media of interest between a separated transmitter and receiver as a function of the vertical distance of travel within the rock. One
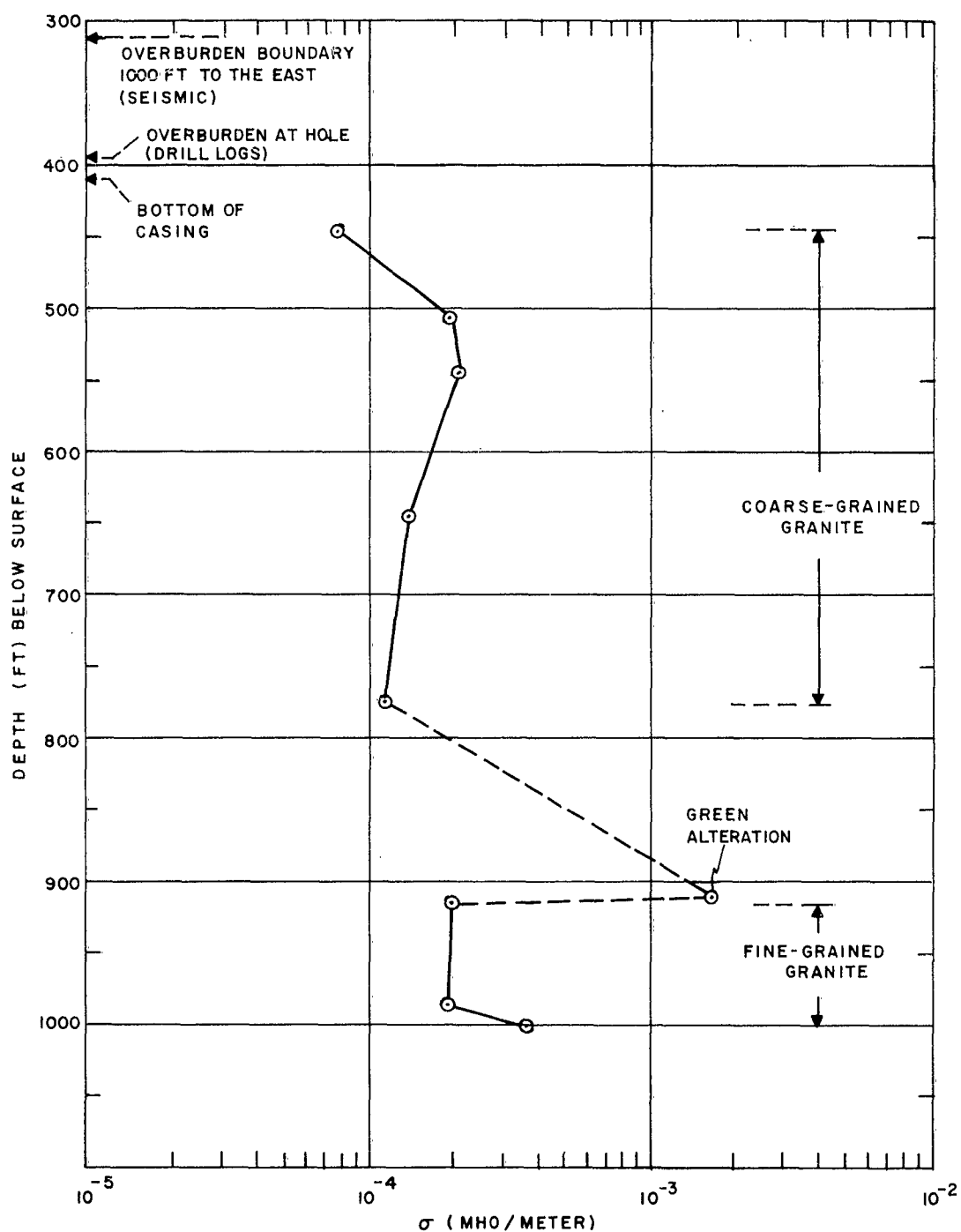
Figure V. 6.   Conductivity of core samples vs depth –
Tubman Road drill hole (Cantwell)

variant of the method for use in vertical drill holes is shown in some detail

in Figure V.7. In this case both transmitting and receiving antennas are

located within the rock medium below a highly conducting overburden. The

decay of the axial electric field between an electric dipole source at A and a

receiving probe at B is a function of the axial antenna separation distance R.

The distance R is varied by changing the relative depths of antennas at A and

B.

Variations of the method from that shown in Figure V.7 can be

employed. These include:

—— interchanging the positions of the source at A and
receiving probe at B;

—— locating a high-power source at A and, at the surface in
air, measuring the field which penetrates the overburden
as the depth of the source is varied. (In practice the
transmitting dipole is fed from a high-power transmitter
on the surface; the effect of the feeder must be taken
into account.);

—— locating a variable depth receiving probe at A and meas-
uring the field at A due to attenuation of known source
fields on the surface. (The fields on the surface may
be ground wave fields due to remote transmitters or
atmosphere noise sources. For ready analysis, it must
be known that the field arriving at A is due to such ground
wave fields as attenuated only by the overburden nearby.);

—— using dipoles other than vertical electric types. (Horizontal
electric dipoles are impractical here principally because
of the small diameters of drill holes, usually 3 to 7 inches.
Small loops might be used but we do not have correspond-
ing experimental data to cite at this writing.).

COAXIAL
FEEDER

C

TO RECEIVER
(FIELD INTENSITY
METER)

AIR

OVERBURDEN

CASING
PIPE

NEOPRENE JACKET
REMOVED

"GROUNDING
CAGE"

INSULATED
ANTENNA

ROCK

B

SHORT CIRCUIT
ELECTRODE

DRILL
HOLE

R

INSULATED, SHORT—
CIRCUITED DIPOLE
ANTENNA

ENCAPSULATED
TRANSMITTER

A
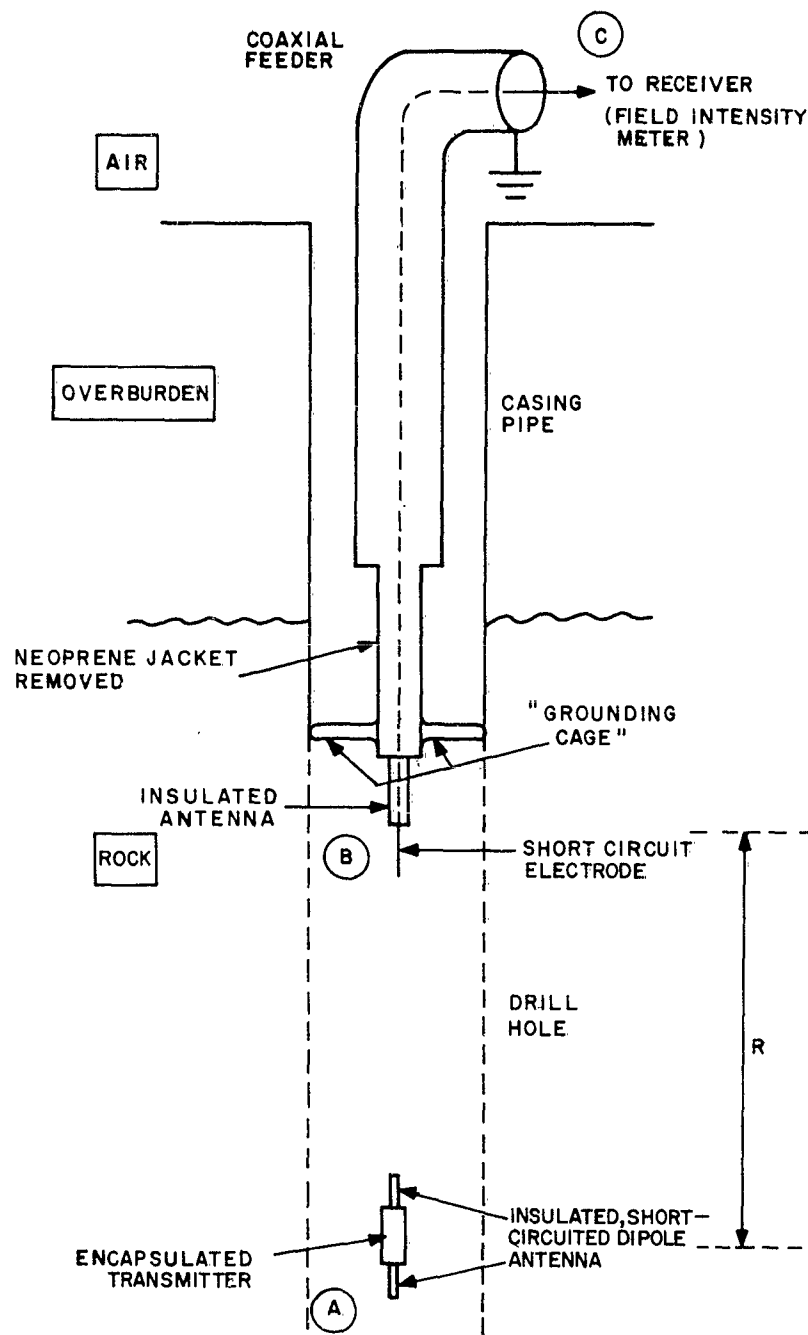
Figure V.7.   A depth attenuation method for obtaining electrical constants
               rock media.   Transmitter at A separated a distance R from
               a receiving dipole at B, with R varied.   The receiver is at
               on surface.

2. Theory

Development of appropriate field expressions for the depth attenuation method depends upon the arrangement of antennas being used. For the particular arrangement in Figure V.7 wherein a thin vertical electric dipole source is used (shown at A), it is desired to calculate the electric field as a function of distance along the axis of the dipole. Consider first that the dipole source is located at the origin of a rectangular coordinate (x, y, z) system and is situated in a homogeneous, dissipative, non-magnetic medium of infinite extent. The center-driven dipole lies along the vertical z-axis and carries a current which is constant along its length at the input value $I_T(0)$. The finite dipole length is $2h_T$ and is assumed physically and electrically short, i.e., $\left(\dfrac{h_T}{R}\right)^2 << 1$ and $\left| kh_T \right|^2 << 1$. Along the z-axis $(x = y = 0)$, the electric field has only a z-component. At a point where $z = R$, the complex amplitude of this field may be written[5] as

$$E_z(0,0,R) = \frac{\omega \mu_0 k}{2\pi} \left[2 h_T I_T(0) \right] \frac{e^{-jkR}}{(kR)^2} \left[1 - j \frac{1}{kR} \right] \qquad (V.11)$$

and the usual time dependence $e^{j\omega t}$ is assumed. In the above k is the complex phase constant of the medium given

$$k = \beta - j\alpha = \omega \sqrt{\mu_0 \xi} = \omega \sqrt{\mu_0 \epsilon} \sqrt{1 - jp} \qquad (V.12)$$

in which β and α are the real phase and attenuation constants, respectively, and p is the loss tangent $(p = \sigma/\omega\epsilon)$. The constants are discussed in Section II.

To measure the field given by equation (V. 11) an electric receiving dipole may be introduced at the point $P(0, 0, R)$ lying along the z-axis. Its half-length h_R is assumed such that $\left(\frac{h_R}{R}\right)^2 << 1$ and $\left|k h_R\right|^2 << 1$. The open-circuit voltage V_{R_o} induced in receiving dipole will depend upon the integrated value of equation (V. 11) along its length. It is also assumed that the receiver antenna current is the same at all points along that antenna. With the aforementioned assumptions regarding the receiver antenna and for distances R such that $\left|kR\right|^2 >> 1$, the voltage V_{R_o} will be proportional to the receiving dipole length $(2 h_R)$ and to the field $E_z(0, 0, R)$ given by equation (V. 11). We are principally interested in the distance dependence of V_R. Squaring the magnitude of equation (V. 11) one obtains

$$\left|V_{R_o}\right|^2 = M \frac{e^{-2 \propto R}}{R^4} L^2 \tag{V. 13}$$

where L is the magnitude $\left|1 - j \frac{1}{kR}\right|$ which is then close to unity. The real quantity M is a constant for given dipole lengths, frequency, electrical constants of the dissipative medium, and current $I_T(0)$. M does not depend upon distance if $I_T(0)$ remains constant with R. For a homogeneous dissipative medium and for a given transmitter power, $I_T(0)$ is not seriously affected by the presence (mutual impedance) of the receiver antenna probe when $\left|kR\right|^2 >> 1$.

Referring again to Figure V. 7, insulated dipoles are located in the semi-infinite dissipative medium being measured (rock) below a highly conducting overburden. The effect of the latter on the impedance of the finite

V. 30

short dipole source has not been solved precisely for the model shown. It is expected that the effect will be negligible when $\left|kR\right|^2 \gg 1$. This is because the amplitude of the axial fields will vary at least by 8.7 db per skin depth, or 55 db per wavelength in large loss tangent media (rock). For a receiver antenna located in the rock just below the rock-overburden boundary, variation in receiver voltage V_{R_o} with separation distance R should then follow that indicated in equation (V. 13). The method so far, then, involves a measurement of the magnitude of the mutual impedance between transmitting and receiving dipoles, and in particular the measured variation of such impedance with distance R.

The values of V_R across the load impedance of the receiver antenna will be proportional to V_{R_o}. For a given configuration, V_R is read as R varies and a relative field decay curve is obtained. Using decibel notation, we may rearrange the relation of V_R and R and write

$$C \cong V_R(\text{dbuv}) + 40 \log_{10} R(\text{ft}) \qquad \text{(V. 14a)}$$

$$= M' - 8.69 \propto R + \log_{10} L^2 \qquad \text{(V. 14b)}$$

In equation (V. 14), $V_R(\text{dbuv})$ is the receiver load voltage expressed in db relative to 1 microvolt, R(ft) is the separation distance R in feet and M' is a new constant which includes the change in units. Observed values of C are plotted vs R on a linear scale; the linear portion of the curve observed at larger values of R has a slope which yields the attenuation constant $\propto$ (as written in equation (V. 14b) the quantity $\propto R$ is in nepers).

3. Example of Measurements and Results

a. Location

Depth attenuation measurements have been made in various drill holes in New Hampshire and Cape Cod using several antenna arrangements. A typical measurement was that made in a 1000-foot drill hole at the Town Dump site in Brewster, Massachusetts, using the antenna configuration of Figure V.7. The cast iron casing pipe, about 7 5/8" in diameter, extends downwards 464 feet through the overburden and into the rock where it was sealed. The drill hole diameter in the rock was about 6". Overburden thickness was 433 feet deduced from well log data. The rock below was fractured granite and water filled the hole to within 20 feet of the surface.

b. Equipment

The antennas employed were linear insulated wire types. The transmitting dipole was made of #12 vinyl insulated wire 25 feet long for each half-length. The output ends of the dipole were "short-circuited" by axially arranged pieces of #12 bare wire, each about 25 feet long. The phase constant of the current distribution for the insulated antenna is small compared with that of the surrounding medium and it turns out that the condition $\left|k\,h_T\right|^2 \ll 1$ is well satisfied. The data analysis indicates that useful separation distances R should exceed 250 feet so that the condition $(h_T/R)^2 \ll 1$ is then well satisfied. The current distribution for the electrically short, short-circuited, insulated dipole is constant along its length (resembling a top-loaded vertical whip antenna in air). The actual impedance of the dipole used

V 32

was not measured in situ but measurements on similar antennas indicated a low inductive impedance of about 30 to 35 ohms at 150 kc.

The receiving antenna probe was a short-circuited, insulated monopole 25 feet long and made of #12 wire covered with polyethylene. (RG-8/U cable stripped of outer conductor and neoprene jacket) The short-circuited output electrode was again 25 feet of #12 bare wire. A coaxial cable, about 700 feet of RG-58/U, was used to connect the probe to the receiver on the surface. The desired large metallic ground plane was not practical. As a compromise the input electrode was the casing pipe; this was accomplished via the grounding cage near the monopole input point. The overburden then acted as the ground plane for the probe antenna immersed in the rock.

Two views of an experimental encapsulated transmitter[*] are shown in the photographs of Figure V.8. The assembled device is about 4 feet long and the tube is about 1 1/2" in diameter in order to be accommodated in the smaller diameter drill holes. It was designed, constructed and tested at AFCRL Communication Sciences Lab, Transmission Branch. Watertight end seals were attached with insulated feed-through connections for the antennas. An insulating oil was poured into the tube just prior to use. After an initial warm-up period of about half an hour, antenna current drift was negligible. Battery life of half a day was typical. Output constancy was checked by remeasuring received signal levels at the same transmitter depths during a variable depth run.

---

[*] Earlier versions suitable for larger diameter drill holes were designed and used by G. J. Harmon.
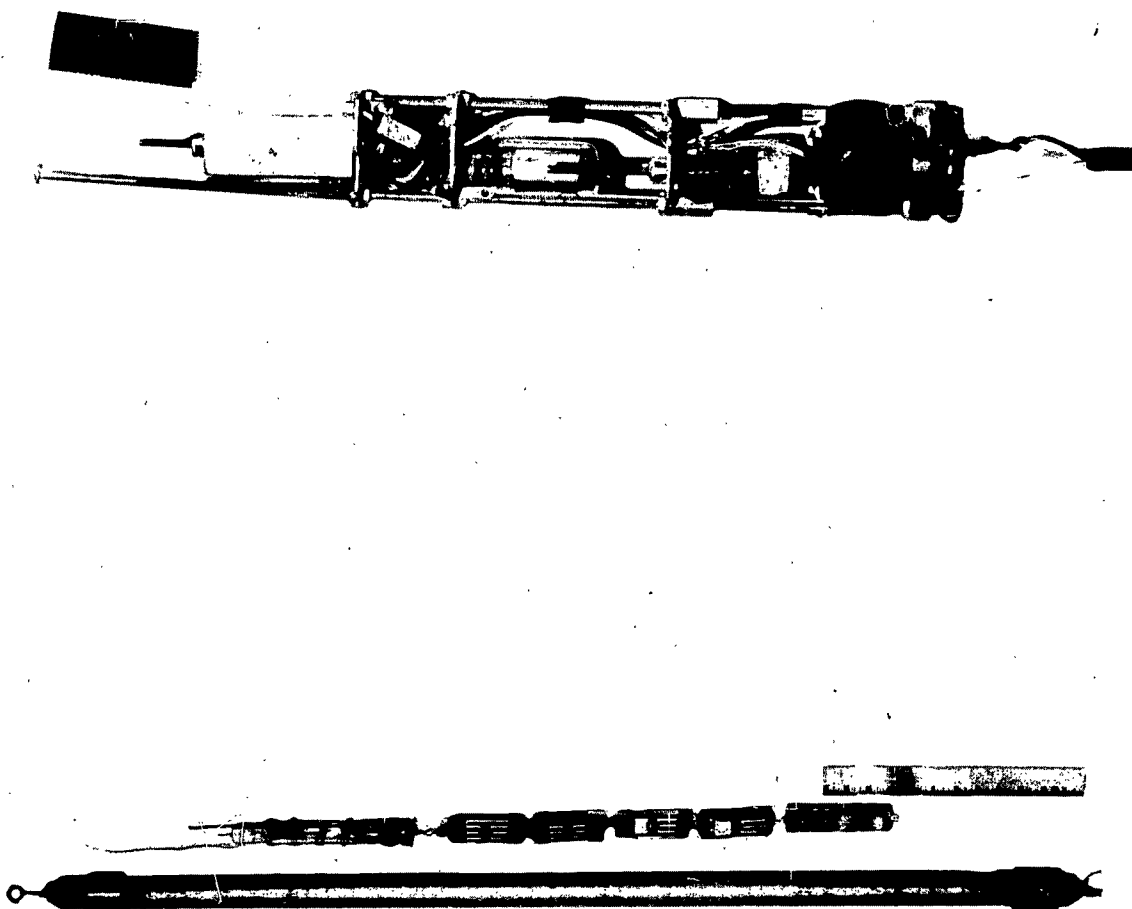
Figure V. 8.   Photographs of experimental encapsulated transmitter.   Top
              shows complete transmitter plus batteries prior to insertion
              into tubular housing.   At bottom is the transmitter.

The encapsulated transmitter and insulated dipole antenna were supported by a nylon rope which was calibrated for measuring transmitter depth from the surface. The receiver coaxial cable was similarly calibrated so that the separation distance R could be determined.

The receiver used was a Stoddard Field Intensity Meter, battery operated, and calibrated several times during a depth run.

The transmitter shown in the photograph of Figure V.8 operated at a fundamental frequency of about 150 kc. Useful signals were detected at the second harmonic over the full depth range and at the third and fourth harmonic frequencies for smaller values of R.

c. Data, Analysis and Results

The first measurements cited were those made at 155 kc in the Brewster hole. The receiver probe input point was maintained at a constant depth a few feet below the bottom of the casing. The depth of the encapsulated transmitter was varied and values of receiver voltage V_R observed as a function of transmitter depth. Constancy of transmitter power output was checked by remeasuring V_R at several depths during a run.

Values of the quantity $\left[V_R \text{ (dbuv)} + 40 \log R\text{(ft)} \right]$ in equation (V.14a) were determined and are indicated by the circled points plotted in Figure V.9. The curve labeled C, the sum of a linear and an exponential distance dependence, was fitted to all the data. Interest is confined to the linear portion where the slope (-6.67 db/100 ft) gives the observed attenuation constant α_1.
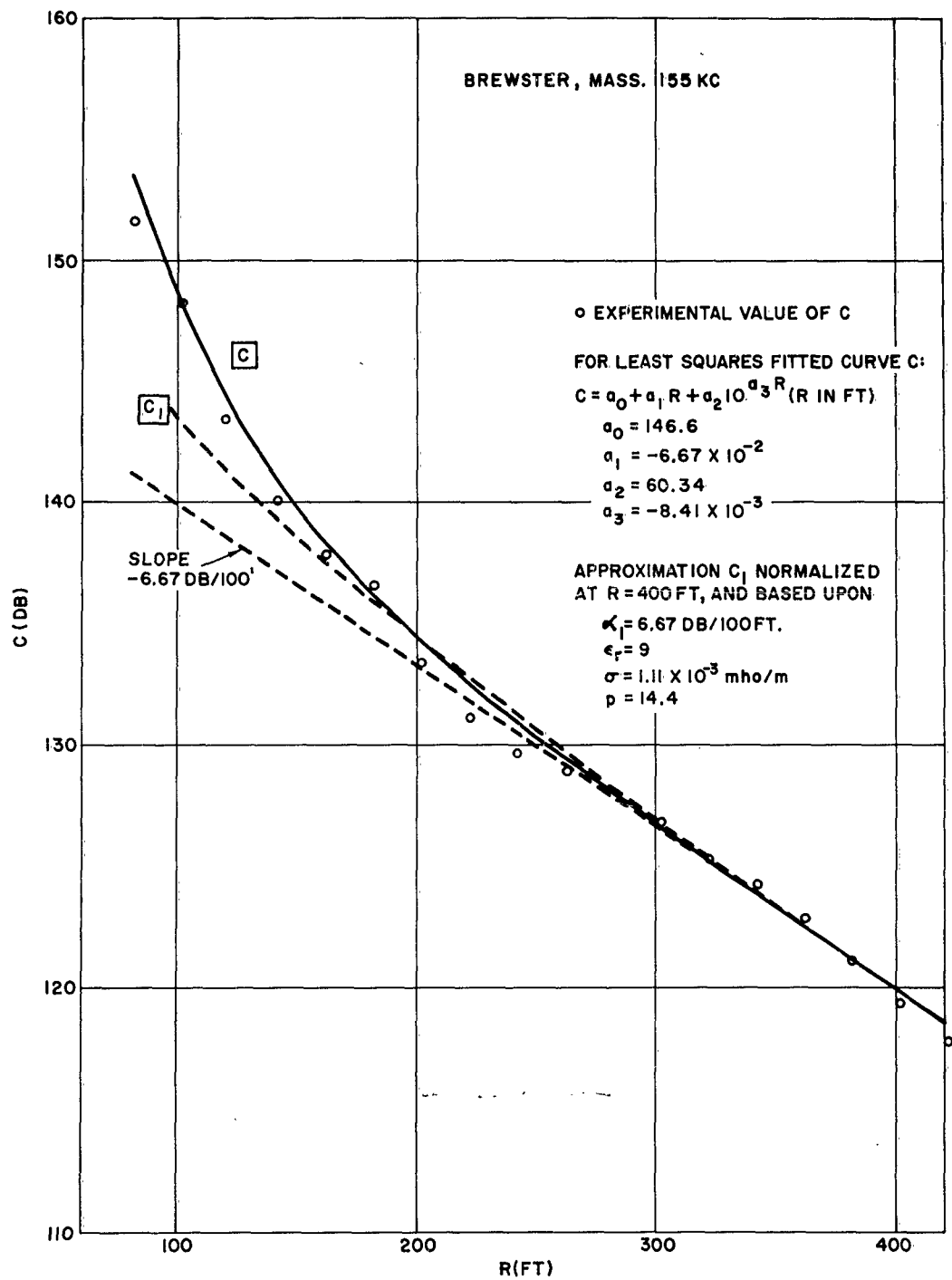
Figure V.9.   Typical plot of C vs R. $C = 40 \log R(ft) + V_R$ (dbuv). Brewster, Mass., site, 155 kc.

Using the relations of Section II, the attenuation constant is given by

$$\alpha = \beta_o \sqrt{\epsilon_r} \, g(p) \qquad \text{(nepers/meter)} \qquad \text{(V. 15)}$$

where

$$g(p) = \left[\frac{(1+p^2)^{1/2} - 1}{2} \right]^{1/2} \qquad \text{(V. 16)}$$

Let α_1 be the observed attenuation constant in db/100 ft. Using equation (V. 15)

$$\alpha_1 = 5.544 \times 10^{-3} \, f_{kc} \sqrt{\epsilon_r} \, g(p), \qquad \text{(db/100 ft)} \qquad \text{(V. 17)}$$

where f_{kc} is the frequency of observation in kc. Rather than calculate and plot families of curves of, say, α_1 vs σ with ϵ_r as a parameter for a given f_{kc}, it is useful to plot implied or interconnected values of σ vs ϵ_r for a given f_{kc} and observed α_1. Using equation (V. 16) in equation (V. 17), the interconnecting relationship between σ and ϵ_r which must combine to give the observed α_1 becomes

$$\sigma = B \sqrt{\epsilon_r + A^2} \qquad \text{(mhos/m)} \qquad \text{(V. 18)}$$

where

$$A = \sqrt{\epsilon_r} \, g(p) = \frac{1.804 \times 10^2}{f_{kc}} \, \alpha_1 \qquad \text{(V. 19)}$$

$$B = \omega \epsilon_o A = 2.004 \times 10^{-5} \, \alpha_1 \qquad \text{(V. 20)}$$

and where α_1 is in db/100 ft.

The value of α_1 is 6.67 db/100 feet in Figure V.9 at 155 kc. The interconnecting values of σ and ϵ_r are shown plotted in Figure V.10
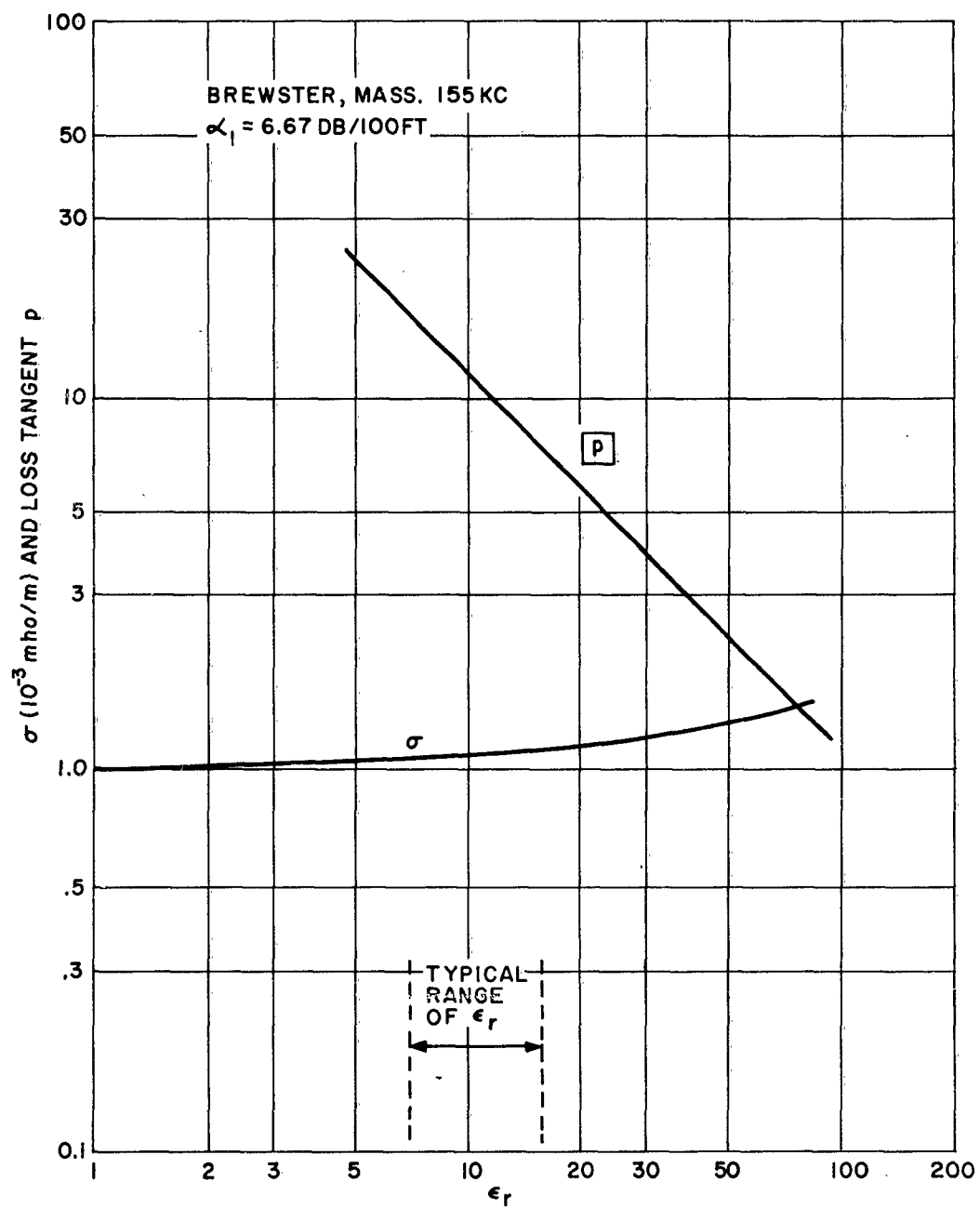
Figure V. 10.   Dependence of conductivity (σ) and loss tangent (p) with assumed relative dielectric constant (ε_r) for observed attenuation constant (α_1) of rock.   Brewster, Mass., site, 155 kc.

on the curve labeled "σ". The consequent values of loss tangent calculated from the paired values of σ and ϵ_r are also shown plotted on the curve labeled p in Figure V. 10. Note that the σ curve is not to be interpreted as a dependence of σ on ϵ_r for the rock; the curve is that of paired values of σ and ϵ_r which give the observed value of α_1.

Referring to Figure V. 10, the curve of σ is relatively flat over a wide range of values of ϵ_r. From other measurements typical values of ϵ_r may vary from 7 to 15; over this range, σ increases from 1. 10 to 1. 16 millimhos/m and p is large and decreasing from 18. 2 to 9, respectively. Thus, σ is well determined from α_1.

Returning to Figure V.9, the curve labeled C_1 is a calculated first approximation from the data obtained from equation (V. 14b). For α_1 = 6. 67 db/100 ft and a typical value of ϵ_r = 9, then σ = 1. 11 x 10^{-3} mhos/m and p = 14. 4. To evaluate k needed in the evaluation of L^2, the quantity $\sqrt{1 - j\,p}$ = 2. 773 - j 2. 587 as determined from tabular values of f(p) and g(p) mentioned in Appendix A. The effect of the constant M' in equation (V. 14) is included by normalizing the calculated values to the value at R = 400 feet on the smoothed data curve C. The agreement between observed (C) and calculated (C_1) values is very good for values of R exceeding 300 feet. For R = 300 ft, $\left| k\,R \right|^2$ = 11. 4.

A second set of data to be cited is that taken from measurements in the drill hole on Tubman Road in Brewster, at 314 kc. The dimensions of this hole are given in Section III. The resulting data, similar to the

plots in Figure V.9, are shown plotted as circled points in Figure V.11. The first approximate value of α_1 was estimated in this case by drawing a straight line through the points, giving $\alpha_1 = 4.03$ db/100 feet. The interconnected values of σ and ϵ_r for this value are shown in the curve of Figure V.12 labeled "σ" for the value α_1; the corresponding value of loss tangent is shown in the curve labeled "p" for the value of α_1. Note that here the values of p are smaller than those in Figure V.10 so that α_1 is not completely dependent upon σ. For assumed typical values of ϵ_r such that $7 \leq \epsilon_r \leq 16$, the values of σ must lie in the range $2.6 \times 10^{-4} \leq \sigma \leq 3.5 \times 10^{-4}$ and $2.14 \geq p \geq 1.24$.

Taking $\epsilon_r = 9$ as a typical value, $\sigma = 2.82 \times 10^{-4}$ and $p = 1.795$ for the observed first approximate value $\alpha_1 = 4.03$ db/100 feet. Then the curve C_1 in Figure V.11 was calculated, normalized to the observed curve at $R = 500$ feet. The curve C_1 departs from the first approximation curve through the data. Noting the departure at $R = 300$ feet was 0.75 db, i.e., the slope of C_1 from $R = 300$ to 500 was too great by $0.75/2 = .38$ db/100 ft, the second approximate value α_2 was determined to be $\alpha_2 = \alpha_1 - 0.38 = 3.67$ db/100 ft. The process was repeated in Figure V.12 with the curves labeled α_2; with $\epsilon_r = 9$, $\sigma = 2.69 \times 10^{-4}$, $p = 1.713$ for the estimated α_2. These data yielded the curve labeled C_2 in Figure V.11, normalized to the observed value at $R = 500$ feet. The curve C_2 is a much better fit to the data points, particularly for R larger than 250 feet. Accordingly, for the Tubman hole at 314 kc, one has for an assumed range of ϵ_r such that $7 \leq \epsilon_r \leq 16$
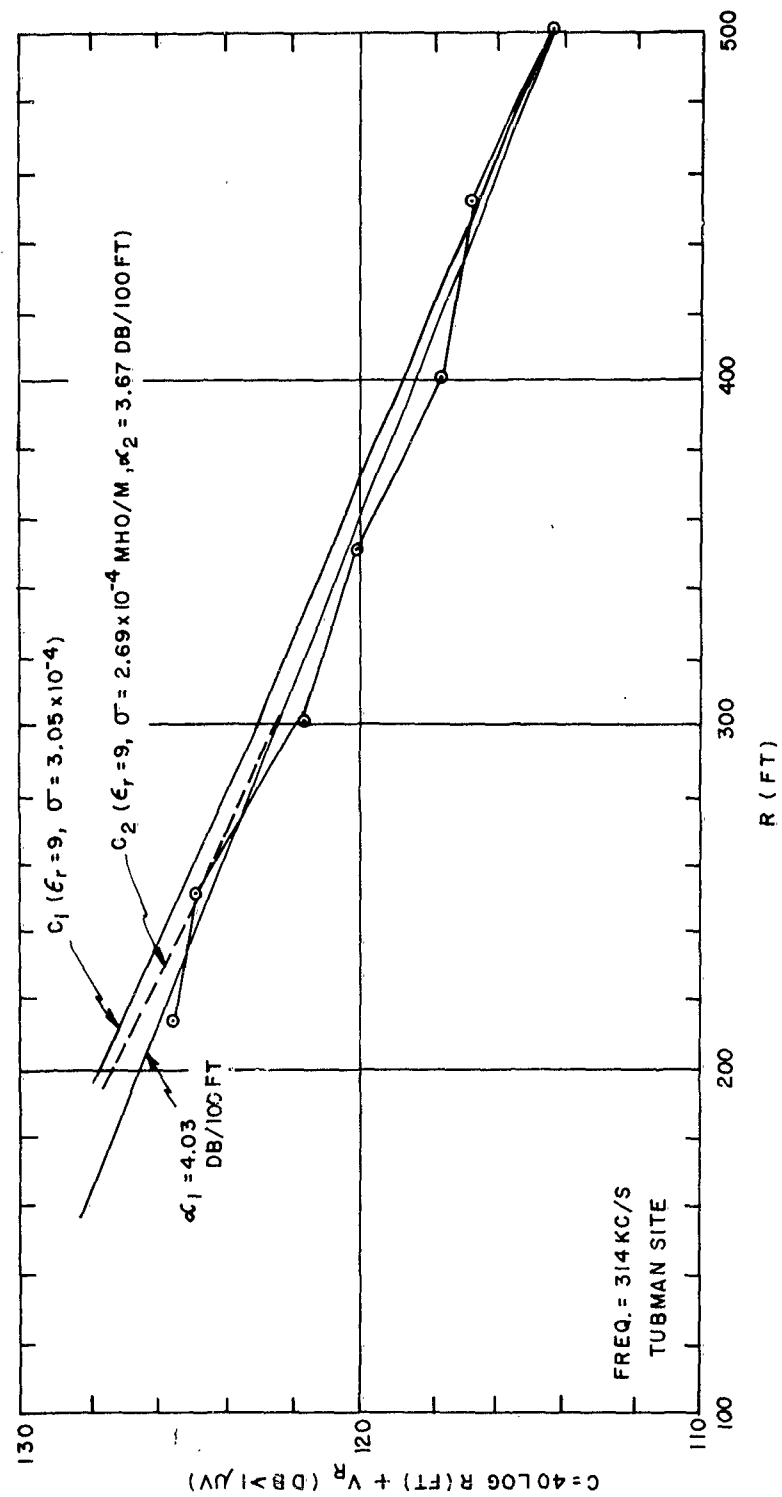
Figure V.11.   Typical plot of C vs R. $C = 40 \log R(\text{ft}) + V_R$ (dbuv).   Tubman Road site, 314 kc.
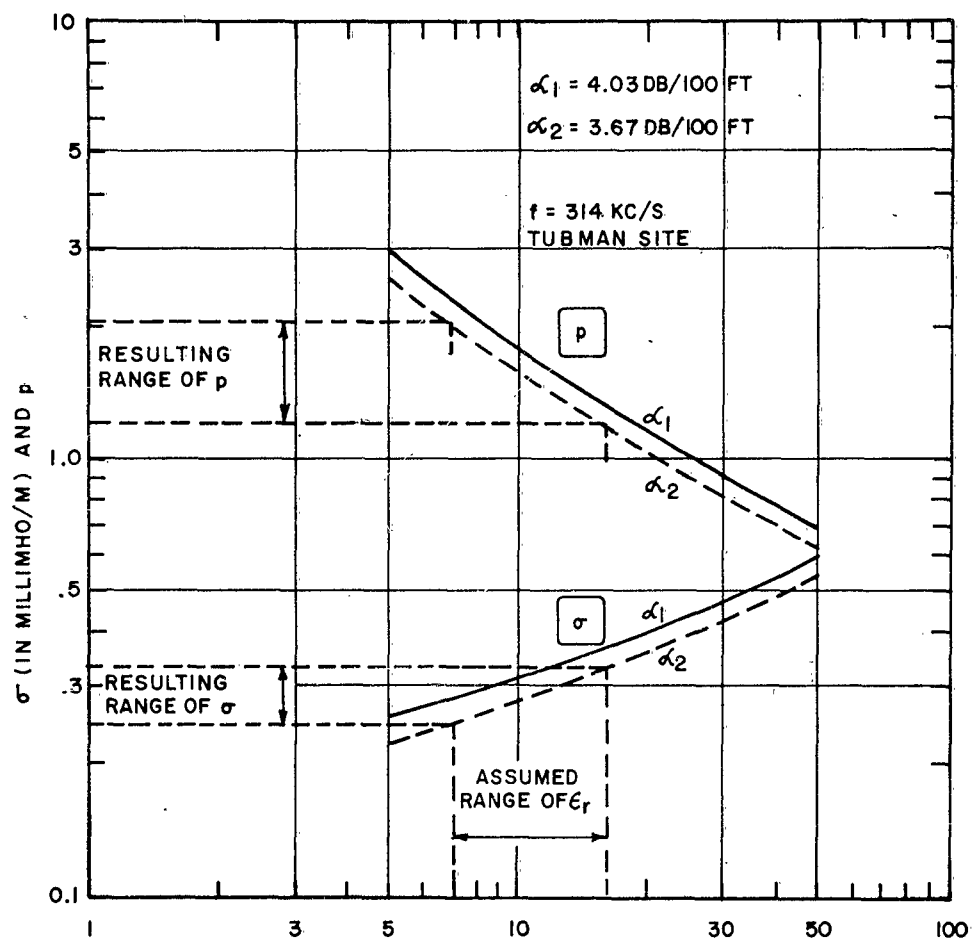
Figure V. 12.   Dependence of conductivity (σ) and loss tangent (p) with
                  assumed relative dielectric constant (ε_r) for observed at-
                  tenuation constant (α_1) of rock.   Tubman Road site, 314 kc.

$$2.5 \times 10^{-4} \leq \sigma \leq 3.3 \times 10^{-4}$$

$$2.03 \gtrsim p \gtrsim 1.19$$

4. Discussion of Results

The depth attenuation method yields values of the attenuation constant (α) by a measurement of the decay of received signal as the receiver-transmitter antenna separation (R) is increased. Analysis is simplified if $|kR| > 1$ for the scheme illustrated in which both antennas were colinear insulated elements (physically and electrically short) and both immersed within the rock being measured. In such case the axial electric field amplitude varies inversely with the square of the distance R and exponentially as $e^{-\alpha R}$.

When the loss tangent (p) is large compared with unity, the observed value of α yields a reasonably well-defined value of σ. When p is small, α depends on the ratio $\sigma / \sqrt{\epsilon_r}$. It is suggested that ϵ_r may be obtained from a knowledge of α if σ and ϵ_r are independent of frequency. Thus, one obtains an estimate of σ from α observed at a low frequency where p is large. A new value of α is observed from measurements repeated at a much higher frequency where p is small. The higher frequency value of α would then yield ϵ_r upon substituting the value of σ deduced at the lower frequency. Homogeneous media are assumed in the analysis.

For the scheme illustrated the simplifying assumption $|kR| > 1$ limits the lowest frequency for useful observations in holes having limited penetration depths into the rock. For rock media similar to that for Cape Cod at the depths investigated, frequencies higher than 50 kc should be employed.

A complete depth run, using the scheme of Figure V.7 can be made within one hour, including observations at 20 ft increments in depth and frequent calibration rechecks.

Measurements have been made using other variations of the scheme, such as the measurement of the attenuation with depth of the signals received in the drill hole due to nearby and remote sources. The use of insulated loop source antennas and receiving probes is under investigation.

G. Estimates from Antenna Impedance Measurements

In principle it was thought feasible to obtain the characteristics of the surrounding medium from a measurement of the input impedance of antennas immersed therein. For bare antennas the agreement of theory with experimental data using media of known electrical constants is good, as discussed in Section IV for model measurements made at VHF. However, the data we have obtained with bare monopoles on full scale measurements at VLF have not been completely analyzed. The difficulty is that the input impedance of the monopole antennas has a comparable component due to the loss in the ground plane, i.e., the overburden, as discussed in Section IV.

In the case of insulated antennas, the input quarter-wave resonant frequency may be used to estimate the propagation constant k_3 of the dissipative medium. This is based upon the theory and the curves in Section IV used for predicting the resonant length (h_x) and showing the effect of conductivity σ_3 on the values of that length. However, those curves were based upon the assumption that the loss tangent was large. The modification when this is not the case is used below.

V-44

Reviewing the theory for the moment, the complex phase constant k of the current was developed in Appendix F in terms of the radial dimensions a_1 (inner conductor) and a_2 (insulation) and the complex phase constants k_2 of the insulation and k_3 of the dissipative medium. Important assumptions are that a_1 and a_2 are small compared with the wavelength λ_3 of the medium and that $|k|^2 << |k_3|^2$. With $k = \beta(1-j \alpha/\beta)$, it was shown for practical antennas that $\alpha^2 << \beta^2$. Assuming a loss-less insulation, then we may write

$$\frac{k^2 \ln(a_2/a_1)}{k_2^2} \doteq \frac{\beta^2}{\beta_2^2} \ln \frac{a_2}{a_1} = \frac{\lambda_2^2}{\lambda^2} \ln \frac{a_2}{a_1} = P_{31}^2 \quad (V.21)$$

in which

$$P_{31}^2 = \ln \frac{2}{\gamma a_1 |k_3|} \quad (V.22)$$

where $\ln \gamma = C = 0.5772 - - - =$ Euler's constant and $\gamma \doteq 1.7810$. Using the definitions in Section IID and the $f(p_3)$ and $g(p_3)$ functions of Section IIB and Appendix A, then one has

$$k_3 = \beta_3 - j \alpha_3 = \beta_0 \sqrt{\epsilon_{r_3}} \sqrt{1 - j p_3} = \beta_0 \sqrt{\epsilon_{r_3}} S_3 \quad (V.23)$$

$$= \beta_0 \sqrt{\epsilon_{r_3}} \left[f(p_3) - j \, g(p_3) \right]$$

and

$$|k_3| = \beta_0 \sqrt{\epsilon_{r_3}} |S_3| = \beta_0 \sqrt{\epsilon_{r_3}} (1 + p_3^2)^{1/4} \quad (V.24)$$

in which $S_3 = \sqrt{1 - j p_3}$.

Input quarter-wave resonance occurs where

$$(\beta h)_r = \pi/2, \quad \lambda_r = 4h \quad (V.25)$$

and when $\alpha^2 << \beta^2$ this condition occurs at a frequency very close to that for which the input reactance is zero. Using the latter to determine λ_r in equation (V. 25), one may write equation (V. 21) as

$$\left(P_{31}^2\right)_r = C_1 \Big/ f_{kc}^2 \qquad \text{(V. 26)}$$

where $(P_{31}^2)_r$ is the value of equation (V. 22) at the observed resonant frequency f_{kc} (in kc) and C_1 is an antenna constant given by

$$C_1 = \left(\frac{3 \times 10^5}{4h}\right)^2 \epsilon_{r_2} \ln \frac{a_2}{a_1} \qquad \text{(V. 27)}$$

in which ϵ_{r_2} is the relative dielectric constant of the insulation and h is the monopole length (in meters).

Finally, after substituting equation (V. 24) in equation (V. 26) and rearranging terms, one has the relation

$$\ln \left[\epsilon_{r_3} \left| S_3 \right|^2 \right] = C_3 \qquad \text{(V. 28)}$$

where C_3 is a constant for a given observed resonant frequency f_{kc} and dimensions and given by

$$C_3 = 2 \left(C_2 - \frac{C_1}{f_{kc}^2} - \ln f_{kc} \right) \qquad \text{(V. 29)}$$

In equation (V. 29),

$$C_2 = \ln \frac{3 \times 10^5}{\pi \gamma a_1} \qquad \text{(V. 30)}$$

with a_1 measured in meters.

Rewriting equation (V.28)

$$\mathcal{E}_{r_3} (1 + p_3^2)^{1/2} = C_4 \qquad (V.31)$$

one has

$$(\mathcal{E}_{r_3})^2 + \left(\frac{1.8 \times 10^7 \ \sigma_3}{f_{kc}} \right)^2 = C_4^2 \qquad (V.32)$$

where σ_3 is the conductivity of the medium (in mhos/meter) and where

$$C_4 = (\ln)^{-1} (C_3) \qquad (V.33)$$

Now C_4 is the constant calculated from the measurements and we desire to know $\mathcal{E}_{r_3}$ and σ_3 of the medium. It is possible to determine σ_3 if it is known that the loss tangent p_3 is large; or it is possible to determine $\mathcal{E}_{r_3}$ if the loss tangent is sufficiently small so that $p_3^2 \ll 1$. The analysis is similar to that encountered in the depth attenuation method discussed in Subsection VF. However, we have found from measurements yielding resonant frequencies f_{kc} in the VLF range that the constant C_4 is such that $C_4^2 \gg \mathcal{E}_{r_3}^2$ for all reasonable values of $\mathcal{E}_{r_3}$ whence values of σ_3 result directly from equation (V.32); the relatively large value of C_4^2 is another way of indicating that p_3 is large.

The results of two sets of data are used for illustration. The first data were the measurements made in 1961 in Goffstown, N.H., the site described in Section IIIA. The antenna was an insulated monopole of the RG-8/U type so that $\mathcal{E}_{r_2} = 2.25$, $a_1 = 0.0408$ in. $= 1.036$ mm, and $\ln a_2/a_1 = 1.25$. The earlier measurements were concerned with measurements in the MF range and it was desired to have an antenna quarter-wave resonant at 500 kc.

Using the prediction curves of Figure IV. 3 for large loss tangent, it was

estimated that a resonant length of 123 ft. would be required based upon an

estimated $\sigma_3^- = 5 \times 10^{-3}$ mhos/m. The impedance data are plotted in Figure

III. 19 and reference to Figure III. 19(a) or Figure III. 19(c) indicates the reso-

nant frequency to be 480 kc. Using these data and calculating the various con-

stants C_1, C_2, and C_3, the value of C_4 worked out to be 48.6. The question

arises as to the value of ϵ_{r_3} to be used. Measurements were not performed

on rock samples at Goffstown, but measurements on random samples of rocks

typical of the area and which were water-soaked (Section VE) gave ϵ_{r_3} of the

order of 9 to 15 for which σ_3^-, using equation (V. 32), works out to be 1. 3 x

10^{-3} and 1. 2 x 10^{-3} mhos/m, respectively. These values are much larger

than the conductivities for those "random" samples shown in Figure V. 4 but

comparable with the conductivity measured for the water in the drill hole. The

resulting value of σ_3^- will vary markedly from those quoted if ϵ_{r_3} exceeds

40.

A second series of measurements were those made early this year

at Harwich, Massachusetts, the site being described in Section IIIA. Again

an insulated antenna of the RG-8/U type was desired. It was desired to obtain

quarter-wave resonance at 120 kc. Using the prediction curves of Figure IV. 4

for large loss tangents, it was estimated that a length of 475 feet would be

required assuming σ_3^- of approximately 10^{-3} mhos/m. The resulting imped-

ance data are plotted on the curves of Figure IV. 7 and IV. 8. Reference to

the curves for the open-circuit termination indicates quarter-wave resonance

occurred very close to 120 kc. The value of C_4 works out to be 189.0 which

is very high compared with plausible values of ϵ_{r_3}, i.e., $C_4^2 >> \epsilon_{r_3}^2$ in

equation (V.32), whence $\sigma_3 = 1.2 \times 10^{-3}$ mhos/m independent of ϵ_{r_3}. Thus,

the loss tangent must be large and Figure IV.4 applies. Such curves imply

that accurate knowledge of antenna constants and f_{kc} must be had for a modest

accuracy in the estimate of σ_3 to obtain. An error of $\pm$ 0.1 kc in the value

of resonant frequency near 120 kc and an error of $\pm$ 0.5 feet in the length of

the antenna near 475 feet means that $\sigma_3 = 1.16 \pm 0.13$ mhos/m, approximately.

H. Estimates from Path Transmission Loss Data - (1-Mile Path,
   Cape Cod)

The total system loss equation was developed in Section II for the

total power loss between parallel linear radiators having the same equatorial

plane. Estimates were given on the power transferred between electrically

short, insulated antenna with short-circuit termination with a known input

resistance, based on theory of Appendices E and F. The estimated losses

can be applied to propagation in a rock stratum below a much more conduc-

tive overburden, ideally of infinite conductivity.

The curves of Section II for the case of the 6000-foot transmission

path were compared with the measurements made on a similar path length

between the drill hole at the Brewster Dump and that at Tubman Road, de-

scribed in Section VI.

The measured total system loss, allowing for mismatch losses, is

slightly larger than the theoretical curve for $\sigma \simeq 10^{-3}$ mhos/m, but the

shape of the curve, i.e., measured loss vs frequency agrees very well with the theoretical curve for that value. This value is only about 3 to 4 times larger than that deduced from surface resistivity measurements for the mid-portion of the path for analysis (see Section VC). In view of the distortion in the profiles of apparent conductivity discussed in Section VC, one concludes such distortion is due to local irregularities, and these were noted near both drill holes. The effect of large but finite values on conductivity of overburden have not yet been taken into account in our analysis, but will be done when better estimates of overburden conductivity are available. The lower the overburden conductivity value the more the effect on resulting transmission loss and hence on the estimate of σ of the rock medium. The resulting value is interpreted as a gross average conductivity of the rock for the transmission path for vertical polarization, and for a conductivity contrast which is very large.

I. Proposed Methods Using Loops

1. Loops for Surface Resistivity Measurements

About ten years ago, Wait[74] developed expressions for the electromagnetic fields from an insulated loop located on the boundary (plane) of two semi-infinite homogeneous dissipative media. In cylindrical coordinates (ρ, ϕ, z) at points along the boundary (z = 0) the magnetic field has no ϕ-component and the electric field has only a ϕ-component. We extend the results where the upper medium (medium 1) is air and the lower medium (medium 2) is the ground. At a radial distance ρ along the ground a second

loop is located, at which the magnetic field z-component is H_z given by

$$H_z = \frac{I_T N_T A_T}{2\pi(\gamma_1^2 - \gamma_2^2)\rho^5}\left[A_H(\gamma_1\rho) - B_H(\gamma_2\rho)\right] \qquad (V.34)$$

where the transmitting loop (electrically small) has N_T turns and area A_T, and carries a current I_T, and A_H and B_H are functions to be described. In equation (V.34)

$$\gamma_n^2 = -\omega^2 \mu_n \epsilon_n + j\,\omega\mu_n\sigma_n = -\omega^2\mu_n\epsilon_n(1-j\,p_n), \quad (n=1,2)$$

$$(V.35)$$

where $n=1$ designates the air and $n=2$ the ground. In equation (V.35) we have μ_n and ϵ_n being the permeability and dielectric constant and σ_n the conductivity of medium n. The loss tangent p_n is

$$p_n = \frac{\sigma_n}{\omega\epsilon_n} = \frac{60\,\sigma_n\,\lambda_o}{\epsilon_{r_n}} \qquad (V.36)$$

where $\epsilon_n = \epsilon_o\epsilon_{r_n}$ and ϵ_{r_n} is the relative dielectric constant of medium n, and λ_o is the free-space wavelength. In what follows, we assume non-magnetic media ($\mu_r = 1$) so that $\mu_n = \mu_o$, $\mu_r = \mu_o = 4\pi \times 10^{-7}$ h/m and $\epsilon_o \cong 10^{-9}/36\pi$ f/m.

We assume σ_1 (air) $= 0 = p_1$, and that the ground has constants at the frequency of measurements that lead to a large loss tangent p_2. Then

$$\gamma_1^2 = -\omega^2\mu_o\epsilon_o = -\beta_o^2 = -(2\pi/\lambda_o)^2$$

$$(V.37)$$

$$\gamma_2^2 \cong j\,\omega\mu_o\sigma_2$$

In equation (V. 34) the quantity $\gamma_1^2 - \gamma_2^2$ becomes $-j \, \omega \mu_o \sigma_2$ approximately where $60 \, \sigma_2 \, \lambda_o >> 1$ which is usually the case of interest. Then equation (V. 34) can be written

$$H_z \cong j \, \frac{I_T \, N_T \, A_T}{2 \, \pi \omega \mu_o \, \sigma_2 \, \rho^5} \left[A_H \, (\gamma_1 \rho) - B_H \, (\gamma_2 \rho) \right] \qquad (V.38)$$

Under the same assumptions, the electric field is in the plane of separation ($z = 0$) and given by

$$E_\phi \cong \frac{I_T \, N_T \, A_T}{2 \, \pi \, \sigma_2 \, \rho^4} \left[B_E \, (\gamma_2 \rho) - A_E \, (\gamma_1 \rho) \right] \qquad (V.39)$$

The A_H and B_H functions for the magnetic field and the A_E and B_E functions for the electric field are of the form

$$\emptyset_H \, (x_n) = (9 + 9 \, x_n + 4 \, x_n^2 + x_n^3) \, e^{-x_n}$$

$$\qquad (V.40)$$

$$\emptyset_E \, (x_n) = (3 + 3 \, x_n + x_n^2) \, e^{-x_n}$$

where

$$x_n = \gamma_n \, \rho \qquad n = 1, 2 \qquad (V.41)$$

At a distance ρ along the boundary we may place a second loop whose plane is parallel to the boundary and responsive only to H_z for inducing an open-circuit voltage V_R. Or we may place an electrically short horizontal wire perpendicular to the direction of propagation and responsive to E_ϕ.

For a secondary consisting of a small loop of area A_R and turns N_R, the open-circuit voltage is V_R, and

V-52

$$V_R = -j \omega \mu_o N_R A_R H_z \qquad (V.42)$$

with H_z given by equation (V.38). The mutual impedance between the loops is Z_m given by

$$Z_m = \frac{V_R}{I_T} = \frac{N^2 A^2}{2\pi \sigma_2 \rho^5} \left[A_H (\gamma_1 \rho) - B_H (\gamma_2 \rho) \right] \qquad (V.43)$$

assuming identical loops with $N_T = N_R = N$ and $A_T = A_R = A$.

In what follows it is assumed that $\beta_o \rho < 1$, i.e., $\rho < \frac{\lambda_o}{2\pi}$ say $\rho_{km} \le \frac{\lambda_o}{30} = 10^4 / f_{kc}$ where f_{kc} is the frequency in kc and ρ_{km} is the distance in kilometers. The evaluation of $B_H (\gamma_2 \rho)$ depends upon the ratio $\rho/\lambda_2 = \rho/2\pi \tau_2$ and simplications result when this ratio is small and when it is large. Otherwise, it must be calculated using equation (V.40),

a. $\rho \ll 2\pi \tau_2$

At very short distances compared with the skin depth τ_2 where

$$\tau_2 = \sqrt{\frac{2}{\omega \mu_o \sigma_2}} = \frac{15.92}{\sqrt{f_{kc} \sigma_2}} \quad \text{meters} \qquad (V.44)$$

and expanding the square brackets out to terms including ρ^4, it can be shown that the mutual impedance is

$$Z_m \cong 0 + j X_m = 0 + j \omega M$$

$$\qquad (V.45)$$

$$M = \frac{\mu_o}{4\pi} N^2 A^2 \frac{1}{\rho^3}$$

i.e., the impedance is purely inductive where the mutual inductance M does not depend on σ_2 and varies as ρ^{-3}.

b. $\rho \geq \lambda_2 = 2\pi \, \tau_2$

At these larger distances, the term $B_H (\gamma_2 \rho)$ becomes negligible compared with $A_H (\gamma_1 \rho)$ because of the exponential damping in equation (V. 40). Under these conditions, it can be shown that the mutual impedance is purely resistive and the mutual resistance R_m is given by

$$R_m = \frac{9}{2\pi} \frac{N^2 A^2}{\sigma_2 \, \rho^5} \qquad (V.\,46)$$

and the conductivity is given by

$$\sigma_2 = \frac{(3\,N\,A)^2}{2\pi\,R_m\,\rho^5} \qquad (V.\,47)$$

Let $I_T = 1.0$ amp. We assume a detector capable of determining the open-circuit voltage V_R and for illustration assume that the minimum detectable signal voltage is 1 microvolt. Then $R_m \leq 10^6$ ohms. As an illustration, consider two identical 500 turn loops each having a diameter of 3 m ($\sim$ 10 ft). With the assumed limitation on maximum value of $R_m = 1$ megohm, then the detectable conductivity is limited by

$$\sigma_2 \leq 1.8 \times 10^{-2} / (\rho_{km})^5 \quad \text{mhos/m} \qquad (V.\,48)$$

and the upper bound on measuring σ_2 varies inversely as the fifth power of distance.

For these assumptions we may bracket the detectable range of σ_2 as

$$\frac{6.8}{(f_{kc})^{5/3}} \leq \sigma_2 \text{ (millimhos/m)} = \frac{17.9}{(\rho_{km})^5} \qquad (V.\,49)$$

V-54

or the restriction on the distance may be stated as

$$\frac{0.10}{\sqrt{f_{kc} \ \sigma_2}} \leq \rho_{km} \leq \frac{10^4}{f_{kc}} \qquad\qquad (V.40)$$

These expressions are the limits resulting from the assumptions of identical loops and distances small compared with the free-space wavelength but large compared with the skin-depth of the ground.

The method can be used for measuring the apparent conductivity σ_a of a horizontally stratified ground where σ_2 above becomes σ_a. Techniques for obtaining overburden and rock conductivities for a two-layer or three-layer model were discussed in Section VB.

Loops have the advantage over horizontal dipoles in portability and freedom from struggles with stringing out horizontal wires through brambles, brush, ponds and the like. Loop impedances are relatively less affected by ground electrode resistance compared with horizontal dipoles. Both loops in the horizontal plane and horizontal electric dipoles will be less affected by atmospheric noise than loops in the vertical plane or vertical electric dipoles because atmospheric noise is predominantly vertically polarized. Distance limits imposed by signal-to-noise ratios require further study. Actual sizes of loops and number of turns will also be dictated by circuit considerations of impedance as a load on a transmitter and the receiver antenna impedance vs its detector impedance.

2. Impedance of a Single Loop in a Dissipative Medium

The impedance of a loop inside an insulating cavity immersed in

a dissipative medium will depend upon the constants of the medium under certain conditions. The problem is similar to that encountered in shielded coils in calculating the effect of the metallic shield can upon the impedance of the coil in air insulation inside the can. If the coil dimensions are small compared with those of the shield can, the coil impedance will not be affected greatly by the presence of the can and will be approximately its value in air. If the coil dimensions are near those of the shield, the coil impedance will be influenced markedly the presence of the can and its electrical properties.

Recently, Wait[78] has analyzed the impedance of loop of radius b inside an insulating spherical cavity of radius a immersed in a homogeneous, isotropic dissipative medium with electrical constants σ, ϵ_r, and μ. Let ΔZ represent the change in the impedance of the coil so immersed from the impedance Z_o in air. Since $b \leq a$, then Wait's expressions for a non-magnetic medium ($\mu = \mu_o = 4\pi \times 10^{-7}$ h/m) may be written

$$\Delta Z = \Delta R + j \; \Delta X \doteq \frac{(\omega \mu_o NS)^2}{6\pi a} (\sigma + j\omega \epsilon_o \epsilon_r) \quad \text{ohms} \qquad (V.41)$$

where $S = \pi b^2$ is the area of the loop, N the number of turns, and a and b are given in meters. All other quantities being the same, then ΔZ varies as b^4/a. Setting $b \doteq a$, then equation (V.41) can be expressed as

$$\Delta R \doteq 5.349 \times 10^{-4} \; (b_{in})^3 \; f_{mc}^2 \; N^2 \sigma, \quad \text{ohms} \qquad (V.42a)$$

$$\Delta X = \frac{\Delta R}{p} \quad , \quad \text{ohms} \qquad (V.42b)$$

in which b_{in} is the loop radius in inches, f_{mc} is the frequency in mc, σ is the conductivity in mhos/m, and p is the loss tangent $p = \dfrac{18 \times 10^3 \, \sigma}{f_{mc} \, \epsilon_r}$.

If we desire to use ΔZ to determine the constants σ and ϵ_r according to equations (V. 41) or (V. 42), the question arises as to the sensitivity of the method, i.e., as to the magnitude of the ratios $\Delta R/R_o$ and $\Delta X/X_o$ where $R_o + j X_o = Z_o$ is the loop impedance in air. In particular, it is desired to determine ΔZ for an insulated loop immersed in a drill hole into the rock basement. In such a case, the cavity diameter must be less than the drill hole diameter, and a typical cavity (or maximum loop) diameter might be 5". For expected values of σ, inspection of equation (V. 42a) indicates that the measurement must be accomplished at frequencies in the HF region to give detectable values of ΔR for nominal values of σ. This is illustrated in the sample calculations below using somewhat idealized assumptions. Limits are imposed on the minimum or detectable change ΔZ by the measuring technique. Let us assume that the change $\Delta R'$ or 0.1 ohm is detectable if R_o is 20 ohms or less, but that if R_o exceeds 20 ohms then the detectable change $\Delta R'' = 5 \times 10^{-3} R_o$. An estimate of R_o may be obtained from the coil-reactance $X_o = \omega L$ and the Q of the coil. For simplicity let us assume that Q is independent of coil constants and frequency and that the coil inductance L is the low frequency value L_o. Further, the coil (spherical) is assumed to occupy such a small segment of the sphere that its inductance is close to that for a thin, single-layer solenoid. In such case $L_o = F N^2 (2 b_{in}) \times 10^{-6}$ henry where F is a function of the ratio of coil diameter to coil length (Nagaoka formula).

For diameter-to-length ratios of 20 to 100, F approaches 0.1 and $L_o = 2 N^2 b_{in} \times 10^{-7}$ henry. Then

$$R_o = \frac{\omega L}{Q} \doteq \frac{\omega L_o}{Q} \doteq \frac{1.25 \, f_{mc} \, N^2 \, b_{in}}{Q} \qquad (V.43)$$

To further typify the calculations for a loop in a drill hole, let $2b = 5''$ and $Q = 250$. Then if $R_o = 20$ ohms,

$$f_{mc} \, N^2 = 1600 \qquad (V.44)$$

The conditions on ΔR may then be written

$$R_o \leqq 20 \text{ ohms}, \quad f_{mc} N^2 \leqq 1600, \quad \Delta R' = 8.36 \times 10^{-3} f_{mc}^2 \, N^2 \, \sigma_m = 0.1 \qquad (V.45a)$$

$$f_{mc}^2 \, N^2 \, \sigma_m = 12.0 \qquad (V.45b)$$

$$R_o \geqq 20 \text{ ohms}, \quad f_{mc} N^2 \geqq 1600, \quad \frac{\Delta R''}{R_o} = 0.67 \, f_{mc} \, \sigma_m = 5 \times 10^{-3} \qquad (V.46a)$$

$$f_{mc} \, \sigma_m = 7.5 \times 10^{-3} \qquad (V.46b)$$

where σ_m is the minimum observable value of the conductivity σ.

If the observing frequency is 16 mc, then a 10-turn coil will have $R_o = 20$ ohms according to equations (V.43) and (V.44). The minimum value of σ which could then be measured is 4.7×10^{-4} mhos/meter, according to equations (V.45b) or (V.46b). At this frequency, increasing N does not help in detecting lower values of σ because equation (V.46b) is independent of N. The only way to detect a lower value of σ would be to use higher frequencies. Under the assumed limiting conditions for $\Delta R'$ and $\Delta R''$ in equations (V.45) and (V.46),

respectively, it appears that equation (V. 46b) represents the best that can be done for detecting as low a value of σ as possible.

Imposing limiting conditions on ΔX similar to those for ΔR yields expressions for minimum detectable values of ϵ_r, called ϵ_{r_m}. Then

$$\frac{\Delta X''}{X_o} = 5 \times 10^{-3} = \frac{\Delta X''}{\Delta R''} \frac{\Delta R''}{R_o} \frac{R_o}{X_o} = \frac{1}{p'' Q} \frac{\Delta R''}{R_o} \qquad (V. 47a)$$

$$p'' = \frac{1}{Q} = \frac{18 \times 10^3 \; \sigma_m}{f_{mc} \; \epsilon_{r_m}} \qquad (V. 47b)$$

where p'' is the maximum allowable loss tangent. With equation (V. 46b) and Q = 250, then

$$f_{mc}^2 \; \epsilon_{r_m} = 135 \, Q = 3.375 \times 10^4 \qquad (V. 47c)$$

To detect ϵ_r = 9, then $f_{mc} \gtrsim 61.2$.

To summarize sample calculations, let us assume the measuring frequency to be 64 mc, a 5-inch diameter coil with 5 turns and Q = 250. Then R_o = 20 ohms and X_o = 5000 ohms. Suppose the change ΔR was such that $\sigma = 10^{-3}$ mhos/m, i.e., $\Delta R = 0.86$ ohm which should be detectable since $\Delta R'' = 0.1$ ohm. The loss tangent would then be $0.028/\epsilon_r$. If the measured change ΔX were such that ϵ_r = 9, i.e., if $\Delta X = 27.4$ ohms, such a value is detectable because $\Delta X'' = 5 \times 10^{-3} \times 5000 = 25$ ohms.

In practice, our idealized assumptions would be changed if the measuring apparatus required different detection sensitivities for ΔR and ΔX from those assumed and if the coil Q differed from 250 at the measuring

frequency. It appears that use of the scheme in drill holes is limited to measurements at HF to obtain values of σ and to the lower VHF frequencies to obtain both σ and ϵ_r. In mine shafts or tunnels where much larger diameter coils may be employed, then the measurements may be made at much lower frequencies; this is because the change ΔZ is proportional to the cube of coil radius, in accordance with equation (V.42).

Somewhat parenthetically, when using coils in drill holes for other purposes at VLF, the change ΔZ should be negligible compared with the impedance Z_o in air provided, of course, that the insulated coil is immersed in a homogeneous medium. If we let k_1 and k_2 be the complex phase constants of the insulating region within the cavity and of the dissipative region exterior to the cavity, respectively, then the equivalent dipole moment of the coil in the cavity is approximately the same as the dipole moment in air, when the cavity radius is so small that $\left|k_1 a\right| << 1$ and $\left|k_2 a\right| << 1$. The cavity then has little or no effect on external fields. Such conditions are readily achievable in practice. The power then radiated by the loop, i.e., the power transferred across the surface of the cavity to be dissipated in the surrounding medium[78] is

$$P \doteq I^2 \Delta R \qquad \qquad (V.48)$$

where I is the rms current flowing in the (small) loop and ΔR is given by equation (V.41) or by equation (V.42a) when $b \doteq a$. Such relations would be useful when employing loops instead of linear dipoles for transmission experiments in deep strata.

3. Loops for Depth Attenuation Methods

For the depth attenuation method described in Section VF, the linear antennas would be replaced by small insulated loops. Consider the transmitting loop (near or around the encapsulated transmitter) to be arranged to lie in a horizontal plane at a distance R below a coaxial receiving loop which is located just below the overburden and connected to the receiver on the surface by a balanced, shielded-pair, transmission line. The receiving loop voltage, i.e., the magnitude of the mutual impedance between the loops, will be proportional to the axial component of the magnetic field of the transmitting loop. If $|kR|$ is sufficiently large, the variation of the received voltage with distance will yield the attenuation constant α of the medium just like that when end-fire electric dipoles were used. The loops would afford more accurate measurement of the separation distance R, and conceivably could give greater sensitivity when the induced voltages in the receiving loop due to external noise (atmospheric noise attenuated by the overburden) are smaller.

Section VI.   TRANSMISSION PATH TESTS

A.   Introduction

Some earlier transmission tests were performed between antennas immersed in drill holes at Goffstown, New Hampshire, and Bedford, New Hampshire.   The overburden was so thin (5 to 30 feet) that questions arose as to whether signals received at LF were transmitted via the direct path in the rock or via the up-over-and-down mode (Section IB).   The preliminary tests included a phase comparison technique.   Initial conclusions were that a significant component was transmitted through the air.   Further tests were most desirable but efforts were transferred to the Cape Cod test sites which were then becoming available.

Attempts were made to transmit signals between antennas immersed deep in the three drill holes on Cape Cod, located on the map of Figure III. 2.

The first two holes were drilled at Harwich and at the Brewster Town Dump (referred hereafter as the Brewster site).   Transmission tests between antennas deep in the two holes (3.8 miles apart) were unsuccessful in that signals were not detected at Harwich from 100 to 300 watt transmitters located at Brewster, at any frequency from 1 to 150 kc.   Antennas employed were 475 feet insulated types of the RG-8/U variety with open- or short-circuit terminations.   For frequencies below 10 kc, a Hewlett-Packard 302A wave analyzer was employed as a receiver, and at higher frequencies a Hammar-lund SP-600 VLF receiver was used.   The tests were attempted when pre-liminary values of rock conductivity (from samples for each hole) seemed to

be lower than 10^{-4} mhos/m. Subsequent tests indicated higher values of conductivity (Section V). Theoretically the average rock conductivity over the whole path must be lower than 10^{-4} mhos/m in order to detect a signal readily, for the transmitter power and antennas and distances employed (see Section II, Figures II. 19 and II. 20).

When the third drill hole at the Tubman Road Site became available, it was possible to attempt tests on other path lengths. Time did not permit tests between Tubman and Harwich drill holes. Some preliminary tests were conducted with successful transmissions between antennas in the Brewster and Tubman drill holes with signals being readily detected at frequencies up to 10 kc. These tests are described below, in Subsection VID.

B. Azimuthal Patterns on the Surface Due to Transmissions from Antenna in Drill Hole - Surface Field Intensities

1. 150 kc Azimuthal Patterns at Several Ranges

Some abnormal behavior with range and azimuth was observed in the field intensity measurements of the field in air at the surface due to signals being transmitted from an antenna immersed in the Brewster drill hole. It was decided to investigate the phenomena further to ascertain the extent of anisotropic effects radially and azimuthally in the surface field intensity.

Measurements were made at 150 kc using the output of the GRN-6 beacon transmitter fed through 1000 feet of RG-8/U coaxial line to an insulated monopole 475 feet long (RG-8/U type) which was terminated in a "short circuit" consisting of 50 feet of #12 wire. The ground cage was used and the

monopole input point was just below and within one foot of the end of the casing pipe 464 feet down. The field intensity meter was a Stoddard NM-10A, battery operated. Antennas in air consisted of the 6" loop or 1 meter whip.

Data was obtained for field intensity receiver voltage as a function of azimuthal bearing about the casing, for each of three radii R = 50, 100, and 200 feet measured from the pipe. Since relative data were desired, receiver voltages were read in db above 1 microvolt, but were not converted to field intensities. Receiver voltages were noted when using the loop and also when using the whip antenna in three positions. The plane of the loop was vertical and oriented for maximum voltage; the voltage was recorded as was the orientation of the plane of the loop relative to the vertical plane containing the hole and observing point. For the 1 meter whip antenna, voltages were noted when the whip was vertical and when it was horizontal and about 1 foot above the ground for two orientations, one aimed at the hole (axial or end-fire component) and the other when the whip was transverse to the direction to the hole (normal or broadside component).

The observations are plotted on polar coordinate paper in Figures VI. 1 through VI. 5. The magnetic bearings were converted to approximate true bearings by assuming the 16° W declination indicated on 1940 CGS maps, plus a compass error. The relative bearing plotted is the approximate true bearing, with the Tubman Road site indicated at a true bearing of 76.5° from the Brewster drill hole.
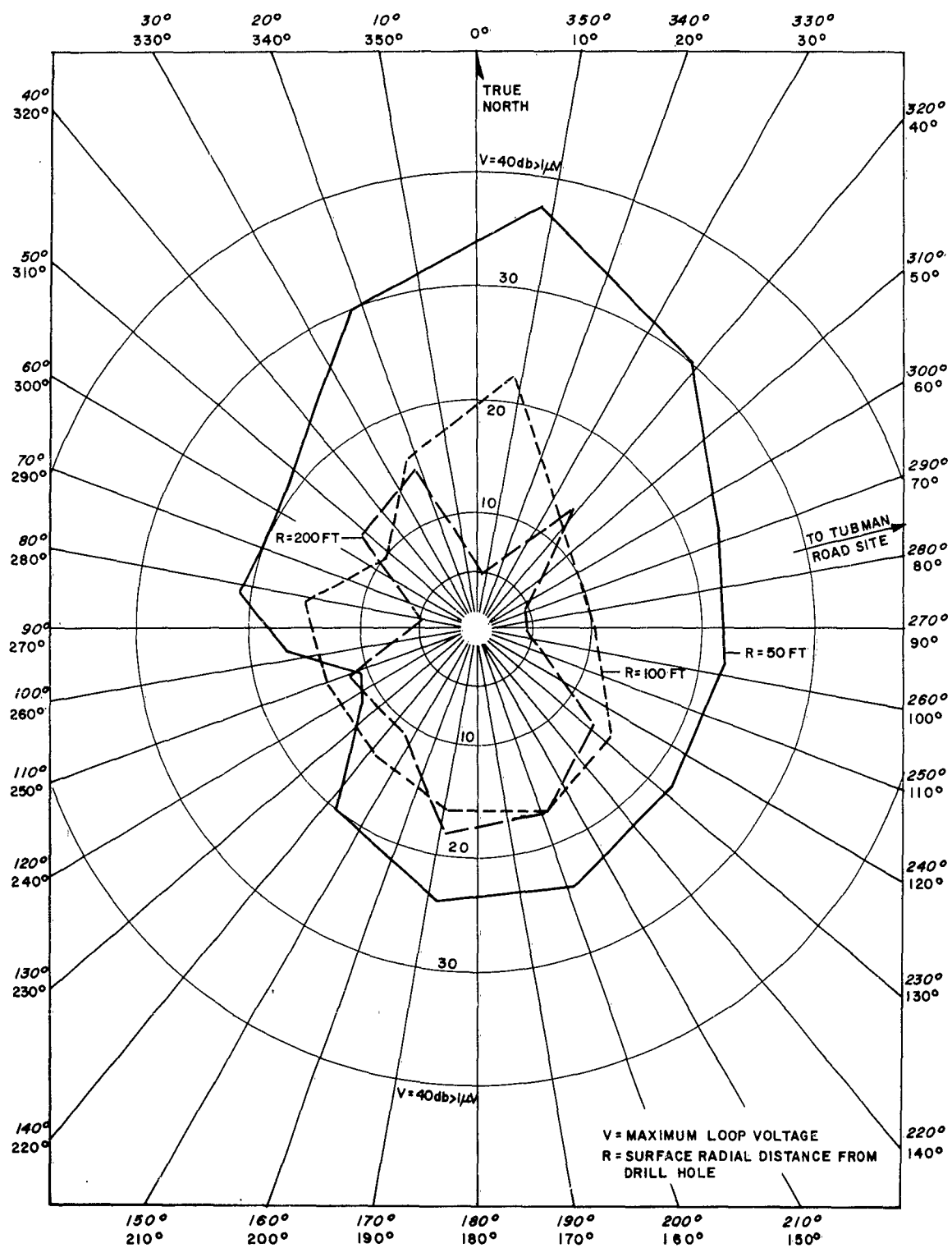
Figure VI.1.   Azimuthal variation of maximum vertical loop voltage of field on surface in air due to vertical radiator deep in drill hole. Brewster, 150 kc.
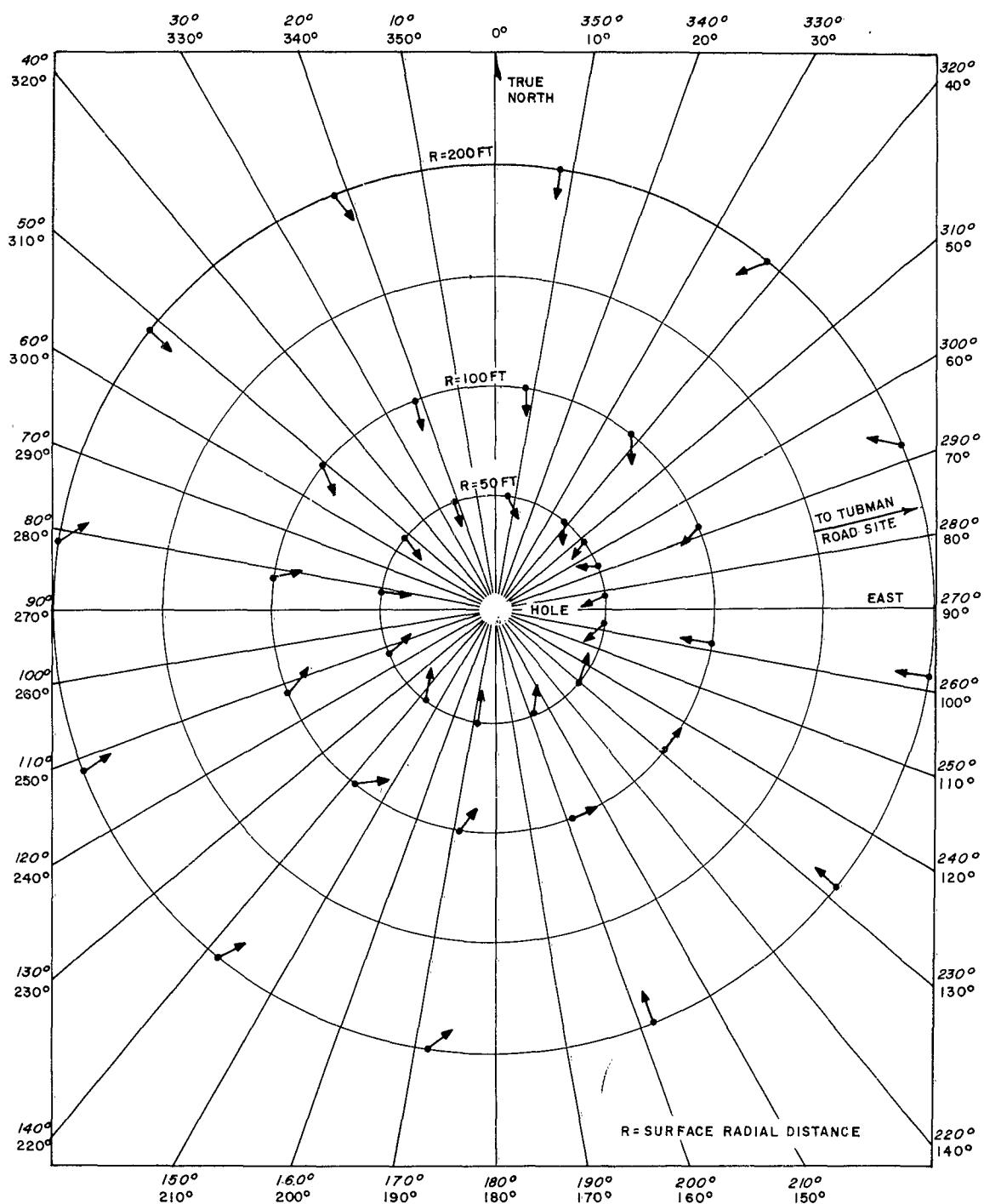
Figure VI. 2. Orientation of plane of vertical loop for maximum surface signal vs azimuth due to field from vertical radiator deep in drill hole. Brewster, 150 kc.
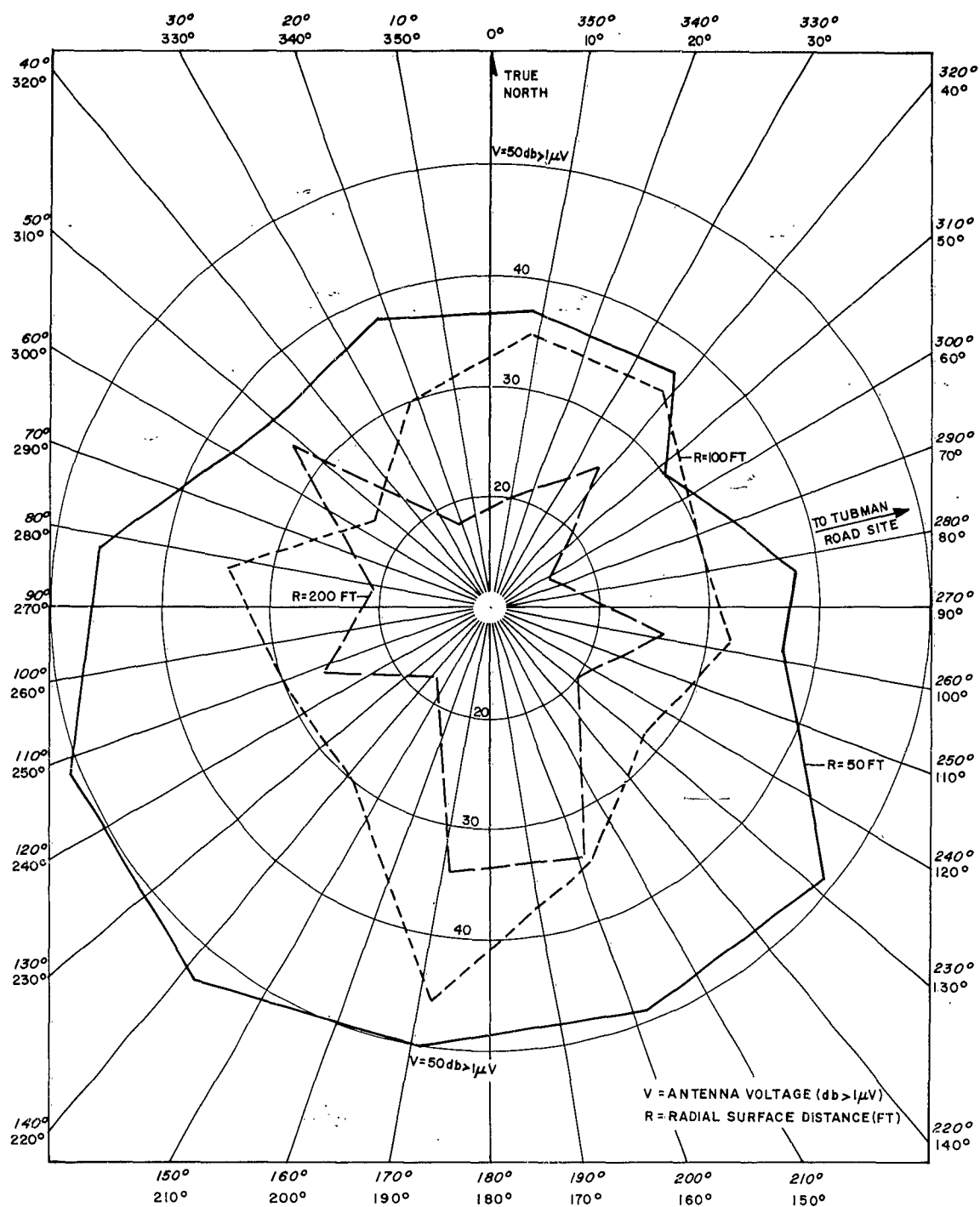
Figure VI. 3.   Azimuthal patterns of relative vertical electric field on surface
due to vertical radiator deep in drill hole.   Brewster, 150 kc.
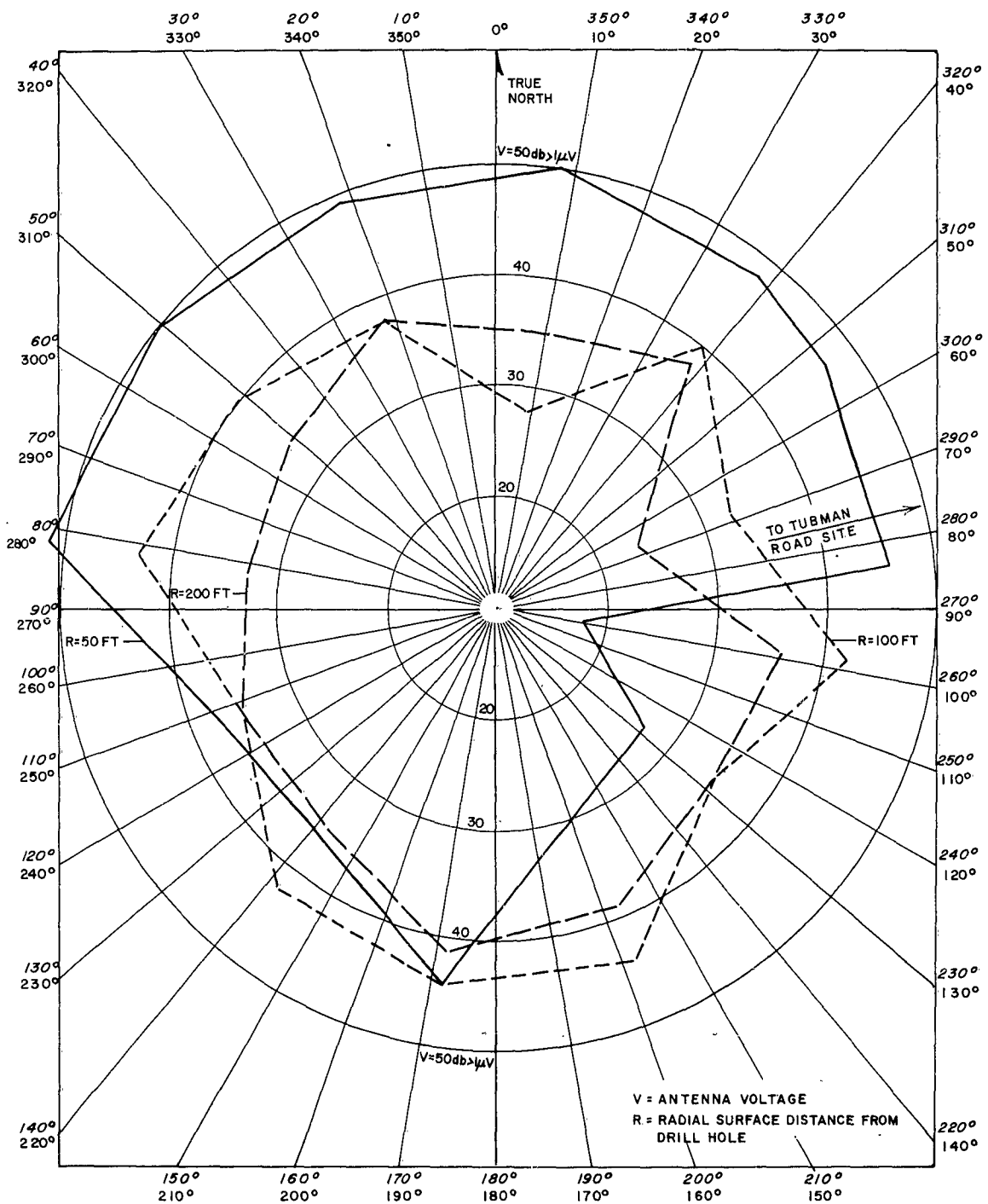
Figure VI. 4.   Azimuthal patterns of horizontal field in air (axial or end-fire components) due to vertical radiator deep in drill hole. Brewster, 150 kc.
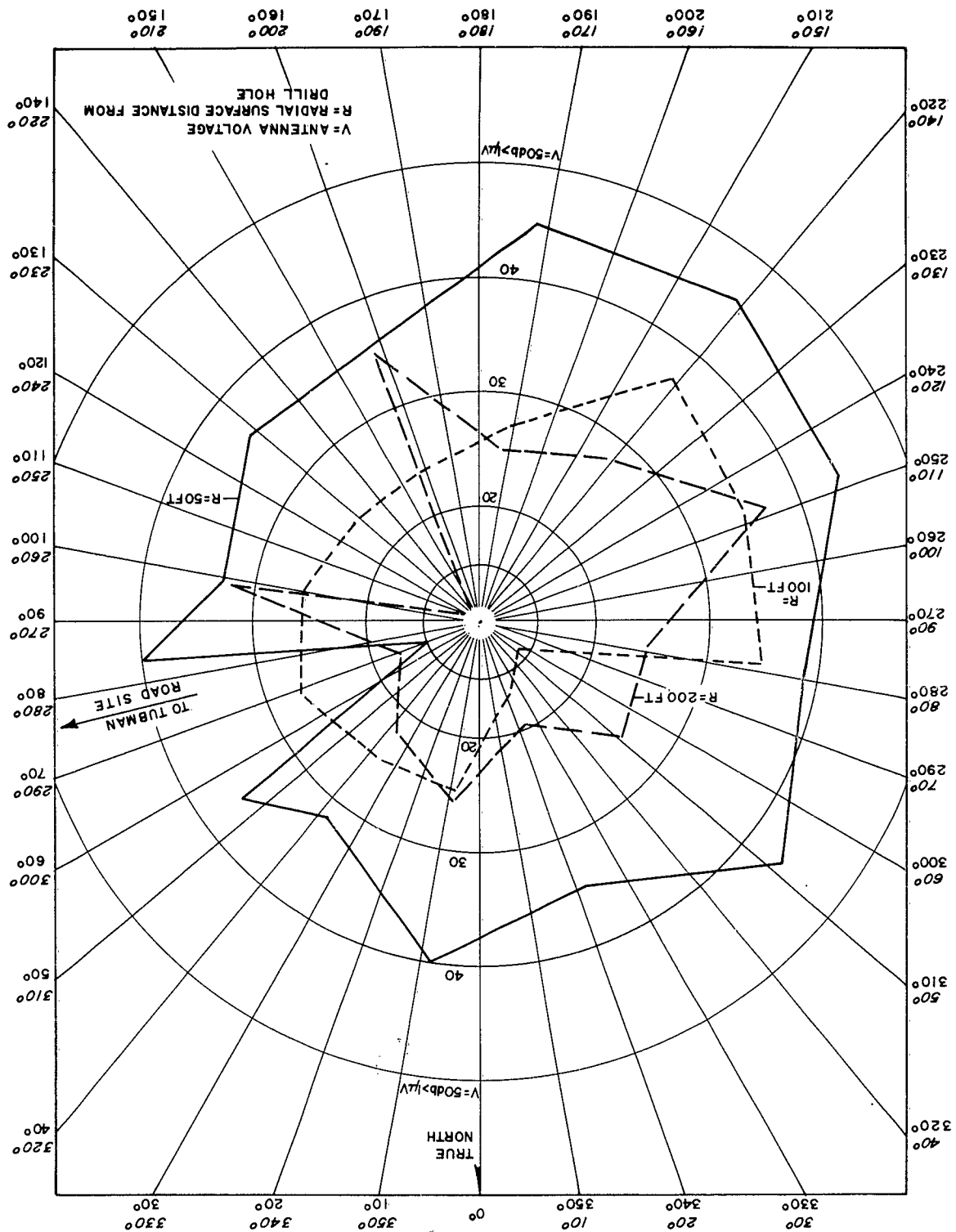
Figure VI. 5. Azimuthal patterns of horizontal field in air (normal or broadside component) due to vertical radiator deep in drill hole. Brewster, 150 kc.

The first two plots refer to the measurements with the loop antenna. In Figure VI. 1, the maximum loop voltages are plotted as a function of azimuth for each of the three radial distances. Note that the voltages are plotted on a decibel scale 0 to 40 db > 1 microvolt. The patterns show skewness and some anomalies. There appears to be a certain "bulging" to the south, and a "notching" in the general direction of Tubman. Further at some azimuths, loop voltages are greater for the larger ranges. The anomalies are further compounded by reference to the loop orientation plots of Figure VI. 2 which attempts to depict by arrows, on circles of radii proportional to R, the orientation of the plane of the loop for the maximum voltages observed and plotted in the previous figure. Note that the plane of the loop for maximum voltage is often at large angles with respect to the vertical plane through the pipe and hole containing the antenna. The "depolarization" is most severe in the easterly quadrants but begins to disappear at the larger ranges.

Some but not all of the anomalous pattern and range behavior of the loop is clarified by reference to the patterns taken with the whip antenna. Thus Figure VI. 3 depicts the azimuthal patterns for the vertical electric field voltage as read when the whip antenna was vertical. (Note that the voltage plotted radially on a db scale runs from 10 to 50 db > 1 microvolt only because the induced voltage was larger for the whip than for the loop.) The vertical electric field patterns "bulge" to the south and the "notching" towards the general direction of Tubman appears at the larger ranges. The anomalous range behavior noted for the loop voltages is not as severe for the vertical

whip voltages, although some appears to the northeast and northwest.

Reference is now made to the next two figures which depict the relative horizontal electric field patterns. The voltages are plotted on the same decibel scale as for the relative electric field in the previous figure; however, the "effective length" of the horizontal whip was not known so inter-comparison of horizontal and electric field intensities cannot be made. The patterns for the axial component of the relative horizontal field are shown in Figure VI. 4 and those for the broadside component are shown in Figure VI. 5. The relative fields in these two cases may be intercompared since the effective length, although unknown, remained the same. The axial component is se-verely scalloped in the southeast where there is also a severe range reversal. Notching occurs in the general direction of Tubman. The normal component pattern bulges to the southwest and there is severe notching in the pattern at the lar est range.

The relative values of axial and broadside components of the horizontal field (voltages) can be used to explain some of the loop orientation observations, but only when one is much larger than the other. For most azimuths, at R = 200 ft, the broadside horizontal component is much weaker than the axial component; for example, at a SE bearing, it is about 25 db weaker than the horizontal axial component. Hence, the electric field in air must lie in the vertical plane, through the observer and the casing, and the plane of the loop should be directed towards the hole, as is seen in Figure VI. 2. More generally, however, one must know the relative phases as well

as amplitudes of all three electric field components to make closer correlation with loop bearings. The phenomena is like that encountered for loop bearing errors at HF due to ionospheric reflections and rotation of the plane of polarization, the so-called "night effect."

2. Measurements of Vertical Electric Field on the Surface at ELF and VLF Close to Brewster Hole

When it was realized that path propagation tests must be conducted at frequencies in the ELF rather than in the VLF spectrum, further measurements of surface field intensities at VLF ceased and efforts were concentrated on obtaining ELF data. On the day (6/20/62) and just prior to the first successful path transmissions to be described, surface field intensities were measured at various ranges from the Brewster drill hole, at 0.5 to 50 kc.

For such frequencies, the only receiver available was a Hewlett Packard 302A wave analyzer (see Section IIID). The device has an input impedance of about 100,000 ohms, and the most sensitive scale is 30 microvolts full-scale on which we could detect a reading of 1/4 microvolt on the meter. The bandwidth was about 6 cps.

A 6-foot whip (used with the Stoddard NM-10A) was used as a vertical antenna, and a short coaxial cable was used to connect the antenna with its coaxial fitting to the terminals of the analyzer. The ground terminal was connected to a 3' ground stake for all readings.

Realizing some of the azimuthal and range anomalies observed in the vertical field at 150 kc might occur at lower frequencies, a radial run

along the same bearing was made, the voltages vs frequency at each of several ranges being observed. The radial chosen was roughly NE of the drill hole, and several ranges 27' to 750' were chosen across the rather rat-inhabited dump. At the extreme range of 750' the azimuth was changed to ENE, approximately the direction of the Tubman site, in order to observe any azimuthal anomaly at such range.

The resulting wave analyzer voltages are shown plotted in Figure VI.6. The solid curves pertain to the NE radial and the dashed one the ENE radial towards Tubman. The transmitting antenna was the 475' insulated monopole with short-circuit termination used before, but the transmitter was the high power audio amplifier. The line current was maintained as close to 1 ampere as possible, and observed voltages were normalized to this value. Except for possibly small feeder attenuation at these frequencies, the line current is close to the monopole input current.

The values of receiver voltage denoted by V_R and plotted in Figure VI.6 show two important effects which were evaluated more closely later. First, there was a distinct range anomaly in that values of V_R at 100' were lower than those at 210' and 300'. Second, values of V_R showed an optimum at about 15 kc. By repeated measurements, the range anomaly at 100' could not be reproduced in measurements at a later date, and discussed below. We must attribute these first observations to an experimental error or in poor "grounding" of the ground stake at the time. The "optimum values" of V_R were not observed in the hole-to-hole measurements to be described.
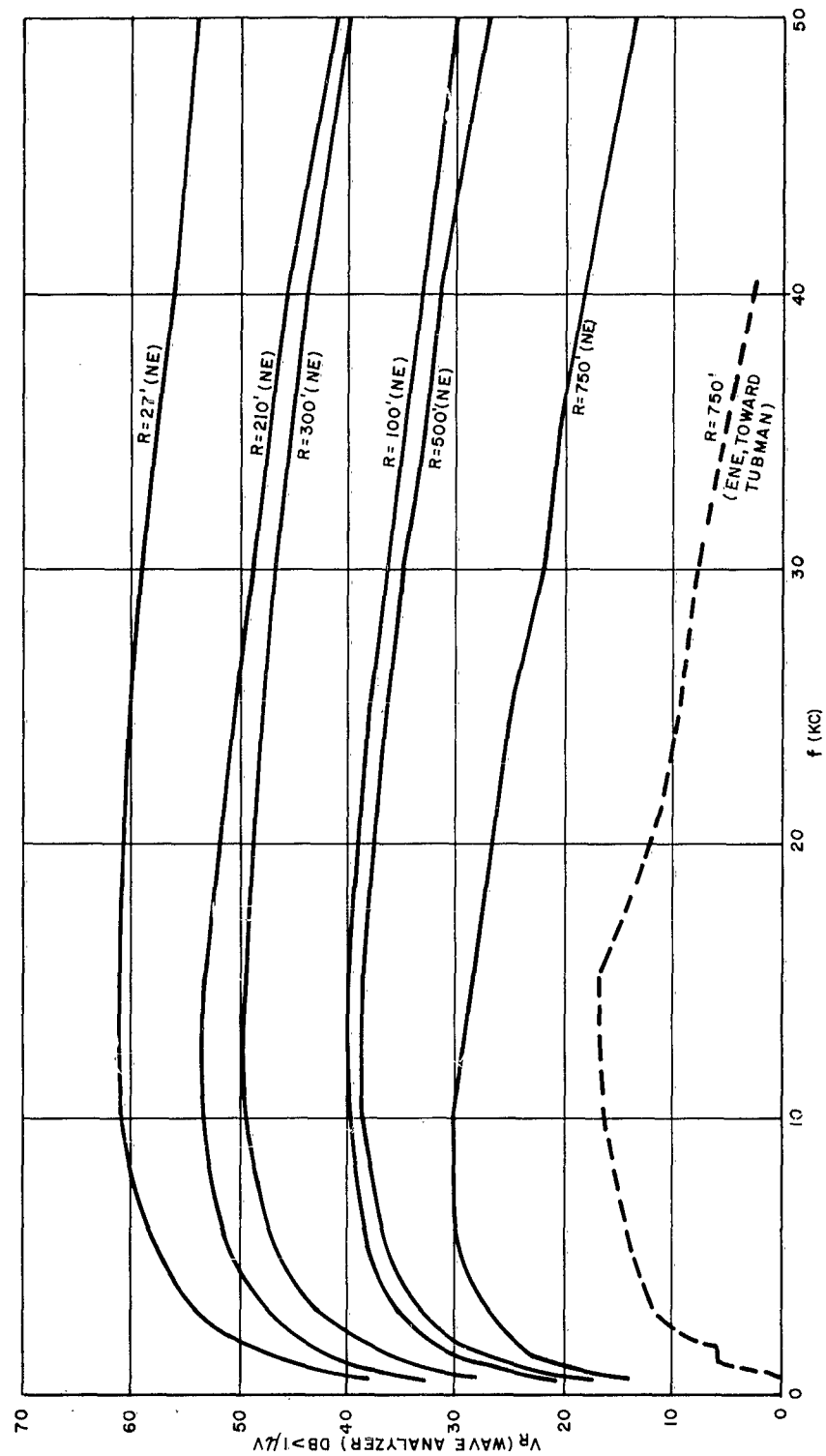
Figure VI. 6.   Surface vertical field intensity in air due to transmissions
from hole antenna.   Wave analyzer voltage V_R at ELF and
LF vs frequency at several ranges R and bearings.   Brewster
Town Dump site (6/20/62).   HP 302A wave analyzer with 6'
vertical whip and grounded with 3' ground stake.

In spite of the high impedance of the wave analyzer, it was then realized that the antenna capacitative reactance might be much larger. In the hole-to-hole tests using the wave analyzer as the receiver, the receiver antenna impedance is very much smaller than the wave analyzer impedance, and in such case V_R, read on the wave analyzer, is a better approximation to the open-circuit antenna voltage V(OC) than it is for the 6-foot whip. A correction factor for the whip antenna $C_V = V(OC)/V_R$ was derived by measuring the antenna capacitance C_A, the antenna connecting cable capacitance C_{AC} and the input admittance of the wave analyzer, Y_{WA}. C_A was about 30 $\mu\mu$f, the cable C_{AC} was about 10 $\mu\mu$f, and the wave analyzer conductance and shunt capacitance were about 9 micromhos and 65 $\mu\mu$f, respectively. The resistance-capacitance divider "network" then yielded values of C_V which were quite frequency sensitive at the lower frequencies. The desired open-circuit antenna voltage is then V(OC) = $C_V V_R$.

Measurements were repeated, in which the 100' range anomaly aforementioned disappeared, and the corrected values of V(OC) are shown in Figure VI.7 for three ranges R = 50, 100, and 210 feet, along the NE radial, shown as solid lines. Also included are the values of V(OC) obtained from V_R in the previous figure for the range R = 750' in a direction towards Tubma Assuming we have properly corrected V_R to obtain V(OC) and that the effective length of the 6-foot whip is about 1 meter, the values of V(OC) in db above 1 microvolt will be the same as the field intensities in db above 1 microvolt/ meter.
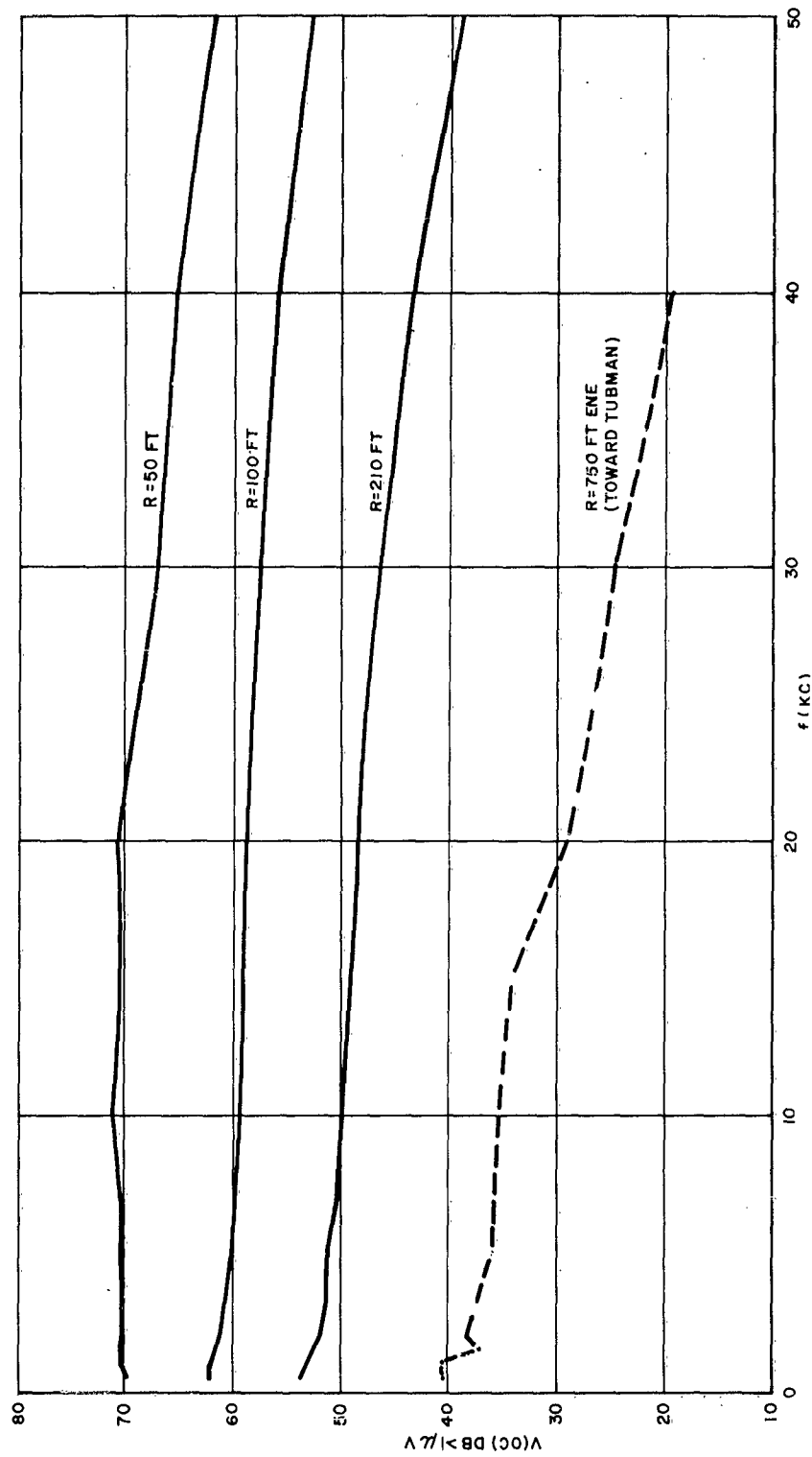
Figure VI. 7.   Surface vertical electric field intensity.   Corrected open-cir-
cuit voltages V(OC) in 6' vertical whip at various ranges NE
(60° magnetic) of drill hole.   Brewster, Mass.

Note the slow frequency dependence of V(OC) and the small increase in the slope of the curves at the greater ranges. This is contrast with the very much greater slope of V(OC) vs frequency observed in the hole-to-hole tests to be described.

During the later observations recorded in Figure VI.7, the noise voltages were observed. The average values of V_R for noise decreased from about 0.5 microvolts at 0.5 kc to about 0.25 microvolts at 7 kc, increasing slightly at 10 kc and then fell off to about 0.1 microvolt at 50 kc; peaks of noise to 2 to 3 microvolts occurred at various frequencies throughout. Some of the very low frequency values may be attributed to internal noise of the wave analyzer.

The observed values of V_R were not affected by changing shielding arrangements at the transmitter (opening the screen room door, removing shield can around feeder at casing pipe, interchanging leads on the screen room filter, etc.). This must mean that leakage fields of the transmitter proper are small. Measured screen room attenuations exceeded 40 db at 1 kc and 76 db at 50 kc, respectively.

3. Effect of Transmitter Antenna Depth on Surface Field Intensity

The transmitting antenna was changed to be very short electrically and so that its depth might be varied while observing the effect on the vertical electric field in air near the surface. The transmitting antenna was a 50-foot insulated antenna (RG-8/U type) with a short-circuit termination

consisting of a 50-foot length of #12 buss wire. We denote by D the depth of the monopole input point where it is joined to the coaxial feeder (RG-8/U cable) inner conductor and waterproofed. (D = 464' corresponds to the depth of the bottom of the casing pipe.) The surface field was observed at the "R = 210', NE" point used previously. At each of several depths readings of V_R with the 6-foot whip were made as a function of frequency 1 to 50 kc.

Resulting values of V_R are plotted vs depth D in Figure VI.8 for frequencies of 10 and 50 kc. Certain detailed features need further investigation but gross results are useful. The values of line input current and voltage were noted, and the values of V_R were normalized to a constant line current of 1 ampere. (It was noted that line voltages changed with depth indicating an effective antenna impedance variation with depth, needing further study.) It is noted that V_R increases by about 15 to 20 db as depth D is decreased, depending on frequency. Further when the antenna plus short circuit was completely inside the pipe, no voltage V_R could be observed above 0.1 microvolt. This must mean that the antenna, when below the pipe, must be the source of V_R observed within a large factor of 50 to 60 db. Further, the lack of an observed signal when the antenna is completely within the pipe means that leakage of the transmitter proper within the screen room must be very small.

Regarding the "plateau" for V_R for depths exceeding D = 464' by distances up to 150', this may mean that the lower conductivity rock may not commence until depths beyond 600' are encountered, at this particular drill
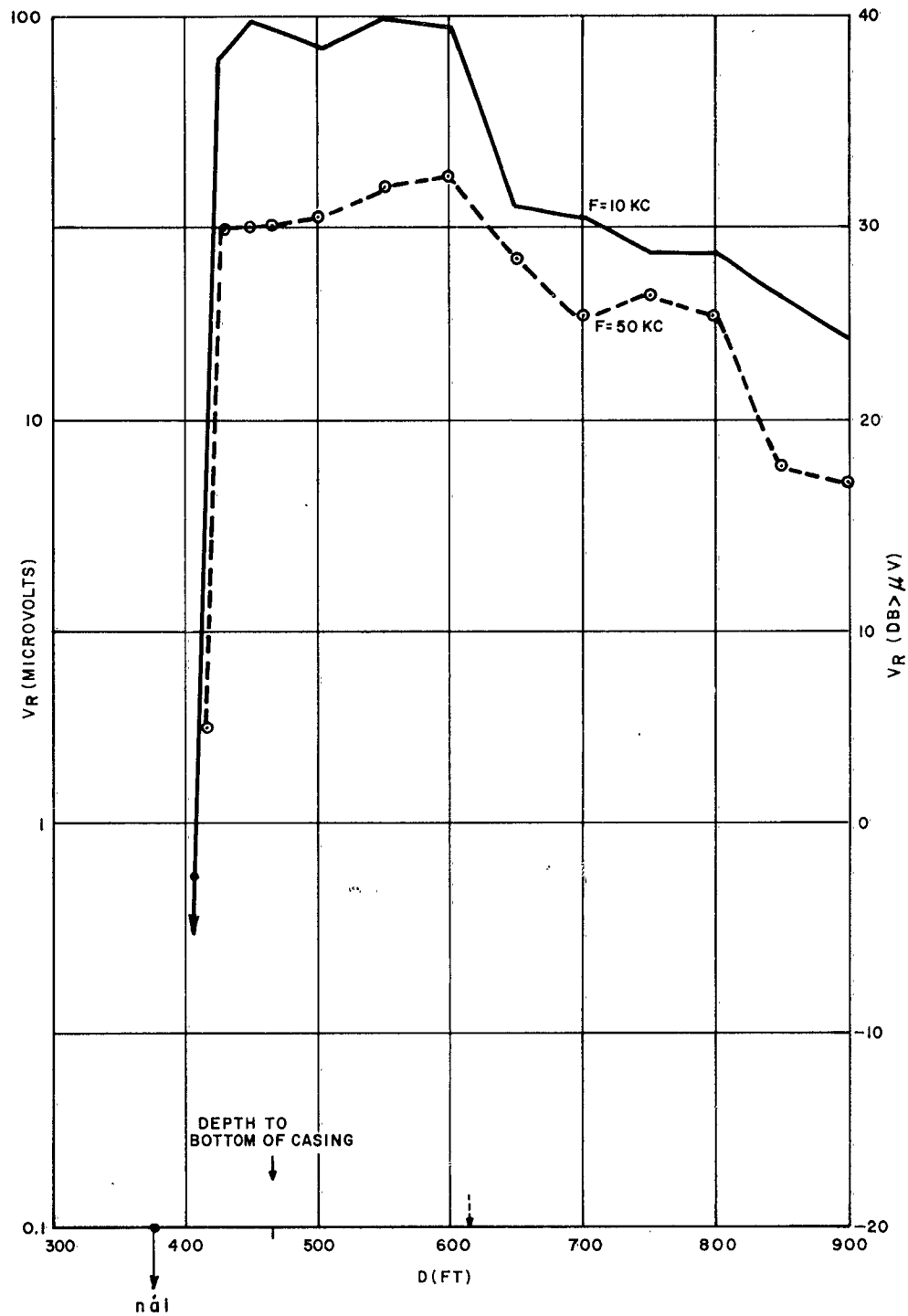
Figure VI. 8. Effect of transmitting antenna depth on surface electric field intensity (vertical).

hole. The phenomenon may also be related to the effect of the finite length (150') of "input braid electrode". It would be useful to reduce the amount of exposed braid on the feeder to 50'; when D then exceeds 514 feet, the antenna behaves as a probe with electrodes at input and output and insulated. The behavior of the feeder at ELF needs examination for depth variation tests.

The curves might be used to infer the contribution to a received signal in hole-to-hole propagation by the up-over-and-down mode. This supposes that the field at the surface observing point closely approximates that of the ground wave portion of the already launched up-and-over component. Thus, if the field should decrease by 15 db with depth at the transmitter and similarly at the receiver, then the potential up-over-and-down mode contribution should decrease with depth (simultaneously) of both transmitting and receiving antenna by 30 db (see reference 40 and Appendix C).

4. Vertical Electric Field Intensity for Greater Ranges at ELF and VLF

Ten differenct sites were chosen to compare measurements of the vertical electric field intensity, in particular to explore the anomalous behavior in that no field was observed on the surface close to the receiving van at Tubman when signals were received on the antenna in that drill hole, and further that there was some evidence of anomalous azimuthal variation at shorter ranges. The sites are identified by the symbol "T-n" where n is a digit running from 0 to 9 to identify the site, somewhat randomly. They are described below.

There were two sites at range R = 750' at two different bearings, referred to in Figure VI.6. These are

Site #	Range (ft.)	Bearing (true)	Description
T-9	750	NE	Edge of Town Dump
T-8	750	76°	In woods towards Tubman

There were next a group of sites along Great Field Road at ranges 2100-2400 feet and different bearings. These are

T-6	2400	31.5°	Edge of road, 100 yds from junction with Setucket Rd.; low voltage power line 50 feet away toward transmitting hole.
T-4	2300	51°	Edge of road
T-2	2100	89°	Edge of road, near cranberry bog towards hole
T-3	2400	119°	Off road, about 200 yds away from high voltage distribution line

Finally there were four sites at ranges 4900 to 6100 feet. These are

T-1	4900	76°	On Tubman property, near Tubman home
T-5	6100	28.5°	Off road, north of School House Pond, a few hundred yds south of intersection with Lower Road, adjacent to abandoned cranberry bog
T-0	6000	76°	At receiver van off Tubman Road, about 40 feet south of the van

Site #	Range (ft.)	Bearing (true)	Description
T-7	6000	76°	Near van, but about 200 yds north, adjacent to stone wall on edge of property, low power lines about 20 feet to the north.

For the surface ranges R exceeding 2000 feet, it was decided to use a taller antenna than the 6-foot whip used previously in anticipation of improved signal-to-noise voltages observed. For this purpose, a portable 33' whip with telescoping sections was used. This created another calibration problem similar to that encountered with the 6-foot whip, which had to be solved in order to obtain the equivalent open-circuit induced voltage from which to obtain the field intensity. A simple expedient of comparing V_R read by the analyzer when using the 33-foot antenna with that when using the 6-foot whip at the same location (site T-9) yielded a "height correction factor C_h" where $C_h = V_R$ (33 foot)$/V_R$ (6 foot). This result gave C_h varying from 18.5 to 20 db. If V_R were simply proportional to height, C_h would be expected to be about 15 db. But C_h as measured should include any changes in antenna capacitance so that one might use the "voltage correction factor C_V" used previously for the 6-foot whip. Normalizing the values of V_R measured with 33-foot whip to those that might have been observed with a 6-foot whip yields the final correction factor $C_V' = C_V/C_h$ to be applied. If the values of V_R are expressed in db $>$ 1 μv, the equivalent open-circuit voltage V(OC) for a 6-foot whip becomes simply $V'(OC)_{db} = V_{Rdb} + C_{Vdb}'$. Assuming the effective

height of a 6-foot whip is 1 meter, then the values of field intensity E in db > 1 μv/m are the same as V'(OC) in db > 1 μv.

The resulting values of E so normalized at those sites where there were observable values of V_R are shown in Figure VI.9 with E in db > μv/m plotted vs frequency for each of 5 sites. Values for the two sites at R = 750' (T-9 and T-8), based on data from Figure VI.6, are included for comparison. (It was the different azimuthal behavior in these curves, plus the results at shorter ranges discussed previously, which led to the exploratory measurements at greater ranges discussed here.)

To illustrate the interesting behavior with range and azimuth, the curves are arranged in two groups, roughly according to bearing. The solid curves are for three different ranges roughly at bearings NE to NNE. In particular, there is noted a strong field at 6100 feet at 28.5° bearing (T-5) in contrast with no observable signals V_R on the 33-foot antenna at sites at and close to the van* (sites T-0, T-1, T-7). The dashed curves are for sites generally easterly and towards Tubman (T-8, T-2, and T-3). There generally appears to be a measurable field towards the NNE-NE at greater ranges up to 6100 feet, whereas at sites toward Tubman, the field could be observed only at ranges up to 2100 feet.

The presence of the field to the NNE at large distances and its absence at Tubman Road is not understood, but may be attributable in part to

---

* A minor exception occurred at site T-7 near a power line where V_R (signal plus noise) was 0.8 db above noise (10 microvolts), at 2 kc but at no other frequencies 0.3 and 20 kc.

Figure VI.9. Vertical electric intensity on surface due to transmissions from vertical dipole in drill hole vs frequency at several test sites.

SOLID CURVES-APPROXIMATELY SAME BEARINGS NORTH OF PATH

● SITE T-9, R = 750 FT, BEARING "NE"
⊙—⊙ SITE T-6, R = 2400 FT, BEARING 31.5°
□—□ SITE T-5, R = 6100 FT, BEARING 28.5°

DASHED CURVES — APPROXIMATELY SAME EASTERLY BEARINGS

▽--▽ SITE T-8, R = 750 FT, BEARING 76° (TUBMAN)
△--△ SITE T-3, R = 2400 FT, BEARING 119°
●--● SITE T-2, R = 2100 FT, BEARING 89°

the irregularities in the overburden alluded to in the surface resistivity meas-
urements (Section V). Smith Pond, located near and just north of the paths
to sites T-6 and T-5 might be an important irregularity in this sense. Power
line re-radiation may be a factor but there were sites quite close to low and
high voltage lines where the field was weak (T-3, T-2) or unobservable (T-1,
T-7). It is possibly happen-stance that the field on the surface at the van
(T-0) was unobservable compared with that at the antenna in the hole for this
would indicate the lack of a potential up-over-and-down mode contribution in
the latter.

C. Noise - 60 cps Interference

While making signal level measurements on an antenna in the Tubman
hole due to transmissions from an antenna in the Brewster hole, it was often
necessary to vary the transmitted frequency to avoid large interfering signals
and noise. This was the case when measuring signals in the air, and signal
detection was the more difficult at frequencies below 10 kc.

Where feasible, noise levels at the time of a measurement were noted,
but the character of the noise was not always that expected of atmospheric
noise. It was while listening to the transmissions with a wideband audio am-
plifier plus tuned filter that 60 cps interference was suspected (Section VID).
Measurements were then made of the 60 cps voltages and its numerous har-
monics up to the order of 3 kc, on antennas in the holes at both sites.

At the Brewster site, the antenna was 475 feet long, of polyethylene
covered #12 wire (RG-8/U type) with a 50-foot short-circuit termination of

#12 wire. The receiver was the Hewlett-Packard 302A wave analyzer. The analyzer was switched to battery operation. It made no essential difference in the readings whether the AC main switch was closed or not. However, it was necessary to shut off the auxiliary AC generator outside the van at the Tubman site to obtain useful data at some frequencies, but essentially there was little difference in those readings above a few microvolts whether that generator was on or off.

The resulting receiver voltages are shown in Figure VI.10. The 60 cps harmonic voltages are indicated by dots and those at Tubman by small triangles. For comparison the received signal voltages at Tubman are indicated by circled points, for two different receiver antenna lengths (h), obtained at the end of this measurement phase. Parameters pertinent to the measurements are indicated on the figure.

The results indicate the difficulty in ascribing on "atmospheric noise level" to that indicated when the frequency is close to the 60 cps harmonics. The amplitudes generally fall off with increasing frequency, the first few odd harmonics being stronger than the even harmonics. There was an enhancement noted near 3 kc at Tubman.

It is not believed that the observed voltages are due to internal generation in the receiving instrument due to overload. It is believed rather that the observed voltages are due to the fields generated by nearby power lines, particularly a high voltage transmission line 1/2 to 1 mile to the south of the area. Some of the voltages observed may be due to the effects of rotating
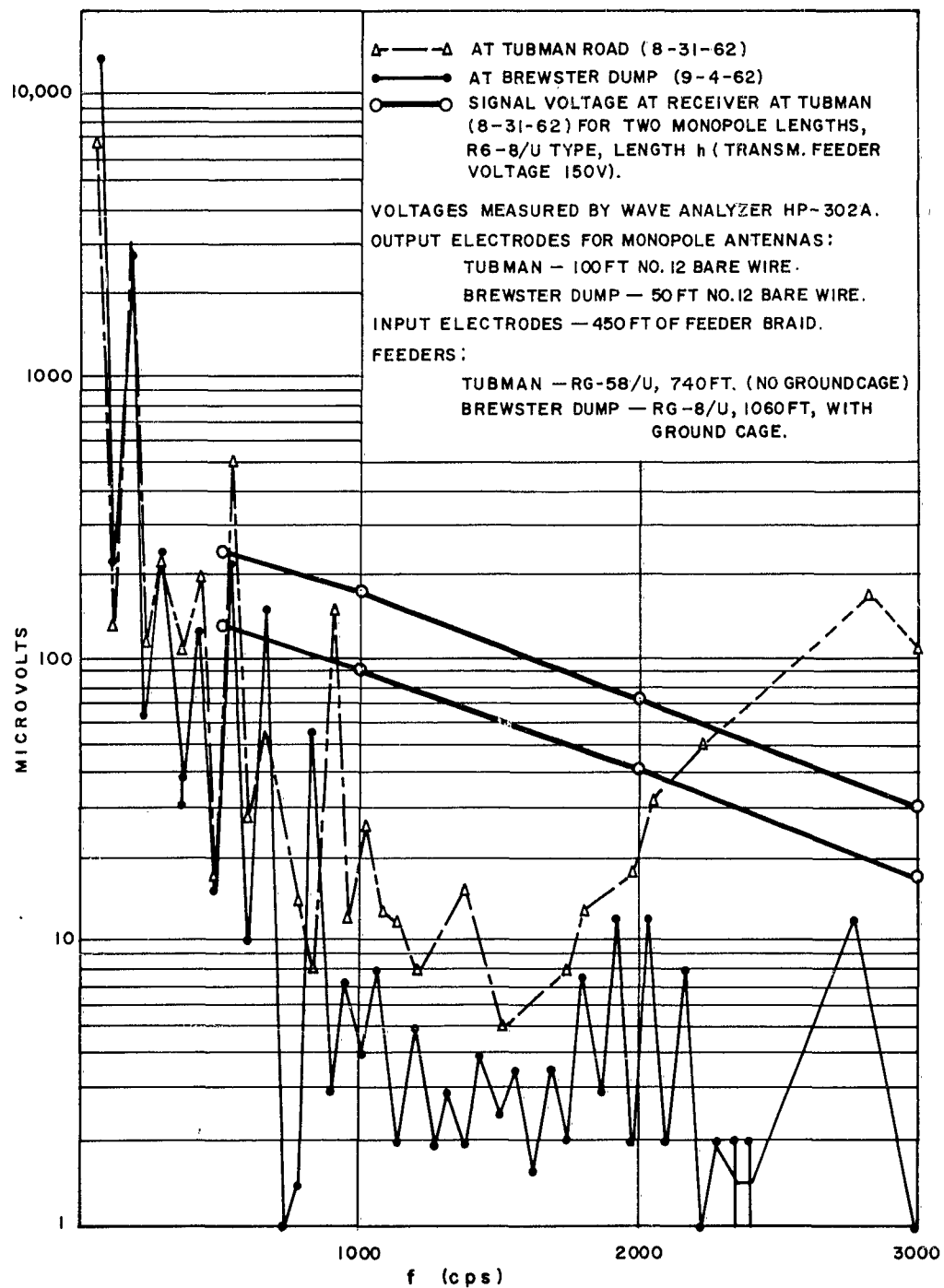
Figure VI. 10.   60 cycle harmonic interference spectra voltages V measured on short-circuit monopoles inserted into rock strata.

machinery or other devices connected to the distribution system in the neighborhood.

The observations do point up the difficulty to be encountered with receiving modulated signals over a wide bandwidth and indicate that care must be taken in the design of a communication system application involving rock propagation. The overburden must be a much better shield against such fields than that encountered in Brewster, assuming that the propagation mechanism for these interfering fields is that of leakage through the overburden of a ground wave propagated mode. Other modes are possible depending upon how they are excited at the source of interference.

D. Signal Transmission Tests on 1-Mile Path (Cape Cod)

1. Description

As mentioned in Section VIA, successful transmissions were accomplished on the 1.1-mile path between antennas in the drill holes at the Brewster Town Dump and on Tubman Road. Various insulated antennas, principally of the RG-8/U type, were employed with open- or short-circuit terminations. The transmitter was the high power (100 to 300 watts) audio amplifier driven by an external oscillator which controlled the frequency. The receiver was the wave analyzer, Hewlett-Packard 302A. Input line voltage or current at the transmitter was maintained constant, there being but a small line input impedance change over the frequency range.

2. First Tests

Following the surface field intensity measurements up to 750-ft

ranges near and around the Brewster site described in Section VIB, tests were commenced the evening of June 20, 1962. The receiving antenna at Tubman was an insulated wire but with vinyl insulation, 312 ft. long, and having a short-circuit termination made of #12 wire. The monopole input depth was held constant at 410 ft, flush with the casing. The transmitting antenna at Brewster was the 475', RG-8/U type insulated antenna with short circuit used previously and the transmitting monopole input depth was maintained constant at 464 ft, flush with the casing.

The received voltages are plotted vs frequency in Figure VI. 11. The scale of the curves for plotting the data was chosen to be similar to that for the surface field intensity curves in Section VIB for easier visual comparison. The solid curves were values of V_R read on the wave analyzer. The impedance of the antenna (short-circuit termination) was of the order of 100 ohms with a slight inductive component. The feedline being electrically short and the impedance of the wave analyzer being much higher than that of the antenna, then V_R closely approximates V(OC) since there are small line attenuation and mismatch effects.

The dashed curves are values of V_R when the receiving antenna was terminated in an open circuit. The reduction in observed voltages are believed to be due to the reduced "effective length" and the effect of antenna mismatch; time did not permit measurement and analysis of these effects.

Note that the curves have apparently much greater slopes than those for the surface field intensity along the path to Tubman discussed in Section VIB.
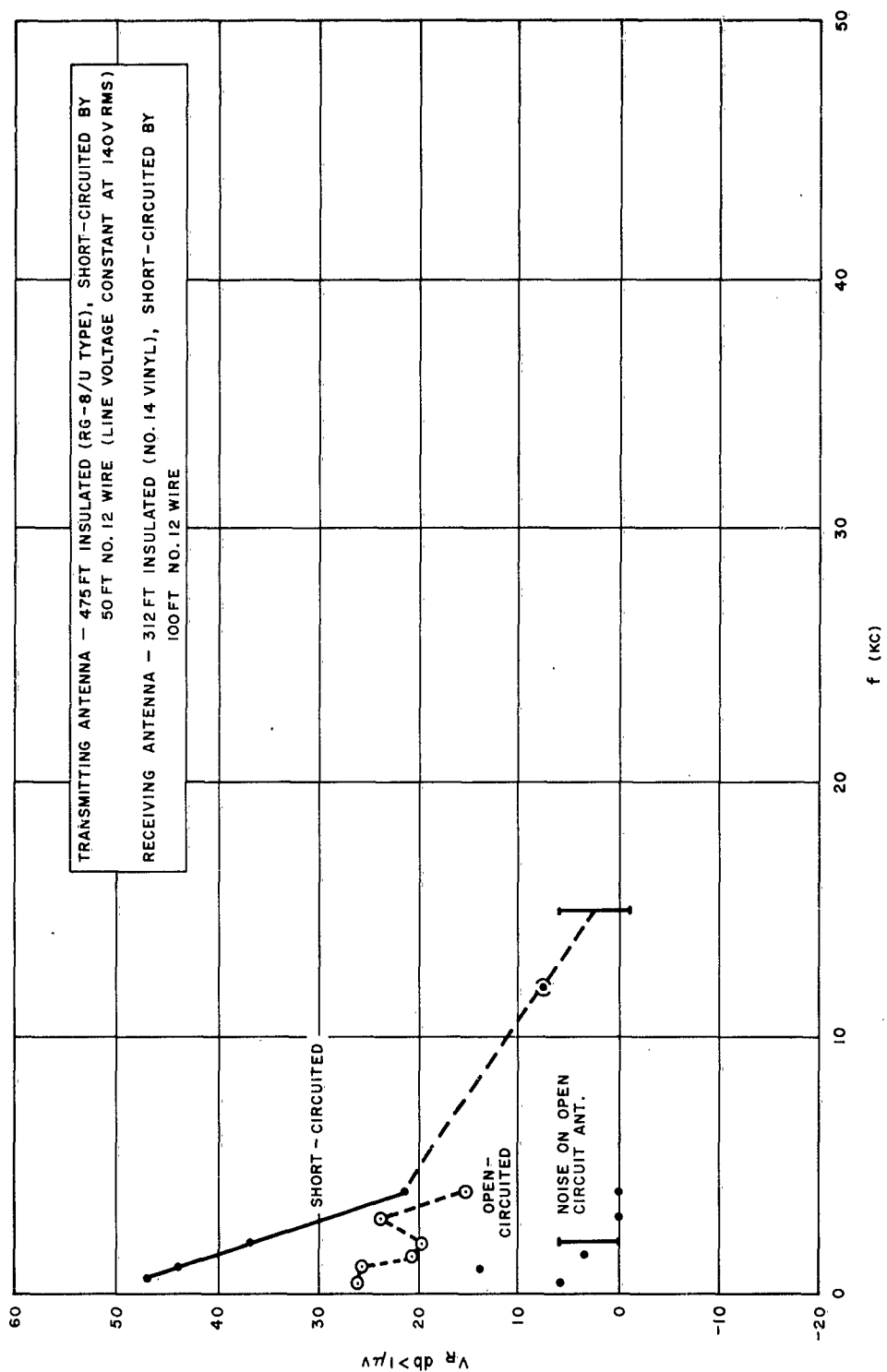
Figure VI.11. Signal voltages received on Tubman drill hole antenna from transmissions on antenna in Brewster drill hole. R = 1.1 mile 6/20/62.

3. Effect of Receiving Antenna Depth

It was noted that increasing the receiving antenna depth increased the values of V_R when using the 312-foot insulated antenna with short-circuit termination. It was also noted that when the insulated portion was entirely in the pipe leaving the bare wire "short-circuit" exposed, then the previously received signal disappeared into the noise at all frequencies. This indicated in a qualitative fashion that the "modified power gain G, " discussed in Sections IIF, IVB, and Appendix F for the bare wire must be much less than that for the insulated antenna, perhaps by as much as 30 db or so at frequencies near 1 kc.

The effect of receiving antenna depth was explored a bit further with a shorter insulated monopole of 123 ft length, with a short-circuit termination. Let D be the depth to the input of the insulated antenna. The voltages V_R for D = 410 feet were about 5 db weaker than those for a greater depth of D = 631 feet (221 feet below the casing) at frequencies from 0.5 to 4 kc. At the greater depth, signals were still being readily detected at levels (4 microvolts) above noise (1 microvolt) as frequency extended byond 5 kc. The depth range was limited by the feeder (RG-58/U cable) length. The results are shown plotted in Figure VI. 12. The remarks on p. VI-19 concerning the effect of "input braid electrode" on Figure VI. 8 apply here at ELF as well.

4. Effect of Receiving Antenna Length

Insulated receiving monopoles of different lengths were used, with short-circuit termination. The resulting receiver voltages V_R are shown plotted on an expanded frequency scale on the curves of Figure VI. 13.
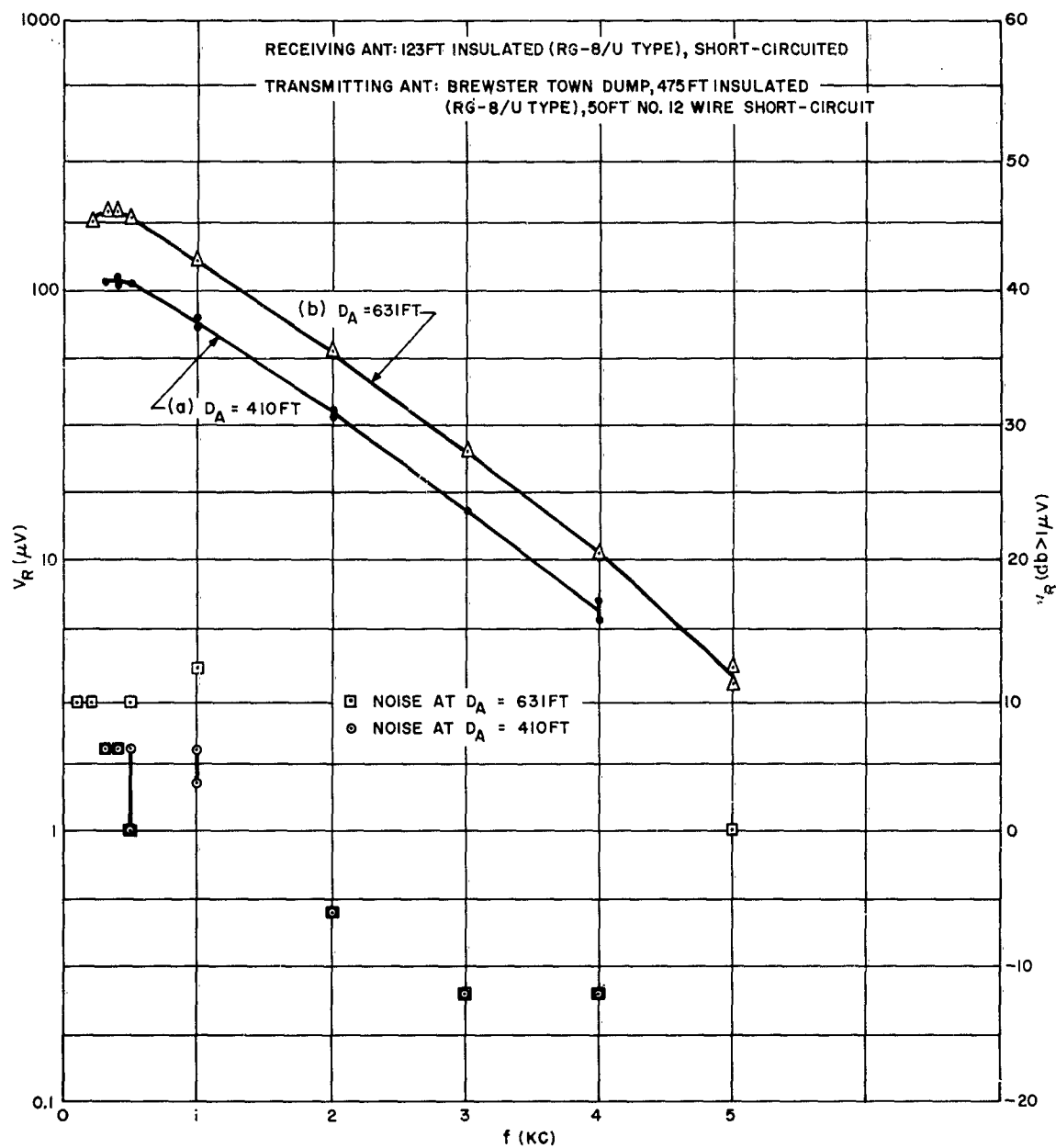
Figure VI. 12.   Path propagation tests.   Effect of Tubman receiver
antenna depth D_A on receiver voltage V_R.
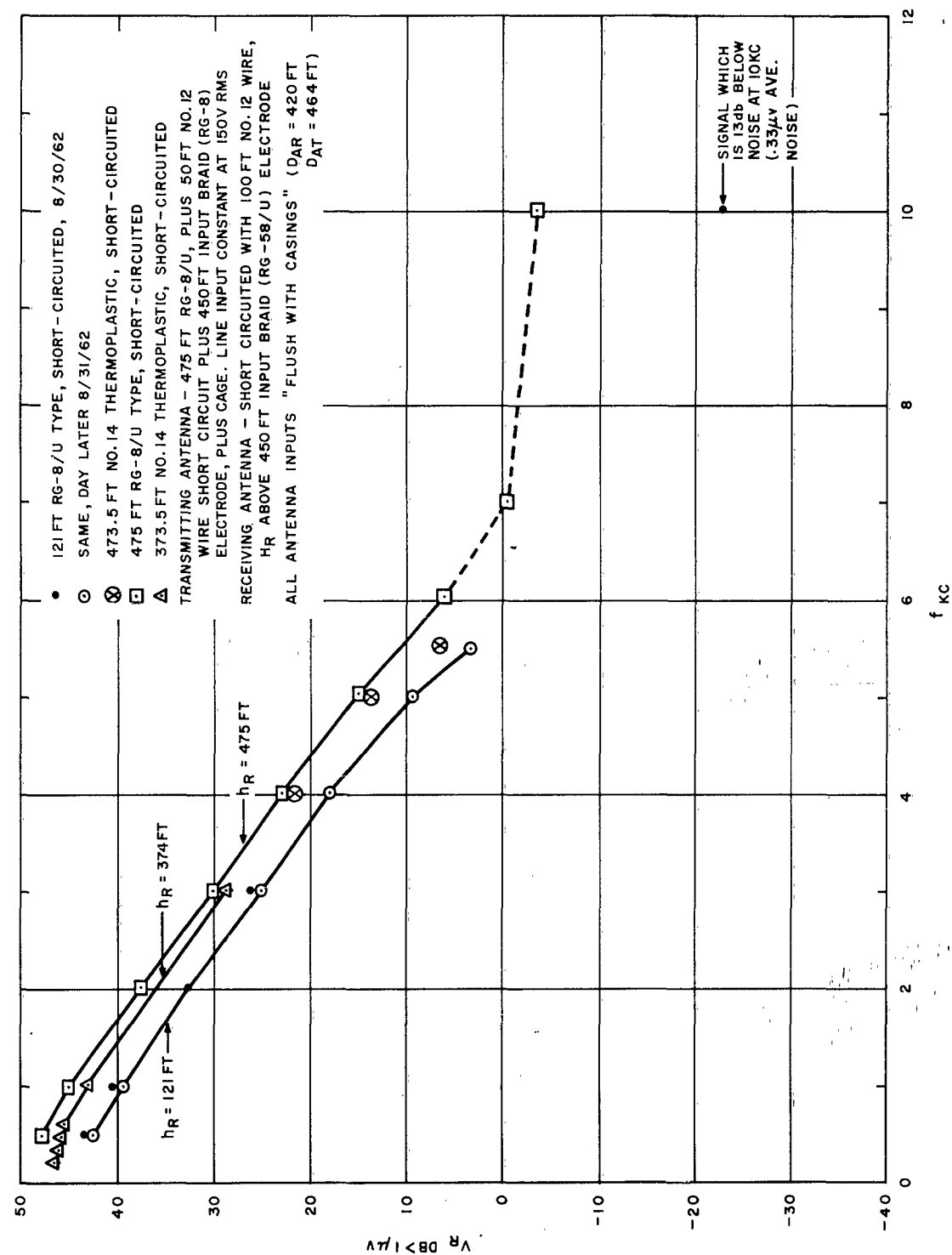
Figure VI. 13   Comparison of signal voltages received at Tubman Road with various antennas from transmissions at town dump site, Brewster.

V_R is generally larger for greater lengths h_R of the receiving antenna. The input depth was flush with the casing at 410 feet.

    5. Field Intensities in the Rock vs Some Surface Field Intensities

    It was not possible to compare values of (or field intensities) for V_R to an antenna in the hole with those at the surface at the receiving site simply because the latter could not be observed on a vertical whip (Section VIB) nor on a length (123 feet) of insulated wire laid on the ground aimed towards the transmitter.

    If one assumes the values of V_R closely approximate the open-circuit induced voltages V(OC) in the electrically short receiving antenna and that the effective length is the actual length h_R of the insulated antenna (short-circuit termination), then the field along the antenna is $E = V(OC)/h_R$, if E is constant along the antenna. Values of E so deduced are shown plotted in Figure VI.14 vs frequency for two antenna lengths 121 and 475 feet. There is a difference where there should be agreement if the field E is constant with depth. The voltage V(OC) is actually proportional to the integrated value of E along its length. If E increases with depth near the overburden (Section VID and also theoretical discussion in Appendix C), then the effective length is not simply h_R unless the antennas are remote from the overburden. Another way of viewing the result is that the effective length is less than h_R for antennas near the overburden, which would tend to bring the two curves nearer to agreement. The remarks apply to a rock medium which is homogeneous with depth. The local irregularity in conductivity with depth, Figure VI.13, may
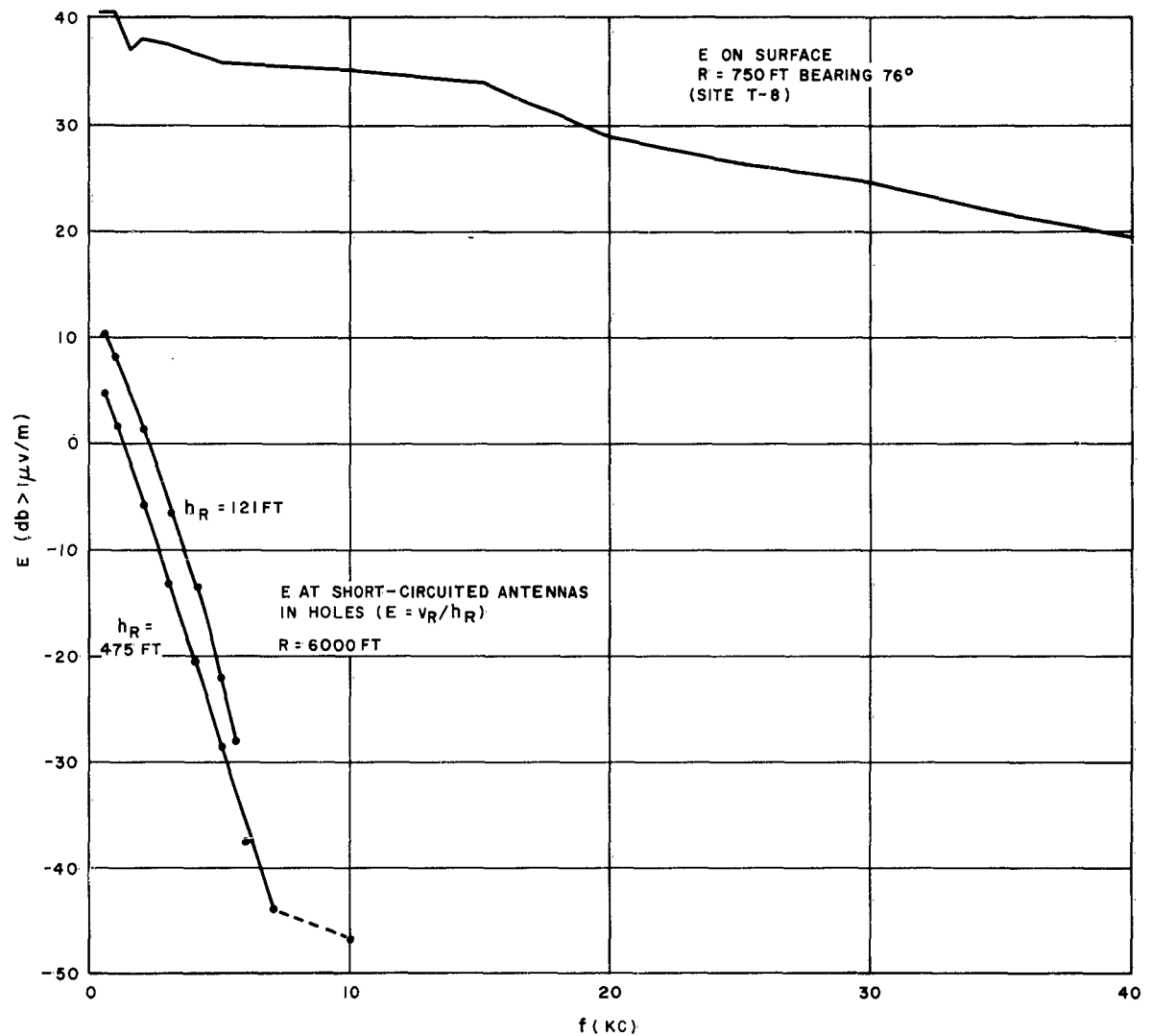
Figure VI. 14. Comparison of "field intensity" E at antenna in drill hole (with range R = 6000 ft) with field intensity on surface along the path at shorter range (R = 750 ft).

be important and its effect should be examined further.

Finally, the surface field intensity at site T-8 (R = 750 feet, bearing 76°) is shown for comparison. Note the vast change in the slopes of the two curves. Again the values of E for site T-8 are not vastly different from those for site T-5 (R = 6100 feet, bearing 31.5°) at a range which is approximately that to Tubman, albeit at a more northerly bearing. That is, the slope of E on the surface vs frequency at great range is vastly different from that in the hole.

The evidence at hand indicates that the observed field intensities measured in the hole are due principally to propagation in the rock below the overburden, and not due to the up-over-and-down mode. This is based upon

— The signals were detected in the hole, but not at the surface close by;

— The signals in the hole increased with increasing antenna depth;

— The variation with frequency of E at the antenna in the hole is much greater than that observed at shorter ranges along the path (where they could be observed) and at comparable ranges somewhat more to the north and away from the direct path.

It is considered necessary to employ other techniques to supplement the evidence. It would be useful to use reference phase techniques, to use a longer antenna in air and to use ground radials at the receiver for further distinction of the two modes. It is considered necessary to conduct further tests on depth variation effects on received field by varying the depths of both antennas once the feedline and probe problems are solved.

6. Preliminary Modulation Tests

In a very preliminary fashion, attempts were made to detect an amplitude-modulated signal. The transmitter, operated near 10 kc, was keyed and the received signal was recorded on magnetic tape. The wave analyzer was connected to the output of the Super Pro receiver with BFO on. The character of the audible beat note out of the wave analyzer for nominal keying speeds (code wheel of GRN-6 used) was as expected in that the signals had a "ringing" sound due to the narrow bandwidth of the analyzer. A tunable filter was of wider bandwidth was then employed and improved audio results when noise levels at the receiver were sufficiently low.

Amplified speech transmissions were attempted with a wideband audio amplifier plus tuned filter used as the "receiver." Results were unsuccessful due to the higher noise figure of the "receiver" and the presence of 60 cps harmonics.

A tone modulated carrier was tried with some success. The carrier was 5 kc and it was modulated with a 1000 cps tone. The lower side-and was detected with the wave analyzer but not the upper. This is in accord with the steep slope of received voltage vs frequency. The implication is that single sideband systems might be employed to advantage for Deep Strata Communications. Consideration should be given to use of some "pre-emphasis plus de-emphasis" scheme to overcome the "filter" characteristic of the propagation medium.

Section VII. DISCUSSION, CONCLUSIONS AND RECOMMENDATIONS

A. Propagation Models

We have used a simple model of an overburden above a semi-infinite rock stratum, with antennas immersed in the latter, to explain certain propagation effects observed on waves propagated between the antennas. This has been useful in connection with short range tests. The model points up the desirability of a thick, highly conducting overburden to shield the receiver from external atmospheric noise, when considering optimum signal-to-noise ratios at the receiver.

We recommend continued theoretical studies regarding the effect of rock conductivity which may vary with depth, and theoretical studies of waveguide propagation modes.

There are disagreements regarding the magnitude of the possibly very low values of rock conductivity which may be found in the earth's crust. Lower conductivities indicate greater communication ranges. The only point we might add is that such low conductivity strata must extend laterally over the large range indicated if such ranges are to be achieved in practice, and such isotropic behavior is difficult to believe. This point is not answered completely and we await results of deep resistivity measurements and surveys.

B. Propagation Tests

Based on limited evidence to date, we conclude that successful transmissions on the 1.1 mile path on Cape Cod were principally by means of signal propagation through the rock near the overburden rather than by the

up-over-and-down mode. The evidence includes absence of a detectable field on the surface when strong fields existed below, the apparent increase of signal received with increasing depth below the overburden, and the difference in shapes of the field intensity vs frequency curves in the hole and in the air at shorter ranges along the path and at comparable ranges off path. The effect of the cable and braid at ELF on depth variation measurements should be more thoroughly studied. More evidence from other techniques is highly recommended.

The surface field intensity patterns show marked abnomalies in azimuth and range at ELF and VLF, when due to transmis ons from an antenna in the rock. It is believed most of this is due to the anisotropic behavior of the overburden. The results indicate that anisotropic behavior of the propagation constant must be taken into account, and that constants derived from path transmission tests are average integrated values.

The use of ground screens on the surface at the receiver and trans-mitter holes might afford another means to discriminate between propagation modes.

Signal amplitude measurements should be implemented by phase measurements.

It is recommended that measurements of the depth variation be continued with electrically short dipoles and with coaxial feeders having better shielding characteristics. Triaxial cable is on hand and should be used after testing for shielding. Such cable may afford a means of obtaining

VII-2

a good probe for exploring the field. The use of insulated loops should be studied, and measurements made with balanced feeders.

The rapid variation of received voltage with frequencies indicates that from a system point of view single sideband schemes should be considered.

Difficulty with 60 cps harmonics should be anticipated where power distribution systems exist.

Ranges exceeding 5 to 10 miles are not expected in practice unless rock conductivities 10^{-4} mhos/m and lower are encountered over these ranges.

Holes with depths of several thousand feet would be useful in order to allow antennas to operate nearer quarter-wave resonance. It should be possible to use frequencies in the lower VLF range.

Transmissions between Tubman and Harwich should be attempted, and possibly short period tests in New Hampshire should be performed using more recent techniques.

Other holes, preferably deeper, should be explored if low rock conductivities are indicated.

C. Antennas

Practically useful results have been achieved with polyethylene covered wire made from RG-8/U cable. The use of Teflon insulation is indicated because of its better water absorption characteristics.

While experimental results agree with essential results of theory, it is thought worthwhile to make measurements of various sizes and types of insulation for such antennas in known homogeneous dissipative media to

confirm details. Of importance are studies aimed at improving antenna efficiency. An example is the use of a low-loss matching section at the input of an insulated antenna which is terminated in an open circuit.

The use of insulated loop antennas should be explored, although vertical drill holes limit the radial dimensions of such loops.

The pattern factor for linear antennas developed theoretically should be confirmed by pattern measurements at frequencies near resonance of an insulated antenna.

D. Measurements of Constants of Rock Media

The major problem of proper measurements of rock media is that measurements should be made in situ. Thus care must be taken on rock samples to reproduce the water content, particularly because of the effect on conductivity and on the frequency dependence of the electric constants.

If it is assumed that interest is in the region adjacent to drill holes because of its influence on antennas and further that the rock is so fractured with water representative of that in the drill hole, then measurements of the drill hole water characteristics are useful. In particular, the water conductivity should closely approximate that of the water infiltrated rock if water conductivity is high and the conductivity of the rock, when dry, is low.

When measuring water conductivity, difficulty is encountered at very low frequencies in the ELF spectrum when using electrodes in contact with the water. This occurs in measuring cells where abnormally high values of "apparent" dielectric constant result. The values measured are apparently

affected by polarization phenomena at the electrodes; values obtained at much higher frequencies are not so affected and represent true values but only at those frequencies. The phenomena need further study for practical application. In the use of insulated antennas, the polarization problem is avoided but questions remain as to the true values of the constants at the frequencies employed at ELF.

The depth attenuation technique with antennas separated vertically is quite useful when drill holes exist and extend far into the rock. The encapsulated transmitter version of the scheme is the most practical. Limited hole depth into the rock restricts minimum frequencies which may be usefully employed to the higher VLF range. Observations at two widely different frequencies may assist separation of conductivity and dielectric constant from attenuation data at the two frequencies. Another variant on the scheme is to measure the phase constant as well as attenuation constant particularly when the loss tangent is less than 1, say. Measurements with loop antennas should be made.

Whether or not drill holes exist, measurements made on the surface of deep resistivity are quite useful. First, surveys should be made with such techniques before new holes are drilled. Second, results from such measurements can be used to assess the value of using existing drill holes for propagation tests. Third, results may be used to help interpret results of successful propagation between two holes. However, the technique suffers in that resulting values are those encountered at fractions to a few cps

frequency, thus yielding values of conductivity valid strictly at those frequencies. It is recommended that some short tests be performed with large horizontal loops in place of long dipoles.

E. Noise

While some noise data were assembled during the course of investigations, we recommend more systematic measurements of noise in air and in the hole be performed. These should be correlated with measurements on fields due to remote ELF and VLF transmitters. The use of a well shielded coaxial feeder for linear probes is recommended. The use of small, ferrite core, loops with balanced, shielded feeder is also recommended.

F. Modulation

Very preliminary tests were performed on the 1 mile path on Cape Cod. Further studies are indicated to assist evaluation of the appropriate modulation scheme to be recommended for communication. Included are the effects of attenuation, phase and noise and interference as functions of frequency.

Section VIII. PERSONNEL

At the Raytheon Company the Deep Strata Research Program was carried out in the Propagation Systems and Research Department under the general direction of Mr. D. A. Hedlund. Mr. G. J. Harmon was the Project Engineer.

Others participating in the program included: Mr. R. A. Sutcliffe, engineer; Dr. J. T. deBettencourt, consultant and consulting scientist; Mr. A. A. Massicott, Northeastern University cooperative student; Mr. A. N. Zaconni, Northeastern University cooperative student; and Mr. M. R. Towne, engineer assistant-technical.

Actively participating in the program were the members of the Transmission Branch, Communication Sciences Laboratory, AFCRL, mentioned in the next Section.

Section IX. ACKNOWLEDGEMENT

Chapman and Company and E. J. Longyear Company.

The early work of Mr. G. J. Harmon is cited and the authors add a note of thanks to him for his loyalty, ideas, and hard work, to Mr. D. A. Hedlund for his general guidance of and technical participation in the program and to our other Raytheon colleagues notably Messrs. Z. Esper and R. Cutter in connection with site surveys and facilities.

Finally, the authors owe a debt of gratitude for the fine work of Miss N. L. Cushing for typing and preparing this Report and related papers for several stages up to the final draft.

Section X. BIBLIOGRAPHY

Text Books and Tables

1. Boudouris, Georges, Propagation Tropospherique, Centre du Documentation Universitaire, Paris; 1957.

2. Jahnke, E., F. Emde, and F. Losch, Tables of Higher Functions, 6th Edition, McGraw-Hill Book Company; 1960.

3. Jordan, E. C., Electromagnetic Waves and Radiation Systems, Prentice-Hall, Inc.; 1958.

4. King, R. W. P., Electromagnetic Engineering, Vol. I. Fundamentals, McGraw-Hill; 1945.

5. King, R. W. P., The Theory of Linear Antennas, Harvard University Press; 1956.

6. King, R. W. P., Transmission-Line Theory, McGraw-Hill; 1955.

7. King, R. W. P., H. R. Mimno, and A. H. Wing, Transmission Lines Antennas and Waveguides, McGraw-Hill; 1945.

8. Schelkunoff, S. A. and H. T. Friis, Antennas Theory and Practice, John Wiley & Sons; 1952.

9. Schelkunoff, S. A., Electromagnetic Waves, D. Van Nostrand Co.; 1944.

10. Sokolnifoff, I. S. and Elizabeth Sokolnifoff, Higher Mathematics for Engineers and Physicists, McGraw-Hill; 1941.

11. Stratton, J. A., Electromagnetic Theory, McGraw-Hill; 1941.

12. Sunde, E. D., Earth Conduction Effects in Transmission Systems, D. Van Nostrand; 1949.

13. American Institute of Physics Handbook, McGraw-Hill; 1957.

14. Dielectric Materials and Applications, A. von Hippel editor, The Technology Press of M. I. T. & John Wiley & Sons, Inc.; 1958.

15. Handbook of Chemistry and Physics, Chemical Rubber Publishing Co.,
    22nd Edition; 1937.

16. Reference Data for Radio Engineers, International Telephone and Tele-
    graph Corp., 4th Edition; 1956.

17. Tables of Circular and Hyperbolic Sines and Cosines for Radian Argu-
    ments, National Bureau of Standards, Applied Mathematics Series 36;
    1953.

18. Table of Circular and Hyperbolic Tangents and Cotangents for Radian
    Arguments, Mathematical Tables Project, National Bureau of Standards,
    Columbia University Press; 1947.

19. Tables of the Exponential Integral for Complex Argument, National
    Bureau of Standards, Applied Mathematics Series 51, U.S.G.P.O.,
    Washington, D.C.; May 15, 1958.

20. Van Nostrand's Scientific Encyclopedia, D. Van Nostrand Co., 3rd
    Edition; January, 1958.

Publications, Meeting Papers, and Reports

21. Banos, A., Jr., and J. P. Wesley, The horizontal electric dipole in a
    conducting half-space, Parts I and II, Reports by Marine Physical
    Laboratory of the Scripps Institution of Oceanography, University of
    California, La Jolla, California; 1953.

22. Budden, K. G., The propagation of radio-atmospheric, The Philosoph-
    ical Magazine, vol. 42, no. 324, pp. 1-19; January, 1951.

23. Budden, K. G., The propagation of radio atmospheric-II, The Philosoph-
    ical Magazine, vol. 43, no. 346, pp. 1179-1200; November, 1952.

24. Budden, K. G., The reflection of very low frequency radio waves at the
    surface of a sharply bounded ionosphere with superimposed magnetic
    field, The Philosophical Magazine, vol. 42, no. 331, pp. 833-850;
    August, 1951.

25. Budden, K. G., The "waveguide" theory of the propagation of very-low-
    frequency radio waves, Proc. IRE, vol. 45, no. 6, pp. 772-774; June,
    1957.

26. Burrows, C. R., *Transient response in a lossy dielectric*, Paper presented at the 1962 Spring URSI Meeting, Georgetown University, Washington, D. C.; April 30-May 3, 1962.

27. Cagniard, L., *Basic theory of the magneto-telluric method of geophysical prospecting*, Geophysics, vol. 18, no. 3, pp. 605-635; July, 1953.

28. Cantwell, T. and T. R. Madden, *Preliminary report on crustal magneto telluric measurements*, Journal of Geophysical Research, 65, p. 4202; 1960.

29. Card, R. H., *Earth resistivity and geological structure*, Electrical Engineering, vol. 54, no. 11; November, 1935.

30. Corrington, M. S., *Applications of the complex exponential integral*, Mathematics of Computation, vol. 15, no. 73, pp. 1-6; January, 1961.

31. Crichlow, W. Q., *Noise investigation at VLF by the National Bureau of Standards*, Proc. IRE, vol. 45, no. 6, pp. 778-782; June, 1957.

32. deBettencourt, J. T., *Studies in deep strata radio communications, half wave antennas and systems*, Technical Report, Raytheon Company, Equipment Division, CADPO; January 27, 1961 (Rev. March 22, 1961).

33. deBettencourt, J. T., *Insulated and bare linear antennas for deep strata propagation*, Paper presented at the 1962 Spring URSI Meeting, Georgetown University, Washington, D. C.; April 20-May 3, 1962. Also paper presented at Boston Section PGAP Meeting, February, 1961.

34. deBettencourt, J. T., *Deep strata research - transmission equation, antenna gains and efficiency in slightly dissipative media*, Memo JTD-1-61 to D. A. Hedlund, Raytheon Company, Equipment Division, CADPO; May 29, 1961.

35. deBettencourt, J. T., *Deep strata research - studies on coaxial antennas in water filled holes*, Memo JTD-2-61 to D. A. Hedlund, Raytheon Company, Equipment Division, CADPO; November 27, 1961.

36. deBettencourt, J. T., *Deep strata research - estimates of VLF and LF noise field strengths and interference effects*, Memo JTD-4-61 to D. A. Hedlund, Raytheon Company, Equipment Division, CADPO; November 21, 1961.

37. deBettencourt, J. T., Deep strata research - linear antennas in dissipative media: current distribution and far fields, Memo JTD-5-61 to D. A. Hedlund, Raytheon Company, Equipment Division, CADPO; November 29, 1961.

38. deBettencourt, J. T., Deep strata research - current distribution on linear antennas in dissipative media, Memo JTD-6-61 to D. A. Hedlund, Raytheon Company, Equipment Division, CADPO; December 11, 1961.

39. deBettencourt, J. T., Deep strata research - linear antennas in dissipative media: Poynting Vector, directivity, power gain, transmission equation, Memo JTD-7-61 to D. A. Hedlund, Raytheon Company, Equipment Division, CADPO; December 18, 1961.

40. deBettencourt, J. T., Deep strata propagation - depth variation technique to determine effective conductivity and to separate deep strata mode from the up-over-and-down mode, Memo JTD-62-1 to D. A. Hedlund, Raytheon Company, Equipment Division, CADPO; 28 May 1962.

41. deBettencourt, J. T., Deep strata research - coaxial feeder cable characteristic impedance and propagation constant at LF and ELF, Memo JTD-62-2 to D. A. Hedlund, Raytheon Company, Equipment Division, CADPO; 20 August 1962.

42. Furutsu, K., On communication in the sea by VLF electromagnetic waves, Journal of the Radio Res. Labs, vol. 5, no. 19, pp. 19-32; January, 1958.

43. Guy, A. W. and G. Hasserjian, Impedance properties of long subsurface antennas, Paper presented at the 1962 Spring URSI Meeting, Georgetown University, Washington, D. C.; April 30-May 3, 1962.

44. Harmon, G. J., Electrical characteristics of granitic media for deep strata propagation, Paper presented at the 1962 Spring URSI Meeting, Georgetown University, Washington, D. C.; April 30-May 3, 1962.

45. Hasserjian, G. and A. W. Guy, Low frequency, subsurface radiating structures, Paper presented at the 1962 Spring URSI Meeting, Georgetown University, Washington, D. C.; April 30-May 3, 1962.

46. Herman, J. R., Reliability of atmospheric radio noise predictions, U.S. Bureau of Standards, Journal of Research, vol. 65D, no. 6, pp. 565-574; November-December, 1961.

47. Hill, E. L., Very low-frequency radiation from lightning strokes, Proc. IRE, vol. 45, no. 6, pp. 775-777; June, 1957.

48. Iizuka, K. and R. W. P. King, Apparatus for the study of the properties of antennas in a conducting medium, Scientific Report No. 1, Cruft Lab, Harvard University, Cambridge, Mass., under contract AF 19(604)7262; May 20, 1961.

49. Iizuka, K. and R. W. P. King, An experimental study of the properties of antennas immersed in conducting media, Scientific Report No. 2, Cruft Lab, Harvard University, Cambridge, Mass., under contract AF 19(604)7262; December 15, 1961.

50. Jean, A. G., H. E. Taggart, and J. R. Wait, Calibration of loop antennas at VLF, U. S. Bureau of Standards, Journal of Research, vol. 65C, no. 3, pp. 189-193; July-September, 1961.

51. King, R. W. P., Dipoles in dissipative media, Harvard University, Cruft Lab, Technical Report No. 336; February 1, 1961.

52. King, R. W. P., Linear arrays: currents, impedances and fields, I, Scientific Report No. 1 (Series 2), Cruft Lab, Harvard University, Cambridge, Mass., under contract AF 19(604)-4118; May 1, 1959. ASTIA No. AD 217 409.

53. King, R. W. P. and C. W. Harrison, Half-wave cylindrical antenna in a dissipative medium: current and impedance, Journal of Research, NBS, vol. 64D, pp. 365-380; July-August, 1960.

54. King, R. W. P., C. W. Harrison, and D. H. Denton, The electrically short antenna as a probe for measuring free electron densities and collision frequencies in an ionized region, U.S. Bureau of Standards, Journal of Research, vol. 65D, no. 4, pp. 371-384; July-August, 1961.

55. Kirkscether, E., Ground constant measurements using a section of balanced two-wire transmission line, IRE Transactions on Antennas & Propagation, vol. AP-8, pp. 307-312; May, 1960.

56. Kownacki, S., A method of investigating air-to-subsurface VLF Propagation, Paper presented at the 1962 Spring URSI Meeting, Georgetown University, Washington, D. C.; April 30-May 3, 1962.

57. Lahiri, B. N. and A. T. Price, Electromagnetic induction in non-uniform conductors, and the determination of the conductivity of the earth from terrestrial magnetic variations, Royal Society of London, Philosophical Transactions, vol. 237A, no. 784, pp. 509-540; January 20, 1939.

58. Macrakis, M., Cylindrical antenna immersed in a dissipative medium (input-impedance), Technical Report No. 256, Cruft Lab, Harvard University, Cambridge, Mass., under contract NOr 1866(16); April 2, 1957.

59. Madden, T. R., T. Cantwell, D. Greenewalt, A. Kelly, and A. Regier, Progress report on geomagnetic studies and electrical conductivity in the earth's crust and upper mantle, M.I.T. Geophysics Lab Report, Project NR-371-401; April 15, 1962.

60. Moore, R. K., The theory of radio communication between submerged submarines, Ph.D. Thesis, Cornell University; 1951.

61. Moore, R. K. and W. E. Blair, Dipole radiation in a conducting half space, U.S. Bureau of Standards, Journal of Research, vol. 65D, no. 6, pp. 547-563; November-December, 1961.

62. Norton, K. A., The propagation of radio waves over the earth and in the atmosphere, Part I, Proc. IRE, vol. 24, p. 1367; October, 1936, and Part II, Proc. IRE, vol. 25, p. 1203; September, 1937.

63. Norton, K. A., System loss in radio wave propagation, Journal of Research, NBS, vol. 64D, pp. 365-380; July-August, 1960.

64. Pierce, G. W., Proc. Am. Acad. Arts and Sciences, vol. 57, p. 175; 1922. Also lecture notes, Cruft Lab, Engineering Course 223, Harvard University; 1937.

65. Raemer, H. R., On the spectrum of terrestrial radio noise at extremely low frequencies, NBS, Journal of Research, vol. 65D, no. 6, pp. 581-593; November-December, 1961.

66. Schlicter, L. B., An electrical problem in geophysics, Tech. Engineering News; 1934.

67. Skehan, J. W., Report on the nature of the water content of the glacial deposits and bedrock of Cape Cod, Massachusetts, for the Raytheon Company; March, 1962.

68. Storer, J. E., Variational solution to the problem of the symmetrical cylindrical antenna, Harvard University, Cruft Lab, Technical Report No. 101; 1951. Also Ph.D. Thesis, Harvard University; 1951.

69. Tai, C. T., Radiation of a Hertzian dipole immersed in a dissipative medium, Tech. Report No. 21, Cruft Lab, Harvard University, Cambrige, Mass., under contract N5 ori-76; 1947. ASTIA No. ATI 19 468.

70. Tai, C. T., A variational solution to the problem of cylindrical antennas, Tech. Report No. 12, Stanford Res. Institute, Aircraft Radiation Systems Lab, California, under contract No. AF 19(122)78. ASTIA No. ATI 94 772.

71. Tai, C. T., Biconical antenna in dissipative media, Paper presented at 1962 Spring URSI-IRE Meeting, Washington, D.C.; May 4, 1962.

72. Tartakovskii, L. S., General design formulae for the field of an arbitrarily orientated dipole placed above a flat uniform earth, Radio Engineering (English Trans. of Radiotekhnika, vol. 13, no. 4; 1958), pp. 47-57; April, 1959.

73. Volland, H., Comparison between mode theory and ray theory of VLF propagation, NBS, Journal of Research, vol. 65D, no. 4, pp. 357-361; July-August, 1961.

74. Wait, J. R., Current-carrying wire loops in a simple inhomogeneous region, Journal of Applied Physics (Correspondence), vol. 23, no. 4, pp. 497-498; April, 1952.

75. Wait, J. R., The magnetic dipole antenna immersed in a conducting medium, Proc. IRE, vol. 40, no. 10, pp. 1244-1245; October, 1952.

76. Wait, J. R., The attenuation versus frequency characteristics of VLF radio waves, Proc. IRE, vol. 45, no. 6, pp. 768-771; June, 1957.

77. Wait, J. R., The mode theory of VLF ionospheric propagation for finite ground conductivity, Proc. IRE, vol. 45, no. 6, pp. 760-767; June, 1957.

78. Wait, J. R., Insulated loop antenna immersed in a conducting medium, NBS, Journal of Research, vol. 59, no. 2, pp. 133-137; (RP 2781); August, 1957.

79. Wait, J. R., Transmission and reflection of electromagnetic waves in the presence of stratified media, NBS, Journal of Research, vol. 61, no. 3, pp. 205-232; September, 1958 (RP 2899).

80. Wait, J. R., Transmission of power in radio propagation, Electronic & Radio Engineer, vol. 36, no. 4, pp. 146-150; April, 1959.

81. Wait, J. R., On the thoery of mixed-path ground-wave propagation on a spherical earth, NBS, Journal of Research, vol. 65D, no. 4, pp. 401-410; July-August, 1961.

82. Wait, J. R., On the impedance of long wire suspended over the ground, Proc. IRE, vol. 49, no. 10, p. 1576; October, 1961.

83. Wait, J. R., Introduction to the theory of VLF propagation, Proc. IRE, vol. 50, no. 7, pp. 1624-1647; July, 1962.

84. Wait, J. R., Theory of magneto-telluric fields, NBS, Journal of Research, vol. 66D, no. 5, pp. 509-541; September-October, 1962.

85. Wait, J. R. and A. M. Conda, On the measurement of ground conductivity at VLF, IRE Trans. on Antennas & Propagation, vol. AP-6, no. 3, pp. 273-277; July, 1958.

86. Wait, J. R. and A. Murphy, The geometrical optics of VLF sky wave propagation, Proc. IRE, vol. 45, no. 6, pp. 754-759; June, 1957.

87. Watt, A. D. and E. L. Maxwell, Characteristics of atmospheric noise from 1 to 100 kc, Proc. IRE, vol. 45, no. 6, pp. 787-794; June, 1957.

88. Waynick, A. H., The present state of knowledge concerning the lower ionosphere, Proc. IRE, vol. 45, no. 6, pp. 741-749; June, 1957.

89. Wheeler, H. A., Fundamental limitations of a small VLF antenna for submarines, IRE Trans. on Antennas & Propagation, vol. AP-6, no. 1, pp. 123-125; January, 1958.

90. Wheeler, H. A., Radio wave propagation in the earth's crust, NBS, Journal of Research, vol. 65D, no. 2, pp. 189-191; March-April, 1961.

91. Wu, Tai Tsum, The imperfectly conducting coaxial line, Technical Report No. 282, Cruft Lab, Harvard University, Cambridge, Mass., under contract Nonr-1866 (26), NR-371-015; April 20, 1958.

92. Yabroff, I. W., Reflections at a sharply bounded ionosphere, Proc. IRE, vol. 45, no. 6, pp. 750-753; June, 1957.

93. Yungul, S. H., Magneto-telluric sounding three-layer interpretation curves, Geophysics, vol. 26, no. 4, pp. 465-476; August, 1961.

94. Geoscience, Inc., Resistivity investigation on Cape Cod, Geoscience, Inc., Natick, Mass., AF Report GAF 13-26; August, 1962.

95. Revision of atmospheric radio noise data, CCIR VIII th Plenary Assembly, Warsaw, vol. I, Report No. 65; 1956. Published by Int. Tele. Union, Geneva; 1957.

96. Stanford Res. Inst., A summary of literature pertaining to VLF and ELF Propagation, Vol. I & Vol. II prepared by Stanford Res. Inst. for the Office of the Secretary of Defense under contract SD-66, SRI Project 3311.

97. Weston Geophysical Engineers, Inc., Report on seismic and magnetic survey Brewster and Harwich, Massachusetts, for Raytheon Company, Weston Geophysical Engineers, Inc., Weston, Mass.; March, 1962.

TABLE 1

$0.0000 \leq p \leq 0.0099$ in steps of 0.0001

p	f(p)	g(p)	$\dfrac{g(p)}{f(p)}$	|S|	θ
.0000	1.00000	0.00000	.00000	1.00000	.00000
1	.00000	.00005	.00005	.00000	.00005
2	.00000	.00010	.00010	.00000	.00010
3	.00000	.00015	.00015	.00000	.00015
4	.00000	.00020	.00020	.00000	.00020
.0005	1.00000	0.00025	.00025	1.00000	.00025
6	.00000	.00030	.00030	.00000	.00030
7	.00000	.00035	.00035	.00000	.00035
8	.00000	.00040	.00040	.00000	.00040
9	.00000	.00045	.00045	.00000	.00045
.0010	1.00000	0.00050	.00050	1.00000	.00050
1	.00000	.00055	.00055	.00000	.00055
2	.00000	.00060	.00060	.00000	.00060
3	.00000	.00065	.00065	.00000	.00065
4	.00000	.00070	.00070	.00000	.00070
.0015	1.00000	0.00075	.00075	1.00000	.00075
6	.00000	.00080	.00080	.00000	.00080
7	.00000	.00085	.00085	.00000	.00085
8	.00000	.00090	.00090	.00000	.00090
9	.00000	.00095	.00095	.00000	.00095
.0020	1.00000	0.00100	.00100	1.00000	.00100
1	.00000	.00105	.00105	.00000	.00105
2	.00000	.00110	.00110	.00000	.00110
3	.00000	.00115	.00115	.00000	.00115
4	.00000	.00120	.00120	.00000	.00120
.0025	1.00000	0.00125	.00125	1.00000	.00125
6	.00000	.00130	.00130	.00000	.00130
7	.00000	.00135	.00135	.00000	.00135
8	.00000	.00140	.00140	.00000	.00140
9	.00000	.00145	.00145	.00000	.00145
.0030	1.00000	0.00150	.00150	1.00000	.00150
1	.00000	.00155	.00155	.00000	.00155
2	.00000	.00160	.00160	.00000	.00160
3	.00000	.00165	.00165	.00000	.00165
4	.00000	.00170	.00170	.00000	.00170
.0035	1.00000	0.00175	.00175	1.00000	.00175
6	.00000	.00180	.00180	.00000	.00180
7	.00000	.00185	.00185	.00000	.00185
8	.00000	.00190	.00190	.00000	.00190
9	.00000	.00195	.00195	.00000	.00195
.0040	1.00000	0.00200	.00200	1.00000	.00200
1	.00000	.00205	.00205	.00000	.00205
2	.00000	.00210	.00210	.00000	.00210
3	.00000	.00215	.00215	.00000	.00215
4	.00000	.00220	.00220	.00000	.00220
.0045	1.00000	0.00225	.00225	1.00001	.00225
6	.00000	.00230	.00230	.00001	.00230
7	.00000	.00235	.00235	.00001	.00235
8	.00000	.00240	.00240	.00001	.00240
9	.00000	.00245	.00245	.00001	.00245

p	f(p)	g(p)	$\frac{g(p)}{f(p)}$	$|S|$	θ
.0050	1.00000	0.00250	.00250	1.00001	.00250
1	.00000	.00255	.00255	.00001	.00255
2	.00000	.00260	.00260	.00001	.00260
3	.00000	.00265	.00265	.00001	.00265
4	.00000	.00270	.00270	.00001	.00270
.0055	1.00000	0.00275	.00275	1.00001	.00275
6	.00000	.00280	.00280	.00001	.00280
7	.00000	.00285	.00285	.00001	.00285
8	.00000	.00290	.00290	.00001	.00290
9	.00000	.00295	.00295	.00001	.00295
.0060	1.00000	0.00300	.00300	1.00001	.00300
1	.00000	.00305	.00305	.00001	.00305
2	.00000	.00310	.00310	.00001	.00310
3	.00000	.00315	.00315	.00001	.00315
4	.00001	.00320	.00320	.00001	.00320
.0065	1.00001	0.00325	.00325	1.00001	.00325
6	.00001	.00330	.00330	.00001	.00330
7	.00001	.00335	.00335	.00001	.00335
8	.00001	.00340	.00340	.00001	.00340
9	.00001	.00345	.00345	.00001	.00345
.0070	1.00001	0.00350	.00350	1.00001	.00350
1	.00001	.00355	.00355	.00001	.00355
2	.00001	.00360	.00360	.00001	.00360
3	.00001	.00365	.00365	.00001	.00365
4	.00001	.00370	.00370	.00001	.00370
.0075	1.00001	0.00375	.00375	1.00001	.00375
6	.00001	.00380	.00380	.00001	.00380
7	.00001	.00385	.00385	.00001	.00385
8	.00001	.00390	.00390	.00002	.00390
9	.00001	.00395	.00395	.00002	.00395
.0080	1.00001	0.00400	.00400	1.00002	.00400
1	.00001	.00405	.00405	.00002	.00405
2	.00001	.00410	.00410	.00002	.00410
3	.00001	.00415	.00415	.00002	.00415
4	.00001	.00420	.00420	.00002	.00420
.0085	1.00001	0.00425	.00425	1.00002	.00425
6	.00001	.00430	.00430	.00002	.00430
7	.00001	.00435	.00435	.00002	.00435
8	.00001	.00440	.00440	.00002	.00440
9	.00001	.00445	.00445	.00002	.00445
.0090	1.00001	0.00450	.00450	1.00002	.00450
1	.00001	.00455	.00455	.00002	.00455
2	.00001	.00460	.00460	.00002	.00460
3	.00001	.00465	.00465	.00002	.00465
4	.00001	.00470	.00470	.00002	.00470
.0095	1.00001	0.00475	.00475	1.00002	.00475
6	.00001	.00480	.00480	.00002	.00480
7	.00001	.00485	.00485	.00002	.00485
8	.00001	.00490	.00490	.00002	.00490
9	.00001	.00495	.00495	.00002	.00495

TABLE 2

$0 \leq p \leq 0.099$ in steps of 0.001

p	f(p)	g(p)	$\frac{g(p)}{f(p)}$	|S|	θ
.000	1.00000	0.00000	.00000	1.00000	.00000
1	.00000	.00050	.00050	.00000	.00050
2	.00000	.00100	.00100	.00000	.00100
3	.00000	.00150	.00150	.00000	.00150
4	.00000	.00200	.00200	.00000	.00200
.005	1.00000	0.00250	.00250	1.00001	.00250
6	.00000	.00300	.00300	.00001	.00300
7	.00001	.00350	.00350	.00001	.00350
8	.00001	.00400	.00400	.00002	.00400
9	.00001	.00450	.00450	.00002	.00450
.010	1.00001	0.00500	.00500	1.00002	.00500
1	.00002	.00550	.00550	.00003	.00550
2	.00002	.00600	.00600	.00004	.00600
3	.00002	.00650	.00650	.00004	.00650
4	.00002	.00700	.00700	.00005	.00700
.015	1.00003	0.00750	.00750	1.00006	.00750
6	.00003	.00800	.00800	.00006	.00800
7	.00004	.00850	.00850	.00007	.00850
8	.00004	.00900	.00900	.00008	.00900
9	.00005	.00950	.00950	.00009	.00950
.020	1.00005	0.01000	.01000	1.00010	.01000
1	.00006	.01050	.01050	.00011	.01050
2	.00006	.01100	.01100	.00012	.01100
3	.00007	.01150	.01150	.00013	.01150
4	.00007	.01200	.01200	.00014	.01200
.025	1.00008	0.01250	.01250	1.00016	.01250
6	.00008	.01300	.01300	.00017	.01300
7	.00009	.01350	.01350	.00018	.01350
8	.00010	.01400	.01400	.00020	.01400
9	.00011	.01450	.01450	.00021	.01450
.030	1.00011	0.01500	.01500	1.00022	.01500
1	.00012	.01550	.01550	.00024	.01550
2	.00013	.01600	.01600	.00026	.01599
3	.00014	.01650	.01650	.00027	.01649
4	.00014	.01700	.01700	.00029	.01699
.035	1.00015	0.01750	.01749	1.00031	.01749
6	.00016	.01800	.01799	.00032	.01799
7	.00017	.01850	.01849	.00034	.01849
8	.00018	.01900	.01899	.00036	.01899
9	.00019	.01950	.01949	.00038	.01949
.040	1.00020	0.02000	.01999	1.00040	.01999
1	.00021	.02050	.02049	.00042	.02049
2	.00022	.02100	.02099	.00044	.02099
3	.00023	.02150	.02149	.00046	.02149
4	.00024	.02199	.02199	.00048	.02199
.045	1.00025	0.02249	.02249	1.00051	.02248
6	.00026	.02299	.02299	.00053	.02298
7	.00028	.02349	.02349	.00055	.02348
8	.00029	.02399	.02399	.00058	.02398
9	.00030	.02449	.02449	.00060	.02448

p	f(p)	g(p)	$\dfrac{g(p)}{f(p)}$	$|S|$	θ
.050	1.00031	0.02499	.02498	1.00062	.02498
1	.00032	.02549	.02548	.00065	.02548
2	.00034	.02599	.02598	.00068	.02598
3	.00035	.02649	.02648	.00070	.02648
4	.00036	.02699	.02698	.00073	.02697
.055	1.00038	0.02749	.02748	1.00076	.02747
6	.00039	.02799	.02798	.00078	.02797
7	.00041	.02849	.02848	.00081	.02847
8	.00042	.02899	.02898	.00084	.02897
9	.00043	.02949	.02947	.00087	.02947
.060	1.00045	0.02999	.02997	1.00090	.02996
1	.00046	.03049	.03047	.00093	.03046
2	.00048	.03099	.03097	.00096	.03096
3	.00050	.03148	.03147	.00099	.03146
4	.00051	.03198	.03197	.00102	.03196
.065	1.00053	0.03248	.03247	1.00105	.03245
6	.00054	.03298	.03296	.00109	.03295
7	.00056	.03348	.03346	.00112	.03345
8	.00058	.03398	.03396	.00115	.03395
9	.00059	.03448	.03446	.00119	.03445
.070	1.00061	0.03498	.03496	1.00122	.03494
1	.00063	.03548	.03546	.00126	.03544
2	.00065	.03598	.03595	.00129	.03594
3	.00067	.03648	.03645	.00133	.03644
4	.00068	.03697	.03695	.00137	.03693
.075	1.00070	0.03747	.03745	1.00140	.03743
6	.00072	.03797	.03795	.00144	.03793
7	.00074	.03847	.03844	.00148	.03842
8	.00076	.03897	.03894	.00152	.03892
9	.00078	.03947	.03944	.00156	.03942
.080	1.00080	0.03997	.03994	1.00160	.03992
1	.00082	.04047	.04043	.00164	.04041
2	.00084	.04097	.04093	.00168	.04091
3	.00086	.04146	.04143	.00172	.04141
4	.00088	.04196	.04193	.00176	.04190
.085	1.00090	0.04246	.04242	1.00180	.04240
6	.00092	.04296	.04292	.00184	.04289
7	.00094	.04346	.04342	.00189	.04339
8	.00097	.04396	.04392	.00193	.04389
9	.00099	.04446	.04441	.00197	.04438
.090	1.00101	0.04495	.04491	1.00202	.04488
1	.00103	.04545	.04541	.00206	.04538
2	.00106	.04595	.04590	.00211	.04587
3	.00108	.04645	.04640	.00216	.04637
4	.00110	.04695	.04690	.00220	.04686
.095	1.00112	0.04745	.04739	1.00225	.04736
6	.00115	.04794	.04789	.00230	.04785
7	.00117	.04844	.04839	.00234	.04835
8	.00120	.04894	.04888	.00239	.04884
9	.00122	.04944	.04938	.00244	.04934

TABLE 3

$0.00 \leq p \leq 0.99$ in steps of 0.01

p	f(p)	g(p)	$\dfrac{g(p)}{f(p)}$	|S|	θ
.00	1.00000	0.00000	.00000	1.00000	.00000
1	.00001	.00500	.00500	.00002	.00500
2	.00005	.01000	.01000	.00010	.01000
3	.00011	.01500	.01500	.00022	.01500
4	.00020	.02000	.01999	.00040	.01999
.05	1.00031	0.02499	.02498	1.00062	.02498
6	.00045	.02999	.02997	.00090	.02996
7	.00061	.03498	.03496	.00122	.03494
8	.00080	.03997	.03994	.00160	.03992
9	.00101	.04495	.04491	.00202	.04488
.10	1.00125	0.04994	.04988	1.00249	.04983
1	.00151	.05492	.05483	.00301	.05478
2	.00179	.05989	.05979	.00358	.05971
3	.00210	.06486	.06473	.00420	.06464
4	.00244	.06983	.06966	.00486	.06955
.15	1.00279	0.07479	.07458	1.00558	.07444
6	.00317	.07975	.07949	.00634	.07933
7	.00358	.08470	.08439	.00715	.08420
8	.00401	.08964	.08928	.00800	.08905
9	.00446	.09458	.09416	.00891	.09388
.20	1.00494	0.09951	.09902	1.00985	.09870
1	.00544	.10443	.10387	.01085	.10350
2	.00596	.10935	.10870	.01189	.10828
3	.00651	.11426	.11352	.01297	.11303
4	.00707	.11916	.11832	.01410	.11777
.25	1.00766	0.12405	.12311	1.01527	.12249
6	.00828	.12893	.12787	.01649	.12718
7	.00891	.13381	.13263	.01775	.13186
8	.00957	.13867	.13736	.01905	.13650
9	.01025	.14353	.14207	.02039	.14113
.30	1.01095	0.14838	.14677	1.02178	.14573
1	.01167	.15321	.15144	.02320	.15030
2	.01241	.15804	.15610	.02467	.15485
3	.01317	.16285	.16074	.02618	.15937
4	.01396	.16766	.16535	.02773	.16387
.35	1.01476	0.17245	.16995	1.02931	.16834
6	.01559	.17724	.17452	.03093	.17278
7	.01643	.18201	.17907	.03260	.17719
8	.01729	.18677	.18360	.03430	.18157
9	.01817	.19152	.18810	.03603	.18593
.40	1.01908	0.19626	.19258	1.03780	.19025
1	.02000	.20098	.19704	.03961	.19455
2	.02094	.20569	.20148	.04145	.19881
3	.02189	.21039	.20589	.04333	.20305
4	.02287	.21508	.21027	.04524	.20725
.45	1.02386	0.21976	.21463	1.04718	.21143
6	.02487	.22442	.21897	.04916	.21557
7	.02590	.22907	.22328	.05116	.21968
8	.02695	.23370	.22757	.05320	.22376
9	.02801	.23833	.23183	.05527	.22781

p	f(p)	g(p)	$\dfrac{g(p)}{f(p)}$	|S|	θ
.50	1.02909	0.24293	.23607	1.05737	.23182
1	.03018	.24753	.24028	.05950	.23581
2	.03129	.25211	.24446	.06166	.23976
3	.03242	.25668	.24862	.06385	.24368
4	.03356	.26123	.25275	.06606	.24757
.55	1.03472	0.26577	.25686	1.06830	.25142
6	.03589	.27030	.26094	.07057	.25524
7	.03707	.27481	.26499	.07287	.25903
8	.03827	.27931	.26901	.07519	.26279
9	.03949	.28379	.27301	.07753	.26652
.60	1.04072	0.28826	.27698	1.07990	.27021
1	.04196	.29272	.28093	.08230	.27387
2	.04322	.29716	.28485	.08471	.27750
3	.04449	.30158	.28874	.08715	.28109
4	.04577	.30599	.29260	.08962	.28466
.65	1.04706	0.31039	.29644	1.09210	.28819
6	.04837	.31477	.30025	.09461	.29169
7	.04969	.31914	.30403	.09713	.29515
8	.05102	.32349	.30779	.09968	.29859
9	.05237	.32783	.31152	.10225	.30199
.70	1.05372	0.33216	.31522	1.10483	.30536
1	.05509	.33647	.31890	.10744	.30870
2	.05646	.34076	.32255	.11006	.31201
3	.05785	.34504	.32617	.11270	.31529
4	.05925	.34930	.32976	.11536	.31854
.75	1.06066	0.35355	.33333	1.11803	.32175
6	.06208	.35779	.33688	.12073	.32494
7	.06351	.36201	.34039	.12343	.32809
8	.06495	.36622	.34388	.12616	.33121
9	.06640	.37041	.34734	.12889	.33431
.80	1.06785	0.37458	.35078	1.13165	.33737
1	.06932	.37874	.35419	.13441	.34040
2	.07080	.38289	.35758	.13720	.34341
3	.07228	.38703	.36094	.13999	.34638
4	.07378	.39114	.36427	.14280	.34933
.85	1.07528	0.39525	.36758	1.14562	.35225
6	.07679	.39934	.37086	.14845	.35514
7	.07830	.40341	.37412	.15130	.35800
8	.07983	.40747	.37735	.15415	.36083
9	.08136	.41152	.38055	.15702	.36363
.90	1.08290	0.41555	.38374	1.15990	.36641
1	.08445	.41957	.38689	.16279	.36916
2	.08601	.42357	.39003	.16569	.37188
3	.08757	.42756	.39313	.16859	.37457
4	.08914	.43153	.39622	.17151	.37724
.95	1.09071	0.43549	.39928	1.17444	.37988
6	.09230	.43944	.40231	.17738	.38250
7	.09388	.44337	.40532	.18032	.38509
8	.09548	.44729	.40831	.18328	.38765
9	.09708	.45120	.41127	.18624	.39019

TABLE 4

$0.0 \leq p \leq 99.9$ in steps of 0.1

p	f(p)	g(p)	$\frac{g(p)}{f(p)}$	|S|	θ
0.0	1.00000	0.00000	.00000	1.00000	.00000
1	.00125	.04994	.04988	.00249	.04983
2	.00494	.09951	.09902	.00985	.09870
3	.01095	.14838	.14677	.02178	.14573
4	.01908	.19626	.19258	.03780	.19025
0.5	1.02909	0.24293	.23607	1.05737	.23182
6	.04072	.28826	.27698	.07990	.27021
7	.05372	.33216	.31522	.10483	.30536
8	.06785	.37458	.35078	.13165	.33737
9	.08290	.41555	.38374	.15990	.36641
1.0	1.09868	0.45509	.41421	1.18921	.39270
1	.11504	.49326	.44237	.21926	.41649
2	.13182	.53012	.46837	.24982	.43803
3	.14894	.56574	.49240	.28067	.45755
4	.16629	.60019	.51462	.31166	.47527
1.5	1.18380	0.63355	.53518	1.34267	.49140
6	.20142	.66588	.55425	.37361	.50610
7	.21908	.69725	.57195	.40439	.51954
8	.23676	.72771	.58840	.43497	.53185
9	.25441	.75733	.60373	.46530	.54316
2.0	1.27202	0.78615	.61803	1.49535	.55357
1	.28956	.81423	.63140	.52510	.56319
2	.30702	.84161	.64391	.55454	.57208
3	.32438	.86833	.65565	.58366	.58033
4	.34164	.89443	.66667	.61245	.58800
2.5	1.35878	0.91994	.67703	1.64091	.59514
6	.37580	.94490	.68680	.66903	.60181
7	.39270	.96934	.69601	.69683	.60805
8	.40947	.99328	.70472	.72430	.61389
9	.42611	1.01675	.71296	.75145	.61937
3.0	1.44262	1.03978	.72076	1.77828	.62452
1	.45899	.06238	.72816	.80480	.62938
2	.47523	.08458	.73519	.83101	.63396
3	.49134	.10639	.74188	.85693	.63828
4	.50732	.12783	.74824	.88255	.64237
3.5	1.52316	1.14892	.75430	1.90789	.64625
6	.53888	.16968	.76009	.93295	.64992
7	.55447	.19012	.76561	.95774	.65342
8	.56993	.21024	.77089	.98227	.65674
9	.58527	.23007	.77594	2.00653	.65990
4.0	1.60049	1.24962	.78078	2.03054	.66291
1	.61558	.26890	.78541	.05431	.66578
2	.63055	.28791	.78986	.07784	.66853
3	.64541	.30667	.79413	.10113	.67115
4	.66015	.32518	.79823	.12420	.67366
4.5	1.67478	1.34346	.80217	2.14704	.67606
6	.68930	.36151	.80597	.16966	.67837
7	.70370	.37935	.80962	.19208	.68058
8	.71800	.39697	.81314	.21429	.68270
9	.73220	.41439	.81653	.23629	.68474

p	f(p)	g(p)	$\dfrac{g(p)}{f(p)}$	|S|	θ
5.0	1.74628	1.43161	.81980	2.25810	.68670
1	.76027	.44864	.82296	.27972	.68859
2	.77416	.46548	.82602	.30115	.69040
3	.78795	.48215	.82897	.32239	.69215
4	.80164	.49863	.83182	.34346	.69384
5.5	1.81524	1.51495	.83458	2.36435	.69547
6	.82874	.53111	.83725	.38508	.69704
7	.84215	.54710	.83983	.40563	.69856
8	.85548	.56294	.84234	.42602	.70003
9	.86871	.57863	.84477	.44625	.70145
6.0	1.88186	1.59417	.84713	2.46633	.70282
1	.89492	.60957	.84941	.48625	.70415
2	.90790	.62483	.85163	.50602	.70544
3	.92079	.63995	.85379	.52564	.70669
4	.93360	.65494	.85588	.54512	.70790
6.5	1.94634	1.66980	.85792	2.56446	.70907
6	.95900	.68454	.85990	.58367	.71021
7	.97157	.69915	.86182	.60273	.71132
8	.98408	.71364	.86370	.62167	.71239
9	.99651	.72802	.86552	.64047	.71344
7.0	2.00886	1.74228	.86730	2.65915	.71445
1	.02115	.75643	.86902	.67770	.71544
2	.03336	.77047	.87071	.69613	.71640
3	.04550	.78440	.87235	.71444	.71733
4	.05758	.79823	.87395	.73263	.71824
7.5	2.06959	1.81196	.87552	2.75070	.71912
6	.08153	.82558	.87704	.76867	.71998
7	.09340	.83911	.87853	.78651	.72082
8	.10521	.85254	.87998	.80425	.72164
9	.11696	.86588	.88140	.82189	.72244
8.0	2.12864	1.87913	.88278	2.83941	.72322
1	.14027	.89229	.88414	.85683	.72398
2	.15183	.90535	.88546	.87415	.72472
3	.16333	.91834	.88675	.89137	.72545
4	.17478	.93123	.88801	.90849	.72615
8.5	2.18616	1.94404	.88925	2.92551	.72684
6	.19749	.95678	.89046	.94244	.72752
7	.20876	.96943	.89164	.95927	.72818
8	.21998	.98200	.89280	.97601	.72882
9	.23114	.99449	.89393	.99266	.72945
9.0	2.24225	2.00691	.89504	3.00922	.73007
1	.25331	.01925	.89613	.02569	.73067
2	.26431	.03153	.89719	.04207	.73126
3	.27526	.04372	.89824	.05837	.73184
4	.28616	.05585	.89926	.07458	.73241
9.5	2.29701	2.06791	.90026	3.09071	.73296
6	.30781	.07990	.90124	.10676	.73350
7	.31856	.09182	.90221	.12272	.73403
8	.32926	.10367	.90315	.13861	.73455
9	.33991	.11546	.90408	.15442	.73506

p	f(p)	g(p)	$\dfrac{g(p)}{f(p)}$	|S|	θ
10.0	2.35052	2.12719	.90499	3.17015	.73556
1	.36108	.13885	.90588	.18581	.73605
2	.37159	.15045	.90676	.20139	.73653
3	.38206	.16199	.90761	.21690	.73701
4	.39248	.17347	.90846	.23233	.73747
10.5	2.40286	2.18489	.90929	3.24769	.73792
6	.41320	.19625	.91010	.26298	.73837
7	.42349	.20756	.91090	.27820	.73880
8	.43374	.21881	.91168	.29336	.73923
9	.44395	.23000	.91246	.30844	.73965
11.0	2.45411	2.24113	.91321	3.32346	.74007
1	.46424	.25222	.91396	.33841	.74047
2	.47432	.26324	.91469	.35329	.74087
3	.48437	.27422	.91541	.36811	.74127
4	.49437	.28515	.91612	.38286	.74165
11.5	2.50434	2.29602	.91682	3.39756	.74203
6	.51426	.30684	.91750	.41219	.74240
7	.52415	.31761	.91818	.42676	.74277
8	.53400	.32834	.91884	.44126	.74313
9	.54381	.33901	.91949	.45571	.74348
12.0	2.55359	2.34964	.92013	3.47010	.74383
1	.56332	.36022	.92076	.48443	.74417
2	.57302	.37075	.92139	.49870	.74451
3	.58269	.38124	.92200	.51292	.74484
4	.59232	.39168	.92260	.52707	.74516
12.5	2.60192	2.40208	.92319	3.54118	.74548
6	.61148	.41243	.92378	.55522	.74580
7	.62100	.42274	.92436	.56922	.74611
8	.63049	.43300	.92492	.58316	.74641
9	.63995	.44323	.92548	.59704	.74672
13.0	2.64938	2.45341	.92603	3.61087	.74701
1	.65877	.46355	.92657	.62465	.74730
2	.66813	.47364	.92711	.63838	.74759
3	.67746	.48370	.92763	.65206	.74787
4	.68675	.49372	.92815	.66569	.74815
13.5	2.69601	2.50370	.92867	3.67926	.74843
6	.70525	.51363	.92917	.69279	.74870
7	.71445	.52353	.92967	.70627	.74897
8	.72362	.53340	.93016	.71970	.74923
9	.73276	.54322	.93064	.73309	.74949
14.0	2.74187	2.55300	.93112	3.74642	.74974
1	.75095	.56275	.93159	.75971	.75000
2	.76000	.57247	.93205	.77295	.75024
3	.76902	.58214	.93251	.78615	.75049
4	.77801	.59178	.93296	.79930	.75073
14.5	2.78697	2.60139	.93341	3.81241	.75097
6	.79591	.61096	.93385	.82547	.75120
7	.80481	.62049	.93428	.83849	.75144
8	.81369	.62999	.93471	.85146	.75167
9	.82254	.63946	.93514	.86439	.75189

p	f(p)	g(p)	$\frac{g(p)}{f(p)}$	|S|	θ
15.0	2.83137	2.64890	.93555	3.87728	.75211
1	.84017	.65830	.93597	.89013	.75233
2	.84893	.66766	.93637	.90293	.75255
3	.85768	.67700	.93677	.91569	.75276
4	.86639	.68630	.93717	.92841	.75298
15.5	2.87508	2.69557	.93756	3.94109	.75318
6	.88375	.70481	.93795	.95373	.75339
7	.89239	.71402	.93833	.96634	.75359
8	.90100	.72320	.93871	.97890	.75379
9	.90959	.73234	.93908	.99142	.75399
16.0	2.91815	2.74146	.93945	4.00390	.75419
1	.92669	.75055	.93982	.01634	.75438
2	.93520	.75960	.94018	.02875	.75457
3	.94369	.76863	.94053	.04112	.75476
4	.95216	.77763	.94088	.05345	.75495
16.5	2.96060	2.78660	.94123	4.06574	.75513
6	.96901	.79554	.94157	.07800	.75531
7	.97741	.80445	.94191	.09022	.75549
8	.98578	.81334	.94225	.10241	.75567
9	.99412	.82219	.94258	.11455	.75585
17.0	3.00245	2.83102	.94291	4.12667	.75602
1	.01075	.83983	.94323	.13875	.75619
2	.01903	.84860	.94355	.15079	.75636
3	.02728	.85735	.94387	.16280	.75653
4	.03552	.86607	.94418	.17477	.75669
17.5	3.04373	2.87477	.94449	4.18671	.75686
6	.05192	.88343	.94479	.19862	.75702
7	.06008	.89208	.94510	.21049	.75718
8	.06823	.90070	.94540	.22233	.75734
9	.07635	.90929	.94569	.23414	.75749
18.0	3.08446	2.91786	.94599	4.24591	.75765
1	.09254	.92640	.94628	.25765	.75780
2	.10060	.93491	.94656	.26936	.75795
3	.10864	.94341	.94685	.28104	.75810
4	.11666	.95188	.94713	.29269	.75825
18.5	3.12466	2.96032	.94741	4.30430	.75840
6	.13264	.96874	.94768	.31588	.75854
7	.14060	.97714	.94795	.32744	.75869
8	.14854	.98551	.94822	.33896	.75883
9	.15646	.99386	.94849	.35045	.75897
19.0	3.16436	3.00219	.94875	4.36191	.75911
1	.17224	.01049	.94901	.37335	.75924
2	.18010	.01878	.94927	.38475	.75938
3	.18794	.02704	.94953	.39612	.75951
4	.19576	.03527	.94978	.40747	.75965
19.5	3.20356	3.04349	.95003	4.41878	.75978
6	.21135	.05168	.95028	.43007	.75991
7	.21911	.05985	.95053	.44132	.76004
8	.22686	.06800	.95077	.45255	.76017
9	.23459	.07613	.95101	.46376	.76029

p	f(p)	g(p)	$\frac{g(p)}{f(p)}$	|S|	θ
20.0	3.24230	3.08423	.95125	4.47493	.76042
1	.24999	.09232	.95149	.48607	.76054
2	.25766	.10038	.95172	.49719	.76067
3	.26532	.10843	.95195	.50828	.76079
4	.27296	.11645	.95218	.51935	.76091
20.5	3.28058	3.12445	.95241	4.53038	.76103
6	.28818	.13243	.95263	.54139	.76115
7	.29577	.14039	.95286	.55238	.76126
8	.30333	.14833	.95308	.56333	.76138
9	.31088	.15626	.95330	.57427	.76149
21.0	3.31842	3.16416	.95351	4.58517	.76161
1	.32593	.17204	.95373	.59605	.76172
2	.33343	.17990	.95394	.60690	.76183
3	.34092	.18775	.95415	.61773	.76194
4	.34838	.19557	.95436	.62854	.76205
21.5	3.35583	3.20338	.95457	4.63931	.76216
6	.36327	.21116	.95477	.65007	.76227
7	.37068	.21893	.95498	.66080	.76237
8	.37809	.22668	.95518	.67150	.76248
9	.38547	.23441	.95538	.68218	.76258
22.0	3.39284	3.24212	.95558	4.69284	.76269
1	.40019	.24982	.95577	.70347	.76279
2	.40753	.25749	.95597	.71408	.76289
3	.41485	.26515	.95616	.72466	.76299
4	.42216	.27279	.95635	.73522	.76309
22.5	3.42945	3.28041	.95654	4.74576	.76319
6	.43672	.28802	.95673	.75627	.76329
7	.44398	.29560	.95692	.76676	.76339
8	.45123	.30317	.95710	.77723	.76348
9	.45846	.31073	.95728	.78767	.76358
23.0	3.46567	3.31826	.95747	4.79810	.76367
1	.47287	.32578	.95765	.80850	.76377
2	.48005	.33328	.95783	.81887	.76386
3	.48722	.34077	.95800	.82923	.76395
4	.49438	.34824	.95818	.83956	.76404
23.5	3.50152	3.35569	.95835	4.84987	.76413
6	.50864	.36312	.95852	.86016	.76422
7	.51576	.37054	.95870	.87043	.76431
8	.52285	.37794	.95887	.88068	.76440
9	.52994	.38533	.95903	.89090	.76449
24.0	3.53701	3.39270	.95920	4.90110	.76458
1	.54406	.40005	.95937	.91129	.76466
2	.55110	.40739	.95953	.92145	.76475
3	.55813	.41472	.95969	.93159	.76483
4	.56514	.42202	.95986	.94171	.76492
24.5	3.57214	3.42931	.96002	4.95181	.76500
6	.57913	.43659	.96018	.96189	.76508
7	.58610	.44385	.96033	.97194	.76517
8	.59306	.45110	.96049	.98198	.76525
9	.60000	.45833	.96065	.99200	.76533

p	f(p)	g(p)	$\dfrac{g(p)}{f(p)}$	|S|	θ
25.0	3.60694	3.46554	.96080	5.00200	.76541
1	.61386	.47274	.96095	.01198	.76549
2	.62076	.47993	.96110	.02194	.76557
3	.62765	.48710	.96126	.03187	.76565
4	.63453	.49426	.96140	.04179	.76572
25.5	3.64140	3.50140	.96155	5.05169	.76580
6	.64825	.50853	.96170	.06157	.76588
7	.65510	.51564	.96185	.07143	.76595
8	.66192	.52274	.96199	.08128	.76603
9	.66874	.52982	.96214	.09110	.76610
26.0	3.67554	3.53689	.96228	5.10090	.76618
1	.68233	.54395	.96242	.11069	.76625
2	.68911	.55099	.96256	.12046	.76632
3	.69588	.55802	.96270	.13021	.76640
4	.70263	.56503	.96284	.13994	.76647
26.5	3.70937	3.57203	.96298	5.14965	.76654
6	.71610	.57902	.96311	.15934	.76661
7	.72282	.58599	.96325	.16902	.76668
8	.72952	.59295	.96338	.17867	.76675
9	.73621	.59990	.96352	.18831	.76682
27.0	3.74289	3.60683	.96365	5.19793	.76689
1	.74956	.61375	.96378	.20754	.76696
2	.75622	.62066	.96391	.21712	.76702
3	.76287	.62755	.96404	.22669	.76709
4	.76950	.63444	.96417	.23624	.76716
27.5	3.77612	3.64130	.96430	5.24578	.76722
6	.78273	.64816	.96442	.25529	.76729
7	.78933	.65500	.96455	.26479	.76736
8	.79592	.66183	.96468	.27428	.76742
9	.80249	.66865	.96480	.28374	.76748
28.0	3.80906	3.67545	.96492	5.29319	.76755
1	.81561	.68224	.96505	.30262	.76761
2	.82215	.68902	.96517	.31204	.76768
3	.82869	.69579	.96529	.32143	.76774
4	.83521	.70254	.96541	.33082	.76780
28.5	3.84171	3.70928	.96553	5.34018	.76786
6	.84821	.71601	.96565	.34953	.76792
7	.85470	.72273	.96576	.35886	.76798
8	.86118	.72943	.96588	.36818	.76804
9	.86764	.73613	.96600	.37748	.76810
29.0	3.87410	3.74281	.96611	5.38676	.76816
1	.88054	.74948	.96623	.39603	.76822
2	.88697	.75614	.96634	.40529	.76828
3	.89340	.76278	.96645	.41452	.76834
4	.89981	.76942	.96656	.42374	.76840
29.5	3.90621	3.77604	.96668	5.43295	.76846
6	.91260	.78265	.96679	.44214	.76851
7	.91898	.78925	.96690	.45131	.76857
8	.92535	.79584	.96701	.46047	.76863
9	.93171	.80241	.96711	.46962	.76868

p	f(p)	g(p)	$\frac{g(p)}{f(p)}$	$|S|$	θ
30.0	3.93806	3.80898	.96722	5.47875	.76874
1	.94440	.81553	.96733	.48786	.76879
2	.95073	.82208	.96744	.49696	.76885
3	.95705	.82861	.96754	.50604	.76890
4	.96336	.83513	.96765	.51511	.76896
30.5	3.96966	3.84164	.96775	5.52416	.76901
6	.97595	.84814	.96785	.53320	.76906
7	.98223	.85463	.96796	.54223	.76912
8	.98850	.86110	.96806	.55124	.76917
9	.99476	.86757	.96816	.56023	.76922
31.0	4.00101	3.87402	.96826	5.56921	.76927
1	.00725	.88047	.96836	.57818	.76933
2	.01348	.88690	.96846	.58713	.76938
3	.01970	.89333	.96856	.59607	.76943
4	.02591	.89974	.96866	.60499	.76948
31.5	4.03211	3.90614	.96876	5.61390	.76953
6	.03831	.91253	.96886	.62279	.76958
7	.04449	.91891	.96895	.63168	.76963
8	.05066	.92528	.96905	.64054	.76968
9	.05683	.93165	.96914	.64940	.76973
32.0	4.06298	3.93800	.96924	5.65823	.76978
1	.06913	.94434	.96933	.66706	.76983
2	.07526	.95067	.96943	.67587	.76988
3	.08139	.95699	.96952	.68467	.76992
4	.08751	.96330	.96961	.69345	.76997
32.5	4.09362	3.96960	.96970	5.70223	.77002
6	.09972	.97589	.96980	.71098	.77007
7	.10581	.98217	.96989	.71973	.77011
8	.11189	.98844	.96998	.72846	.77016
9	.11796	.99470	.97007	.73718	.77021
33.0	4.12402	4.00095	.97016	5.74588	.77025
1	.13008	.00719	.97024	.75457	.77030
2	.13612	.01342	.97033	.76325	.77034
3	.14216	.01964	.97042	.77192	.77039
4	.14819	.02585	.97051	.78057	.77043
33.5	4.15421	4.03205	.97059	5.78921	.77048
6	.16022	.03825	.97068	.79783	.77052
7	.16622	.04443	.97077	.80645	.77057
8	.17222	.05060	.97085	.81505	.77061
9	.17820	.05677	.97094	.82364	.77065
34.0	4.18418	4.06292	.97102	5.83221	.77070
1	.19015	.06907	.97110	.84078	.77074
2	.19611	.07521	.97119	.84933	.77078
3	.20206	.08133	.97127	.85786	.77083
4	.20800	.08745	.97135	.86639	.77087
34.5	4.21393	4.09356	.97143	5.87490	.77091
6	.21986	.09966	.97152	.88340	.77095
7	.22578	.10575	.97160	.89189	.77099
8	.23169	.11183	.97168	.90037	.77103
9	.23759	.11791	.97176	.90883	.77108

p	f(p)	g(p)	$\dfrac{g(p)}{f(p)}$	|S|	θ
35.0	4.24348	4.12397	.97184	5.91729	.77112
1	.24937	.13003	.97192	.92573	.77116
2	.25524	.13607	.97199	.93416	.77120
3	.26111	.14211	.97207	.94257	.77124
4	.26697	.14814	.97215	.95098	.77128
35.5	4.27283	4.15416	.97223	5.95937	.77132
6	.27867	.16017	.97230	.96775	.77136
7	.28451	.16617	.97238	.97612	.77140
8	.29034	.17217	.97246	.98448	.77144
9	.29616	.17815	.97253	.99282	.77147
36.0	4.30197	4.18413	.97261	6.00116	.77151
1	.30777	.19010	.97268	.00948	.77155
2	.31357	.19606	.97276	.01779	.77159
3	.31936	.20201	.97283	.02609	.77163
4	.32514	.20795	.97290	.03438	.77167
36.5	4.33092	4.21389	.97298	6.04266	.77170
6	.33668	.21981	.97305	.05092	.77174
7	.34244	.22573	.97312	.05918	.77178
8	.34819	.23164	.97320	.06742	.77181
9	.35394	.23754	.97327	.07565	.77185
37.0	4.35967	4.24344	.97334	6.08387	.77189
1	.36540	.24932	.97341	.09208	.77192
2	.37112	.25520	.97348	.10028	.77196
3	.37684	.26107	.97355	.10847	.77200
4	.38254	.26693	.97362	.11665	.77203
37.5	4.38824	4.27278	.97369	6.12481	.77207
6	.39393	.27863	.97376	.13297	.77210
7	.39962	.28446	.97383	.14111	.77214
8	.40529	.29029	.97389	.14925	.77217
9	.41096	.29611	.97396	.15737	.77221
38.0	4.41663	4.30193	.97403	6.16548	.77224
1	.42228	.30773	.97410	.17358	.77228
2	.42793	.31353	.97416	.18167	.77231
3	.43357	.31932	.97423	.18975	.77235
4	.43920	.32510	.97430	.19782	.77238
38.5	4.44483	4.33088	.97436	6.20588	.77241
6	.45045	.33664	.97443	.21393	.77245
7	.45606	.34240	.97449	.22197	.77248
8	.46166	.34815	.97456	.23000	.77251
9	.46726	.35390	.97462	.23802	.77255
39.0	4.47285	4.35963	.97469	6.24602	.77258
1	.47844	.36536	.97475	.25402	.77261
2	.48401	.37108	.97482	.26201	.77265
3	.48958	.37680	.97488	.26999	.77268
4	.49515	.38250	.97494	.27795	.77271
39.5	4.50070	4.38820	.97500	6.28591	.77274
6	.50625	.39389	.97507	.29386	.77277
7	.51180	.39958	.97513	.30179	.77281
8	.51733	.40526	.97519	.30972	.77284
9	.52286	.41093	.97525	.31764	.77287

p	f(p)	g(p)	$\dfrac{g(p)}{f(p)}$	|S|	θ
40.0	4.52838	4.41659	.97531	6.32554	.77290
1	.53390	.42224	.97537	.33344	.77293
2	.53941	.42789	.97543	.34133	.77296
3	.54491	.43353	.97549	.34920	.77299
4	.55041	.43917	.97555	.35707	.77302
40.5	4.55589	4.44479	.97561	6.36493	.77305
6	.56138	.45041	.97567	.37278	.77309
7	.56685	.45602	.97573	.38062	.77312
8	.57232	.46163	.97579	.38845	.77315
9	.57778	.46723	.97585	.39627	.77318
41.0	4.58324	4.47282	.97591	6.40408	.77321
1	.58869	.47840	.97597	.41188	.77324
2	.59413	.48398	.97602	.41967	.77326
3	.59957	.48955	.97608	.42745	.77329
4	.60500	.49511	.97614	.43522	.77332
41.5	4.61043	4.50067	.97619	6.44298	.77335
6	.61584	.50622	.97625	.45074	.77338
7	.62125	.51176	.97631	.45848	.77341
8	.62666	.51730	.97636	.46622	.77344
9	.63206	.52283	.97642	.47394	.77347
42.0	4.63745	4.52835	.97647	6.48166	.77350
1	.64284	.53387	.97653	.48937	.77352
2	.64822	.53937	.97658	.49706	.77355
3	.65359	.54488	.97664	.50475	.77358
4	.65896	.55037	.97669	.51243	.77361
42.5	4.66432	4.55586	.97675	6.52010	.77364
6	.66968	.56134	.97680	.52777	.77366
7	.67502	.56682	.97685	.53542	.77369
8	.68037	.57229	.97691	.54306	.77372
9	.68570	.57775	.97696	.55070	.77375
43.0	4.69104	4.58321	.97701	6.55832	.77377
1	.69636	.58866	.97707	.56594	.77380
2	.70168	.59410	.97712	.57355	.77383
3	.70699	.59954	.97717	.58115	.77385
4	.71230	.60497	.97722	.58874	.77388
43.5	4.71760	4.61040	.97728	6.59632	.77391
6	.72289	.61581	.97733	.60390	.77393
7	.72818	.62122	.97738	.61146	.77396
8	.73347	.62663	.97743	.61902	.77398
9	.73874	.63203	.97748	.62657	.77401
44.0	4.74402	4.63742	.97753	6.63411	.77404
1	.74928	.64281	.97758	.64164	.77406
2	.75454	.64819	.97763	.64916	.77409
3	.75979	.65356	.97768	.65667	.77411
4	.76504	.65893	.97773	.66418	.77414
44.5	4.77028	4.66429	.97778	6.67167	.77416
6	.77552	.66965	.97783	.67916	.77419
7	.78075	.67500	.97788	.68664	.77421
8	.78598	.68034	.97793	.69411	.77424
9	.79120	.68568	.97798	.70158	.77426

p	f(p)	g(p)	$\dfrac{g(p)}{f(p)}$	$\lvert S \rvert$	θ
45.0	4.79641	4.69101	.97802	6.70903	.77429
1	.80162	.69633	.97807	.71648	.77431
2	.80682	.70165	.97812	.72392	.77434
3	.81202	.70696	.97817	.73135	.77436
4	.81721	.71227	.97822	.73877	.77439
45.5	4.82239	4.71757	.97826	6.74618	.77441
6	.82758	.72287	.97831	.75359	.77444
7	.83275	.72816	.97836	.76099	.77446
8	.83792	.73344	.97840	.76838	.77448
9	.84308	.73872	.97845	.77576	.77451
46.0	4.84824	4.74399	.97850	6.78313	.77453
1	.85339	.74925	.97854	.79050	.77455
2	.85854	.75451	.97859	.79785	.77458
3	.86368	.75977	.97863	.80520	.77460
4	.86882	.76502	.97868	.81255	.77462
46.5	4.87395	4.77026	.97873	6.81988	.77465
6	.87907	.77550	.97877	.82720	.77467
7	.88419	.78073	.97882	.83452	.77469
8	.88931	.78595	.97886	.84183	.77472
9	.89442	.79117	.97891	.84914	.77474
47.0	4.89952	4.79639	.97895	6.85643	.77476
1	.90462	.80159	.97899	.86372	.77478
2	.90971	.80680	.97904	.87100	.77481
3	.91480	.81199	.97908	.87827	.77483
4	.91989	.81719	.97913	.88553	.77485
47.5	4.92496	4.82237	.97917	6.89279	.77487
6	.93004	.82755	.97921	.90004	.77490
7	.93510	.83273	.97926	.90728	.77492
8	.94016	.83790	.97930	.91451	.77494
9	.94522	.84306	.97934	.92174	.77496
48.0	4.95027	4.84822	.97938	6.92895	.77498
1	.95532	.85337	.97943	.93617	.77500
2	.96036	.85852	.97947	.94337	.77503
3	.96540	.86366	.97951	.95056	.77505
4	.97043	.86880	.97955	.95775	.77507
48.5	4.97546	4.87393	.97959	6.96493	.77509
6	.98048	.87905	.97964	.97211	.77511
7	.98549	.88417	.97968	.97927	.77513
8	.99050	.88929	.97972	.98643	.77515
9	.99551	.89440	.97976	.99358	.77517
49.0	5.00051	4.89950	.97980	7.00073	.77520
1	.00551	.90460	.97984	.00787	.77522
2	.01050	.90969	.97988	.01500	.77524
3	.01548	.91478	.97992	.02212	.77526
4	.02046	.91986	.97996	.02923	.77528
49.5	5.02544	4.92494	.98000	7.03634	.77530
6	.03041	.93001	.98004	.04344	.77532
7	.03538	.93508	.98008	.05054	.77534
8	.04034	.94014	.98012	.05762	.77536
9	.04530	.94520	.98016	.06470	.77538

p	f(p)	g(p)	$\frac{g(p)}{f(p)}$	$\lvert S \rvert$	θ
50.0	5.05025	4.95025	.98020	7.07177	.77540
1	.05519	.95530	.98024	.07884	.77542
2	.06014	.96034	.98028	.08590	.77544
3	.06507	.96538	.98032	.09295	.77546
4	.07001	.97041	.98036	.09999	.77548
50.5	5.07493	4.97543	.98039	7.10703	.77550
6	.07986	.98046	.98043	.11406	.77552
7	.08477	.98547	.98047	.12109	.77554
8	.08969	.99048	.98051	.12810	.77556
9	.09460	.99549	.98055	.13511	.77558
51.0	5.09950	5.00049	.98058	7.14211	.77560
1	.10440	.00549	.98062	.14911	.77561
2	.10929	.01048	.98066	.15610	.77563
3	.11418	.01546	.98070	.16308	.77565
4	.11907	.02044	.98073	.17006	.77567
51.5	5.12395	5.02542	.98077	7.17703	.77569
6	.12882	.03039	.98081	.18399	.77571
7	.13370	.03536	.98084	.19094	.77573
8	.13856	.04032	.98088	.19789	.77575
9	.14342	.04528	.98092	.20483	.77577
52.0	5.14828	5.05023	.98095	7.21177	.77578
1	.15313	.05518	.98099	.21870	.77580
2	.15798	.06012	.98103	.22562	.77582
3	.16283	.06505	.98106	.23253	.77584
4	.16767	.06999	.98110	.23944	.77586
52.5	5.17250	5.07491	.98113	7.24635	.77588
6	.17733	.07984	.98117	.25324	.77589
7	.18216	.08476	.98120	.26013	.77591
8	.18698	.08967	.98124	.26701	.77593
9	.19179	.09458	.98128	.27389	.77595
53.0	5.19661	5.09948	.98131	7.28076	.77597
1	.20141	.10438	.98134	.28762	.77598
2	.20622	.10928	.98138	.29448	.77600
3	.21102	.11417	.98141	.30133	.77602
4	.21581	.11905	.98145	.30817	.77604
53.5	5.22060	5.12393	.98148	7.31501	.77605
6	.22539	.12881	.98152	.32184	.77607
7	.23017	.13368	.98155	.32866	.77609
8	.23494	.13855	.98159	.33548	.77611
9	.23972	.14341	.98162	.34229	.77612
54.0	5.24449	5.14826	.98165	7.34910	.77614
1	.24925	.15312	.98169	.35590	.77616
2	.25401	.15797	.98172	.36269	.77617
3	.25876	.16281	.98175	.36948	.77619
4	.26352	.16765	.98179	.37626	.77621
54.5	5.26826	5.17248	.98182	7.38303	.77622
6	.27300	.17731	.98185	.38980	.77624
7	.27774	.18214	.98189	.39656	.77626
8	.28248	.18696	.98192	.40332	.77628
9	.28721	.19178	.98195	.41007	.77629

p	f(p)	g(p)	$\dfrac{g(p)}{f(p)}$	|S|	θ
55.0	5.29193	5.19659	.98198	7.41681	.77631
1	.29665	.20140	.98202	.42355	.77632
2	.30137	.20620	.98205	.43028	.77634
3	.30608	.21100	.98208	.43700	.77636
4	.31079	.21579	.98211	.44372	.77637
55.5	5.31550	5.22058	.98214	7.45044	.77639
6	.32020	.22537	.98218	.45714	.77641
7	.32489	.23015	.98221	.46384	.77642
8	.32959	.23493	.98224	.47054	.77644
9	.33427	.23970	.98227	.47723	.77645
56.0	5.33896	5.24447	.98230	7.48391	.77647
1	.34364	.24923	.98233	.49059	.77649
2	.34831	.25399	.98236	.49726	.77650
3	.35298	.25875	.98240	.50392	.77652
4	.35765	.26350	.98243	.51058	.77653
56.5	5.36232	5.26825	.98246	7.51724	.77655
6	.36697	.27299	.98249	.52388	.77657
7	.37163	.27773	.98252	.53053	.77658
8	.37628	.28246	.98255	.53716	.77660
9	.38093	.28719	.98258	.54379	.77661
57.0	5.38557	5.29192	.98261	7.55042	.77663
1	.39021	.29664	.98264	.55703	.77664
2	.39485	.30136	.98267	.56365	.77666
3	.39948	.30607	.98270	.57025	.77667
4	.40411	.31078	.98273	.57685	.77669
57.5	5.40873	5.31548	.98276	7.58345	.77670
6	.41335	.32018	.98279	.59004	.77672
7	.41796	.32488	.98282	.59662	.77673
8	.42258	.32957	.98285	.60320	.77675
9	.42718	.33426	.98288	.60977	.77676
58.0	5.43179	5.33894	.98291	7.61634	.77678
1	.43639	.34362	.98294	.62290	.77679
2	.44098	.34830	.98297	.62946	.77681
3	.44557	.35297	.98299	.63601	.77682
4	.45016	.35764	.98302	.64255	.77684
58.5	5.45475	5.36230	.98305	7.64909	.77685
6	.45933	.36696	.98308	.65562	.77687
7	.46390	.37162	.98311	.66215	.77688
8	.46848	.37627	.98314	.66867	.77690
9	.47305	.38091	.98317	.67519	.77691
59.0	5.47761	5.38556	.98319	7.68170	.77692
1	.48217	.39020	.98322	.68820	.77694
2	.48673	.39483	.98325	.69470	.77695
3	.49129	.39946	.98328	.70120	.77697
4	.49584	.40409	.98331	.70769	.77698
59.5	5.50038	5.40872	.98333	7.71417	.77700
6	.50492	.41333	.98336	.72065	.77701
7	.50946	.41795	.98339	.72712	.77702
8	.51400	.42256	.98342	.73359	.77704
9	.51853	.42717	.98344	.74005	.77705

p	f(p)	g(p)	$\dfrac{g(p)}{f(p)}$	|S|	θ
60.0	5.52306	5.43177	.98347	7.74650	.77707
1	.52758	.43637	.98350	.75296	.77708
2	.53210	.44097	.98353	.75940	.77709
3	.53662	.44556	.98355	.76584	.77711
4	.54113	.45015	.98358	.77228	.77712
60.5	5.54564	5.45473	.98361	7.77871	.77713
6	.55015	.45932	.98363	.78513	.77715
7	.55465	.46389	.98366	.79155	.77716
8	.55915	.46847	.98369	.79796	.77718
9	.56364	.47303	.98371	.80437	.77719
61.0	5.56813	5.47760	.98374	7.81077	.77720
1	.57262	.48216	.98377	.81717	.77722
2	.57710	.48672	.98379	.82356	.77723
3	.58158	.49127	.98382	.82995	.77724
4	.58606	.49582	.98385	.83633	.77726
61.5	5.59053	5.50037	.98387	7.84271	.77727
6	.59500	.50491	.98390	.84908	.77728
7	.59947	.50945	.98392	.85545	.77730
8	.60393	.51399	.98395	.86181	.77731
9	.60839	.51852	.98398	.86817	.77732
62.0	5.61285	5.52305	.98400	7.87452	.77733
1	.61730	.52757	.98403	.88087	.77735
2	.62175	.53209	.98405	.88721	.77736
3	.62619	.53661	.98408	.89354	.77737
4	.63063	.54112	.98410	.89987	.77739
62.5	5.63507	5.54563	.98413	7.90620	.77740
6	.63950	.55013	.98415	.91252	.77741
7	.64393	.55464	.98418	.91884	.77742
8	.64836	.55913	.98420	.92515	.77744
9	.65278	.56363	.98423	.93145	.77745
63.0	5.65720	5.56812	.98425	7.93775	.77746
1	.66162	.57261	.98428	.94405	.77747
2	.66604	.57709	.98430	.95034	.77749
3	.67045	.58157	.98433	.95663	.77750
4	.67485	.58605	.98435	.96291	.77751
63.5	5.67925	5.59052	.98438	7.96918	.77752
6	.68365	.59499	.98440	.97545	.77754
7	.68805	.59946	.98442	.98172	.77755
8	.69244	.60392	.98445	.98798	.77756
9	.69683	.60838	.98447	.99424	.77757
64.0	5.70122	5.61283	.98450	8.00049	.77759
1	.70560	.61729	.98452	.00673	.77760
2	.70998	.62173	.98455	.01298	.77761
3	.71436	.62618	.98457	.01921	.77762
4	.71873	.63062	.98459	.02544	.77763
64.5	5.72310	5.63506	.98462	8.03167	.77765
6	.72747	.63949	.98464	.03789	.77766
7	.73183	.64392	.98466	.04411	.77767
8	.73619	.64835	.98469	.05032	.77768
9	.74054	.65277	.98471	.05653	.77769

p	f(p)	g(p)	$\frac{g(p)}{f(p)}$	$\lvert S \rvert$	θ
65.0	5.74490	5.65719	.98473	8.06273	.77771
1	.74925	.66161	.98476	.06893	.77772
2	.75359	.66602	.98478	.07513	.77773
3	.75794	.67043	.98480	.08132	.77774
4	.76228	.67484	.98483	.08750	.77775
65.5	5.76661	5.67924	.98485	8.09368	.77777
6	.77095	.68364	.98487	.09985	.77778
7	.77528	.68804	.98490	.10602	.77779
8	.77960	.69243	.98492	.11219	.77780
9	.78393	.69682	.98494	.11835	.77781
66.0	5.78825	5.70121	.98496	8.12450	.77782
1	.79256	.70559	.98499	.13066	.77783
2	.79688	.70997	.98501	.13680	.77785
3	.80119	.71435	.98503	.14294	.77786
4	.80549	.71872	.98505	.14908	.77787
66.5	5.80980	5.72309	.98508	8.15521	.77788
6	.81410	.72746	.98510	.16134	.77789
7	.81840	.73182	.98512	.16747	.77790
8	.82269	.73618	.98514	.17358	.77791
9	.82698	.74053	.98516	.17970	.77792
67.0	5.83127	5.74489	.98519	8.18581	.77794
1	.83556	.74924	.98521	.19191	.77795
2	.83984	.75358	.98523	.19801	.77796
3	.84412	.75793	.98525	.20411	.77797
4	.84839	.76227	.98527	.21020	.77798
67.5	5.85267	5.76660	.98529	8.21629	.77799
6	.85694	.77094	.98532	.22237	.77800
7	.86120	.77527	.98534	.22845	.77801
8	.86547	.77959	.98536	.23452	.77802
9	.86973	.78392	.98538	.24059	.77803
68.0	5.87398	5.78824	.98540	8.24666	.77805
1	.87824	.79255	.98542	.25272	.77806
2	.88249	.79687	.98544	.25877	.77807
3	.88674	.80118	.98547	.26482	.77808
4	.89098	.80548	.98549	.27087	.77809
68.5	5.89522	5.80979	.98551	8.27691	.77810
6	.89946	.81409	.98553	.28295	.77811
7	.90370	.81839	.98555	.28899	.77812
8	.90793	.82268	.98557	.29501	.77813
9	.91216	.82697	.98559	.30104	.77814
69.0	5.91639	5.83126	.98561	8.30706	.77815
1	.92061	.83555	.98563	.31308	.77816
2	.92483	.83983	.98565	.31909	.77817
3	.92905	.84411	.98567	.32510	.77818
4	.93326	.84838	.98569	.33110	.77819
69.5	5.93747	5.85266	.98572	8.33710	.77820
6	.94168	.85693	.98574	.34309	.77821
7	.94589	.86119	.98576	.34908	.77823
8	.95009	.86546	.98578	.35507	.77824
9	.95429	.86972	.98580	.36105	.77825

p	f(p)	g(p)	$\dfrac{g(p)}{f(p)}$	$|S|$	θ
70.0	5.95849	5.87397	.98582	8.36703	.77826
1	.96268	.87823	.98584	.37300	.77827
2	.96687	.88248	.98586	.37897	.77828
3	.97106	.88673	.98588	.38493	.77829
4	.97524	.89097	.98590	.39089	.77830
70.5	5.97943	5.89521	.98592	8.39685	.77831
6	.98361	.89945	.98594	.40280	.77832
7	.98778	.90369	.98596	.40875	.77833
8	.99196	.90792	.98598	.41469	.77834
9	.99613	.91215	.98600	.42063	.77835
71.0	6.00029	5.91638	.98601	8.42657	.77836
1	.00446	.92060	.98603	.43250	.77837
2	.00862	.92482	.98605	.43843	.77838
3	.01278	.92904	.98607	.44435	.77839
4	.01693	.93325	.98609	.45027	.77840
71.5	6.02109	5.93747	.98611	8.45618	.77841
6	.02524	.94167	.98613	.46209	.77842
7	.02939	.94588	.98615	.46800	.77843
8	.03353	.95008	.98617	.47390	.77843
9	.03767	.95428	.98619	.47980	.77844
72.0	6.04181	5.95848	.98621	8.48569	.77845
1	.04595	.96267	.98623	.49158	.77846
2	.05008	.96686	.98625	.49747	.77847
3	.05421	.97105	.98626	.50335	.77848
4	.05834	.97524	.98628	.50922	.77849
72.5	6.06246	5.97942	.98630	8.51510	.77850
6	.06658	.98360	.98632	.52097	.77851
7	.07070	.98777	.98634	.52683	.77852
8	.07482	.99195	.98636	.53269	.77853
9	.07893	.99612	.98638	.53855	.77854
73.0	6.08304	6.00029	.98640	8.54440	.77855
1	.08715	.00445	.98641	.55025	.77856
2	.09126	.00861	.98643	.55610	.77857
3	.09536	.01277	.98645	.56194	.77858
4	.09946	.01693	.98647	.56778	.77859
73.5	6.10356	6.02108	.98649	8.57361	.77860
6	.10765	.02523	.98651	.57944	.77861
7	.11174	.02938	.98652	.58527	.77861
8	.11583	.03352	.98654	.59109	.77862
9	.11992	.03766	.98656	.59690	.77863
74.0	6.12400	6.04180	.98658	8.60272	.77864
1	.12808	.04594	.98660	.60853	.77865
2	.13216	.05007	.98661	.61433	.77866
3	.13623	.05420	.98663	.62013	.77867
4	.14031	.05833	.98665	.62593	.77868
74.5	6.14438	6.06245	.98667	8.63173	.77869
6	.14844	.06658	.98669	.63752	.77870
7	.15251	.07070	.98670	.64330	.77871
8	.15657	.07481	.98672	.64909	.77871
9	.16063	.07893	.98674	.65486	.77872

p	f(p)	g(p)	g(p)/f(p)	|S|	θ
75.0	6.16468	6.08304	.98676	8.66064	.77873
1	.16874	.08714	.98677	.66641	.77874
2	.17279	.09125	.98679	.67218	.77875
3	.17684	.09535	.98681	.67794	.77876
4	.18088	.09945	.98683	.68370	.77877
75.5	6.18493	6.10355	.98684	8.68945	.77878
6	.18897	.10764	.98686	.69521	.77878
7	.19300	.11173	.98688	.70095	.77879
8	.19704	.11582	.98689	.70670	.77880
9	.20107	.11991	.98691	.71244	.77881
76.0	6.20510	6.12399	.98693	8.71818	.77882
1	.20913	.12807	.98695	.72391	.77883
2	.21315	.13215	.98696	.72964	.77884
3	.21718	.13623	.98698	.73536	.77885
4	.22120	.14030	.98700	.74108	.77885
76.5	6.22521	6.14437	.98701	8.74680	.77886
6	.22923	.14844	.98703	.75252	.77887
7	.23324	.15250	.98705	.75823	.77888
8	.23725	.15656	.98706	.76393	.77889
9	.24125	.16062	.98708	.76964	.77890
77.0	6.24526	6.16468	.98710	8.77533	.77891
1	.24926	.16873	.98711	.78103	.77891
2	.25326	.17278	.98713	.78672	.77892
3	.25725	.17683	.98715	.79241	.77893
4	.26125	.18088	.98716	.79809	.77894
77.5	6.26524	6.18492	.98718	8.80377	.77895
6	.26923	.18896	.98720	.80945	.77896
7	.27321	.19300	.98721	.81513	.77896
8	.27720	.19703	.98723	.82079	.77897
9	.28118	.20107	.98725	.82646	.77898
78.0	6.28516	6.20510	.98726	8.83212	.77899
1	.28913	.20912	.98728	.83778	.77900
2	.29311	.21315	.98729	.84344	.77900
3	.29708	.21717	.98731	.84909	.77901
4	.30105	.22119	.98733	.85474	.77902
78.5	6.30501	6.22521	.98734	8.86038	.77903
6	.30898	.22922	.98736	.86602	.77904
7	.31294	.23323	.98737	.87166	.77905
8	.31690	.23724	.98739	.87729	.77905
9	.32085	.24125	.98741	.88292	.77906
79.0	6.32481	6.24525	.98742	8.88855	.77907
1	.32876	.24925	.98744	.89417	.77908
2	.33271	.25325	.98745	.89979	.77909
3	.33665	.25725	.98747	.90541	.77909
4	.34060	.26124	.98748	.91102	.77910
79.5	6.34454	6.26523	.98750	8.91663	.77911
6	.34848	.26922	.98752	.92224	.77912
7	.35241	.27321	.98753	.92784	.77912
8	.35635	.27719	.98755	.93344	.77913
9	.36028	.28117	.98756	.93903	.77914

p	f(p)	g(p)	$\dfrac{g(p)}{f(p)}$	|S|	θ
80.0	6.36421	6.28515	.98758	8.94462	.77915
1	.36813	.28913	.98759	.95021	.77916
2	.37206	.29310	.98761	.95579	.77916
3	.37598	.29707	.98762	.96137	.77917
4	.37990	.30104	.98764	.96695	.77918
80.5	6.38382	6.30501	.98765	8.97253	.77919
6	.38773	.30897	.98767	.97810	.77920
7	.39164	.31293	.98769	.98366	.77920
8	.39555	.31689	.98770	.98923	.77921
9	.39946	.32085	.98772	.99479	.77922
81.0	6.40337	6.32480	.98773	9.00034	.77923
1	.40727	.32875	.98775	.00590	.77923
2	.41117	.33270	.98776	.01145	.77924
3	.41507	.33665	.98778	.01699	.77925
4	.41896	.34059	.98779	.02254	.77926
81.5	6.42285	6.34453	.98781	9.02807	.77926
6	.42675	.34847	.98782	.03361	.77927
7	.43063	.35241	.98784	.03914	.77928
8	.43452	.35634	.98785	.04467	.77929
9	.43840	.36027	.98786	.05020	.77929
82.0	6.44229	6.36420	.98788	9.05572	.77930
1	.44617	.36813	.98789	.06124	.77931
2	.45004	.37205	.98791	.06676	.77932
3	.45392	.37597	.98792	.07227	.77932
4	.45779	.37989	.98794	.07778	.77933
82.5	6.46166	6.38381	.98795	9.08328	.77934
6	.46553	.38772	.98797	.08879	.77935
7	.46939	.39164	.98798	.09429	.77935
8	.47325	.39555	.98800	.09978	.77936
9	.47711	.39945	.98801	.10527	.77937
83.0	6.48097	6.40336	.98802	9.11076	.77937
1	.48483	.40726	.98804	.11625	.77938
2	.48868	.41116	.98805	.12173	.77939
3	.49253	.41506	.98807	.12721	.77940
4	.49638	.41896	.98808	.13269	.77940
83.5	6.50023	6.42285	.98810	9.13816	.77941
6	.50407	.42674	.98811	.14363	.77942
7	.50792	.43063	.98812	.14910	.77942
8	.51176	.43451	.98814	.15456	.77943
9	.51560	.43840	.98815	.16002	.77944
84.0	6.51943	6.44228	.98817	9.16548	.77945
1	.52326	.44616	.98818	.17093	.77945
2	.52709	.45004	.98819	.17638	.77946
3	.53092	.45391	.98821	.18183	.77947
4	.53475	.45778	.98822	.18727	.77947
84.5	6.53857	6.46165	.98824	9.19271	.77948
6	.54240	.46552	.98825	.19815	.77949
7	.54622	.46939	.98826	.20358	.77950
8	.55003	.47325	.98828	.20901	.77950
9	.55385	.47711	.98829	.21444	.77951

p	f(p)	g(p)	$\frac{g(p)}{f(p)}$	|S|	θ
85.0	6.55766	6.48097	.98830	9.21986	.77952
1	.56147	.48482	.98832	.22528	.77952
2	.56528	.48868	.98833	.23070	.77953
3	.56909	.49253	.98835	.23612	.77954
4	.57289	.49638	.98836	.24153	.77954
85.5	6.57670	6.50022	.98837	9.24694	.77955
6	.58050	.50407	.98839	.25234	.77956
7	.58429	.50791	.98840	.25774	.77956
8	.58809	.51175	.98841	.26314	.77957
9	.59188	.51559	.98843	.26854	.77958
86.0	6.59567	6.51943	.98844	9.27393	.77958
1	.59946	.52326	.98845	.27932	.77959
2	.60325	.52709	.98847	.28471	.77960
3	.60703	.53092	.98848	.29009	.77960
4	.61082	.53475	.98849	.29547	.77961
86.5	6.61460	6.53857	.98851	9.30085	.77962
6	.61837	.54239	.98852	.30622	.77962
7	.62215	.54621	.98853	.31159	.77963
8	.62592	.55003	.98855	.31696	.77964
9	.62970	.55384	.98856	.32233	.77964
87.0	6.63347	6.55766	.98857	9.32769	.77965
1	.63723	.56147	.98858	.33305	.77966
2	.64100	.56528	.98860	.33840	.77966
3	.64476	.56908	.98861	.34375	.77967
4	.64852	.57289	.98862	.34910	.77968
87.5	6.65228	6.57669	.98864	9.35445	.77968
6	.65604	.58049	.98865	.35979	.77969
7	.65979	.58429	.98866	.36513	.77970
8	.66355	.58808	.98868	.37047	.77970
9	.66730	.59188	.98869	.37580	.77971
88.0	6.67104	6.59567	.98870	9.38113	.77972
1	.67479	.59946	.98871	.38646	.77972
2	.67854	.60324	.98873	.39179	.77973
3	.68228	.60703	.98874	.39711	.77974
4	.68602	.61081	.98875	.40243	.77974
88.5	6.68976	6.61459	.98876	9.40774	.77975
6	.69349	.61837	.98878	.41306	.77976
7	.69722	.62215	.98879	.41837	.77976
8	.70096	.62592	.98880	.42367	.77977
9	.70469	.62969	.98881	.42898	.77977
89.0	6.70841	6.63346	.98883	9.43428	.77978
1	.71214	.63723	.98884	.43958	.77979
2	.71586	.64099	.98885	.44487	.77979
3	.71958	.64476	.98886	.45016	.77980
4	.72330	.64852	.98888	.45545	.77981
89.5	6.72702	6.65228	.98889	9.46074	.77981
6	.73073	.65603	.98890	.46602	.77982
7	.73445	.65979	.98891	.47130	.77982
8	.73816	.66354	.98893	.47658	.77983
9	.74187	.66729	.98894	.48185	.77984

p	f(p)	g(p)	$\frac{g(p)}{f(p)}$	|S|	θ
90.0	6.74557	6.67104	.98895	9.48713	.77984
1	.74928	.67479	.98896	.49239	.77985
2	.75298	.67853	.98897	.49766	.77986
3	.75668	.68227	.98899	.50292	.77986
4	.76038	.68601	.98900	.50818	.77987
90.5	6.76408	6.68975	.98901	9.51344	.77987
6	.76777	.69349	.98902	.51869	.77988
7	.77147	.69722	.98904	.52394	.77989
8	.77516	.70095	.98905	.52919	.77989
9	.77885	.70468	.98906	.53444	.77990
91.0	6.78253	6.70841	.98907	9.53968	.77990
1	.78622	.71213	.98908	.54492	.77991
2	.78990	.71586	.98910	.55016	.77992
3	.79358	.71958	.98911	.55539	.77992
4	.79726	.72330	.98912	.56062	.77993
91.5	6.80094	6.72702	.98913	9.56585	.77993
6	.80461	.73073	.98914	.57107	.77994
7	.80828	.73444	.98915	.57630	.77995
8	.81195	.73815	.98917	.58152	.77995
9	.81562	.74186	.98918	.58673	.77996
92.0	6.81929	6.74557	.98919	9.59195	.77996
1	.82295	.74928	.98920	.59716	.77997
2	.82662	.75298	.98921	.60237	.77998
3	.83028	.75668	.98922	.60757	.77998
4	.83394	.76038	.98924	.61277	.77999
92.5	6.83759	6.76407	.98925	9.61797	.77999
6	.84125	.76777	.98926	.62317	.78000
7	.84490	.77146	.98927	.62836	.78000
8	.84855	.77515	.98928	.63356	.78001
9	.85220	.77884	.98929	.63874	.78002
93.0	6.85585	6.78253	.98931	9.64393	.78002
1	.85950	.78621	.98932	.64911	.78003
2	.86314	.78990	.98933	.65429	.78003
3	.86678	.79358	.98934	.65947	.78004
4	.87042	.79726	.98935	.66464	.78005
93.5	6.87406	6.80093	.98936	9.66982	.78005
6	.87769	.80461	.98937	.67499	.78006
7	.88133	.80828	.98938	.68015	.78006
8	.88496	.81195	.98940	.68532	.78007
9	.88859	.81562	.98941	.69048	.78007
94.0	6.89222	6.81929	.98942	9.69563	.78008
1	.89584	.82295	.98943	.70079	.78008
2	.89947	.82661	.98944	.70594	.78009
3	.90309	.83027	.98945	.71109	.78010
4	.90671	.83393	.98946	.71624	.78010
94.5	6.91033	6.83759	.98947	9.72138	.78011
6	.91395	.84125	.98949	.72652	.78011
7	.91756	.84490	.98950	.73166	.78012
8	.92117	.84855	.98951	.73680	.78012
9	.92478	.85220	.98952	.74193	.78013

p	f(p)	g(p)	$\frac{g(p)}{f(p)}$	|S|	θ
95.0	6.92839	6.85585	.98953	9.74706	.78014
1	.93200	.85949	.98954	.75219	.78014
2	.93561	.86314	.98955	.75732	.78015
3	.93921	.86678	.98956	.76244	.78015
4	.94281	.87042	.98957	.76756	.78016
95.5	6.94641	6.87405	.98958	9.77268	.78016
6	.95001	.87769	.98959	.77779	.78017
7	.95360	.88132	.98961	.78290	.78017
8	.95720	.88496	.98962	.78801	.78018
9	.96079	.88859	.98963	.79312	.78018
96.0	6.96438	6.89221	.98964	9.79822	.78019
1	.96797	.89584	.98965	.80333	.78020
2	.97156	.89946	.98966	.80842	.78020
3	.97514	.90309	.98967	.81352	.78021
4	.97872	.90671	.98968	.81861	.78021
96.5	6.98231	6.91032	.98969	9.82370	.78022
6	.98588	.91394	.98970	.82879	.78022
7	.98946	.91756	.98971	.83388	.78023
8	.99304	.92117	.98972	.83896	.78023
9	.99661	.92478	.98973	.84404	.78024
97.0	7.00018	6.92839	.98974	9.84912	.78024
1	.00375	.93200	.98975	.85419	.78025
2	.00732	.93560	.98976	.85927	.78025
3	.01089	.93921	.98978	.86434	.78026
4	.01445	.94281	.98979	.86940	.78026
97.5	7.01802	6.94641	.98980	9.87447	.78027
6	.02158	.95000	.98981	.87953	.78028
7	.02514	.95360	.98982	.88459	.78028
8	.02870	.95719	.98983	.88965	.78029
9	.03225	.96079	.98984	.89470	.78029
98.0	7.03580	6.96438	.98985	9.89975	.78030
1	.03936	.96797	.98986	.90480	.78030
2	.04291	.97155	.98987	.90985	.78031
3	.04646	.97514	.98988	.91489	.78031
4	.05000	.97872	.98989	.91993	.78032
98.5	7.05355	6.98230	.98990	9.92497	.78032
6	.05709	.98588	.98991	.93001	.78033
7	.06063	.98946	.98992	.93504	.78033
8	.06417	.99303	.98993	.94007	.78034
9	.06771	.99661	.98994	.94510	.78034
99.0	7.07125	7.00018	.98995	9.95013	.78035
1	.07478	.00375	.98996	.95515	.78035
2	.07831	.00732	.98997	.96017	.78036
3	.08184	.01089	.98998	.96519	.78036
4	.08537	.01445	.98999	.97021	.78037
99.5	7.08890	7.01801	.99000	9.97522	.78037
6	.09243	.02157	.99001	.98023	.78038
7	.09595	.02513	.99002	.98524	.78038
8	.09947	.02869	.99003	.99025	.78039
9	.10299	.03225	.99004	.99525	.78039

TABLE 5

$0 \leq p \leq 999$ in steps of 1

p	f(p)	g(p)	$\frac{g(p)}{f(p)}$	|S|	θ
0	1.00000	0.00000	.00000	1.00000	.00000
1	.09868	.45509	.41421	.18921	.39270
2	.27202	.78615	.61803	.49535	.55357
3	.44262	1.03978	.72076	.77828	.62452
4	.60049	.24962	.78078	2.03054	.66291
5	1.74628	1.43161	.81980	2.25810	.68670
6	.88186	.59417	.84713	.46633	.70282
7	2.00886	.74228	.86730	.65915	.71445
8	.12864	.87913	.88278	.83941	.72322
9	.24225	2.00691	.89504	3.00922	.73007
10	2.35052	2.12719	.90499	3.17015	.73556
1	.45412	.24113	.91321	.32346	.74007
2	.55359	.34964	.92013	.47010	.74383
3	.64938	.45341	.92603	.61087	.74701
4	.74187	.55300	.93112	.74642	.74974
15	2.83137	2.64890	.93555	3.87728	.75211
6	.91815	.74146	.93945	4.00390	.75419
7	3.00245	.83102	.94291	.12667	.75602
8	.08446	.91786	.94599	.24591	.75765
9	.16436	3.00219	.94875	.36191	.75911
20	3.24230	3.08423	.95125	4.47493	.76042
1	.31842	.16416	.95351	.58517	.76161
2	.39284	.24212	.95558	.69284	.76269
3	.46567	.31826	.95747	.79810	.76367
4	.53701	.39270	.95920	.90110	.76458
25	3.60694	3.46554	.96080	5.00200	.76541
6	.67554	.53689	.96228	.10090	.76618
7	.74289	.60683	.96365	.19793	.76689
8	.80906	.67545	.96492	.29319	.76755
9	.87410	.74281	.96611	.38676	.76816
30	3.93806	3.80898	.96722	5.47875	.76874
1	4.00101	.87402	.96826	.56921	.76927
2	.06298	.93800	.96924	.65823	.76978
3	.12402	4.00095	.97016	.74588	.77025
4	.18418	.06292	.97102	.83221	.77070
35	4.24348	4.12397	.97184	5.91729	.77112
6	.30197	.18413	.97261	6.00116	.77151
7	.35967	.24344	.97334	.08387	.77189
8	.41663	.30193	.97403	.16548	.77224
9	.47285	.35963	.97469	.24602	.77258
40	4.52838	4.41659	.97531	6.32554	.77290
1	.58324	.47282	.97591	.40408	.77321
2	.63745	.52835	.97647	.48166	.77350
3	.69104	.58321	.97701	.55832	.77377
4	.74402	.63742	.97753	.63411	.77404
45	4.79641	4.69101	.97802	6.70903	.77429
6	.84824	.74399	.97850	.78313	.77453
7	.89952	.79639	.97895	.85643	.77476
8	.95027	.84822	.97938	.92895	.77498
9	5.00051	.89950	.97980	7.00073	.77520

p	f(p)	g(p)	$\frac{g(p)}{f(p)}$	|S|	θ
50	5.05025	4.95025	.98020	7.07177	.77540
1	.09950	5.00049	.98058	.14211	.77560
2	.14828	.05023	.98095	.21177	.77578
3	.19661	.09948	.98131	.28076	.77597
4	.24449	.14826	.98165	.34910	.77614
55	5.29193	5.19659	.98198	7.41681	.77631
6	.33896	.24447	.98230	.48391	.77647
7	.38557	.29192	.98261	.55042	.77663
8	.43179	.33894	.98291	.61634	.77678
9	.47761	.38556	.98319	.68170	.77692
60	5.52306	5.43177	.98347	7.74650	.77707
1	.56813	.47760	.98374	.81077	.77720
2	.61285	.52305	.98400	.87452	.77733
3	.65720	.56812	.98425	.93775	.77746
4	.70122	.61283	.98450	8.00049	.77759
65	5.74490	5.65719	.98473	8.06273	.77771
6	.78825	.70121	.98496	.12450	.77782
7	.83127	.74489	.98519	.18581	.77794
8	.87398	.78824	.98540	.24666	.77805
9	.91639	.83126	.98561	.30706	.77815
70	5.95849	5.87397	.98582	8.36703	.77826
1	6.00029	.91638	.98601	.42657	.77836
2	.04181	.95848	.98621	.48569	.77845
3	.08304	6.00029	.98640	.54440	.77855
4	.12400	.04180	.98658	.60272	.77864
75	6.16468	6.08304	.98676	8.66064	.77873
6	.20510	.12399	.98693	.71818	.77882
7	.24526	.16468	.98710	.77533	.77891
8	.28516	.20510	.98726	.83212	.77899
9	.32481	.24525	.98742	.88855	.77907
80	6.36421	6.28515	.98758	8.94462	.77915
1	.40337	.32480	.98773	9.00034	.77923
2	.44229	.36420	.98788	.05572	.77930
3	.48097	.40336	.98802	.11076	.77937
4	.51943	.44228	.98817	.16548	.77945
85	6.55766	6.48097	.98830	9.21986	.77952
6	.59567	.51943	.98844	.27393	.77958
7	.63347	.55766	.98857	.32769	.77965
8	.67104	.59567	.98870	.38113	.77972
9	.70841	.63346	.98883	.43428	.77978
90	6.74557	6.67104	.98895	9.48713	.77984
1	.78253	.70841	.98907	.53968	.77990
2	.81929	.74557	.98919	.59195	.77996
3	.85585	.78253	.98931	.64393	.78002
4	.89222	.81929	.98942	.69563	.78008
95	6.92839	6.85585	.98953	9.74706	.78014
6	.96438	.89221	.98964	.79822	.78019
7	7.00018	.92839	.98974	.84912	.78024
8	.03580	.96438	.98985	.89975	.78030
9	.07125	7.00018	.98995	.95013	.78035

p	f(p)	g(p)	$\dfrac{g(p)}{f(p)}$	|S|	θ
100	7.10651	7.03580	.99005	10.00025	.78040
1	.14160	.07124	.99015	.05012	.78045
2	.17652	.10651	.99024	.09975	.78050
3	.21127	.14160	.99034	.14913	.78054
4	.24585	.17652	.99043	.19827	.78059
105	7.28027	7.21127	.99052	10.24718	.78064
6	.31453	.24585	.99061	.29586	.78068
7	.34863	.28027	.99070	.34431	.78073
8	.38257	.31453	.99078	.39253	.78077
9	.41635	.34863	.99087	.44053	.78081
110	7.44998	7.38257	.99095	10.48831	.78085
1	.48347	.41635	.99103	.53587	.78089
2	.51680	.44998	.99111	.58322	.78093
3	.54998	.48346	.99119	.63035	.78097
4	.58302	.51679	.99127	.67728	.78101
115	7.61592	7.54998	.99134	10.72401	.78105
6	.64867	.58302	.99142	.77053	.78109
7	.68128	.61591	.99149	.81685	.78112
8	.71376	.64867	.99156	.86298	.78116
9	.74610	.68128	.99163	.90890	.78120
120	7.77831	7.71376	.99170	10.95464	.78123
1	.81038	.74610	.99177	11.00019	.78127
2	.84232	.77831	.99184	.04555	.78130
3	.87414	.81038	.99190	.09072	.78133
4	.90582	.84232	.99197	.13571	.78137
125	7.93738	7.87413	.99203	11.18052	.78140
6	.96881	.90582	.99209	.22515	.78143
7	8.00012	.93738	.99216	.26960	.78146
8	.03131	.96881	.99222	.31388	.78149
9	.06238	8.00012	.99228	.35799	.78152
130	8.09333	8.03131	.99234	11.40192	.78155
1	.12416	.06238	.99240	.44569	.78158
2	.15487	.09332	.99245	.48929	.78161
3	.18547	.12415	.99251	.53273	.78164
4	.21595	.15487	.99257	.57600	.78167
135	8.24632	8.18547	.99262	11.61911	.78169
6	.27658	.21595	.99267	.66206	.78172
7	.30673	.24632	.99273	.70486	.78175
8	.33677	.27658	.99278	.74749	.78178
9	.36671	.30673	.99283	.78998	.78180
140	8.39653	8.33677	.99288	11.83231	.78183
1	.42625	.36671	.99293	.87449	.78185
2	.45587	.39653	.99298	.91652	.78188
3	.48538	.42625	.99303	.95841	.78190
4	.51480	.45587	.99308	12.00014	.78193
145	8.54410	8.48538	.99313	12.04174	.78195
6	.57331	.51479	.99317	.08319	.78197
7	.60242	.54410	.99322	.12450	.78200
8	.63144	.57331	.99327	.16566	.78202
9	.66035	.60242	.99331	.20669	.78204

p	f(p)	g(p)	$\dfrac{g(p)}{f(p)}$	$|S|$	θ
150	8.68917	8.63143	.99336	12.24758	.78206
1	.71789	.66035	.99340	.28834	.78209
2	.74652	.68917	.99344	.32896	.78211
3	.77506	.71789	.99349	.36945	.78213
4	.80350	.74652	.99353	.40980	.78215
155	8.83185	8.77506	.99357	12.45003	.78217
6	.86011	.80350	.99361	.49012	.78219
7	.88828	.83185	.99365	.53009	.78221
8	.91637	.86011	.99369	.56993	.78223
9	.94436	.88828	.99373	.60964	.78225
160	8.97227	8.91636	.99377	12.64923	.78227
1	9.00009	.94436	.99381	.68870	.78229
2	.02782	.97227	.99385	.72804	.78231
3	.05547	9.00009	.99388	.76727	.78233
4	.08303	.02782	.99392	.80637	.78235
165	9.11052	9.05547	.99396	12.84535	.78237
6	.13792	.08303	.99399	.88422	.78239
7	.16523	.11052	.99403	.92296	.78240
8	.19247	.13791	.99407	.96160	.78242
9	.21962	.16523	.99410	13.00011	.78244
170	9.24670	9.19247	.99413	13.03852	.78246
1	.27370	.21962	.99417	.07681	.78247
2	.30062	.24670	.99420	.11499	.78249
3	.32746	.27370	.99424	.15306	.78251
4	.35422	.30061	.99427	.19101	.78252
175	9.38091	9.32746	.99430	13.22886	.78254
6	.40752	.35422	.99433	.26661	.78256
7	.43406	.38091	.99437	.30424	.78257
8	.46052	.40752	.99440	.34177	.78259
9	.48691	.43406	.99443	.37919	.78260
180	9.51322	9.46052	.99446	13.41651	.78262
1	.53946	.48691	.99449	.45373	.78264
2	.56563	.51322	.99452	.49084	.78265
3	.59173	.53946	.99455	.52785	.78267
4	.61776	.56563	.99458	.56476	.78268
185	9.64372	9.59173	.99461	13.60157	.78270
6	.66961	.61776	.99464	.63828	.78271
7	.69543	.64372	.99467	.67489	.78272
8	.72118	.66961	.99470	.71141	.78274
9	.74686	.69543	.99472	.74782	.78275
190	9.77248	9.72118	.99475	13.78414	.78277
1	.79803	.74686	.99478	.82037	.78278
2	.82351	.77248	.99481	.85650	.78279
3	.84892	.79803	.99483	.89254	.78281
4	.87427	.82351	.99486	.92848	.78282
195	9.89956	9.84892	.99488	13.96433	.78283
6	.92478	.87427	.99491	14.00009	.78285
7	.94994	.89956	.99494	.03576	.78286
8	.97503	.92478	.99496	.07134	.78287
9	10.00006	.94994	.99499	.10682	.78289

p	f(p)	g(p)	$\frac{g(p)}{f(p)}$	|S|	θ
200	10.02503	9.97503	.99501	14.14222	.78290
1	.04994	.00006	.99504	.17753	.78291
2	.07478	.02503	.99506	.21276	.78292
3	.09957	.04994	.99509	.24789	.78294
4	.12429	.07478	.99511	.28294	.78295
205	10.14895	10.09957	.99513	14.31791	.78296
6	.17355	.12429	.99516	.35278	.78297
7	.19810	.14895	.99518	.38758	.78298
8	.22258	.17355	.99520	.42229	.78299
9	.24701	.19810	.99523	.45691	.78301
210	10.27138	10.22258	.99525	14.49146	.78302
1	.29569	.24701	.99527	.52592	.78303
2	.31994	.27138	.99529	.56030	.78304
3	.34414	.29569	.99532	.59460	.78305
4	.36828	.31994	.99534	.62882	.78306
215	10.39236	10.34414	.99536	14.66296	.78307
6	.41639	.36828	.99538	.69702	.78308
7	.44036	.39236	.99540	.73100	.78309
8	.46428	.41639	.99542	.76490	.78310
9	.48814	.44036	.99544	.79873	.78312
220	10.51195	10.46428	.99546	14.83247	.78313
1	.53571	.48814	.99549	.86614	.78314
2	.55941	.51195	.99551	.89974	.78315
3	.58306	.53571	.99553	.93326	.78316
4	.60665	.55941	.99555	.96670	.78317
225	10.63020	10.58306	.99557	15.00007	.78318
6	.65369	.60665	.99559	.03337	.78319
7	.67713	.63020	.99560	.06659	.78320
8	.70052	.65369	.99562	.09974	.78321
9	.72386	.67713	.99564	.13282	.78321
230	10.74714	10.70052	.99566	15.16582	.78322
1	.77038	.72386	.99568	.19876	.78323
2	.79357	.74714	.99570	.23162	.78324
3	.81670	.77038	.99572	.26441	.78325
4	.83979	.79357	.99574	.29713	.78326
235	10.86283	10.81670	.99575	15.32978	.78327
6	.88582	.83979	.99577	.36236	.78328
7	.90876	.86283	.99579	.39487	.78329
8	.93165	.88582	.99581	.42732	.78330
9	.95450	.90876	.99582	.45969	.78331
240	10.97730	10.93165	.99584	15.49200	.78331
1	11.00005	.95450	.99586	.52424	.78332
2	.02275	.97730	.99588	.55642	.78333
3	.04541	11.00005	.99589	.58852	.78334
4	.06802	.02275	.99591	.62056	.78335
245	11.09058	11.04541	.99593	15.65254	.78336
6	.11310	.06802	.99594	.68445	.78337
7	.13557	.09058	.99596	.71630	.78337
8	.15800	.11310	.99598	.74808	.78338
9	.18038	.13557	.99599	.77980	.78339

p	f(p)	g(p)	$\frac{g(p)}{f(p)}$	|S|	θ
250	11.20272	11.15800	.99601	15.81145	.78340
1	.22502	.18038	.99602	.84304	.78341
2	.24727	.20272	.99604	.87457	.78341
3	.26947	.22502	.99606	.90604	.78342
4	.29163	.24727	.99607	.93744	.78343
255	11.31375	11.26947	.99609	15.96878	.78344
6	.33583	.29163	.99610	16.00006	.78345
7	.35786	.31375	.99612	.03128	.78345
8	.37985	.33583	.99613	.06244	.78346
9	.40180	.35786	.99615	.09354	.78347
260	11.42370	11.37985	.99616	16.12457	.78348
1	.44556	.40180	.99618	.15555	.78348
2	.46739	.42370	.99619	.18647	.78349
3	.48917	.44556	.99620	.21733	.78350
4	.51091	.46739	.99622	.24813	.78350
265	11.53260	11.48917	.99623	16.27888	.78351
6	.55426	.51091	.99625	.30956	.78352
7	.57588	.53260	.99626	.34019	.78353
8	.59745	.55426	.99628	.37076	.78353
9	.61899	.57588	.99629	.40128	.78354
270	11.64049	11.59745	.99630	16.43173	.78355
1	.66194	.61899	.99632	.46213	.78355
2	.68336	.64049	.99633	.49248	.78356
3	.70474	.66194	.99634	.52277	.78357
4	.72608	.68336	.99636	.55300	.78357
275	11.74738	11.70474	.99637	16.58318	.78358
6	.76864	.72608	.99638	.61330	.78359
7	.78986	.74738	.99640	.64337	.78359
8	.81105	.76864	.99641	.67339	.78360
9	.83220	.78986	.99642	.70335	.78361
280	11.85331	11.81105	.99643	16.73325	.78361
1	.87438	.83220	.99645	.76311	.78362
2	.89541	.85331	.99646	.79291	.78363
3	.91641	.87438	.99647	.82266	.78363
4	.93737	.89541	.99649	.85235	.78364
285	11.95830	11.91641	.99650	16.88199	.78364
6	.97918	.93737	.99651	.91159	.78365
7	12.00004	.95830	.99652	.94113	.78366
8	.02085	.97918	.99653	.97061	.78366
9	.04163	12.00004	.99655	17.00005	.78367
290	12.06237	12.02085	.99656	17.02944	.78367
1	.08308	.04163	.99657	.05877	.78368
2	.10375	.06237	.99658	.08806	.78369
3	.12439	.08308	.99659	.11729	.78369
4	.14499	.10375	.99660	.14648	.78370
295	12.16556	12.12439	.99662	17.17561	.78370
6	.18609	.14499	.99663	.20470	.78371
7	.20659	.16556	.99664	.23374	.78371
8	.22705	.18609	.99665	.26272	.78372
9	.24748	.20659	.99666	.29166	.78373

p	f(p)	g(p)	$\dfrac{g(p)}{f(p)}$	|S|	θ
300	12.26788	12.22705	.99667	17.32056	.78373
1	.28824	.24748	.99668	.34940	.78374
2	.30857	.26788	.99669	.37819	.78374
3	.32886	.28824	.99671	.40694	.78375
4	.34912	.30857	.99672	.43564	.78375
305	12.36935	12.32886	.99673	17.46430	.78376
6	.38954	.34912	.99674	.49290	.78376
7	.40971	.36935	.99675	.52146	.78377
8	.42984	.38954	.99676	.54997	.78377
9	.44993	.40971	.99677	.57844	.78378
310	12.47000	12.42984	.99678	17.60686	.78379
1	.49003	.44993	.99679	.63524	.78379
2	.51003	.47000	.99680	.66357	.78380
3	.53000	.49003	.99681	.69185	.78380
4	.54993	.51003	.99682	.72009	.78381
315	12.56984	12.53000	.99683	17.74828	.78381
6	.58971	.54993	.99684	.77643	.78382
7	.60955	.56984	.99685	.80454	.78382
8	.62936	.58971	.99686	.83260	.78383
9	.64914	.60955	.99687	.86061	.78383
320	12.66889	12.62936	.99688	17.88859	.78384
1	.68861	.64914	.99689	.91652	.78384
2	.70830	.66889	.99690	.94440	.78385
3	.72795	.68861	.99691	.97224	.78385
4	.74758	.70830	.99692	18.00004	.78385
325	12.76718	12.72795	.99693	18.02780	.78386
6	.78674	.74758	.99694	.05551	.78386
7	.80628	.76718	.99695	.08318	.78387
8	.82578	.78674	.99696	.11081	.78387
9	.84526	.80628	.99697	.13840	.78388
330	12.86471	12.82578	.99697	18.16594	.78388
1	.88413	.84526	.99698	.19345	.78389
2	.90352	.86471	.99699	.22091	.78389
3	.92288	.88413	.99700	.24833	.78390
4	.94221	.90352	.99701	.27571	.78390
335	12.96151	12.92288	.99702	18.30305	.78391
6	.98078	.94221	.99703	.33034	.78391
7	13.00003	.96151	.99704	.35760	.78391
8	.01924	.98078	.99705	.38482	.78392
9	.03843	13.00003	.99705	.41199	.78392
340	13.05759	13.01924	.99706	18.43913	.78393
1	.07672	.03843	.99707	.46622	.78393
2	.09583	.05759	.99708	.49328	.78394
3	.11490	.07672	.99709	.52030	.78394
4	.13395	.09583	.99710	.54728	.78394
345	13.15297	13.11490	.99711	18.57421	.78395
6	.17197	.13395	.99711	.60111	.78395
7	.19093	.15297	.99712	.62797	.78396
8	.20987	.17197	.99713	.65480	.78396
9	.22878	.19093	.99714	.68158	.78397

p	f(p)	g(p)	$\frac{g(p)}{f(p)}$	|S|	θ
350	13.24767	13.20987	.99715	18.70832	.78397
1	.26653	.22878	.99716	.73503	.78397
2	.28536	.24767	.99716	.76170	.78398
3	.30416	.26653	.99717	.78833	.78398
4	.32294	.28536	.99718	.81492	.78399
355	13.34169	13.30416	.99719	18.84148	.78399
6	.36042	.32294	.99719	.86800	.78399
7	.37911	.34169	.99720	.89448	.78400
8	.39779	.36042	.99721	.92092	.78400
9	.41643	.37911	.99722	.94733	.78401
360	13.43505	13.39779	.99723	18.97370	.78401
1	.45365	.41643	.99723	19.00004	.78401
2	.47222	.43505	.99724	.02633	.78402
3	.49076	.45365	.99725	.05259	.78402
4	.50928	.47222	.99726	.07882	.78402
365	13.52777	13.49076	.99726	19.10501	.78403
6	.54624	.50928	.99727	.13116	.78403
7	.56468	.52777	.99728	.15728	.78404
8	.58310	.54624	.99729	.18336	.78404
9	.60150	.56468	.99729	.20941	.78404
370	13.61986	13.58310	.99730	19.23542	.78405
1	.63821	.60150	.99731	.26139	.78405
2	.65652	.61986	.99732	.28734	.78405
3	.67482	.63821	.99732	.31324	.78406
4	.69309	.65652	.99733	.33911	.78406
375	13.71133	13.67482	.99734	19.36495	.78406
6	.72955	.69309	.99734	.39075	.78407
7	.74775	.71133	.99735	.41652	.78407
8	.76592	.72955	.99736	.44226	.78408
9	.78407	.74775	.99736	.46796	.78408
380	13.80220	13.76592	.99737	19.49362	.78408
1	.82030	.78407	.99738	.51925	.78409
2	.83838	.80220	.99739	.54485	.78409
3	.85643	.82030	.99739	.57042	.78409
4	.87446	.83838	.99740	.59595	.78410
385	13.89247	13.85643	.99741	19.62145	.78410
6	.91045	.87446	.99741	.64692	.78410
7	.92841	.89247	.99742	.67235	.78411
8	.94635	.91045	.99743	.69775	.78411
9	.96426	.92841	.99743	.72312	.78411
390	13.98215	13.94635	.99744	19.74845	.78412
1	14.00002	.96426	.99745	.77375	.78412
2	.01787	.98215	.99745	.79902	.78412
3	.03569	14.00002	.99746	.82426	.78413
4	.05349	.01787	.99747	.84946	.78413
395	14.07127	14.03569	.99747	19.87464	.78413
6	.08903	.05349	.99748	.89978	.78414
7	.10676	.07127	.99748	.92489	.78414
8	.12447	.08903	.99749	.94997	.78414
9	.14216	.10676	.99750	.97502	.78415

p	f(p)	g(p)	$\frac{g(p)}{f(p)}$	|S|	θ
400	14.15982	14.12447	.99750	20.00003	.78415
1	.17747	.14216	.99751	.02502	.78415
2	.19509	.15982	.99752	.04997	.78415
3	.21269	.17747	.99752	.07489	.78416
4	.23027	.19509	.99753	.09978	.78416
405	14.24783	14.21269	.99753	20.12464	.78416
6	.26536	.23027	.99754	.14947	.78417
7	.28288	.24783	.99755	.17427	.78417
8	.30037	.26536	.99755	.19904	.78417
9	.31784	.28288	.99756	.22378	.78418
410	14.33529	14.30037	.99756	20.24849	.78418
1	.35272	.31784	.99757	.27316	.78418
2	.37013	.33529	.99758	.29781	.78418
3	.38752	.35272	.99758	.32243	.78419
4	.40488	.37013	.99759	.34702	.78419
415	14.42223	14.38752	.99759	20.37158	.78419
6	.43955	.40488	.99760	.39611	.78420
7	.45685	.42223	.99760	.42061	.78420
8	.47414	.43955	.99761	.44508	.78420
9	.49140	.45685	.99762	.46952	.78420
420	14.50864	14.47414	.99762	20.49393	.78421
1	.52586	.49140	.99763	.51831	.78421
2	.54306	.50864	.99763	.54267	.78421
3	.56024	.52586	.99764	.56699	.78422
4	.57740	.54306	.99764	.59129	.78422
425	14.59454	14.56024	.99765	20.61556	.78422
6	.61166	.57740	.99766	.63980	.78422
7	.62876	.59454	.99766	.66401	.78423
8	.64584	.61166	.99767	.68819	.78423
9	.66290	.62876	.99767	.71234	.78423
430	14.67994	14.64584	.99768	20.73647	.78424
1	.69696	.66290	.99768	.76057	.78424
2	.71396	.67994	.99769	.78464	.78424
3	.73094	.69696	.99769	.80868	.78424
4	.74790	.71396	.99770	.83269	.78425
435	14.76484	14.73094	.99770	20.85668	.78425
6	.78176	.74790	.99771	.88064	.78425
7	.79867	.76484	.99771	.90457	.78425
8	.81555	.78176	.99772	.92848	.78426
9	.83242	.79867	.99772	.95235	.78426
440	14.84926	14.81555	.99773	20.97620	.78426
1	.86609	.83242	.99774	21.00003	.78426
2	.88289	.84926	.99774	.02382	.78427
3	.89968	.86609	.99775	.04759	.78427
4	.91645	.88289	.99775	.07133	.78427
445	14.93320	14.89968	.99776	21.09505	.78427
6	.94993	.91645	.99776	.11874	.78428
7	.96665	.93320	.99777	.14240	.78428
8	.98334	.94994	.99777	.16604	.78428
9	15.00002	.96665	.99778	.18965	.78428

p	f(p)	g(p)	$\frac{g(p)}{f(p)}$	|S|	θ
450	15.01668	14.98334	.99778	21.21323	.78429
1	.03331	15.00002	.99779	.23679	.78429
2	.04994	.01668	.99779	.26032	.78429
3	.06654	.03331	.99779	.28382	.78429
4	.08312	.04994	.99780	.30730	.78430
455	15.09969	15.06654	.99780	21.33075	.78430
6	.11623	.08312	.99781	.35418	.78430
7	.13276	.09969	.99781	.37758	.78430
8	.14928	.11623	.99782	.40096	.78431
9	.16577	.13276	.99782	.42431	.78431
460	15.18224	15.14928	.99783	21.44764	.78431
1	.19870	.16577	.99783	.47094	.78431
2	.21514	.18224	.99784	.49421	.78432
3	.23156	.19870	.99784	.51746	.78432
4	.24797	.21514	.99785	.54068	.78432
465	15.26436	15.23156	.99785	21.56388	.78432
6	.28072	.24797	.99786	.58706	.78433
7	.29708	.26436	.99786	.61021	.78433
8	.31341	.28072	.99787	.63333	.78433
9	.32973	.29708	.99787	.65643	.78433
470	15.34603	15.31341	.99787	21.67951	.78433
1	.36231	.32973	.99788	.70256	.78434
2	.37857	.34603	.99788	.72559	.78434
3	.39482	.36231	.99789	.74859	.78434
4	.41105	.37857	.99789	.77157	.78434
475	15.42727	15.39482	.99790	21.79452	.78435
6	.44346	.41105	.99790	.81745	.78435
7	.45964	.42727	.99791	.84035	.78435
8	.47580	.44346	.99791	.86323	.78435
9	.49195	.45964	.99791	.88609	.78435
480	15.50808	15.47580	.99792	21.90893	.78436
1	.52419	.49195	.99792	.93174	.78436
2	.54029	.50808	.99793	.95452	.78436
3	.55637	.52419	.99793	.97728	.78436
4	.57243	.54029	.99794	22.00002	.78437
485	15.58847	15.55637	.99794	22.02274	.78437
6	.60450	.57243	.99794	.04543	.78437
7	.62052	.58847	.99795	.06810	.78437
8	.63651	.60450	.99795	.09074	.78437
9	.65249	.62052	.99796	.11337	.78438
490	15.66846	15.63651	.99796	22.13597	.78438
1	.68440	.65249	.99797	.15854	.78438
2	.70033	.66846	.99797	.18110	.78438
3	.71625	.68440	.99797	.20363	.78438
4	.73215	.70033	.99798	.22613	.78439
495	15.74803	15.71625	.99798	22.24862	.78439
6	.76390	.73215	.99799	.27108	.78439
7	.77975	.74803	.99799	.29352	.78439
8	.79558	.76390	.99799	.31594	.78439
9	.81140	.77975	.99800	.33833	.78440

p	f(p)	g(p)	$\frac{g(p)}{f(p)}$	$|S|$	θ
500	15.82721	15.79558	.99800	22.36070	.78440
1	.84300	.81140	.99801	.38305	.78440
2	.85877	.82721	.99801	.40538	.78440
3	.87452	.84300	.99801	.42768	.78440
4	.89026	.85877	.99802	.44997	.78441
505	15.90599	15.87452	.99802	22.47223	.78441
6	.92170	.89026	.99803	.49447	.78441
7	.93739	.90599	.99803	.51668	.78441
8	.95307	.92170	.99803	.53888	.78441
9	.96873	.93739	.99804	.56105	.78442
510	15.98438	15.95307	.99804	22.58320	.78442
1	16.00002	.96873	.99805	.60533	.78442
2	.01563	.98438	.99805	.62744	.78442
3	.03123	16.00002	.99805	.64952	.78442
4	.04682	.01563	.99806	.67159	.78443
515	16.06239	16.03123	.99806	22.69363	.78443
6	.07795	.04682	.99806	.71565	.78443
7	.09349	.06239	.99807	.73765	.78443
8	.10902	.07795	.99807	.75963	.78443
9	.12453	.09349	.99808	.78159	.78443
520	16.14003	16.10902	.99808	22.80353	.78444
1	.15551	.12453	.99808	.82545	.78444
2	.17098	.14003	.99809	.84734	.78444
3	.18643	.15551	.99809	.86921	.78444
4	.20187	.17098	.99809	.89107	.78444
525	16.21729	16.18643	.99810	22.91290	.78445
6	.23270	.20187	.99810	.93471	.78445
7	.24809	.21729	.99810	.95650	.78445
8	.26347	.23270	.99811	.97827	.78445
9	.27883	.24809	.99811	23.00002	.78445
530	16.29418	16.26347	.99812	23.02175	.78445
1	.30952	.27884	.99812	.04346	.78446
2	.32484	.29419	.99812	.06515	.78446
3	.34015	.30952	.99813	.08681	.78446
4	.35544	.32484	.99813	.10846	.78446
535	16.37072	16.34015	.99813	23.13009	.78446
6	.38598	.35544	.99814	.15169	.78447
7	.40123	.37072	.99814	.17328	.78447
8	.41647	.38598	.99814	.19485	.78447
9	.43169	.40123	.99815	.21639	.78447
540	16.44690	16.41647	.99815	23.23792	.78447
1	.46209	.43169	.99815	.25943	.78447
2	.47727	.44690	.99816	.28091	.78448
3	.49244	.46209	.99816	.30238	.78448
4	.50759	.47727	.99816	.32383	.78448
545	16.52273	16.49244	.99817	23.34525	.78448
6	.53785	.50759	.99817	.36666	.78448
7	.55296	.52273	.99817	.38805	.78448
8	.56806	.53785	.99818	.40942	.78449
9	.58314	.55296	.99818	.43077	.78449

p	f(p)	g(p)	$\frac{g(p)}{f(p)}$	|S|	θ
550	16.59821	16.56806	.99818	23.45210	.78449
1	.61326	.58314	.99819	.47341	.78449
2	.62830	.59821	.99819	.49470	.78449
3	.64333	.61326	.99819	.51597	.78449
4	.65834	.62830	.99820	.53722	.78450
555	16.67335	16.64333	.99820	23.55846	.78450
6	.68833	.65834	.99820	.57967	.78450
7	.70331	.67335	.99821	.60087	.78450
8	.71827	.68833	.99821	.62204	.78450
9	.73321	.70331	.99821	.64320	.78450
560	16.74815	16.71827	.99822	23.66434	.78451
1	.76307	.73321	.99822	.68546	.78451
2	.77797	.74815	.99822	.70656	.78451
3	.79287	.76307	.99823	.72764	.78451
4	.80775	.77798	.99823	.74870	.78451
565	16.82262	16.79287	.99823	23.76975	.78451
6	.83747	.80775	.99823	.79077	.78451
7	.85231	.82262	.99824	.81178	.78452
8	.86714	.83747	.99824	.83277	.78452
9	.88196	.85231	.99824	.85374	.78452
570	16.89676	16.86714	.99825	23.87469	.78452
1	.91155	.88196	.99825	.89562	.78452
2	.92632	.89676	.99825	.91654	.78452
3	.94109	.91155	.99826	.93744	.78453
4	.95584	.92632	.99826	.95831	.78453
575	16.97058	16.94109	.99826	23.97918	.78453
6	.98530	.95584	.99827	24.00002	.78453
7	17.00001	.97058	.99827	.02084	.78453
8	.01471	.98530	.99827	.04165	.78453
9	.02940	17.00001	.99827	.06244	.78453
580	17.04407	17.01471	.99828	24.08321	.78454
1	.05873	.02940	.99828	.10396	.78454
2	.07338	.04407	.99828	.12469	.78454
3	.08802	.05873	.99829	.14541	.78454
4	.10264	.07338	.99829	.16611	.78454
585	17.11726	17.08802	.99829	24.18679	.78454
6	.13185	.10264	.99830	.20745	.78454
7	.14644	.11726	.99830	.22810	.78455
8	.16101	.13185	.99830	.24873	.78455
9	.17558	.14644	.99830	.26934	.78455
590	17.19013	17.16101	.99831	24.28993	.78455
1	.20466	.17558	.99831	.31051	.78455
2	.21919	.19013	.99831	.33107	.78455
3	.23370	.20466	.99832	.35161	.78455
4	.24820	.21919	.99832	.37213	.78456
595	17.26269	17.23370	.99832	24.39264	.78456
6	.27716	.24820	.99832	.41313	.78456
7	.29163	.26269	.99833	.43360	.78456
8	.30608	.27716	.99833	.45406	.78456
9	.32052	.29163	.99833	.47449	.78456

p	f(p)	g(p)	$\dfrac{g(p)}{f(p)}$	|S|	θ
600	17.33495	17.30608	.99833	24.49491	.78456
1	.34936	.32052	.99834	.51532	.78457
2	.36377	.33495	.99834	.53570	.78457
3	.37816	.34936	.99834	.55607	.78457
4	.39254	.36377	.99835	.57643	.78457
605	17.40691	17.37816	.99835	24.59676	.78457
6	.42126	.39254	.99835	.61708	.78457
7	.43561	.40691	.99835	.63739	.78457
8	.44994	.42126	.99836	.65767	.78458
9	.46426	.43561	.99836	.67794	.78458
610	17.47857	17.44994	.99836	24.69819	.78458
1	.49287	.46426	.99836	.71843	.78458
2	.50715	.47857	.99837	.73865	.78458
3	.52143	.49287	.99837	.75885	.78458
4	.53569	.50715	.99837	.77904	.78458
615	17.54994	17.52143	.99838	24.79921	.78459
6	.56418	.53569	.99838	.81936	.78459
7	.57841	.54994	.99838	.83950	.78459
8	.59262	.56418	.99838	.85962	.78459
9	.60683	.57841	.99839	.87973	.78459
620	17.62102	17.59262	.99839	24.89982	.78459
1	.63520	.60683	.99839	.91989	.78459
2	.64937	.62102	.99839	.93994	.78459
3	.66353	.63520	.99840	.95998	.78460
4	.67768	.64937	.99840	.98001	.78460
625	17.69182	17.66353	.99840	25.00002	.78460
6	.70594	.67768	.99840	.02001	.78460
7	.72006	.69182	.99841	.03998	.78460
8	.73416	.70594	.99841	.05994	.78460
9	.74825	.72006	.99841	.07989	.78460
630	17.76233	17.73416	.99841	25.09982	.78460
1	.77640	.74825	.99842	.11973	.78461
2	.79046	.76233	.99842	.13963	.78461
3	.80450	.77640	.99842	.15951	.78461
4	.81854	.79046	.99842	.17937	.78461
635	17.83257	17.80450	.99843	25.19922	.78461
6	.84658	.81854	.99843	.21906	.78461
7	.86058	.83257	.99843	.23887	.78461
8	.87457	.84658	.99843	.25868	.78461
9	.88855	.86058	.99844	.27846	.78462
640	17.90252	17.87457	.99844	25.29824	.78462
1	.91648	.88855	.99844	.31799	.78462
2	.93043	.90252	.99844	.33773	.78462
3	.94437	.91648	.99845	.35746	.78462
4	.95830	.93043	.99845	.37717	.78462
645	17.97221	17.94437	.99845	25.39687	.78462
6	.98612	.95830	.99845	.41654	.78462
7	18.00001	.97221	.99846	.43621	.78463
8	.01389	.98612	.99846	.45586	.78463
9	.02777	18.00001	.99846	.47549	.78463

p	f(p)	g(p)	$\dfrac{g(p)}{f(p)}$	$\lvert S \rvert$	θ
650	18.04163	18.01389	.99846	25.49511	.78463
1	.05548	.02777	.99847	.51472	.78463
2	.06932	.04163	.99847	.53431	.78463
3	.08315	.05548	.99847	.55388	.78463
4	.09697	.06932	.99847	.57344	.78463
655	18.11078	18.08315	.99847	25.59298	.78463
6	.12458	.09697	.99848	.61251	.78464
7	.13837	.11078	.99848	.63203	.78464
8	.15215	.12458	.99848	.65153	.78464
9	.16591	.13837	.99848	.67101	.78464
660	18.17967	18.15215	.99849	25.69048	.78464
1	.19342	.16591	.99849	.70993	.78464
2	.20715	.17967	.99849	.72938	.78464
3	.22088	.19342	.99849	.74880	.78464
4	.23459	.20715	.99850	.76821	.78465
665	18.24830	18.22088	.99850	25.78761	.78465
6	.26199	.23459	.99850	.80699	.78465
7	.27568	.24830	.99850	.82636	.78465
8	.28935	.26199	.99850	.84571	.78465
9	.30302	.27568	.99851	.86505	.78465
670	18.31667	18.28935	.99851	25.88437	.78465
1	.33031	.30302	.99851	.90368	.78465
2	.34395	.31667	.99851	.92298	.78465
3	.35757	.33031	.99852	.94226	.78466
4	.37118	.34395	.99852	.96152	.78466
675	18.38479	18.35757	.99852	25.98078	.78466
6	.39838	.37118	.99852	26.00001	.78466
7	.41196	.38479	.99852	.01924	.78466
8	.42554	.39838	.99853	.03845	.78466
9	.43910	.41196	.99853	.05764	.78466
680	18.45265	18.42554	.99853	26.07682	.78466
1	.46620	.43910	.99853	.09599	.78466
2	.47973	.45265	.99853	.11514	.78467
3	.49325	.46620	.99854	.13428	.78467
4	.50677	.47973	.99854	.15341	.78467
685	18.52027	18.49325	.99854	26.17252	.78467
6	.53376	.50677	.99854	.19162	.78467
7	.54725	.52027	.99855	.21070	.78467
8	.56072	.53376	.99855	.22977	.78467
9	.57419	.54725	.99855	.24882	.78467
690	18.58764	18.56072	.99855	26.26786	.78467
1	.60108	.57419	.99855	.28689	.78467
2	.61452	.58764	.99856	.30591	.78468
3	.62795	.60109	.99856	.32491	.78468
4	.64136	.61452	.99856	.34389	.78468
695	18.65477	18.62795	.99856	26.36287	.78468
6	.66816	.64136	.99856	.38183	.78468
7	.68155	.65477	.99857	.40077	.78468
8	.69493	.66816	.99857	.41970	.78468
9	.70830	.68155	.99857	.43862	.78468

p	f(p)	g(p)	$\frac{g(p)}{f(p)}$	$\lvert S \rvert$	θ
700	18.72165	18.69493	.99857	26.45753	.78468
1	.73500	.70830	.99857	.47642	.78468
2	.74834	.72165	.99858	.49530	.78469
3	.76167	.73500	.99858	.51416	.78469
4	.77499	.74834	.99858	.53301	.78469
705	18.78830	18.76167	.99858	26.55185	.78469
6	.80160	.77499	.99858	.57067	.78469
7	.81490	.78830	.99859	.58948	.78469
8	.82818	.80161	.99859	.60828	.78469
9	.84145	.81490	.99859	.62707	.78469
710	18.85472	18.82818	.99859	26.64584	.78469
1	.86797	.84145	.99859	.66460	.78469
2	.88122	.85472	.99860	.68334	.78470
3	.89445	.86797	.99860	.70207	.78470
4	.90768	.88122	.99860	.72079	.78470
715	18.92090	18.89445	.99860	26.73950	.78470
6	.93411	.90768	.99860	.75819	.78470
7	.94730	.92090	.99861	.77687	.78470
8	.96049	.93411	.99861	.79553	.78470
9	.97368	.94730	.99861	.81419	.78470
720	18.98685	18.96049	.99861	26.83283	.78470
1	19.00001	.97368	.99861	.85146	.78470
2	.01316	.98685	.99862	.87007	.78471
3	.02631	19.00001	.99862	.88867	.78471
4	.03944	.01316	.99862	.90726	.78471
725	19.05257	19.02631	.99862	26.92584	.78471
6	.06568	.03944	.99862	.94440	.78471
7	.07879	.05257	.99863	.96295	.78471
8	.09189	.06569	.99863	.98149	.78471
9	.10498	.07879	.99863	27.00001	.78471
730	19.11806	19.09189	.99863	27.01852	.78471
1	.13114	.10498	.99863	.03702	.78471
2	.14420	.11806	.99863	.05551	.78472
3	.15725	.13114	.99864	.07399	.78472
4	.17030	.14420	.99864	.09245	.78472
735	19.18333	19.15725	.99864	27.11090	.78472
6	.19636	.17030	.99864	.12933	.78472
7	.20938	.18334	.99864	.14776	.78472
8	.22239	.19636	.99865	.16617	.78472
9	.23539	.20938	.99865	.18457	.78472
740	19.24839	19.22239	.99865	27.20295	.78472
1	.26137	.23539	.99865	.22133	.78472
2	.27434	.24839	.99865	.23969	.78472
3	.28731	.26137	.99866	.25804	.78473
4	.30027	.27434	.99866	.27638	.78473
745	19.31322	19.28731	.99866	27.29470	.78473
6	.32616	.30027	.99866	.31301	.78473
7	.33909	.31322	.99866	.33131	.78473
8	.35201	.32616	.99866	.34960	.78473
9	.36493	.33909	.99867	.36788	.78473

p	f(p)	g(p)	$\dfrac{g(p)}{f(p)}$	$\lvert S\rvert$	θ
750	19.37783	19.35201	.99867	27.38614	.78473
1	.39073	.36493	.99867	.40439	.78473
2	.40362	.37783	.99867	.42263	.78473
3	.41650	.39073	.99867	.44086	.78473
4	.42937	.40362	.99867	.45907	.78474
755	19.44223	19.41650	.99868	27.47727	.78474
6	.45508	.42937	.99868	.49547	.78474
7	.46793	.44223	.99868	.51364	.78474
8	.48077	.45509	.99868	.53181	.78474
9	.49360	.46793	.99868	.54997	.78474
760	19.50642	19.48077	.99869	27.56811	.78474
1	.51923	.49360	.99869	.58624	.78474
2	.53203	.50642	.99869	.60436	.78474
3	.54483	.51923	.99869	.62247	.78474
4	.55762	.53203	.99869	.64056	.78474
765	19.57039	19.54483	.99869	27.65864	.78474
6	.58316	.55762	.99870	.67672	.78475
7	.59593	.57039	.99870	.69478	.78475
8	.60868	.58316	.99870	.71282	.78475
9	.62142	.59593	.99870	.73086	.78475
770	19.63416	19.60868	.99870	27.74889	.78475
1	.64689	.62143	.99870	.76690	.78475
2	.65961	.63416	.99871	.78490	.78475
3	.67232	.64689	.99871	.80289	.78475
4	.68503	.65961	.99871	.82087	.78475
775	19.69772	19.67232	.99871	27.83883	.78475
6	.71041	.68503	.99871	.85679	.78475
7	.72309	.69772	.99871	.87473	.78475
8	.73576	.71041	.99872	.89266	.78476
9	.74843	.72309	.99872	.91058	.78476
780	19.76108	19.73576	.99872	27.92849	.78476
1	.77373	.74843	.99872	.94639	.78476
2	.78637	.76108	.99872	.96427	.78476
3	.79900	.77373	.99872	.98215	.78476
4	.81162	.78637	.99873	28.00001	.78476
785	19.82424	19.79900	.99873	28.01786	.78476
6	.83684	.81162	.99873	.03570	.78476
7	.84944	.82424	.99873	.05353	.78476
8	.86203	.83684	.99873	.07135	.78476
9	.87461	.84944	.99873	.08915	.78476
790	19.88719	19.86203	.99873	28.10695	.78477
1	.89976	.87461	.99874	.12473	.78477
2	.91232	.88719	.99874	.14251	.78477
3	.92487	.89976	.99874	.16027	.78477
4	.93741	.91232	.99874	.17802	.78477
795	19.94994	19.92487	.99874	28.19576	.78477
6	.96247	.93741	.99874	.21348	.78477
7	.97499	.94995	.99875	.23120	.78477
8	.98750	.96247	.99875	.24890	.78477
9	20.00001	.97499	.99875	.26660	.78477

p	f(p)	g(p)	$\frac{g(p)}{f(p)}$	$\lvert S \rvert$	θ
800	20.01250	19.98750	.99875	28.28428	.78477
1	.02499	20.00001	.99875	.30195	.78477
2	.03747	.01250	.99875	.31962	.78477
3	.04995	.02499	.99876	.33727	.78478
4	.06241	.03747	.99876	.35490	.78478
805	20.07487	20.04995	.99876	28.37253	.78478
6	.08732	.06241	.99876	.39015	.78478
7	.09976	.07487	.99876	.40776	.78478
8	.11219	.08732	.99876	.42535	.78478
9	.12462	.09976	.99876	.44294	.78478
810	20.13704	20.11219	.99877	28.46051	.78478
1	.14945	.12462	.99877	.47807	.78478
2	.16185	.13704	.99877	.49562	.78478
3	.17425	.14945	.99877	.51317	.78478
4	.18664	.16185	.99877	.53070	.78478
815	20.19902	20.17425	.99877	28.54822	.78478
6	.21139	.18664	.99878	.56572	.78479
7	.22376	.19902	.99878	.58322	.78479
8	.23611	.21139	.99878	.60071	.78479
9	.24846	.22376	.99878	.61819	.78479
820	20.26081	20.23611	.99878	28.63565	.78479
1	.27314	.24846	.99878	.65311	.78479
2	.28547	.26081	.99878	.67055	.78479
3	.29779	.27314	.99879	.68799	.78479
4	.31010	.28547	.99879	.70541	.78479
825	20.32241	20.29779	.99879	28.72282	.78479
6	.33471	.31010	.99879	.74023	.78479
7	.34700	.32241	.99879	.75762	.78479
8	.35928	.33471	.99879	.77500	.78479
9	.37156	.34700	.99879	.79237	.78480
830	20.38382	20.35928	.99880	28.80973	.78480
1	.39609	.37156	.99880	.82708	.78480
2	.40834	.38382	.99880	.84442	.78480
3	.42058	.39609	.99880	.86175	.78480
4	.43282	.40834	.99880	.87907	.78480
835	20.44506	20.42059	.99880	28.89638	.78480
6	.45728	.43282	.99880	.91367	.78480
7	.46950	.44506	.99881	.93096	.78480
8	.48171	.45728	.99881	.94824	.78480
9	.49391	.46950	.99881	.96551	.78480
840	20.50610	20.48171	.99881	28.98276	.78480
1	.51829	.49391	.99881	29.00001	.78480
2	.53047	.50610	.99881	.01725	.78480
3	.54265	.51829	.99881	.03447	.78481
4	.55481	.53047	.99882	.05169	.78481
845	20.56697	20.54265	.99882	29.06889	.78481
6	.57912	.55481	.99882	.08609	.78481
7	.59127	.56697	.99882	.10327	.78481
8	.60340	.57912	.99882	.12045	.78481
9	.61554	.59127	.99882	.13761	.78481

p	f(p)	g(p)	$\frac{g(p)}{f(p)}$	|S|	θ
850	20.62766	20.60340	.99882	29.15477	.78481
1	.63977	.61554	.99883	.17191	.78481
2	.65188	.62766	.99883	.18905	.78481
3	.66399	.63977	.99883	.20617	.78481
4	.67608	.65188	.99883	.22329	.78481
855	20.68817	20.66399	.99883	29.24039	.78481
6	.70025	.67608	.99883	.25749	.78481
7	.71232	.68817	.99883	.27457	.78481
8	.72439	.70025	.99884	.29165	.78482
9	.73645	.71232	.99884	.30871	.78482
860	20.74850	20.72439	.99884	29.32577	.78482
1	.76055	.73645	.99884	.34281	.78482
2	.77258	.74850	.99884	.35985	.78482
3	.78462	.76055	.99884	.37687	.78482
4	.79664	.77259	.99884	.39389	.78482
865	20.80866	20.78462	.99884	29.41089	.78482
6	.82067	.79664	.99885	.42789	.78482
7	.83267	.80866	.99885	.44487	.78482
8	.84467	.82067	.99885	.46185	.78482
9	.85666	.83267	.99885	.47882	.78482
870	20.86864	20.84467	.99885	29.49577	.78482
1	.88062	.85666	.99885	.51272	.78482
2	.89259	.86864	.99885	.52966	.78482
3	.90455	.88062	.99886	.54658	.78483
4	.91651	.89259	.99886	.56350	.78483
875	20.92846	20.90455	.99886	29.58041	.78483
6	.94040	.91651	.99886	.59731	.78483
7	.95233	.92846	.99886	.61420	.78483
8	.96426	.94040	.99886	.63107	.78483
9	.97618	.95233	.99886	.64794	.78483
880	20.98810	20.96426	.99886	29.66480	.78483
1	21.00001	.97618	.99887	.68165	.78483
2	.01191	.98810	.99887	.69849	.78483
3	.02380	21.00001	.99887	.71533	.78483
4	.03569	.01191	.99887	.73215	.78483
885	21.04757	21.02380	.99887	29.74896	.78483
6	.05945	.03569	.99887	.76576	.78483
7	.07131	.04757	.99887	.78255	.78483
8	.08318	.05945	.99887	.79934	.78484
9	.09503	.07131	.99888	.81611	.78484
890	21.10688	21.08318	.99888	29.83288	.78484
1	.11872	.09503	.99888	.84963	.78484
2	.13055	.10688	.99888	.86638	.78484
3	.14238	.11872	.99888	.88311	.78484
4	.15420	.13055	.99888	.89984	.78484
895	21.16602	21.14238	.99888	29.91656	.78484
6	.17782	.15420	.99888	.93327	.78484
7	.18963	.16602	.99889	.94997	.78484
8	.20142	.17783	.99889	.96666	.78484
9	.21321	.18963	.99889	.98334	.78484

p	f(p)	g(p)	g(p)/f(p)	|S|	θ
900	21.22499	21.20142	.99889	30.00001	.78484
1	.23677	.21321	.99889	.01667	.78484
2	.24854	.22499	.99889	.03332	.78484
3	.26030	.23677	.99889	.04997	.78484
4	.27205	.24854	.99889	.06660	.78485
905	21.28380	21.26030	.99890	30.08323	.78485
6	.29555	.27205	.99890	.09984	.78485
7	.30728	.28380	.99890	.11645	.78485
8	.31901	.29555	.99890	.13305	.78485
9	.33074	.30728	.99890	.14964	.78485
910	21.34245	21.31901	.99890	30.16622	.78485
1	.35416	.33074	.99890	.18279	.78485
2	.36587	.34245	.99890	.19935	.78485
3	.37756	.35416	.99891	.21590	.78485
4	.38926	.36587	.99891	.23244	.78485
915	21.40094	21.37756	.99891	30.24898	.78485
6	.41262	.38926	.99891	.26550	.78485
7	.42429	.40094	.99891	.28202	.78485
8	.43596	.41262	.99891	.29852	.78485
9	.44762	.42429	.99891	.31502	.78485
920	21.45927	21.43596	.99891	30.33151	.78485
1	.47092	.44762	.99891	.34799	.78486
2	.48256	.45927	.99892	.36446	.78486
3	.49419	.47092	.99892	.38092	.78486
4	.50582	.48256	.99892	.39738	.78486
925	21.51744	21.49419	.99892	30.41382	.78486
6	.52906	.50582	.99892	.43026	.78486
7	.54067	.51744	.99892	.44668	.78486
8	.55227	.52906	.99892	.46310	.78486
9	.56386	.54067	.99892	.47951	.78486
930	21.57546	21.55227	.99893	30.49591	.78486
1	.58704	.56386	.99893	.51230	.78486
2	.59862	.57546	.99893	.52868	.78486
3	.61019	.58704	.99893	.54506	.78486
4	.62175	.59862	.99893	.56142	.78486
935	21.63331	21.61019	.99893	30.57778	.78486
6	.64487	.62175	.99893	.59413	.78486
7	.65641	.63331	.99893	.61046	.78486
8	.66795	.64487	.99893	.62679	.78487
9	.67949	.65641	.99894	.64312	.78487
940	21.69102	21.66795	.99894	30.65943	.78487
1	.70254	.67949	.99894	.67573	.78487
2	.71406	.69102	.99894	.69203	.78487
3	.72557	.70254	.99894	.70831	.78487
4	.73707	.71406	.99894	.72459	.78487
945	21.74857	21.72557	.99894	30.74086	.78487
6	.76006	.73707	.99894	.75712	.78487
7	.77155	.74857	.99894	.77337	.78487
8	.78303	.76006	.99895	.78962	.78487
9	.79450	.77155	.99895	.80585	.78487

p	f(p)	g(p)	$\dfrac{g(p)}{f(p)}$	$|S|$	θ
950	21.80597	21.78303	.99895	30.82208	.78487
1	.81743	.79450	.99895	.83830	.78487
2	.82889	.80597	.99895	.85451	.78487
3	.84034	.81743	.99895	.87071	.78487
4	.85178	.82889	.99895	.88690	.78487
955	21.86322	21.84034	.99895	30.90308	.78487
6	.87465	.85178	.99895	.91926	.78488
7	.88607	.86322	.99896	.93542	.78488
8	.89749	.87465	.99896	.95158	.78488
9	.90891	.88607	.99896	.96773	.78488
960	21.92032	21.89749	.99896	30.98388	.78488
1	.93172	.90891	.99896	31.00001	.78488
2	.94311	.92032	.99896	.01613	.78488
3	.95450	.93172	.99896	.03225	.78488
4	.96589	.94311	.99896	.04836	.78488
965	21.97727	21.95450	.99896	31.06446	.78488
6	.98864	.96589	.99897	.08055	.78488
7	22.00001	.97727	.99897	.09663	.78488
8	.01137	.98864	.99897	.11271	.78488
9	.02272	22.00001	.99897	.12877	.78488
970	22.03407	22.01137	.99897	31.14483	.78488
1	.04541	.02272	.99897	.16088	.78488
2	.05675	.03407	.99897	.17692	.78488
3	.06808	.04541	.99897	.19296	.78488
4	.07941	.05675	.99897	.20898	.78488
975	22.09073	22.06808	.99897	31.22500	.78489
6	.10204	.07941	.99898	.24101	.78489
7	.11335	.09073	.99898	.25701	.78489
8	.12465	.10204	.99898	.27300	.78489
9	.13595	.11335	.99898	.28898	.78489
980	22.14724	22.12465	.99898	31.30496	.78489
1	.15853	.13595	.99898	.32093	.78489
2	.16980	.14724	.99898	.33689	.78489
3	.18108	.15853	.99898	.35284	.78489
4	.19235	.16981	.99898	.36878	.78489
985	22.20361	22.18108	.99899	31.38472	.78489
6	.21487	.19235	.99899	.40064	.78489
7	.22612	.20361	.99899	.41656	.78489
8	.23736	.21487	.99899	.43248	.78489
9	.24860	.22612	.99899	.44838	.78489
990	22.25983	22.23736	.99899	31.46427	.78489
1	.27106	.24860	.99899	.48016	.78489
2	.28229	.25984	.99899	.49604	.78489
3	.29350	.27106	.99899	.51191	.78489
4	.30471	.28229	.99899	.52777	.78490
995	22.31592	22.29350	.99900	31.54363	.78490
6	.32712	.30471	.99900	.55948	.78490
7	.33831	.31592	.99900	.57531	.78490
8	.34950	.32712	.99900	.59115	.78490
9	.36069	.33831	.99900	.60697	.78490

APPENDIX A

Tables of the Function $\sqrt{1 \pm j\, p} = f(p) \pm j\, g(p)$

By

J. T. deBettencourt

I. Introduction

The complex radical $\sqrt{1 \pm j\, p}$, where p is real, occurs in equations in many fields of application such as wave propagation in dissipative media, transmission lines, and networks. Let us write

$$S = \sqrt{1 \pm j\, p} = f(p) \pm j\, g(p) = \left| S \right| e^{\pm j\,\theta} \tag{A.1}$$

where

$$f(p) = + \left[\frac{+\sqrt{1 + p^2} + 1}{2} \right]^{1/2} = \cosh\left(1/2 \sinh^{-1} p\right) \tag{A.2}$$

$$g(p) = + \left[\frac{+\sqrt{1 + p^2} - 1}{2} \right]^{1/2} = \sinh\left(1/2 \sinh^{-1} p\right) \tag{A.3}$$

II. Tables

The functions f(p) and g(p) were first computed by G. W. Pierce[64] and tables were published by King (reference 4, Appendix II). We have employed a digital computer in order to obtain values of these functions to five decimal places and to correct some typographical errors in previously published values. In addition to tabular values of f(p) and g(p) for various values of p, other useful quantities are tabulated. These are the ratio g(p)/f(p), the magnitude $\left| S \right| = (1 + p^2)^{1/4}$, and the angle $\theta = \tan^{-1} g(p)/f(p)$.

The ranges and steps in the range of p for which the values are computed are:

$$0 \leq p \leq 0.0099 \quad \text{in steps of } 0.0001 \quad (\text{Table 1})$$

$$0 \leq p \leq 0.099 \quad \text{in steps of } 0.001 \quad (\text{Table 2})$$

$$0 \leq p \leq 0.99 \quad \text{in steps of } 0.01 \quad (\text{Table 3})$$

$$0 \leq p \leq 99.9 \quad \text{in steps of } 0.1 \quad (\text{Table 4})$$

$$0 \leq p \leq 999.0 \quad \text{in steps of } 1.0 \quad (\text{Table 5})$$

The tabular values which follow are arranged sequentially according to these ranges of p.

III. Discussion of Tabular Computations

1. Preparation

These tables were computed by an IBM 704 electronic data processing machine. All calculations were made in single precision floating point, i.e., to 27 significant bits. The program was written in FORTRAN.

The functions were evaluated directly from the expressions stated above, with the exception of g(p) for which the algebraically equivalent expression

$$g(p) = \frac{p}{2 f(p)} \qquad (A.4)$$

was used. This avoided loss of accuracy due to subtraction of unity from a quantity differing only slightly from unity when p is small.

2. Verification

For every value of the argument p a checking function

$$r = \left[\left| S \right|^2 - 1 \right] \frac{\cos \theta}{\sin \theta} \qquad\qquad (A.5)$$

was also computed (except in Table 1). The quantity

$$\left| p - r \right|$$

was required to be less than 2^{-13} as a test of both the program and the calculations. (Algebraically $r \cong p$, and the expression for r indirectly includes all five of the computed functions.) In Table 1 the values of $|S|$ were too close to unity to permit calculating r with sufficient accuracy; however, this table was easily verified by inspection due to the regular behavior of the functions near the origin.

The FORTRAN source program was twice compiled and the tables were independently computed several days apart. The times of printing of the two output tapes were separated by a month. The two sets of print sheets were superimposed on a light table and visually inspected for digit overlap and legibility. The final plates from which these tables were printed were prepared by photographic means.

It is hoped that due to these special precautions there are no computer, printer or reproduction errors in the tables.

3. Accuracy

The maximum error (not most probable) which can accumulate due to truncation of calculations at 27 significant bits is:

$f(p)$ 2 parts in 2^{27}

$g(p)$ 3 parts in 2^{27}

$g(p)/f(p)$ 5.5 parts in 2^{27}

$|S|$ 5.5 parts in 2^{27}

θ 4.5 parts in 2^{27}

This implies that for the worst case (p = 999), considering both computational and round-off error, the tabular error (the amount by which the printed five place value may differ from the true value) can be no more than:

$f(p)$ $(0.5 + .04) \times 10^{-5}$

$g(p)$ $(0.5 + .05) \times 10^{-5}$

$g(p)/f(p)$ $(0.5 + .005) \times 10^{-5}$

$|S|$ $(0.5 + .13) \times 10^{-5}$

θ $(0.5 + .004) \times 10^{-5}$

4. Linear Interpolation

Linear interpolation (simple proportion) may be used to estimate values of these functions for arguments lying between those tabulated. Associated with interpolated values are two errors: the double tabular error, due to the combination of two tabular values, and the non-linearity error.

a. Example 1: Find f(1.55):

$$f(1.55) \doteq f(1.5) + \frac{1}{2}\left[f(1.6) - f(1.5)\right]$$

$$= 1.19261 \pm 2(0.54 \times 10^{-5}) \text{ at least}$$

A conservation bound for the non-linearity error, together with

its sign, may be obtained by second-differencing (in most regions of the tables); i.e.,

If $f(p)$ is the function,

p is the tabulation interval,

$0 \leq g < \Delta p$, and

$E\left[f(p)\right] = f(p)$ (interpolated) - $f(p)$ (True),

then

$E\left[f(p_1 + g)\right]$ lies between zero and the smaller of

$$\frac{g}{\Delta p} \left[f(p_2) - 2f(p_1) + f(p_0) \pm 4 \text{ (tabular error)} \right]$$

or

$$\left[1 - \frac{g}{\Delta p} \right] \left[f(p_3) - 2f(p_2) + f(p_1) \pm 4 \text{ (tabular error)} \right].$$

Choose + or - to maximize $|E|$.

b. Example 2: Find $E\left[f(1.55)\right]$:

$$\frac{g}{\Delta p} \left[f(1.6) = 2f(1.5) + f(1.4) \pm 4 \text{ (tabular error)} \right]$$

$$= \frac{1}{2} \left[.00011 + 4(0.54 \times 10^{-5}) \right]$$

$$= .000055 + .000011$$

$$= +.00007$$

Therefore

$$f(1.55) = 1.19261 \begin{array}{l} +0 +.00001 \\ -.00007 -.00001 \end{array}$$

$$= 1.19261 \begin{array}{l} +.00001 \\ -.00008 \end{array}$$

The derivation of this bound for E is valid everywhere except for

$$f(p) \text{ in the interval } (1.6, \ 1.9)$$

$$|S| \text{ in the interval } (1.3, \ 1.6)$$

where there exist points of inflection. We may say that in these regions the value of E is less than that nearby, although the sign is not known.

c. Example 3: Find $f(1.65)$ and $E\left[f(1.65)\right]$:

$$f(1.65) \doteq f(1.6) + \frac{1}{2}\left[f(1.7) = f(1.6)\right]$$

$$= 1.21025 \pm 2(0.54 \times 10^{-5}) \text{ at least}$$

$$\dot{E}\left[f(1.65)\right] = \text{is of the same order as } E\left[f(1.55)\right], \text{ but the sign is unknown.}$$

Hence

$$f(1.65) = 1.21025 \pm (.00007 + .00001)$$

$$= 1.21025 \pm .00008.$$

5. Approximations for Small and Large Values of p

a. Small p

When p is small compared with unity

$$
\left.
\begin{aligned}
f(p) &= 1 + \frac{p^2}{8} - - - - - \\[2mm]
g(p) &= \frac{p}{2}\left(1 - \frac{p^2}{8} - - - -\right) \\[2mm]
\frac{g(p)}{f(p)} &= \frac{p}{2}\left(1 - \frac{p^2}{4} - - - -\right) \\[2mm]
|S| &= 1 + \frac{p^2}{4} - - - - - - \\[2mm]
\theta &= \frac{p}{2}\left(1 - \frac{p^2}{3} - - - -\right)
\end{aligned}
\right\} \qquad \text{(A. 6)}
$$

If $p \leq 0.6$, the following approximate expressions may be used with an accuracy sufficient for many practical applications:

$$f(p) \cong 1 \qquad \text{(too low by 4\% or less)}$$

$$g(p) \cong \frac{p}{2} \qquad \text{(too high by 4\% or less)}$$

$$\frac{g(p)}{f(p)} \cong \frac{p}{2} \qquad \text{(too high by 8\% or less)}$$

$$|S| \cong 1 \qquad \text{(too low by 7\% or less)}$$

$$\theta \cong \frac{p}{2} \qquad \text{(too high by 10\% or less)}$$

$$(A.7)$$

b. Large p

When p is large compared with unity

$$f(p) = \sqrt{\frac{p}{2}} \left(1 + \frac{1}{2p} - - - - -\right)$$

$$g(p) = \sqrt{\frac{p}{2}} \left(1 - \frac{1}{2p} - - - -\right)$$

$$\frac{g(p)}{f(p)} = 1 - \frac{1}{p} - - - - - -$$

$$|S| = \sqrt{p} \left(1 + \frac{1}{4p^2} - - -\right)$$

$$\theta = \frac{\pi}{4} - \frac{1}{2p} \left(1 + \frac{1}{4p} - - - -\right)$$

$$(A.8)$$

If $p \geq 10$, the following approximate expressions may be used with an accuracy sufficient for many practical applications.

$$f(p) \cong \sqrt{\frac{p}{2}} \qquad \text{(too low by 5\% or less)}$$

$$g(p) \cong \sqrt{\frac{p}{2}} \qquad \text{(too high by 5\% or less)}$$

$$\frac{g(p)}{f(p)} \cong 1 \qquad \text{(too high by 10\% or less)} \qquad \qquad \text{(A.9)}$$

$$|S| \cong \sqrt{p} \qquad \text{(too low by 0.2\% or less)}$$

$$\theta \cong \frac{\pi}{4} \qquad \text{(too high by 7\% or less)}$$

c. Relation Between f(p) and g(p + 2)

It can be shown that f(p) exceeds g(p + 2) by less than

$$\frac{1}{4\,p^2\,g(p)}$$

For example, for p greater than 100 the difference is less than 3.6×10^{-6}.

This relation could be useful in extending these tables to large values of p, by eliminating the need to calculate and tabulate f(p) and g(p) separately.

IV. Applications

The various applications of the functions f(p) and g(p) were discussed by Pierce[64] and use has been made of these functions by King[4,5,6] and others.

For example, in radio wave propagation in a dissipative medium, the complex phase constant k of the medium is given by

$$k = +\omega\sqrt{\mu\,\varepsilon} = \beta - j\,\alpha \qquad \qquad \text{(A.10)}$$

A-8

where

$$\omega = 2 \pi f$$

f = wave frequency (cycles/sec)

μ = permeability of the medium = $\mu_o \mu_r$

ξ = complex dielectric factor

β = real phase constant

α = real attenuation constant

The complex dielectric factor ξ is given by

$$\xi = \epsilon - j \, \sigma/\omega = \epsilon (1 - j \, p) \tag{A. 11}$$

where

ϵ = real effective dielectric constant = $\epsilon_o \epsilon_r$

σ = real effective conductivity (mho/m)

p = loss tangent of the medium

The loss tangent p is given by

$$p = \frac{\sigma}{\omega \epsilon} = \frac{60 \sigma \lambda_o}{\epsilon_r} \tag{A. 12}$$

where mks units have been used and

λ_o = free space wavelength (meter)

ϵ_r = real effective relative dielectric constant

In most cases, the permeability μ is real and μ_r is the real effective relative permeability. In the above $\mu_o = 4 \pi \times 10^{-7}$ henry/m and $\epsilon_o \doteq \frac{1}{36 \pi} \times 10^{-9}$ farad/m.

A-9

With μ real and upon substituting equation (A.7) in equation (A.6), and using equation (A.1), then one obtains

$$
\left.
\begin{aligned}
k &= \beta - j\alpha = \beta(1 - j\,\frac{\alpha}{\beta}) = |k|\,e^{j\theta} \\[6pt]
\beta &= \omega\sqrt{\mu\epsilon_0}\ \sqrt{\epsilon_r}\ f(p) \\[6pt]
\alpha &= \omega\sqrt{\mu\epsilon_0}\ \sqrt{\epsilon_r}\ g(p) \\[6pt]
\frac{\alpha}{\beta} &= \frac{g(p)}{f(p)} \\[6pt]
|k| &= \omega\sqrt{\mu\epsilon_0}\ \sqrt{\epsilon_r}\ |S| \\[6pt]
|S| &= (1 + p^2)^{1/4} \\[6pt]
\theta &= \tan^{-1}\frac{\alpha}{\beta} = \tan^{-1}\frac{g(p)}{f(p)}
\end{aligned}
\right\} \qquad \text{(A.13)}
$$

In many cases in radio propagation, the dissipative media are non-magnetic whence $\mu_r = 1$. In such case

$$
\omega\sqrt{\mu\epsilon_0} = \omega\sqrt{\mu_0\epsilon_0} = \beta_0 = \frac{2\pi}{\lambda_0} \quad \text{(rad/meter)} \qquad \text{(A.14)}
$$

is the real phase constant in space.

The tables then provide the quantities needed to compute β, α, α/β, $|k|$ and θ according to the relations in (A.9). The results of course apply for a given set of electrical constants of the dissipative medium μ_r, ϵ_r and σ at the radian frequency ω of the wave, with p (loss tangent) given by equation (A.8).

A-10

For small and for large values of p, the approximate relations (A.7) and (A.9) may be used.

Thus for a non-magnetic, dissipative medium with small loss tangent $(p \leq 0.6)$

$$\beta \cong \beta_o \sqrt{\epsilon_r} \text{ (rad/m)}$$

$$\alpha \cong \frac{60 \pi \sigma}{\sqrt{\epsilon_r}} \text{ (nepers/m)} \tag{A.15}$$

but if the loss tangent is large $(p \geq 10)$, then

$$\beta \cong \alpha = \frac{1}{\tau} = \sqrt{\frac{\omega \mu_o \sigma}{2}} \tag{A.16}$$

where τ is known as the metallic skin depth, in meters.

V. Acknowledgement

The coordination of the computational work and the analysis in Section III was performed by D. H. Copp, Propagation and Systems Research Department, Communication and Data Processing Operation, Norwood. The problem preparation for the computer was written by Miss Carolyn Galante, Applied Mathematics, Bedford Computation Center.

APPENDIX B

Theory of Waveguide Propagation for Very Deep Strata

By

J. T. deBettencourt

I. Introduction

The theory of waveguide propagation in very deep strata in the earth's

crust assumes initially that the guiding walls are horizontal planes of infinite

or finite conductivity and that there is a sharply-bounded propagation medium

(rock) in between having small or zero conductivity such that the loss tangent*

is small ($p_2 \leq 0.6$).

The field expressions for waves guided between parallel planes can be

obtained by reference to many texts such as that of Jordan[3] which includes

the effect of losses in planes of finite but high metallic conductivity. For

our purposes, we prefer to follow the VLF propagation mode theory of

Budden[25] and Wait,[77] the first assuming a plane earth and ionosphere and

the latter treating more completely the same problem with extensions to the

effects of a spherical earth and ionosphere plus a development and discussion

of mode excitation for the waves in the air. We shall follow Wait's treat-

ment[77] for plane boundaries but with a modest extension. Instead of the air

we have slightly lossy propagation medium (rock). The ground is replaced

---

* The subscript "2" on quantities denoting loss tangent, dielectric constant
and conductivity is used to denote the propagation medium in which the waves
are excited and detected.

by the overburden, as one wall. The ionosphere is replaced by a discontinuity such as the Moho, for the other wall. In our case, the antennas stretch downward below the overburden, whereas in Wait's treatment the antennas extend upwards above the ground into air; the difference is in the value of dipole moment for the same power input to the input terminals. Regarding effects of curvature of the walls, wave modes impinging on the Moho would tend to "diverge" whereas those reflected from the ionosphere would tend to "converge." We will not consider curvature effects in any detail.

II. Theory

The field expressions have been developed for vertical electric dipoles. Assuming perfectly conducting planes, the modes are those of the transverse magnetic type $TM_{m,o}$ where subscript m if the mode number. The TM_{oo} mode (m = 0) is the transverse electromagnetic or TEM mode, and is represented in C of Figure I.4 of Section I of the Report by the direct ray between T and R parallel to the walls. Rays for the first order mode m = 1 are also shown and are due to reflections from the upper and lower walls. Excitation for a given mode depends upon whether the wave frequency exceeds or is less than the cut-off frequency f_{cm} for that mode. Let d be the distance between the parallel planes. Then for a loss-less dielectric of relative dielectric constant ϵ_{r2} and infinitely conducting walls, the values of f_{cm} are given by

$$f_{cm} = \frac{m \, v_o}{2 \sqrt{\epsilon_{r2}} \, d} \qquad (m = 0, 1, 2 - - -) \qquad (B.1)$$

B-2

where v_o is the velocity of light in space, with v_o and d measured in the same distance units. As an example of the calculation, let d = 20 km, ϵ_{r_2} = 4, whence

$$f_{cm} = 3.75\,m, \ kc \tag{B.2}$$

For a wave frequency f_{kc} in kc, then

$$\frac{f_{cm}}{f_{kc}} = 3.75\,m \tag{B.3}$$

The phase velocity of a reflected mode m down the "guide" is

$$v_{p_m} = \frac{v_o}{\sqrt{\epsilon_{r_2}}\ \sqrt{1 - f_{cm}^2/f^2}} \tag{B.4}$$

As long as $f > f_{cm}$ the radical is positive, and one has the guide wavelength

$$\lambda_{gm} = \frac{\lambda_o/\sqrt{\epsilon_{r2}}}{\sqrt{1 - (f_{cm}/f)^2}} = \frac{\lambda_2}{\sqrt{1 - (f_{cm}/f)^2}} \tag{B.5}$$

where λ_2 is the plane wave wavelength in the dielectric. At frequencies above cut-off, energy can be propagated down the guide with no exponential attenuation and the allowable modes of transmission are those with m = 0, 1, 2 - - -. The resultant field at a receiver is then the sum of all the waves with appropriate phase shifts and amplitudes for each taken into account.

If f is below cut-off f_{cm}, the propagation constant of the wave mode m along the guide

$$k_{gm} = \beta_{gm} - j\ \alpha_{gm} \tag{B.6}$$

B-3

becomes imaginary and there is no energy propagated as a wave, only exponential damping with attenuation constant α. In the example cited, with equations (B.2) and (B.3), a 10 kc excitation could be propagated down the "guide" with modes $m = 0$ (TEM), $m = 1$ (TM_{10}) and $m = 2$ (TM_{20}) but not the third order mode $m = 3$. All three "rays" identified by the modes $m = 0$, 1, and 2 would be combined at the receiver to give the resultant received field.

In Wait's treatment[77] the ratio f_{cm}/f for the loss-less dielectric and perfectly conducting walls is identified with a cosine symbol

$$C_m = \cos \theta_m = \frac{f_{cm}}{f} \tag{B.7}$$

where θ_m is the angle of incidence of the m-th ray upon the plane wall. For $m = 0$ (TEM), $\theta = 90^\circ$ and this mode wave propagates parallel to the planes. There are many other aspects and the reader is referred to the references cited for further details.

We now consider walls of "finite but very high" conductivity. The terminology is a relative matter but refers to the refractive index of the walls relative to the dielectric, or to the reflection coefficient of the wall to a ray impinging upon it from the dielectric. For infinitely conducting walls the reflection coefficient of the wall R_W is $+1$. The "finite but very high" conductivity condition is that which obtains when $\left| R_W \right|$ departs by only a small amount from $+1$. The reflection coefficient of the wall is related to the refractive index N_W of the wall relative to that of the rock, for the allowable modes m, by

$$R_{W_m} = \frac{N_W C_m - C_{W_m}}{N_W C_m + C_{W_m}} \qquad (B.8)$$

where

$$N_W = \frac{k_W}{k_2} = \sqrt{\frac{\epsilon_{r_W}(1 - j\, p_W)}{\epsilon_{r_2}(1 - j\, p_2)}} \qquad (B.9)$$

with k_W and k_2 being the complex phase constants, ϵ_{r_W} and ϵ_{r_2} the relative dielectric constants, and p_W and p_2 the loss tangents, of the wall and rock, respectively. The loss tangents are

$$
\left.
\begin{aligned}
p_W &= \frac{\sigma_W}{\epsilon_o \epsilon_{r_W} \omega} = \frac{60\, \sigma_W \lambda_o}{\epsilon_{r_W}} \\[2em]
p_2 &= \frac{\sigma_2}{\epsilon_o \epsilon_{r_2} \omega} = \frac{60\, \sigma_2 \lambda_o}{\epsilon_{r_2}}
\end{aligned}
\right\} \qquad (B.10)
$$

with σ_W and σ_2 being the conductivities of the wall and rock, respectively, and λ_o the free space wavelength.

In equation (B.8) the quantity C_{W_m} is like the cosine of an angle of incidence at the wall but given mathematically by

$$C_{W_m} = \sqrt{1 - \frac{\sin^2 \theta}{N_W^2}} \qquad (B.11)$$

For subsequent use, we define the symbol

$$S_m = \sqrt{1 - C_m^2} = \sin \theta_m \qquad (B.12)$$

Now for perfectly conducting walls, $\sigma_W \to \infty$, whence $N_W \to \infty$ $C_{W_m} \to 1$ and $R_{W_m} = +1$. The case considered here assumes a loss-less dielectric $\sigma_2 = 0 = p_2$ and σ_W so high that $p_W >> 1$. From equations (B.9) and (B.10), then

$$N_W \cong \sqrt{-j \; \frac{60 \; \sigma_W \; \lambda_o}{\epsilon_{r_2}}} \qquad \text{(B.13)}$$

If this value of N_W is very high, then C_{W_m} in equation (B.11) is very nearly unity. Hence the reflection coefficient in equation (B.8) can be writte

$$R_{W_m} \cong 1 - 2 \; \frac{C_{W_m}}{N_W C_m} \cong e^{-2} \left(\frac{q}{C_m} \right) \qquad \text{(B.14)}$$

where $\frac{q}{C_m}$ is a small quantity ($|q|^2 << |C_m|^2$), with

$$q = \frac{C_{W_m}}{N_W} \cong \frac{1}{N_W} \qquad \text{(B.15)}$$

The allowable modes m are determined from a knowledge of C_m, i.e., from the allowable incident angles θ_m (complex), where C_m is determined from Wait's reflection condition.[77] For two electrically different walls, media 1 and 3, bounding the propagating dielectric region 2, the resonance condition is

$$R_{W1}(m) \; R_{W3}(m) \; e^{-j \, 2 \, k_2 d} = e^{-j \, 2\pi m} \qquad \text{(B.16)}$$

Let us assume for simplicity that the walls are identical and have "finite but high" conductivity so that $R_{W1} = R_{W3} = R_W$ given by equation (B.14). The resonance condition, equation (B.16), for such a case results in

$$k_2 d\, C_m \cong \pi m + j\, \frac{\Delta}{C_m} \qquad (\text{if } |\Delta\, k_2 d| < < 1) \qquad\qquad \text{(B.17)}$$

where

$$\Delta = 2\, q = 2\, x\, \frac{C_{Wm}}{N_W} \cong \frac{2}{N_W} \qquad\qquad\qquad \text{(B.18)}$$

The resonance condition, equation (B.17), is solved for allowable values of

C_m (complex) and thence for the quantity S_m in equation (B.12) which appears

in the final expressions for field components. Even for a loss-less dielectric

propagating medium ($\sigma_2 = 0 = p_2$), the existence of finite conductivity walls

means that S_m is complex which results in exponential attenuation of the

component of each ray m, "down the guide." The resultant field, being the

sum of all allowable modes m, suffers exponential damping loss attributable

to losses in the walls experienced by each mode "reflection." When the walls

are perfectly conducting, $\sigma_W = \infty$ and C_m in equation (B.17) is a real

quantity if $\sigma_2 = 0$; in this case C_m reduces to the loss-less definition in

equation (B.7) and there is no exponential damping of each mode.

The final expressions for field components was given by Wait[77] for a

cylindrical coordinate system (ρ, $\emptyset$, z) where the exciting dipole is located

along the z-axis at $z = d_T$ and the resultant field is evaluated at radial dis-

tances ρ , angle $\emptyset$ about the z-axis and at a receiver distance $z = d_R$ verti-

cally away from the z = 0 plane. In our case, the z = 0 plane is the lower

boundary of the overburden, with z measured vertically downward. We con-

sider only vertically polarized electric radiators with current directed along

the z-axis. The allowable modes between parallel infinite planes at z = 0 and

z = d are $TM_{m,o}$ modes (m = 0, 1, 2, 3 - - -). The electric field at a point $(\rho, \emptyset, z)$ will have E_z and E_ρ components ($E_\emptyset = 0$) and the magnetic field will have only $H_\emptyset$ -component ($H_\rho = H_z = 0$). We consider only the resulting E_z field component, for plane walls.

For highly conducting walls ($p_W \geq 10$) the propagation constant k_W is

$$k_W = \omega \sqrt{\mu_o \, \epsilon_o \, \epsilon_{r_W} (1 - j \, p_W)} = \beta_W - j \, \alpha_W \cong \frac{1 - j}{\tau_W} \qquad \text{(B. 19)}$$

where the skin depth τ_W is given by

$$\tau_W \cong \frac{504}{\sqrt{f \, \sigma_W}} \quad \text{(in meters)} \qquad \text{(B. 20)}$$

where f is in cps and σ_W is in mhos/m.

For the slightly lossy propagating dielectric ($p_2 \leq 0.6$)

$$k_2 = \omega \sqrt{\mu_o \, \epsilon_o \, \epsilon_{r_2} (1 - j \, p_2)} = \beta_2 - j \, \alpha_2$$

$$= \beta_o \sqrt{\epsilon_{r_2}} \left[f(p_2) - j \, g(p_2) \right]$$

$$\cong \beta_o \sqrt{\epsilon_{r_2}} \left[1 - j \, \frac{p_2}{2} \right] \qquad \text{(B. 21)}$$

whence

$$\beta_2 \cong \beta_o \sqrt{\epsilon_{r_2}}$$

$$\alpha_2 = \beta_o \sqrt{\epsilon_{r_2}} \, \frac{p_2}{2} = \frac{60 \, \pi \, \sigma_2}{\sqrt{\epsilon_{r_2}}} \quad \text{(nepers/m)} \qquad \left. \right\} \qquad \text{(B. 22)}$$

B-8

It is with the case $p_W >> 10$ and $p_2 \leq 0.6$ that we shall be concerned. We further consider that the plane walls are of a thickness much greater than their metallic skin depth given by equation (B.20).

Following Wait's development but with the slight change to a dielectric of small loss tangent, the electric field component E_z is then the sum

$$E_z = \frac{\omega \mu_0 (I\,dz)_{d_T}}{2d} \sum_{m = 0, 1, 2}^{\infty} \delta_m (C_m) \, S_m^2 \, H_o^{(2)} (k_2 S_m \rho)$$

$$f_m (d_T) f_m (d_R) \tag{B.23}$$

where $(I\,dz)_{d_T}$ is the dipole moment of a center-driven, loss-less dipole of total length dz carrying a constant (with z) current I and located at a depth d_T. The quantity $H_o^{(2)} (k_2 S_m \rho)$ is the Hankel function of the second king of complex argument $k_2 S_m \rho$. The quantity S_m is given by equation (B.12) and behaves like a pattern factor. For perfectly conducting walls and a loss-less dielectric, and for frequencies above cut-off, $S_m = \sin \theta_m$. The factor S_m, in equation (B.23), appears once to give the z-component of a ray travelling at an angle θ_m away from the dipole source and once again to give the z-component of the wave reflected towards the receiver.

For a given depth d_T of the dipole having a moment $(I\,dz)_{d_T}$, the function $f_m (d_R)$ behaves as a "height-gain" function for the receiver. The functions $f_m (d_R)$ and $f_m (d_T)$ are given formally by

$$f_m(z) = \frac{e^{j k_2 C_m z} + R_W e^{-j k_2 C_m z}}{2 \sqrt{R_W}} \tag{B.24}$$

B-9

where z is d_T or d_R. For plane walls so highly conducting that $\left| N_W \right|^2 \gg 1$, then the plane wave reflection coefficient for vertical polarization R_W is very nearly unity and given in the exponential approximation by equation (B.14). In such case, the functions $f_m(z)$ can be written

$$f_m(z) = \cos \left(k_2 m z - j \frac{\Delta}{2 C_m} \right) \qquad (B.25)$$

For $z = 0$

$$f_m(z = 0) = \cosh \frac{\Delta}{2 C_m} \cong 1 \qquad (B.26)$$

if $\left| \Delta \right| \ll 2 \left| C_m \right|$, which is true for modes not too near grazing and is true for the cases considered here.

We consider from here on the source and observer to be so close to the boundary (i.e., $2z \ll d$) that $f_m(d_T) \cong 1 \cong f_m(d_R)$. We further assume that the source is so close to the boundary ($d_T \ll \frac{\lambda_2}{2\pi}$) that we can take its dipole moment $(I dz)_{d_T}$ as $(I dz)_o$. Then we may write

$$E_z = E_o' W \qquad (B.27)$$

where E_o' is a reference field and W is the field referred to E_o'. Following Wait's definition, the field E_o of the source $(I dz)_{d_T}$, in the medium at a large distance ρ on a perfectly conducting plane, is

$$E_o = j \frac{\omega \mu_o}{2\pi} (I dz)_{d_T} \frac{e^{-j k_2 \rho}}{\rho} \qquad \text{(far-field)}$$

$$= E_o' e^{-j (k_2 \rho - \pi/2)} \qquad (B.28)$$

B-10

where

$$E_o' = \frac{\omega \mu_o}{2\pi\rho} (I\,dz)_{d_T} \qquad (B.29)$$

If the source is located at $d_T = 0$, then

$$E_o' = \frac{\omega \mu_o}{2\pi\rho} (I\,dz)_o \qquad (B.30)$$

For empty space and a perfectly conducting plane, the value of E_o' in equation (B.30) is the familiar 300 mv/m (rms) at $\rho = 1$ km for 1 kw of radiated power. If the plane is not perfectly conducting, this value of E_o' for 1 kw input is reduced by $\sqrt{\dfrac{R_{rad}}{R_{rad} + R_{SW}}}$ where R_{SW} is the surface resistance of the plane wall. If the plane wall is perfectly conducting but the dielectric is loss-less with $\epsilon_{r_2} > 1$, then the reference value for 1 kw input is reduced by $(\epsilon_{r_2})^{-1/4}$. If the plane wall is not perfectly conducting and if the dielectric is lossy, the relations are more complicated. In any event, for a dipole located very close to the boundary plane, having a given dipole moment $(I\,dz)_o$, we retain the definition E_o' given in equation (B.30). Then W is given by

$$W = \frac{\pi\rho}{d} \sum_{m = 0, 1, 2 \, --}^{\infty} \delta_m (C_m) \, S_m^2 \, H_o^{(2)} (k_2 S_m \rho) \qquad (B.31)$$

In the far-field where it is assumed $|k_2 S_m \rho| > 1$, the Hankel function may be replaced by the first term in the asymptotic series expansion

$$H_o^{(2)} (x) \cong \frac{2}{\pi x} \, e^{j\pi/4} \, e^{-jx} \left[1 + j \frac{1}{8x} --- \right] \qquad (B.32)$$

whence equation (B. 32) may be approximated by

$$W \cong \frac{\pi \rho}{d} \sqrt{\frac{2}{\pi k_2 \rho}} \; e^{j \pi/4} \sum_{m = 0, 1 - - -}^{\infty} \delta_m (C_m) S_m^{3/2} e^{-j k_2 S_m}$$

$$\cong \sqrt{\frac{\rho / \lambda_2}{d / \lambda_2}} \; e^{j(\pi/4 + p_2/4)} \sum_{m = 0, 1 - - -}^{\infty} A_m \, e^{j \psi_m} \qquad \text{(B. 33b)}$$

(B. 33a)

if the propagating medium has a small loss tangent $p_2 \lesssim 0.6$.

In the form written in equation (B. 33b), A_m is the relative amplitude and ψ_m the total relative phase shift of mode m. It is with A_m and ψ_m that we shall be principally concerned, and thence to the evaluation of W which gives the final field relative to the reference value E_o'. Far-field conditions are assumed.

The components in equation (B. 33a) are each complex in general. We write each in complex notation and proceed to evaluate A_m and ψ_m. S_m is complex and may be written

$$S_m = S_m' - j S_m'' = \left| S_m \right| e^{-j \psi_{S_m}} = \sqrt{1 - C_m^2} \qquad \text{(B. 34)}$$

The imaginary component S_m'' gives rise to the exponential attenuation and the real component S_m' gives rise to the phase shift. In the exponential term

$$-j k_2 S_m \rho = -j (\beta_2 - j \alpha_2) (S_m' - j S_m'') \rho = -j (\beta_{gm} - j \alpha_{gm}) \rho$$

$$= - \alpha_{gm} \rho - j \beta_{gm} \rho = - A_{gm} - j \psi_{gm} \qquad \text{(B. 35)}$$

where β_{gm} and α_{gm} are the phase and attenuation constants per unit distance along the guide, and A_{gm} and ψ_{gm} are the total exponential

B-12

attenuation and phase shift of each mode m contributing to the E_z field in the far zone. With small loss tangent $p_2 \leq 0.6$, k_2 is given by equations (B.21) and (B.22)*, whence

$$\beta_{gm} = \beta_2 \, S_m' \left(1 - \frac{p_2}{2} \, \frac{S_m''}{S_m'}\right) \Bigg\}$$

$$\alpha_{gm} = \beta_2 \, S_m' \left(\frac{p_2}{2} + \frac{S_m''}{S_m'}\right) \Bigg\} \qquad \text{(B.36)}$$

$$A_{gm} = \alpha_{gm} \, \rho \Bigg\}$$

$$\gamma_{gm} = \beta_{gm} \, \rho \Bigg\} \qquad \text{(B.37)}$$

In the evaluations of S_m and $\delta_m (C_m)$, we need to evaluate the quantity Δ again by equation (B.18) and the quantity C_m from the resonant condition, equation (B.16). For the case of highly reflecting plane walls, we use equation (B.17) which assumes $\left| \Delta k_2 d \right| \ll 1$, with Δ being a small quantity.

For plane walls of large loss tangent ($p_W \geq 10$) and for a lossy dielectric of small loss tangent($p_2 \leq 0.6$), we may write

$$\Delta = \Delta' + j \, \Delta'' \simeq \frac{2}{N_W} \qquad \text{(B.38)}$$

where

$$\Delta' = \ell \left(1 + \frac{p_2}{2}\right), \quad \Delta'' = \ell \left(1 - \frac{p_2}{2}\right) \qquad \text{(B.39)}$$

$$\ell = \sqrt{2} \sqrt{\frac{\epsilon_{r2}}{60 \, \sigma_W \, \lambda_o}} \quad , \quad p_2 = \frac{60 \, \sigma_2 \, \lambda_o}{\epsilon_{r2}} \qquad \text{(B.40)}$$

---

* If the loss tangent p_2 is large, the values of β_2 and α_2 will have to be evaluated from tables of $f(p_2)$ and $g(p_2)$ in Appendix A.

and where both ℓ and p_2 are small quantities for the conditions assumed.

The restriction $\left| \Delta k_2 d \right| \ll 1$ is solved from

$$\Delta k_2 d \cong \ell \beta_2 d \left[(1 + p_2) + j (1 - p_2) \right]$$

$$\left| \Delta k_2 d \right| \cong \ell \sqrt{2} \; \beta_2 d \ll 1$$

(B. 41)

with $\beta_2 = 2 \pi / \lambda_2$ and $\lambda_2 \cong \lambda_o / \sqrt{\epsilon_{r_2}}$.

The value of C_m is obtained from the quadratic solution of equation (B. 17),
viz.

$$C_m = \frac{\pi m}{2 k_2 d} + \sqrt{ \left(\frac{\pi m}{2 k_2 d} \right)^2 + j \; \frac{\Delta}{k_2 d} }$$

$$= \frac{\pi m}{2 k_2 d} \left[1 + \sqrt{ 1 + j \; \frac{4 \Delta k_2 d}{\pi^2 m^2} } \right]$$

(B. 42)

For the zero-order mode m = 0,

$$C_o = \sqrt{ j \; \frac{\Delta}{k_2 d} }$$

$$S_o = \sqrt{ 1 - C_o^2 } = \sqrt{ 1 - j \frac{\Delta}{k_2 d} }$$

(B. 43)

The quantity $\dfrac{\Delta}{k_2 d}$ is given by

$$\frac{\Delta}{k_2 d} \cong \frac{\ell}{\beta_2 d} \; (1 + j)$$

(B. 44)

so that for m = 0

$$S_o = \sqrt{ 1 + \frac{\ell}{\beta_2 d} - j \frac{\ell}{\beta_2 d} }$$

(B. 45)

B-14

If $\ell/\beta_2 d$ is sufficiently small, then from equations (B.34) and (B.45),

$$S_o' \cong 1 + \frac{\ell}{\beta_2 d} = 1 \qquad |S_o| \cong 1$$

$$S_o'' \cong \frac{\ell}{2\beta_2 d} \qquad \psi_{S_o} \cong \frac{\ell}{2\beta_2 d} \qquad \qquad \text{(B.46)}$$

Before proceeding to modes $m \geq 1$, let us examine the various relations for perfectly conducting walls ($\sigma_W = \infty$) for which $N_W = \infty$, $R_W = 1$, for vertical polarization, and for a loss-less dielectric. Let us designate the resonant condition by C_m^o as that which obtains when $\Delta = 0$ and $p_2 = 0$. Then

$$C_m^o \equiv \left. \frac{\pi m}{k_2 d} \right|_{p_2 = 0} = \frac{\pi m}{\beta_2 d} = \left(\frac{f_{c_m}}{f} \right)_{\substack{\sigma_W = 0 \\ p_2 = 0}} \equiv \left(\frac{f_{c_m}}{f} \right)_o \qquad \text{(B.47)}$$

The corresponding value of S_m^o is

$$S_m^o = \sqrt{1 - (C_m^o)^2} = \sqrt{1 - \left(\frac{f_{c_m}}{f} \right)_o^2} \qquad \text{(B.48)}$$

Let

$$r = \left| 1 - (C_m^o)^2 \right| = \left| 1 - \left(\frac{f_{c_m}}{f} \right)_o^2 \right| \qquad \text{(B.49)}$$

If $f > f_{c_m}$, then S_m^o is real and

$$(S_m^o)' = \sqrt{r} \qquad (S_m^o)'' = 0$$

$$|S_m^o| = \sqrt{r} \qquad (\psi_{S_m^o}) = 0 \qquad \qquad \text{(B.50)}$$

and there is no exponential attenuation of the modes above cut-off.

If $f < f_{cm}$, then S_m^o is purely imaginary

$$S_m^o = -j \sqrt{r} = \left| S_m^o \right| e^{-j \Psi_{S_m^o}}$$

$$(S_m^o)' = 0 \qquad (S_m^o)'' = \sqrt{r} \qquad \qquad \qquad \text{(B.51)}$$

$$\left| S_m^o \right| = \sqrt{r} \qquad (\Psi_{S_m^o}) = \pi/2 = 90^o$$

and "modes" below cut-off are those of energy propagated only with exponential

damping.

For $m = 0$, we rewrite

$$S_o' \cong 1 = S_o^o , \qquad S_o'' = \frac{\ell}{2\beta_2 d}$$

$$\left| S_o \right| \cong 1 = \left| S_o^o \right| , \qquad \Psi_{S_o} = \frac{\ell}{2\beta_2 d} \qquad \qquad \text{(B.46a)}$$

For $m \geq 1$, and recalling that $\left| \Delta k_2 d \right| << 1$, then

$$S_m^2 \cong 1 - \frac{\pi^2 m^2}{k_2^2 d^2} - j \frac{2\Delta}{k_2 d}$$

$$\qquad \qquad \qquad \qquad \qquad \qquad \qquad \qquad \text{(B.52)}$$

$$= 1 - \frac{(C_m^o)^2}{1 - j P_2} - j \frac{2\ell}{\beta_2 d} (1 + j)$$

without further approximation.

If $p_2^2 << 1$, then

$$S_m^2 = (S_m^o)^2 + \frac{2\ell}{\beta_2 d} - j \, u \qquad \qquad \text{(B.53)}$$

where

$$u = \frac{2\ell}{\beta_2 d} + p_2 (C_m^o)^2 \tag{B.54}$$

Finally, with f not too near cut-off, i.e., $\frac{2\ell}{\beta_2 d} \ll (S_m^o)^2$, then for $m \geq 1$

$$\left.\begin{aligned}
S_m &\cong S_m^o - j \frac{u}{2 S_m^o} = S_m' - j S_m'' = |S_m| e^{-j \psi_{S_m}} \\[2mm]
S_m' &\cong S_m^o \qquad\qquad S_m'' \cong \frac{u}{2 S_m^o} \\[2mm]
|S_m| &\cong S_m^o \left[1 + \frac{1}{8} \left(\frac{u}{S_m^o}\right)^2\right] \cong S_m^o \\[2mm]
\psi_{S_m} &= \tan^{-1} \frac{S_m''}{S_m'} \cong \tan^{-1} \frac{u}{2 (S_m^o)^2} \cong \frac{u}{2 (S_m^o)^2}
\end{aligned}\right\} \tag{B.55}$$

For the function $\delta_m(C_m)$, under the restriction $|\Delta k_2 d| \ll 1$ (i.e., excitation of modes is proportional to δ_m), one has

$$\frac{1}{\delta_m(C_m)} \equiv \left[1 + j \frac{1}{2 k_2 d R_W^2} \frac{\partial}{\partial C} (R_W^2)\right]_{C = C_m} \tag{B.56a}$$

$$\cong \left[1 + j \frac{\Delta}{k_2 d C_m^2}\right] \tag{B.56b}$$

For $m = 0$, using C_o in equation (B.43), and writing $\delta_m(C_m)$ in complex form

$$\delta_m(C_m) = \delta_m' - j \delta_m'' = |\delta_m| e^{-j \psi_{\delta_m}} \tag{B.57}$$

we have

$$\delta_0(C_0) = \delta_0' - j\,\delta_0'' = |\delta_0|\,e^{-j\,\psi_{\delta_0}}$$

$$\delta_0' = 1/2 \qquad \delta_0'' = 0$$

$$|\delta_0| = 1/2 \qquad \psi_{\delta_0} = 0$$

$$\left.\right\} \quad \text{(B.58)}$$

For $m \geq 1$, and making use of the resonant condition (B.17), equation (B.56b) becomes

$$\frac{1}{\delta_m(C_m)} = \left[2 - \frac{\pi\,m}{k_2 d\,C_m}\right] = \frac{1}{|\delta_m|}\,e^{j\,\psi_{\delta_m}} \qquad \text{(B.59)}$$

Using the value of C_m from equation (B.42) together with the restriction $|\Delta k_2 d| << (2\pi m)^2$ that applies here,

$$|\delta_m| \cong 1$$

$$\psi_{\delta_m} \cong \ell\frac{\beta_2 d}{\pi^2 m^2} \cong 0$$

$$\left.\right\} \quad \text{(B.60)}$$

In summation, with the values of $\delta_m(C_m)$, S_m, and $e^{-j\,k_2 S_m \rho}$ defined as above for $m = 0$ and for $m \geq 1$, the values of $A_m\,e^{j\,\psi_m}$ in equation (B.33b) can be expressed as follows

$$A_m = |\delta_m|\,|S_m|^{3/2}\,e^{-A_{gm}} \qquad \text{(B.61a)}$$

$$\psi_m = (\psi_\delta + \frac{3}{2}\,\psi_S + \psi_g)_m \qquad \text{(B.61b)}$$

III. Sample Calculations, f = 10 kc

For illustration, we shall consider only those modes of propagation at a frequency f which are above cut-off frequencies f_{c_m}. For $m = 0$, values of $\left| \mathcal{S}_o \right|$ and $\gamma_{\mathcal{S}_o}$, $\left| S_o \right|$ and γ_{S_o}, and A_{g_o} and γ_{g_o} are given, respectively by equations (B.58), (B.46), and (B.37) where appropriate values of S_o' and S_o'' are used. For $m \geq 1$, values of $\left| \mathcal{S}_m \right|$ and $\gamma_{\mathcal{S}_m}$, $\left| S_m \right|$ and $\gamma_{\mathcal{S}_m}$, and A_{g_m} and γ_{g_m} are given, respectively by equations (B.60), (B.55) and (B.37). The results are illustrated by several examples to follow, in which the modes are excited by radiation from a vertically polarized elementary dipole located just below the upper plane, the waves being propagated in a dielectric between this plane and a lower parallel plane at a depth d below the upper plane. The frequency assumed is 10 kc (λ_o = 30 km).

1. Air Dielectric, perfectly conducting identical plane walls, d = 20 km

This simplest of all cases is governed by

$$\epsilon_{r_2} = 1 \qquad \sigma_w = \infty$$

$$\sigma_2 = 0 = p_2 \qquad N_w = \infty \qquad R_w = 1 \qquad \text{(B.62)}$$

For this case $\Delta = 0 = \ell = u$. The cut-off frequency, given by equation (B.1) is

$$f_{c_m} = 7.5 \, m, \; \text{(kc)} \; , \qquad \epsilon_{r_2} = 1 \qquad \text{(B.63)}$$

The TM_{oo} (TEM) will be propagated as will the $TM_{1,0}$ mode. All higher modes will be such that f is below cut-off f_{c_m}.

2. **Loss-Less Dielectric** ($\epsilon_{r_2} > 1$), **perfectly conducting, identical walls,** $d = 20$ km

To illustrate this case, it was assumed that

$$\epsilon_{r_2} = 4 \qquad \sigma_2 = 0 \qquad \sigma_W = \infty \qquad N_W = \infty$$

$$P_2 = 0 \qquad \lambda_2 = 15 \text{ km} \qquad R_W = 1 \qquad\qquad (B.64)$$

$$\Delta = 0 = \ell = u$$

The frequencies of the (loss-less) cut-off modes are given by equation (B. 1) and become

$$f_{cm} = 3.75 \, m \ \ \text{kc} \quad (\epsilon_{r_2} = 4) \qquad\qquad (B.65)$$

Hence, for a 10 kc wave modes $m = 0$, 1 and 2 can be propagated without exponential damping. Values of E_z were calculated for 1 kw radiated into the dielectric (region 2) and for distances $15 \leq \rho \leq 100$ km. For these calculations,

$$m = 0 \quad C_o = 0 \qquad S_o = 1.0000 \qquad \varsigma_o = 1/2 \quad A_o = 0.5000$$

$$m = 1 \quad C_1 = .375 \quad S_1 = .9090 \qquad \varsigma_1 = 1 \qquad A_1 = 0.9090$$

$$m = 2 \quad C_2 = .75 \quad S_2 = .6614 \qquad \varsigma_2 = 2 \qquad A_2 = 0.6614$$

$$(B.66)$$

The TEM mode ($m = 0$) is weaker than the $TM_{1,0}$ mode even though the latter travels a greater distance in the dielectric.

Calculations of $E_o^!$, W and hence E_z were made for $\rho \geq 15$ km for which $2\pi S_m \rho / \lambda_2 > 1$ so that the large argument expansion of $H_o^{(2)} (\beta_2 S_m \rho)$ could be used and the approximate far-field relations employed. The results

are shown plotted on the upper curve in Figure I. 5 of Section I of the Report, with E_o' shown as a reference (this has a value 3 db less than the inverse distance value for air, for one kilowatt radiated power). The minima and maxima in E_z are the result of destructive and constructive interference of the three modes, and E_z will oscillate below and above the inverse distance reference value E_o' as the relative value W varies with distance ρ. On the curve, a minimum occurs at ρ near 28 km, a broad maximum near 50 km and a second minimum near 100 km. If a 10 kc signal were to be propagated under the assumed conditions, an optimum distance occurs at about 50 km.

The curve of Figure I. 5 should serve only as an illustration for further discussion of waveguide modes. In this loss-less case, for the same value of d, use of higher frequencies allows more and more modes of propagation. The resultant mode interference is more complicated. Also, for a given frequency, fewer modes can be propagated as the plane separation depth d decreases. Thus, if d were 10 km, cut-off frequencies are $f_{c_m} = 7.5$ m kc and a 10 kc signal could be propagated only by the TEM (TM_{oo}) and $TM_{1,0}$ modes. If the lower discontinuity were a plane at $d \leq 5$ km, only the TEM (m = 0) mode would be propagated for a 10 kc excitation.

3. **Low-Loss Dielectric**, perfectly conducting identical plane walls

For illustration we assume d = 20 km and f = 10 kc as before, but it is assumed the loss-tangent p_2 is very small and not zero. The electric constants and related factors assumed for calculation are (at 10 kc),

$$\sigma_2 = 10^{-6} \text{ mhos/m} \qquad \sigma_W = \infty$$

$$\mathcal{E}_{r_2} = 4 \qquad\qquad N_W = \infty \qquad\qquad\Bigg\} \quad (B.67)$$

$$P_2 = 0.45 \qquad\qquad R_W = +1$$

Then $\lambda_2 \cong \lambda_0/\sqrt{\mathcal{E}_{r_2}}$ = 15 km and the exponential attenuation constant

$\alpha_2 \cong 60 \, \pi \, \sigma_2/\sqrt{\mathcal{E}_{r_2}}$ = 9.425 x 10^{-2} nepers/km = 0.82 db/km.

One consequence of dielectric losses is that care must be taken in the definition of reference field E_o or E_o' for a given "radiated power," and examination must be made of the term "radiation resistance." The subject has been treated by numerous authors such as King,[51] Tai,[69] and Wait[75] and is touched upon in Appendix G. The current on the dipole may be obtained from a knowledge of the input power P_{in} and the resistance of the dipole at the input terminals. The reference field in the far-zone may be obtained by a reference to P_{in}.

Referring the field to that from a dipole radiator of known dipole moment I dz, another consequence of dissipation in the propagating medium is that higher order modes, travelling greater distances, contribute less and less to the mode sum than lower order modes. This is because values of C_m from the resonance condition for perfectly conducting walls is complex and consequently so is S_m. The imaginary part S_m'' of S_m gives rise principally to exponential attenuation with coefficient $\beta_2 S_m' \cong \dfrac{2\pi}{\lambda_2} S_m'$ per unit distance if the loss tangent p_2 is small.

Calculations of the field E_z vs distance ρ were made using the assumed conditions (B. 67). The dipole moment was assumed to be the same as that for the case $\sigma_2 = 0$, i.e., $Idz = 16,900$ amp. m. (rms). The results are plotted in the lower curve of Figure I. 5 of Section I of the Report, the curve being labelled "E_z ($\sigma_2 = 10^{-6}$ mhos/m)". The two curves of E_z for $\sigma_2 = 0$ and $\sigma_2 = 10^{-6}$ mhos/m may thus be compared for dipoles having the same dipole moment, not input power.

Note that the curve for $\sigma_2 = 10^{-6}$ oscillates about the curve $E_o' \, e^{-\alpha_2 \rho}$ for the TEM (m = 0) mode, the excursions being less and the curve smoother then the upper curve for $\sigma_2 = 0$. Further discussion of the curves is given in the text of Section IB of the Report:

More extensive calculations by digital computers were being planned as this present contract period was completed.

4. Loss-Less Dielectric, highly identical conducting walls

The assumed constants for this case were $\sigma_W = 10^{-2}$ mhos/m with $p_W \gg 1$, $\epsilon_{r_2} = 4$, $\sigma_2 = 10^{-6}$ mhos/m, $d = 20$ km, $f = 10$ kc, $p_2 = 0.45$. Some spot calculations have been made by desk computers, the results (not plotted) showing further smoothing of the previous curve and that mode m = 2 is quite weak.

Calculations should be carried out by digital computers for other depths to the lower discontinuity d and other frequencies f.

B-23

5. Effect of Earth's Curvature

The effect of earth's curvature has not been formalized. Even if the ranges should turn out to be so large that curvature effects might be included, it is not expected that one would find areas in the earth's crust to remain homogeneous and of very low conductivity over such distances. Consequently, it is not planned to study the effect of earth's curvature at this stage.

APPENDIX C

Theory of Radio Wave Propagation in Rock Near and Below an Overburden-Rock Interface

By

J. Carolan

I. Introduction

There are several possible propagation modes between antennas immersed in a rock medium situated below a conducting top layer (e.g. overburden) at VLF or LF frequency ranges. For example, waves may travel via an "up-over-and-down" (UOD) mode, i.e., from the source in the rock, up through the overburden, along the surface, back down through the overburden and to the receiver. This mode is particularly effective when the overburden layer is electrically so thin that its influence may be neglected. The field expressions of Moore,[60,61] specialized for dipoles in sea water, may be extended for use here.

There is a possible deep waveguide mode (reference 89 and Appendix B) which could exist for waves in a rock medium guided between a thick, highly conducting layer on top (e.g., overburden or sea water) and one below (e.g., the Mohorovic discontinuity). This mode would be effective if the conductivity were very small (less than 10^{-7} mhos/m, for example) over large volumes in the earth's crust (see Section IB of Report).

The mode discussed in this note is that of waves in a semi-infinite rock medium below a more highly conducting medium (overburden) guided along the boundary to a receiving point also in the rock. In concept, this "interface

wave" mode is similar to that for the ground wave in air with dipoles above the ground, where the rock with complex phase constant k_1 has replaced the air with real phase constant β_o. The "interface wave" mode would be the resultant of a "direct wave," a "reflected wave" due to reflection from the overburden, and an "interface surface wave" along the rock-overburden boundary.

It was thought intuitively that as transmitting dipole and receiving point were lowered below the interface one would encounter a "depth gain" similar to the "height gain" for dipoles elevated in air above ground. If so, then the "depth gain" for the interface rock wave might afford a means of determining whether a received signal was due predominantly to such a wave or to the possible propagation by the up-over-and-down mode.

It is the purpose of this note to outline the approach and approximate solution for vertical electric dipoles and further to give sample calculations of the interface wave for a particular propagation path being experimentally investigated.

Section II contains a summary of the theoretical approach and approximate solutions. The sample calculations are discussed and results plotted on curves in Section III. The results are discussed in Section IV.

II. Theoretical Development for Vertical Electric Dipoles

The model assumed is shown in the insert in Figure C. 1. A vertical electric dipole source is located along the z-axis of a cylindrical coordinate system (ρ, θ, z) in region 1 (rock) at a distance d below the plane boundary
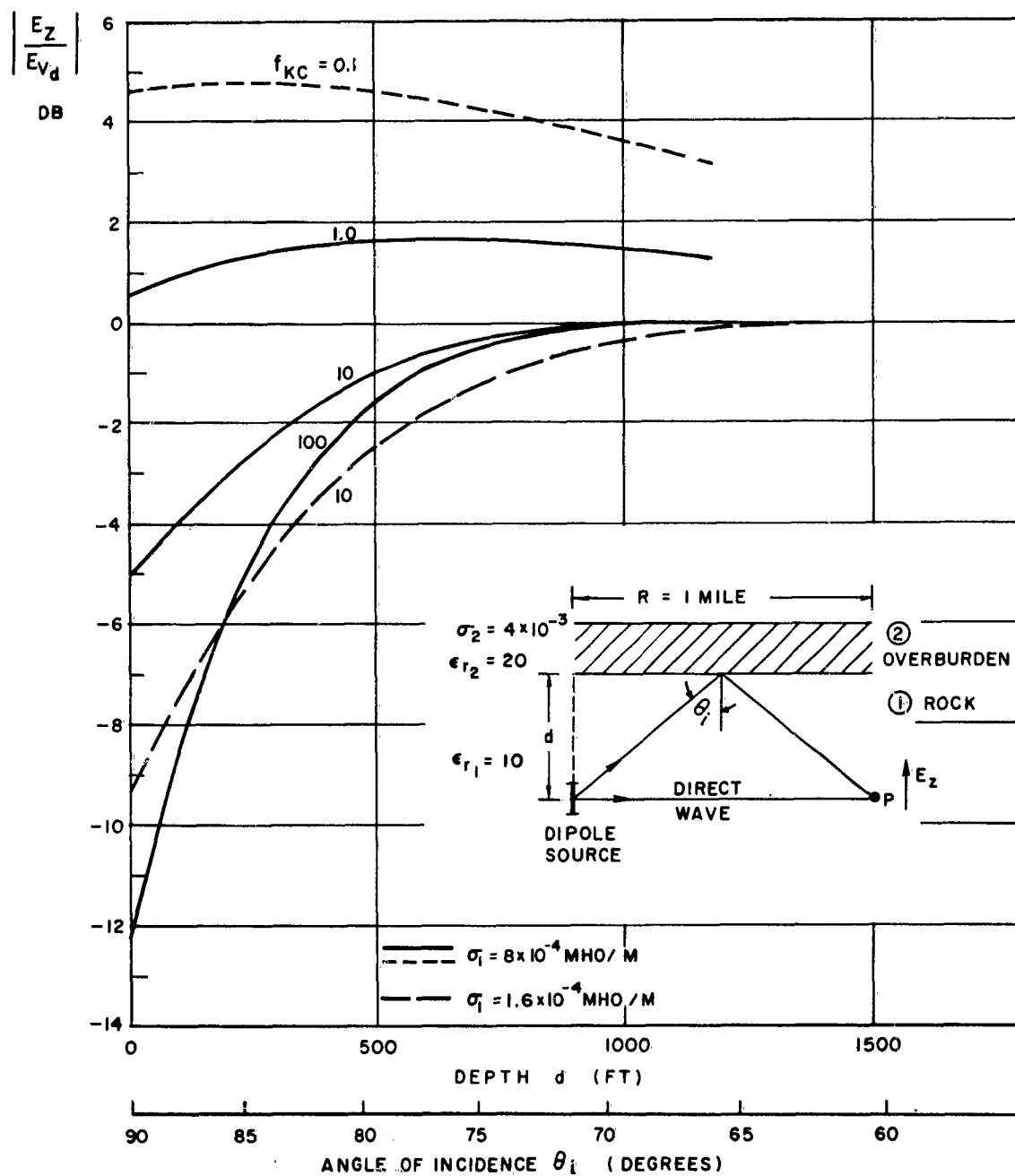
Figure C.1. Normalized vertical electric field $\left|E_z/E_{V_d}\right|$ in rock for vertical electric dipole source and point of observation located at depth d below overburden.

($z = 0$) of region 2 (overburden). Both media are assumed semi-infinite, homogeneous and non-magnetic. It is desired to determine the field at another point in region 1.

The complex phase constant for region n ($n = 1, 2$) is given by

$$k_n = \omega \sqrt{\mu_o \xi_n} \qquad (C.1)$$

where

$$
\left.
\begin{aligned}
&\xi_n = \text{complex dielectric factor} = \epsilon_o \epsilon_{r_n} (1 - j\, p_n) \\
&\epsilon_{r_n} = \text{relative effective dielectric constant} \\
&p_n = \text{loss tangent} = \sigma_n / (\omega \epsilon_o \epsilon_{r_n}) = 60\ \sigma_n \lambda_o / \epsilon_{r_n} \\
&\sigma_n = \text{effective conductivity} \\
&\lambda_o = \text{wavelength in free space}
\end{aligned}
\right\} \qquad (C.2)
$$

and mks units are employed.

For vertical electric dipoles in region 1, the Hertzian potential has only a z-component. The development of expressions for the electric field then follows that for vertical dipoles in air above ground (reference 5, Chapter VII; references 62 and 79) except that for region 1 rock with complex phase constant k_1 has replaced air with real phase constant β_o. Of importance is the relative refractive index N_{21} of waves incident from region 1 upon region 2, where

$$N_{21}^2 = \left(\frac{k_2}{k_1} \right)^2 = \frac{\epsilon_{r_2} (1 - j\, p_2)}{\epsilon_{r_1} (1 - j\, p_1)} \qquad (C.3)$$

It is assumed that $\left|N_{21}\right|^2$ will be moderately large. Frequencies of interest are less than 100 kc, and at such frequencies the loss tangents p_n, given by equation (C.2) will be large ($p_n \geq 10$) for the typical electrical constants assumed for each medium. N_{21}^2 then is essentially real and given approximately by the conductivity contrast ratio σ_2/σ_1 (there is a small imaginary component which is negative when $p_2 > p_1$).

The electrical field in the rock may be considered as the sum of several components like those of Norton[62] for dipoles in air above ground. The resultant wave may be termed the "interface wave" and in the far field it is the resultant of a "direct wave" between dipole and point of observation, a "reflected wave" from the overburden, and an "interface surface wave" guided along the rock-overburden boundary. For the sample calculations, it was necessary to include higher order correction terms (reference 5, Chapter VII).

The complex numberical distance for antennas on the boundary may be written[79] in polar form

$$P_e = \left|P_e\right| e^{-jb} \tag{C.4}$$

In the usual expressions[5,79] for p_e, complex phase constant k_1 for rock replaces real phase constant β_o for air. With large loss tangents for both media, N_{21}^2 in equation (C.3) is practically real and the phase angle b in equation (C.4) is close to 135°. The general complex numerical distance W for antennas below the boundary may be written as

$$W = P e^{-jB} \tag{C.5}$$

and the phase angle B is 135° for N_{21}^2 real.

III. Example of Calculations

Propagation over a one-mile path between antennas in drill holes on Cape Cod was being investigated and physical data typical for such a path were assumed for calculations. The electrical constants assumed were $\epsilon_{r_1} = 10$ and $\sigma_1 = 8 \times 10^{-4}$ mhos/m for the rock, and $\epsilon_{r_2} = 20$ and $\sigma_2 = 4 \times 10^{-3}$ mhos/m for the overburden. (In one case, for 10 kc, a second computation was made for $\sigma_1 = 1.6 \times 10^{-3}$ mhos/m.)

The frequencies of interest were 100 kc and less, at which the loss tangents p_1 and p_2 exceeded 10. Values of $\left| N_{21} \right|^2$ were about 5. Further, the depths below the overburden of the dipole source and of the point of observation were assumed identical, of value d. The curves in King (reference 5, Chapter VII) for the complex "ground wave" attenuation function F were used with B = 135°. For small values of P it was necessary to compute F using the series expansion expressions (references 5, Chapter VII; 62 and 79). It was also necessary to include correction terms in the field equations to account for near-zone conditions, particularly at the lower frequencies.

The vertical and horizontal components of electric field were computed for several frequencies from 0.1 to 100 kc as a function of depth d. The resulting amplitudes were normalized to the amplitude $\left| E_{V_d} \right|$ of the vertical direct-wave component of the electric field, which component contained additional near-field correction terms. Only the magnitudes of the normalized vertical electric field $\left| E_z / E_{V_d} \right|$ at the observing point P are shown plotted on the curves of Figure C. 1.

IV. Discussion of Results

Referring to the curves in Figure C. 1 for angles near grazing incidence, the "interface surface wave" predominates, and at frequencies higher than 1 kc this component is weaker than the "direct wave" component of the total field for the assumed conditions. At frequencies higher than 1 kc, $|E_z|$ increases with depth (angle of incidence decreasing) and approaches the "direct wave" value at larger and larger depths. The increase of $|E_z|$ with depth is the sharper the higher the frequency. Such variations are attributed to the relatively stronger effects of exponential damping in the rock on the "reflected wave" and "interface surface wave" components than on the "direct wave" component. The curve for 0. 1 kc is suspect because the validity of the assumptions is questionable for such low frequencies; it is shown in small dashes in Figure C. 1. At 10 kc, where curves are shown for two values of σ_1, the general remarks on behavior of normalized $|E_z|$ with depth apply, but for the higher conductivity case the "interface surface wave" component is less and hence there is a greater relative increase in normalized $|E_z|$ with increasing depth.

Calculations were made for the radial component of the electric field but are not included here because (a) we have not devised a practical means for its measurement in drill holes, (b) the vertical component $|E_z|$ is the stronger, and (c) the radial component decreases with increased depth (see below).

The measurement of the variation of $|E_z|$ with depth is suggested as one possible means to determine whether the received signal is due predominantly to the rock propagated mode discussed or to a possible up-over-and-down (UOD) mode. Field expressions for the latter three-medium problem are not available. However, for a given source-observer separation one would expect the field for the UOD mode to vary with the depth d according to $e^{-2\alpha_1 d}$ where α_1 is the attenuation constant for the rock. Thus at 10 kc with $\sigma_1 = 8 \times 10^{-4}$ mhos/m, $\alpha_1 = 1.5$ db/100 ft. For a 500 foot increase in depth, the contribution to the received signal should <u>decrease</u> by 15 db whereas $|E_z|$ should <u>increase</u> toward the direct wave value according to Figure C.1, the amount of increase depending upon the starting value of d (e.g., 3 db for the depth range 100 to 600 feet).

While the theory for the vertical electric dipole assumes an overburden of infinite thickness, the expressions for the field in the rock should not be affected seriously by the influence of the air-overburden boundary if the overburden is several skin depths in thickness. This is principally because of the exponential damping of 8.7 db per skin depth (55 db per wavelength) of travel each way in the highly conducting overburden.

With antennas very near the overburden the received field intensity is due principally to the "interface surface wave" component. At frequencies above 1 kc a more effective communication link is achieved by increasing the depth of the transmitting and receiving antennas.

APPENDIX D
Uninsulated (Bare) Cylindrical Antennas In Dissipative Media - Theory
By
J. T. deBettencourt

I. Introduction

In what follows it is assumed that the bare antenna is center driven and is immersed in a homogeneous, isotropic, dissipative medium of infinite extent. The antenna is assumed to have infinite conductivity; in such case Stratton[11] has shown that the complex phase constant k of the current is the same as that of the surrounding medium. The dissipative media with which we shall be concerned have electrical properties such as those for sea water, soil, or rocks (see Section IA for typical constants). A discussion of the complex phase constant of a dissipative medium is given in Section IID, and the complex characteristic impedance $\mathcal{Z}$ of the medium is discussed in Section IIE. For non-magnetic media, one has

$$k = \beta - j\alpha, \quad \alpha \leq \beta \tag{D.1}$$

$$\mathcal{Z} = \frac{\omega \mu_0}{k} = \frac{\mathcal{Z}_e}{(1 - j\alpha/\beta)} \tag{D.2}$$

$$\beta = \text{phase constant} = \beta_0 \sqrt{\epsilon_r} \, f(p) \tag{D.3a}$$

$$\alpha = \text{attenuation constant} = \beta_0 \sqrt{\epsilon_r} \, g(p) \tag{D.3b}$$

$$\beta_0 = \text{phase constant for space} = 2\pi/\lambda_0 \tag{D.4}$$

$$p = \text{loss tangent} = \frac{\sigma}{\omega\epsilon} = \frac{60 \, \sigma \lambda_0}{\epsilon_r} \tag{D.5}$$

in which σ and ϵ_r are the real effective conductivity and relative dielectric constant, respectively, λ_o is the free space wavelength, and mks units are used. The functions f(p) and g(p) are discussed in Section IIB and tabulated in Appendix A.

The antenna is of length 2h and radius a such that $\frac{h}{a} >> 1$. Interest will be concentrated on antennas having an electrical half-length $\pi/2 \lesssim \beta h \leq 3\pi/2$ and on electrically short antennas such that $\beta h \leq 0.3$, in which β is the phase constant of the medium for an loss tangent and given by equation (D.3a).

Formally, the theory is based upon variational formulations of Tai[70] and Storer[68] for antennas in free space but where the complex phase constant k of the dissipative medium is substituted for the real phase constant β_o of free space, and ζ is substituted for the real characteristic impedance $\zeta_o \doteq 120\pi$ ohms of free space. Then the formulas contain exponential, sine, and modified cosine integrals of complex argument. Because we lacked appropriate tables for complex arguments, we resorted to approximations using asymptotic expansions for large arguments and convergent series expansions for small arguments. In the formulas of Storer,[68] the argument of some of the integrals are half as large as the smallest argument in the integral expressions of Tai.[70] Because of the interest in antennas whose half-length was equal to or greater than a quarter-wavelength in the medium, we based our equations on the formulations of Tai[70] since the approximations using the asymptotic expansions were more accurate.

D-2

II. Exponential, Sine, and Modified Cosine Ingetrals - Series Expansions

We wished to check our expansions of sine and modified cosine integrals with values of those integrals calculated from tabulated values of the exponential integral. Tables of the latter have been prepared by the National Bureau of Standards[19] and Corrington[30] have shown how the sine and cosine integrals may be deduced therefrom. For this purpose we use the NBS definition of the exponential integral. Let $z_1 = x + jy = \rho\, e^{j\theta_1}$. The exponential integral is given by

$$E_1(z_1) = \int_{z_1}^{\infty} \frac{e^{-u}}{u}\, du \tag{D.6}$$

and is defined for $-\pi < \theta_1 \leq \pi$. The tabular values are given for the angular range $0 \leq \theta_1 \leq \pi$.

For $z_1 \neq 0$, $E_1(z_1)$ is given by the series

$$E_1(z_1) = -C - \ln z_1 - \sum_{n=1}^{\infty} \frac{(-1)^n z_1^n}{n \cdot n!} \tag{D.7}$$

where $C = 0.5772 - - - - =$ Euler's constant. The series (D.7) is particularly useful when $|z_1| < 1$ so that very few terms in the series are required.

When $|z_1|$ is large, the asymptotic expansion for $E_1(z_1)$ may be written

$$E_1(z_1) = \frac{e^{-z_1}}{z_1}\left(1 - \frac{1}{z_1} + \frac{2!}{z_1^2} - \frac{3!}{z_1^3} + - - -\right) \tag{D.8}$$

For a complex variable W, the following integral relations are employed:

$$Ci(W) = \text{cosine integral} = \int_{\infty}^{W} \frac{\cos t}{t}\, dt = ci(W) \tag{D.9}$$

$$Cin(W) = \text{modified cosine integral} = \int_0^W \frac{1 - \cos t}{t} \, dt$$

$$= C + \ln W - Ci(W) \tag{D.10}$$

$$Si(W) = \text{sine integral} = \int_0^W \frac{\sin t}{t} \, dt = \frac{\pi}{2} \int_\infty^W \frac{\sin t}{t} \, dt$$

$$= \frac{\pi}{2} - si(W) \tag{D.11}$$

and

$$L(W) = Cin(W) + j \, si(W) \tag{D.12}$$

In the theoretical development, we use the complex variable $z = x - jy = \rho \, e^{j\theta}$, and $y \le x$ so that $-\pi/4 \le \theta \le 0$. For this range of θ, $z_1 = z^*$ where the asterisk denotes complex conjugate. Denoting by $f(z_1)$ the exponential, sine, or cosine integrals, then

$$f(z_1^*) = f^*(z_1) = f(z) \tag{D.13}$$

Following Corrington,[30] then the desired integrals may be computed from the tabulated exponential integral as follows:

$$Cin(x - jy) = C + \ln(x - jy) - Ci(x - jy) \tag{D.14}$$

$$Ci(x - jy) = -\frac{1}{2} \left[E_1(y + jx) + E_1^*(-y + jx) \right] \tag{D.15}$$

$$Si(x - jy) = -j \frac{1}{2} \left[E_1(y + jx) - E_1^*(-y + jx) \right] + \frac{\pi}{2} \tag{D.16}$$

$$L(x - jy) = Cin(x - jy) + j \, Si(x - jy) \tag{D.17}$$

in which E_1 is the tabulated value and E_1^* is the complex conjugate of the tabulated value.

D-4

The series representation (D.7) may be used to obtain approximate forms, useful for small z, for the integrals in equations (D.14) through (D.17). With $z = x - jy$, one obtains

$$Cin(z) = \frac{z^2}{2.2!} - \frac{z^4}{4.4!} + \frac{z^6}{6.6!} - - - \qquad (D.18)$$

$$Si(z) = z - \frac{z^3}{3.3!} + \frac{z^5}{5.5!} - - - - \qquad (D.19)$$

$$L(z) \cong \frac{z^2}{4} (1 - \frac{z^2}{24} + \frac{z^4}{1080}) + jz(1 - \frac{z^2}{18} + \frac{z^4}{600}) \qquad (D.20)$$

The series forms (D.18) and (D.19) may be derived readily from the series expressions in Janke-Emde-Losch[2] for $ci(W)$ and $si(W)$ when substituted in equations (D.9) and (D.11).

For large arguments, asymptotic expansions like (D.8) are substituted in equations (D.14) through (D.17) with the result

$$Cin(z) = C + \ln z - \frac{\sin z}{z} (1 - \frac{2}{z^2} - - -) + \frac{\cos z}{z^2} (1 - \frac{6}{z^2} - - -)$$

$$(D.21)$$

$$Si(z) = \frac{\pi}{2} - \frac{\cos z}{z} (1 - \frac{2}{z^2} - - -) - \frac{\sin z}{z^2} (1 - \frac{6}{z^2} - - -) \qquad (D.22)$$

$$L(z) = C + \ln z + j\frac{\pi}{2} - j\frac{e^{-jz}}{z} \left[(1 - \frac{2}{z^2} - - -) + j\frac{1}{z} (1 - \frac{6}{z^2} - - -) \right]$$

$$(D.23)$$

The series (D.21) and (D.22) are formally like those derived from asymptotic

expansions for ci(x) and si(x) for real variable x as given by Janke-Emde-Losch[2] but where the complex variable $z = x - jy$ is substituted for the real variable x.

To illustrate the accuracy of using approximate relations, calculations were made for $L(z)$ with $z = x - jy$, for $y = 0$ and $y = x$ and for $x = 0.5$, 3.0, 4.0, and 5.0. For $y = 0$, the tabular values of $Cin(x)$ and $Si(x)$ were taken from King's text (reference 5, Appendix) from which the tabular value for $L(z)$, defined in equation (D. 12), is readily obtained. For $z = 0.5 - j\,0.5$ and $z = 3 - j\,3$, tabular values of $E_1(y + jx)$ and $E_1(-y + jx)$ exist[19] from which tabular values of $L(z)$ were obtained using equations (D. 14) through (D. 17). The exponential integral for the larger values of $z = 4 - j\,4$ and $z = 5 - j\,5$ were obtained from tabular values[19] of the function $e^z E_1(z)$ and proceeding as above to obtain $L(z)$. For $z = 0.5 - j\,0.5$ and $z = 0.5 - j\,0$, the approximate value of $L(z)$ was calculated from expression (D. 20) using two terms in the parentheses. For the other values of z, approximate values of $L(z)$ were calculated from equation (D. 23) omitting the second terms in the parentheses. The results of such calculations are shown in Table D. 1 with $L(z)$ written in polar form. The error, in percent, between the tabular and approximate values of the magnitude R and phase angle ϕ are also given.

For the smallest z, the error in the approximations using expression (D. 20) is quite small and should reduce for smaller values of z. For larger values of z, using equation (D. 23) with $y = 0$, the error is small and reduces the larger the value of x. For $y = x$, the error is quite small for $x \geq 3$.

D-6

TABLE D. 1

Comparison of Values of L(z) Calculated from
Tabulated Values of the Exponential Integral with Those Calculated
Using Series Approximations

$$z = x - j y \quad y \leq x$$

$$L(z) = Cin(z) + j\ Si(z) = R\ \underline{/\phi} = Re^{j\phi}$$

z	L(z) (deduced from tables of $E_1(z)$)		Approx. L(z) (deduced from series)		Error in % R	Error in % ϕ
0.5 - j 0.5	0.62419	$\underline{/0.67211}$	0.62050	$\underline{/0.67763}$	-0.59	+0.82
0.5 - j 0	0.49697	$\underline{/1.44601}$	0.49697	$\underline{/1.44601}$	0.00	0.00
3 - j 3	2.1633	$\underline{/0.37408}$	2.1627	$\underline{/0.37378}$	-0.03	-0.08
3 - j 0	2.4165	$\underline{/0.87108}$	2.4221	$\underline{/0.89196}$	+0.23	+2.40
4 - j 4	2.4409	$\underline{/0.32884}$	2.4407	$\underline{/0.32886}$	-0.01	+0.01
4 - j 0	2.7423	$\underline{/0.69599}$	2.7629	$\underline{/0.70075}$	+0.75	+0.69
5 - j 5	2.6482	$\underline{/0.30129}$	2.6530	$\underline{/0.30085}$	+0.22	-0.15
5 - j 0	2.8374	$\underline{/0.57788}$	2.8492	$\underline{/0.57580}$	+0.42	-0.36
6 - j 6	2.8270	$\underline{/0.28148}$	2.8266	$\underline{/0.28153}$	-0.01	+0.02
6 - j 0	2.8229	$\underline{/0.52902}$	2.8236	$\underline{/0.52630}$	+0.02	-0.51

Values of z where y $\ll$ x will be seen to represent the case for bare antennas immersed in a dissipative medium having a loss tangent p which is very small. Values of z where y $\doteq$ x will then represent that case for large loss tangent. The quantity x will represent the radian lengths $2\beta h$ or $4\beta h$ in the functions L(2z) and L(4z) used in our modification of Tai's integral expressions.[70] Accordingly, since we lack tables of Cin(z) and Si(z), we shall use approximations (D.20) for electrically short antennas and (D.23) with x $\geq$ π, y $\leq$ x corresponding to antennas with $\beta h \geq \pi/2$.

III. The Variational Solution

The zero-order variational, or EMF, method of solution is based upon a sinusoidal distribution of current. If the antenna lies along the z-axis and z' denotes the position coordinate, the zero-order current distribution is given by

$$I(z') = I(0) \frac{\sin k (h - | z'|)}{\sin k h} \tag{D.24}$$

in which I(0) is the input current at z' = 0. The complex phase constant of the current k is the same as that of the dissipative medium given by equation (D.1). The distribution given in equation (D.24) is the same as that used by King[51] to obtain the approximate electromagnetic field due to a bare antenna in dissipative media and for which $\beta h \leq 3\pi/2$; a different distribution was used, however, to obtain the input impedance.

The input impedance Z_{oo} for the zero-order variational (EMF) method may be written as

$$Z_{00} = \frac{\mathscr{S}}{4} \quad \frac{\nu_{11}}{\sin^2 kh} \qquad\qquad (D.25)$$

where $\mathscr{S}$ is the complex characteristic impedance of the dissipative medium given by equation (D.2), and where

$$\nu_{11} = 2 L(2z) + e^{j2z} \left[\ln 2 - \frac{\varOmega}{2} - L(4z) + 2 L(2z) \right] + e^{j2z} \left[\frac{\varOmega}{2} - \ln 2 \right]$$

$$(D.26)$$

with $z = kh = \beta h (1 - j \frac{\alpha}{\beta})$ and with the thickness parameter $\varOmega = 2 \ln \frac{2h}{a}$.

The functions $L(W)$ are given by equation (D.12) and discussed in Section DII.

The first-order variational solution is based upon Tai's trial current distribution[70] which may be written as

$$I(z') = I(0) \left\{ \frac{\sin k(h - |z'|) + A k(h - |z'|) \cos k(h - |z'|)}{\sin kh + kh A \cos kh} \right\} \qquad (D.27)$$

The first-order input impedance may be written, after evaluating the constant A, as

$$Z_{01} = \frac{\mathscr{S}}{4} \cdot \frac{\nu_{11} \nu_{22} - \nu_{12}^2}{z^2 \nu_{11} \cos^2 z - z \nu_{12} \sin 2z + \nu_{22} \sin^2 z}$$

$$(D.28)$$

The constant A in equation (D.27) is evaluated from the variational method as

$$A = \frac{z \nu_{11} \cos z - \nu_{12} \sin z}{\nu_{22} \sin z - z \nu_{12} \cos z} \qquad\qquad (D.29)$$

The parameter ν_{11} in equations (D.28) and (D.29) is given by equation (D.26). The parameters ν_{12} and ν_{22} are very long expressions which may be

obtained from the equations of Tai[70] but with complex $z = kh$ written $\ldots$ the real value $x = \beta h$ in those equations.

IV. The Half-Wave Antenna ($\beta' = \pi/2$)

1. In Free Space

In free space, $p = 0$, $\varepsilon_r = 1$ and kh become simply $\beta_o h = \dfrac{2\pi h}{\lambda_o}$. The results of several methods for computing the input impedance have been compared previously, sometimes graphically and occasionally in tabular form. Listed below in Table D.2 are numerical values for the input impedance Z_o and admittance Y_o for an antenna the length of which is one-half wavelength in free space, obtained from several methods. The value of Ω chosen was 10. The results for the first-order variational method were computed using the formulas of Tai[70] and tabulated values for the sine and modified cosine integral (reference ?, Appendix). The King-Middleton second order values were taken from King's text.[5] The values obtained by King[51] using a recent approximation to his iterative procedure are also shown. The values deduced from the EMF method are well known.[5, 51]

The comparison of the values of Y_o calculated by the latter three methods was discussed by King.[51] We merely add that the values calculated by the first-order variational method differ but 1% in the conductance and 3% in the susceptance from the corresponding King-Middleton values and thus agree well with experiment.

2. In a Loss-Less Dielectric ($\varepsilon_r \neq 1$, $p = 0$)

In a loss-less dielectric, $p = 0$, if the antenna length is adjusted to